Report Number 97-06

research

UNIVERSITY OF MINNESOTA
CENTER FOR TRANSPORTATION STUDIES

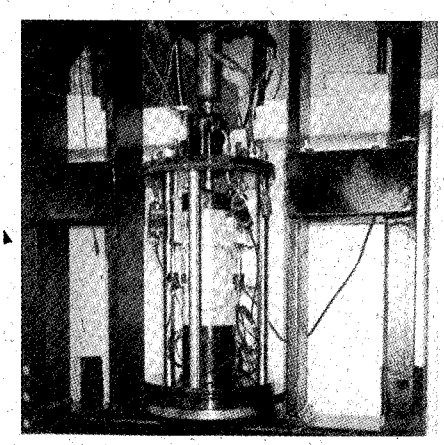

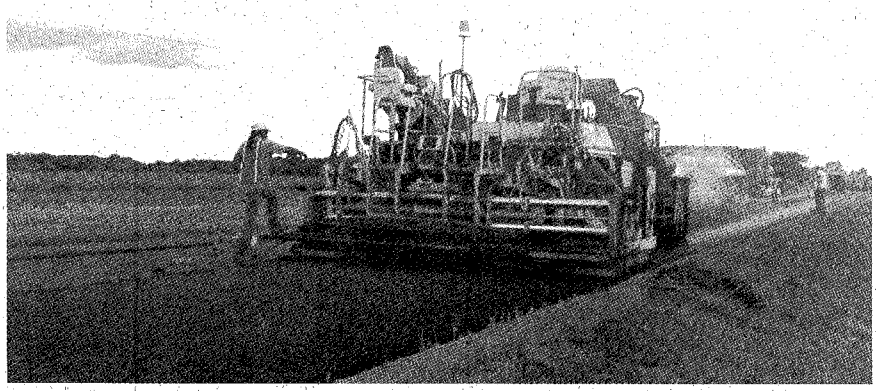

Investigation of Hot Mix Asphalt Mixtures at Mn/ROAD

Local Road Research Board

MnROAD
Office of Minnesota Road Research

Technical Report Documentation Page

1. Report No.	2.	3. Recipient's Accession No.
MN/RC - 97/06		

4. Title and Subtitle	5. Report Date
INVESTIGATION OF HOT MIX ASPHALT MIXTURES AT Mn/ROAD	February 1997
	6.

7. Author(s)	8. Performing Organization Report No.
Mary Stroup-Gardiner and David E. Newcomb	

9. Performing Organization Name and Address	10. Project/Task/Work Unit No.
University of Minnesota Department of Civil Engineering 122 CivE Building 500 Pillsbury Dr. S.E. Minneapolis, Minnesota 55455	11. Contract (C) or Grant (G) No. (C) 68894 TOC #77 (C) 72631 TOC #164

12. Sponsoring Organization Name and Address	13. Type of Report and Period Covered
Minnesota Department of Transportation 395 John Ireland Boulevard Mail Stop 330 St. Paul, Minnesota 55155	Final Report 1992-1996
	14. Sponsoring Agency Code

15. Supplementary Notes

16. Abstract (Limit: 200 words)

This report presents the material characterization for the Minnesota Road Research Project (Mn/ROAD) bituminous materials. This effort will provide the historical base line information on properties needed for the validation of future pavement evaluation and design models. The objectives of the work were to 1) Document construction of Mn/ROAD, 2) Establish a series of test methods for characterizing the materials and 3) Develop a data base of material properties to develop mechanistic pavement design procedures. Documentation on construction included mixture design, construction techniques and a summary of test results. The laboratory test methods represent a wide variety of tests developed by the Strategic Highway Research Program, the National Cooperative Highway Research Program and the Federal Highway Administration. The materials represent those tested during the mixture design, construction and post construction phases of Mn/ROAD.

17. Document Analysis/Descriptors		18. Availability Statement
Bituminous Materials Pavement Design Construction Test Results	Characterization Hot Mix Asphalt	No restrictions. Document available from: National Technical Information Services, Springfield, Virginia 22161

19. Security Class (this report)	20. Security Class (this page)	21. No. of Pages	22. Price
Unclassified	Unclassified	246	

INVESTIGATION OF HOT MIX ASPHALT MIXTURES AT Mn/ROAD

Final Report

Prepared by

Mary Stroup-Gardiner
David Newcomb

University of Minnesota
Department of Civil Engineering
122 CivE Building
500 Pillsbury Dr. S.E.
Minneapolis, MN 55455-0220

February 1997

Published by

Minnesota Department of Transportation
Office of Research Administration
200 Ford Building Mail Stop 330
117 University Avenue
St Paul Minnesota 55155

TABLE OF CONTENTS

LIST OF TABLES

LIST OF FIGURES

EXECUTIVE SUMMARY

This report presents the material characterization for the Minnesota Road Research Project (Mn/ROAD) 5- and 10-Year Mainline and Low Volume Road bituminous test cells. The material characterizations of these mixtures will provide the historical base line information on properties needed for the validation of future pavement evaluation and design models. The initial laboratory testing of the 5-Year Mainline bituminous materials also served as an evaluation of test methods subsequently used in the evaluation of the 10-Year Mainline and Low Volume Road facility materials.

The objectives of this report were to:

1. Document construction of the test cells.

2. Establish a series of laboratory test methods for characterizing the temperature susceptibility, moisture sensitivity, low temperature behavior, and permanent deformation characteristics of asphalt concrete materials.

3. Develop a data base of material properties that will be used in the development of mechanistic pavement designs.

Documentation of the bituminous test cell construction includes mix designs, development of rolling patterns with the construction of test pads, a description of the actual construction, and a summary of construction testing.

The laboratory testing program for materials characterization evaluated a variety of test methods developed by the Strategic Highway Research Program (SHRP), the National Cooperative Highway Research Program (NCHRP) and the Federal Highway Administration (FHWA). The test methods shown in the table below were selected based on the most currently available information as well as the ability for test results to be used in either established empirical-mechanistic or proposed mechanistic pavement design approaches.

Materials tested in this program included laboratory-prepared loose mix (mix design materials), behind-the-paver samples, and cores. The testing program for the cores was limited due to sample size requirements for several of the tests. Specific load levels and variations of each test method are discussed in detail in Chapter Four (Testing Program) in the main report.

Some general observations that can be made about the Mn/ROAD mixtures are as follows:

1. Temperature susceptibility, using resilient modulus testing (ASTM D4123) over a range of test temperatures, showed that mix design materials significantly under-predicted the moduli of the 120/150 pen asphalt mixtures when compared to the behind-the-paver materials. However, the higher viscosity AC 20 mix design moduli were generally similar to those obtained for behind-the-paver

materials. This suggests that the lower viscosity asphalt may be more susceptible to aging (i.e., an increase in moduli) during production than the higher viscosity asphalt.

2. Resilient moduli for mix design materials significantly under-predicted the cold temperature moduli for the cores from the 120/150 pen asphalt 10-Year Mainline test cells and over-predicted the warm temperature moduli. However, it should be noted that wet cores were sealed in plastic containers immediately after coring and then placed in cold storage until testing. This resulted in unplanned moisture conditioning of the cores and may be a significant factor in these comparisons.

Experimental Design for the Laboratory Characterization of Asphalt Concrete Materials for Mn/ROAD.

Source	Fundamental Mixture Properties			
	Temperature Susceptibility	Moisture Sensitivity	Low Temperature Behavior	Permanent Deformation Characteristics
SHRP		Net Adsorption	Indirect Tensile Creep (Constant Stress)	
NCHRP	Diametral Resilient Modulus (ASTM D4123)		Constant Rate of Deformation Indirect Tensile Creep	
FHWA		Modified Lottman (ASTM D4867)		
Other	Axially Loaded Dynamic Modulus Diametral Resilient Modulus (Instrumented over Center 1/4)			Axially Loaded Repeated Load and Static Creep[1]

1: Initially used by SHRP researchers during A-003A contract. The final SHRP recommendation was direct shear but the equipment was not available at the time this work was started.

3. Asphalt content did not have a significant influence on either temperature susceptibility or the magnitude of resilient moduli for a given asphalt grade.

4. Gyratory compaction of materials produced mixtures with similar moduli values at a given test temperature for both the 120/150 pen asphalt and the AC 20. There was also no significant difference between mix design and behind-the-paver materials.

5. The tensile strength of mixtures prepared with the AC 20 asphalt were approximately 20 percent greater than those prepared with the 120/150 pen asphalt. The tensile strengths of the behind-the-paver materials were either similar to or greater than the tensile strengths for mix design materials.

6. There was no clear trend between tensile strength ratios for mix design and behind-the-paver materials.

7. Low temperature [1°C (34°F)] tensile strengths at slow rates of deformation (0.025 mm/min) were similar for the mix design and behind-the-paver materials. The tensile strength of the cores was approximately half of those for either the mix design or behind-the-paver materials. The horizontal strains for cores were about 5 times greater than those for either of the other two sources of materials. The most likely reason for this difference is a difference in air voids between the sample sets (approximately 4 percent for mix design and behind-the-paver, and between 6 and 8 percent for cores).

8. The creep compliance determined from unconfined static creep testing at 25°C (77°F) was similar for both the 120/150 pen and AC 20 mix design mixtures. However, there was a significant difference in the compliance for the behind-the-paver materials with the 120/150 pen asphalt mixtures showing a much greater compliance (i.e, failed) than the AC 20 mixtures.

CHAPTER ONE

INTRODUCTION

In the late 1950's and early 1960's, the American Association of State Highway Officials (AASHO) undertook a large pavement performance experiment in Ottowa, Illinois, in which large cargo trucks were driven over a number of asphalt and concrete road structures for two years. Pavement conditions, in terms of roughness (ride quality) and distress, were monitored to define when pavement sections had failed. These were empirically related to the initial pavement structures in terms of layer thicknesses and material qualities. The resulting performance equations then formed the basis of how most of the pavements in the United States were designed. Local calibrations of these equations were developed to account for deviations in climatic and soil conditions in different parts of the country.

While the AASHO Road Test equations were adequate for the time period in which they were developed, there were several shortcomings. The AASHO Road Test was conducted over a two-year period, so while the contribution of traffic loadings to failure was well related, the contribution of climate was minimized, and the interaction between traffic and climate could not be adequately described. Also, because of the empirical nature of the equations, changing conditions in traffic loads and new materials could not be incorporated in the design procedure. So, while the empirical equations were relatively simple, they lacked the flexibility to handle change. Some examples of changes in traffic loadings included the use of higher pressure tires (from about 75 psi in the late 50's to 105 psi in the late 80's), higher volumes of truck traffic using roadways due to the closure of railheads and the use of radial tires instead of bias-ply tires (they have different contact pressure distributions and tracking characteristics). New materials such as polymer modified asphalt binders and asphalt-rubber could not be accommodated because they did not fit the model used to describe pavement performance at the AASHO Road Test.

Researchers such as Monismith, Finn, Mahoney, Epps and Newcomb began developing mechanistic-empirical approaches to pavement design which offered an improved

flexibility in accounting for changes in loadings and materials. Most of these are based on layered elastic analysis wherein loads are described in terms of their magnitude and geometry, and materials in terms of their elastic parameters (Young's modulus and Poisson's ratio). However, such efforts have met with limited success because of a lack of information concerning traffic and seasonal changes in material properties. The resulting failure criteria (relationships between pavement responses and performance) have been based on sketchy data, so there has been no widespread movement to adopt mechanistic-empirical design procedures. Thus, there was a need to research pavements on a large scale and explain the performance in mechanistic terms.

A number of test tracks have been or are being constructed, artificial loading facilities (ALFs) have been built, and long-term pavement performance (LTPP) studies are being conducted. Specific objectives are being addressed within each of these, and an overview of these will be presented below.

Test tracks are defined as closed facilities with full-scale pavement features, trafficked by typical highway vehicles (trucks). Existing test tracks include the Federal Highway Administration (FHWA) access road into the Turner-Fairbanks Research Center, the Nardo Test Track in Italy, the Virttaa Test Road in Finland, the Penn State Test Track, and WesTrack. The access road at Turner-Fairbanks was more of a study of instrumentation placement and variability in readings than anything to do with pavement performance. Several strain gauges in asphalt concrete were placed longitudinally in a line. The results described the spatial variability in tensile strain under controlled conditions. Only one pavement cross-section was used in this road. The Organization for Economic Cooperation and Development (OECD) sponsored a pavement instrumentation evaluation at Nardo where researchers from several countries gathered to compare results obtained from different methods of instrumenting pavements. The Virttaa Test Road in Finland is actually part of a widened asphalt roadway which is used as an emergency airfield by the Finnish Air Force. Only four pavement sections exist at Virttaa which are instrumented with strain gauges and displacement transducers. Recent modifications have allowed them to investigate the effects of saturation levels in the soil on pavement responses. The Penn State Test Track was built quite a few years ago to study

the effects of construction variables. It is a two-lane facility, three miles in length. It was most recently used to study pavement instrumentation performance. WesTrack was constructed during the fall of 1995 near Fallon, Nevada. This test track is an FHWA project constructed for the purpose of verifying the effects of construction control on pavement performance.

ALFs are devices used to apply a large number of simulated traffic loadings on a pavement in a very short time period. They may either be fixed or mobile devices. These exist in France, Australia, South Africa, FHWA (Turner-Fairbanks), Indiana, Louisiana, California, and Texas. These are used to apply large numbers of load repetitions (usually to failure) to full-scale pavements quickly. It is impossible to incorporate the effects of climate in such studies, but they are useful in terms of investigating the effects of changing load conditions and the effects of new materials.

The Strategic Highway Research Program (SHRP) initiated a long-term pavement performance study in 1987 which is being carried forward by the FHWA. On the order of 2000 existing and new concrete and asphalt pavement sections throughout the U.S. are being monitored in terms of traffic, general ambient climate and performance. A very limited number of these are instrumented to study the effects of moisture and temperature in the pavement. An even more limited number of sections of new concrete and asphalt pavements will be instrumented for responses, and this must be done at the individual state's expense. Tow of these are being constructed in Ohio and one was built in North Carolina.

Mn/ROAD differs from the above facilities and studies in a number of ways. First, it has 40 asphalt, concrete and gravel-surfaced pavement sections which span designs from low-volume roads to interstates. The pavement sections were designed so that different combinations of materials, layer thicknesses, design details and drainage schemes could be evaluated. All pavement sections are instrumented to monitor pavement responses including pressures, strains and displacements, and subsurface conditions of moisture content, moisture state, ground water level and temperature.

The Mn/ROAD facility is located parallel to Interstate 94 (I-94) in Otsego, Minnesota which is approximately 60 km (40 miles) northwest of the Minneapolis-St. Paul metropolitan

area and consists of 4.8 km (3 miles) of two-lane interstate as well as 4 km (2.5 miles) of closed-loop low volume test track. The I-94 traffic, an estimated 14,000 vehicles per day (15 percent trucks), is periodically diverted onto the high volume facility where 23 heavily instrumented test cells will be subjected to live traffic loads. The low volume facility with 17 test cells, including portland cement concrete, asphalt cement concrete, and various aggregate surfaces, will be subjected to controlled loading by a single vehicle circling the two-lane test track. The inside lane is trafficked four days a week with an 80,000 lb. truck; the outside lane is trafficked one day a week with a 102,000 lb. truck.

The interstate portion of the test facility has been divided into two parts, referred to as the 5-Year and 10-Year Mainline. These interstate sections have been designed for an estimated 5- and 10-year design life, respectively. Both the 5- and 10-Year Mainline have both portland cement concrete and asphalt concrete test cells. Figures 1.1, and 1.2 show the various structural layouts of the 5-Year and 10-Year, and Low Volume asphalt concrete test cells, respectively.

The materials characterization results for the asphalt concrete used at Mn/ROAD is presented in this report.

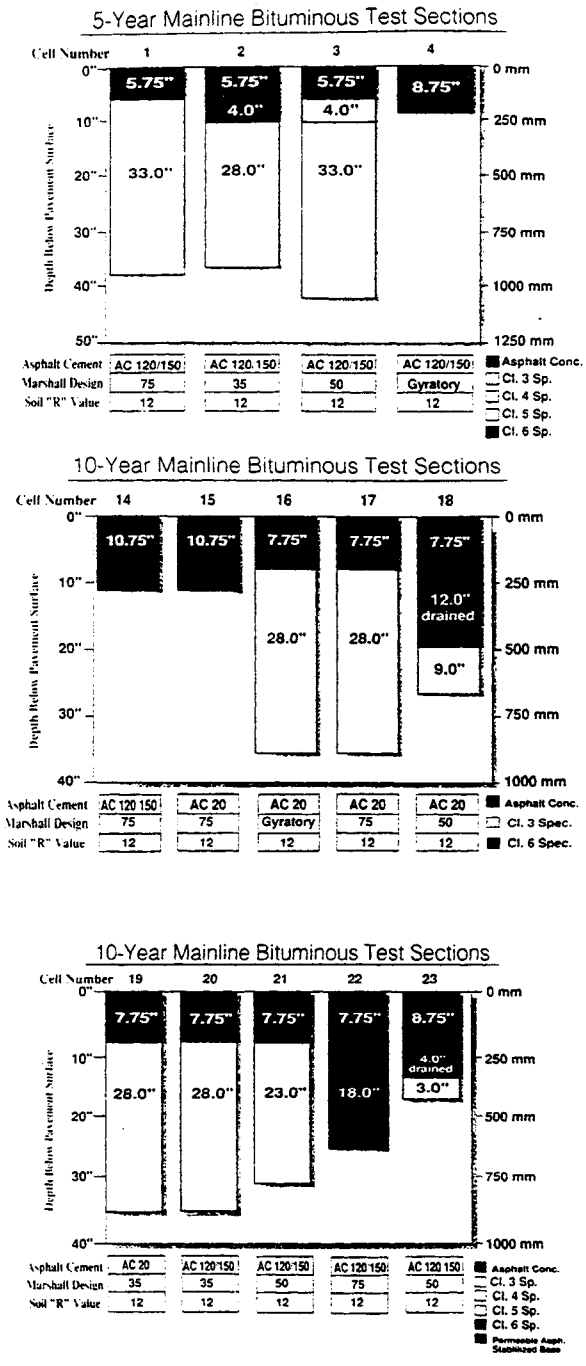

Figure 1.1. Layout of the 5- and 10-Year Mainline Asphalt Concrete Test Cells.

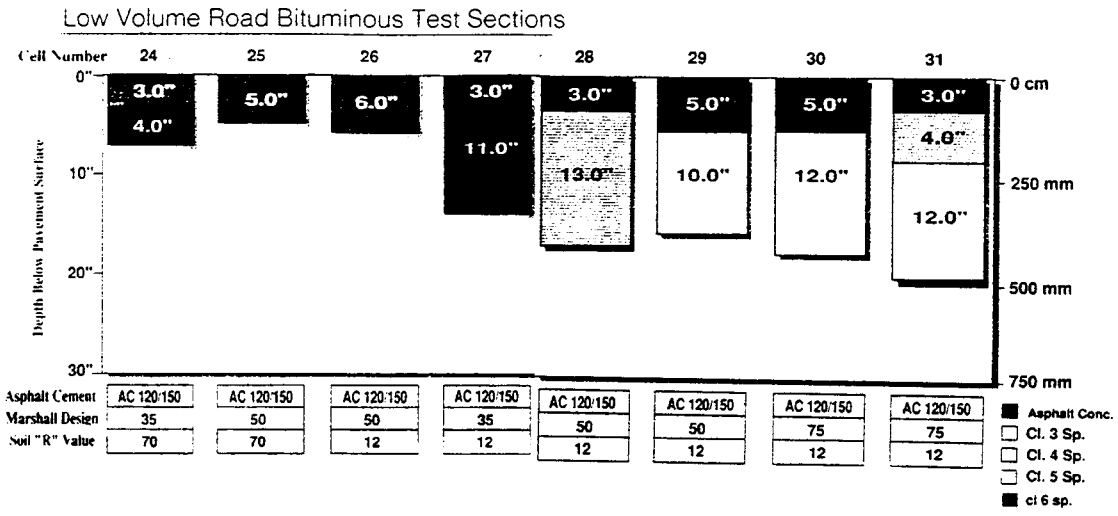

Figure 1.2. Layout for the Low Volume Road Asphalt Concrete Test Cells.

OBJECTIVES

The objectives of this research were to:

1. Document the construction of the test facilities.
2. Establish a series of laboratory test methods for characterizing the temperature susceptibility, moisture sensitivity, low temperature behavior, and permanent deformation characteristics of the asphalt concrete materials.
3. Develop a data base of material properties to be used in the development of mechanistic pavement designs.

SCOPE

Construction of all of the bituminous test cells at Mn/ROAD are documented in this report. The laboratory testing program for the materials characterization used a variety of test methods developed by SHRP, the National Cooperative Highway Research Program (NCHRP) and the FHWA (**1,2,3**). Test methods were selected based upon the available information as well as the ability for test results to be used in either established empirical-mechanistic or proposed mechanistic pavement design approaches. Table 1.1 shows the general approach for this testing program.

Table 1.1. Approach for the Materials Characterization of Asphalt Concrete.

Source	Fundamental Mixture Properties			
	Temperature Susceptibility	Moisture Sensitivity	Low Temperature Behavior	Permanent Deformation Characteristics
SHRP		Modified Lottman (ASTM D4867) Net Adsorption	Indirect Tensile Creep (Constant Stress)	
NCHRP	Diametral Resilient Modulus (ASTM D4123)		Constant Rate of Deformation Indirect Tensile Creep	
Other	Dynamic Modulus (Diametral and Uniaxial)			Axial Repeated Load and Static Creep

Materials tested in this program included laboratory-prepared loose mix (mix design materials), behind-the-paver samples (field-mixed, laboratory compacted), and cores. This testing provided a comparison of mixture properties obtained during mix design to those of the mixtures produced during construction at the same level of compactive effort. Differences in properties between these two sets of samples will be due to changes in the cold feed aggregate gradation, fluctuations in asphalt cement content, and aggregate degradation during production. Test results for the cores will provide information as to the in-place properties prior to traffic loading.

The testing program for the cores was limited due to sample size requirements for several of the tests and the number of cores obtained prior to opening the facilities to traffic. Specific load levels and variations of each test method are discussed in detail in Chapter Three, Testing Program.

CHAPTER TWO
MATERIALS AND MIX DESIGNS

MATERIAL PROPERTIES

Aggregates

Three stockpiles of aggregates were used for the Mn/ROAD asphalt concrete mixtures. The majority of the mix was comprised of two stockpiles obtained from Buffalo Bituminous's Crow River pit in Buffalo, Minnesota; both of these were partially crushed river gravel. The third stockpile was obtained from Meridian, Inc. in St. Cloud, Minnesota and was a 100 percent crushed granite (CA-50) (**4**). The physical properties, stockpile gradations, and blending percentages used to prepare the mix design materials and the adjusted percentages used for construction are shown in Table 2.1.

The combined gradation was held constant for all asphalt concrete mixtures for all test cells, however the blending percentages used in construction were different than those used for preparation of the laboratory-prepared mix design materials. The original gradation blend was selected during the mix design work completed by the Minnesota Department of Transportation (Mn/DOT) prior to construction. Aggregate stockpiles were re-sampled just prior to the start of the construction; this check showed that the gradation blends needed adjustment to compensate for increased and erratic fines content. The construction stockpiles were eventually reworked so that a consistent gradation was achieved during construction and no further blending adjustments were needed.

Table 2.1. Aggregate Properties for Mn/ROAD Asphalt Concrete Test Cells.

Property	Crow River Fines	Crow River Coarse	CA-50	Combined Gradation (Job Mix Formula)
Blending Percentages, % Mix Design Construction	 74 66	 16 24	 10 10	 100 100
Bulk Specific Gravity	2.73	2.66	2.62	2.708 (Mix) 2.702 (Field)
Absorption Capacity, %	NA	NA	NA	NA
Percent Crushed, %	---	61.2	100	---
Cumulative Percent Passing, %				
19 mm (3/4 in)	100	100	100	100
12.5 mm (1/2 in)	100	75	80	92
9.0 mm (3/8 in)	99	53	37	82
4.75 mm (No. 4)	94	19	4	67
2.0 mm (No. 10)	82	11	---	57
1.0 mm (No. 20)	63	8	---	---
0.45 mm (No. 40)	39	6	---	27
0.25 mm (No. 80)	10	4	---	---
0.125 mm (No. 100)	8	3	---	---
0.075 mm (No. 200)	4.9	2.4	----	4

Asphalt Cement

Two grades of binder, a 120/150 penetration grade and and AC 20 viscosity grade, were supplied by the Koch Refinery in Rosemount, Minnesota. Only the 120/150 pen grade was used for the 5-Year Mainline (1 through 4) and the Low Volume Road (24 through 31) test cells. Test cells 14 and 20 through 23 in the 10-Year Mainline were constructed with the 120/150 pen asphalt while test cells 15 through 19 had the AC 20 asphalt. A comparison of the binder properties and the relevant binder specifications are shown in Table 2.2.

Table 2.2. Physical Properties of Asphalt Cements.

Property	Koch 120/150 Penetration Grade	ASTM D946 Specification	Koch AC 20	ASTM D3381 Specification Table 1
Viscosity, 60°C (140°F), Poise	846	---	1987	2,000 ± 400
Viscosity, 135°C (275°F), cSt	271	---	397	210 min
Penetration, 25°C (77°F), 0.1 mm	130	120 min 150 max	76	40 min
Ductility, 25°C (77°F), 5 cm/min	120+	---	120+	---
Flash Point, °C (°F) min	318 (605)	218 (425) min	---	232 (450) min
Tests on Residue from Thin Film Oven Test				
Viscosity, 60°C (140°F), Poise	1,880	---	4662	10,000 max
Viscosity, 135°C (275°F), cSt	439	---	579	---
Penetration, 25°C (77°F), 0.1 mm	71	---	45	---
Ductility, 25°C (77°F), 5 cm/min	120+	100 min	120+	20 min
SUPERPAVE (SHRP) Binder Specifications				
PG Grading	PG 58 - 28	---	PG 58 - 22	---

---: Not applicable

MIX DESIGNS

Preconstruction work consisted of completing four mix designs: 1) 35-blow Marshall, 2) 50-blow Marshall, 3) 75-blow Marshall, and 4) the SHRP Level 1 (volumetric mix design). The first three were performed by the Minnesota Department of Transportation (Mn/DOT) Materials, Research and Engineering Laboratory in Maplewood, Minnesota. The Asphalt Institute in Lexington, Kentucky performed the SHRP mix design. These were used for all of the Mn/ROAD asphalt concrete test cells.

Mix designs were limited to determining the optimum binder content for mixtures prepared with the 120/150 pen asphalt cement. The same optimum asphalt content was used

with the AC-20 so that the binder content for comparisons of the 120/150 and AC 20 test cells would have a consistent amount of asphalt. Mixing temperatures were adjusted to achieve an equivalent viscosity.

Marshall Mix Designs (35, 50, and 75 Blow)

Sample Preparation

The appropriate percentages of each of three aggregate stockpiles were combined and heated to 150°C (300°F) for at least 4 hours prior to mixing. The asphalt cement was heated to 135°C (275°F) for a maximum of 4 hours. A large mixer was used to prepare approximately 10 kg (22 lb) batches at each of five asphalt cement contents. Each batch was used to prepare five samples; three samples were compacted for mix design testing and the remainder was used for determining the theoretical maximum specific gravity. Samples were compacted immediately after mixing with a rotating base, bevel head Marshall hammer.

Marshall Mix Designs

Testing included determining the bulk and theoretical specific gravities, air voids, Marshall stabilities, flow, voids in mineral aggregate (VMA), and the percent of voids filled with asphalt (VFA). The results of the testing are shown in Table 2.3. The optimum asphalt content was selected as the percentage that would produce 4 percent air voids. Based on this criterion and the data in Table 2.3, the optimum binder contents were selected as 6.4, 6.1, and 5.9 by weight of total mix for the 35, 50, and 75 blow mix designs, respectively.

Table 2.3. Marshall Mix Design Results (120/150 Penetration Grade Asphalt Cement). (Reported by Mn/DOT)

Asphalt Content[1]	Air Voids, %	VMA, %	VFA, %	Marshall Stability, kN (lb)	Marshall Flow, 0.25 mm, 0.01 in	Density kg/m^3 (lb/ft^3)
35 Blow Mix Design						
5.0	8.0	18.0	55.4	2,172 (966)	10	2,275 (142.0)
5.5	6.6	17.7	62.8	2,115 (941)	10	2,294 (143.2)
6.0	5.0	17.4	71.3	2,439 (1,085)	11	2,315 (144.5)
6.5	3.7	17.4	78.7	2,455 (1,092)	10	2,328 (145.3)
50 Blow Mix Design						
5.0	7.1	17.2	28.6	2,272 (1,278)	11	2,297 (143.4)
5.5	6.2	17.2	64.0	2,621 (1,166)	10	2,307 (144.0)
6.0	4.3	16.8	74.4	2,779 (1,236)	9	2,331 (145.5)
6.5	3.0	16.8	82.2	2,734 (1,216)	9	2,344 (146.3)
75 Blow Mix Design						
5.0	6.5	16.6	60.9	3,287 (1,462)	10	2,312 (144.3)
5.5	5.4	16.5	67.2	3,536 (1,573)	9	2,329 (145.4)
6.0	4.0	16.6	75.9	3,324 (1,480)	10	2,339 (146.0)
6.5	2.3	16.2	85.8	3,424 (1,523)	10	2,361 (147.4)

1: Percent by weight of mixture.

Gyratory Mix Design

Sample Preparation

Aggregates and asphalt cement were batched as described in the Asphalt Institute's Manual Series No. 2 on "Mix Design Methods" (**5**). Once mixed, the loose-mix was stored for 4 hours in an oven set at the desired compaction temperature which was approximately 135°C (275°F). A set of three samples for each of four percentages of asphalt contents was

then compacted using a Rainhart gyratory compactor with a 1.25° angle of gyration, and a rotational speed of 30 rpm. Samples were cooled and extruded as in the Marshall mix design method.

SHRP Level 1 Mix Design

The SHRP Level 1 mix design uses a volumetric approach to select an optimum asphalt content. This method specifies a preliminary procedure for defining an appropriate aggregate gradation, followed by the selection of an optimum binder content for the selected gradation. In the case of the Mn/ROAD design, the gradation was restricted to that initially selected with the Marshall mix design.

If the gradation had not already been fixed during the Marshall mix designs at the start of the project, the complete gyratory mix design would have consisted of the following steps. First, three different gradations would be selected; typically one fine gradation and two coarse would be used. The optimum asphalt content would be estimated based on the gradation, and this would be used to fabricate one set of three samples for each gradation. The voids, VMA, and VFA would be evaluated according to SHRP criteria and the best would be selected or, if none were acceptable, other gradations would be tried at this point.

Once a gradation is selected, as was the case for the Mn/ROAD materials, a set of three samples is fabricated for the optimum asphalt content and $\pm$ 0.5 percent of optimum asphalt cement contents. The change in density during compaction was monitored at three levels of compaction (i.e., numbers of gyrations) during sample fabrication. The criteria for selecting the optimum asphalt content at a predetermined number of maximum gyrations was:

1. A density of less than 89 percent of maximum at the initial number of gyrations.
2. Four percent air voids at the design compaction effort.
3. A density of less than 98 percent of maximum at refusal.

The gyratory mix design results, based on a design number of 100 gyrations (selected by the Asphalt Institute), for the Mn/ROAD aggregate gradation are shown in Table 2.4. Based on these results, the optimum asphalt content was selected as 5.6 percent.

Table 2.4. Gyratory Mix Design Results.

Asphalt Content[1], %	Air Voids, %	VMA, %	VFA, %	Density with Numbers of Gyrations, %		
				10	100	230
4.7	6.4	15.7	59.0	88.8	93.6	94.8
5.2	5.1	15.5	67.0	89.9	94.9	96.2
5.7	3.8	15.5	76.0	91.1	96.2	97.5
6.2	2.8	15.7	82.0	92.1	97.2	98.5

1: Percent by total weight of mixture.

The numbers of gyrations at which the density was monitored was dependent upon the desired compactive effort and was selected by the Asphalt Institute from (**6**). This selection was based upon the anticipated in-service average high air temperature and the estimated level of design traffic.

Discussion of Results

Table 2.5 compares the optimum binder contents and the corresponding VMA and VFA for each of the four mix designs. As expected, both the asphalt content and the VMA decreased as the compactive effort increased. The VFA is approximately 78 percent for the 35 blow Marshall mix design. This decreased to approximately 74 to 75 percent for the remaining mix designs.

Table 2.5. Comparison of Mix Design Results.

Mix Design Method	Optimum Asphalt Cement Content	VMA %	VFA %
35 Blow Marshall	6.4	17.4	78.5
50 Blow Marshall	6.1	16.8	74.4
75 Blow Marshall	5.9	16.5	75.0
SHRP Gyratory Level 1	5.6	15.5	74.0

While the SHRP Level 1 mix design was used for selecting a gyratory-based optimum binder content, the SHRP gyratory Level 2, or preferably Level 3, mix design is recommended for the design of a high traffic level facility such as Mn/ROAD. Both of these design levels select the optimum asphalt cement content based not only on volumetric parameters but also an evaluation of mixture properties. These advanced levels of mix design were not completed for Mn/ROAD because construction preceded the final development of SHRP equipment and test methods. It is anticipated that this work will be completed at a later date.

CHAPTER THREE
CONSTRUCTION

Materials sampled at the time of construction were taken from behind the paving machine, stored in metal buckets, reheated and compacted in the laboratory prior to testing. The reason for testing the mixtures in this condition was to establish the material properties at the time of construction, and ascertain how they changed from the mixture design phase. Since the compaction methods and compactive effort was the same as that at the time of mixture designed, it is assumed that any differences in the mixture would be the result of the construction process, e.g., changes in aggregate gradation through abrasion, higher asphalt absorption due to plant temperatures being hotter than laboratory mixture temperatures, etc.

During construction Braun Intertec, Inc., St. Paul, Minnesota, provided construction control testing services which included monitoring density, specific gravities, and air voids.

CONSTRUCTION OF TEST PADS

Pavement test pads were constructed to establish compactor rolling patterns September 21 and 22, 1992. Three bituminous mixtures were used over three types of base materials. The gyratory-design mixture was placed on prepared subgrade in two lifts were constructed. The 75 and 35 blow design mixtures were constructed on 33 inches of class 4 special base aggregate and 28 inches of class 4 special topped with 4 inches of class 3 special, respectively. Again, two lifts were constructed. Definitions of base aggregate specifications are shown in Table 3.1.

During construction, the mat density was measured with a nuclear density gauge after every pass of the roller. The final rolling patterns established for the test pads are shown in Table 3.2. Bituminous material samples were also obtained during the test pad construction; the test results for these materials are shown in Table 3.3.

Table 3.1. Base Aggregate Specifications (7).

Property	Aggregate Classification			
	Class 3 Special (Cl3sp)	Class 4 Special (Cl4sp)	Class 5 Special (Cl5sp)	Class 6 Special (Cl6sp)
Sieve Analysis, Percent Passing:				
34.5 mm (1-1/2 in)	---	100	---	---
25 mm (1in)	---	95 - 100	100	100
19 mm (3/4 in)	---	90 - 100	90 - 100	85 - 100
12.5 mm (1/2 in)	100	---	---	---
9.5 mm (3/8 in)	95 -100	80 - 95	70 - 85	50 - 70
4.75 mm (No. 4)	85 - 100	70 - 85	55 - 70	30 - 50
2.0 mm (No. 10)	65 - 90	55 - 70	35 - 55	15 - 30
1.0 mm (No. 40)	30 - 50	15 - 30	15 - 30	5 - 15
0.075 mm (No. 200)	8 - 15	5 - 10	3 - 8	0 - 5
Plasticity:				
Liquid Limit	35 max.	35 max.	25 max.	25 max.
Plastic Limit	< 12	< 12	< 6	< 6
Percent crushed	not specified	not specified	-- min.	100% crushed

Table 3.2. Rolling Patterns Established from the Construction of Test Pads.

Roller Passes	Test Pad			
	1	2	3	4
70 to 76 mm (2.75 and 3 in) Base				
Breakdown Steel (Static)	4	4	4	4
Pneumatic	4	2	2	4
Finish Steel (Static)	4	2	4	4
38 mm (1.5 in) Base and Wear				
Breakdown Steel (Static)	4	4	4	4
Pneumatic	4	2	4	4
Finish Steel (Static)	2	3	2	4

Table 3.3. Bituminous Mixture Properties for Test Pads (8).

Test	Test Cells (Results Average of 4 Tests Per Lift Per Cell)					
	Pad 1 (Representative of 1)		Pad 2 (Representative of 2)		Pad 3 (Representative of 4)	
Course	Base	Base	Base	Base	Base	Base
Lift	1st	2nd	1st	2nd	1st	2nd
Lift Thickness, mm (in.)	70 (2.75)	38 (1.50)	70 (2.75)	38 (1.50)	76 (3.00)	70 (2.75)
Mn/DOT Specification	2331 75 blow	2331 75 blow	2331 35 blow	2331 35 blow	2331 Gyratory	2331 Gyratory
Bulk Specific Gravity	2.406	2.394	2.374	2.356	2.380	2.381
Maximum Specific Gravity	2.457	2.490	2.424	2.464	2.471	2.468
Air Voids, %	2.1	3.9	2.1	4.3	3.7	3.5
VMA, %	13.6	13.6	15.2	15.5	14.1	14.1
Stability, N (lbs.)	8376 (1883)	11898 (2675)	6187 (1391)	7361 (1655)	9083 (2042)	9612 (2161)
Flow, 0.25 mm	9.5	6.7	10.1	8.3	7.7	7.1
Extracted Asphalt Content, %	5.8	5.1	6.7	5.6	5.3	5.5
Sieve Analysis After Extraction:						
19 mm (3/4 in)	100	100	100	100	100	100
16 mm (5/8 in)	99	99	100	99	99	99
12.5 mm (1/2 in)	96	94	94	94	93	94
9.0 mm (3/8 in)	81	84	84	84	85	86
4.75 mm (No. 4)	63	65	65	66	68	69
2.0 mm (No. 10)	51	52	52	53	55	55
1.0 mm (No. 20)	39	39	40	40	42	42
0.45 mm (No. 40)	25	26	26	26	27	27
0.25 mm (No. 80)	---	---	---	---	---	---
0.075 mm (No. 200)	5.1	4.9	5.2	4.9	4.6	4.6

5-YEAR MAINLINE

The test cell layout was shown in Figure 1.3. The base materials for the 5-Year Mainline had been placed and compacted during the spring and summer of 1992; the subsurface instrumentation was also placed at this time. All lifts were placed starting with test cell 4 and ending with test cell 1.

The asphalt content for the binder and wear courses were selected for the 1 through 4 based on the 75 blow, 35 blow, 50 blow, and gyratory mix design, respectively. Test cell 4 was the only full depth pavement structure in the 5-Year Mainline; 8.75 inches of bituminous materials were placed over graded and compacted subgrade.

Originally, plans called for the use of a side-feed conveyor belt for loading the hot mix into the paver so that haul trucks would not be traveling over sensors placed on the top surface of the base. However, equipment difficulties led to the abandonment of this idea within the first three hours of construction. Equipment difficulties that led to this decision included frequent failure of the conveyor and the subsequent delay in construction. The construction process was changed to allow the truck to discharge directly to the paver, and the sensors were continuously monitored by research personnel. A reasonable construction pace was resumed with no damage to the sensors.

Once the construction problems had been corrected, the first lift of test cell 4 was placed on September 23, 1992. The first lift of the remaining three test cells and the second lift of test cell 4 were placed on September 24, 1992. The second and third lifts for 1 through 3, and the third and fourth lifts for 4 were placed on September 25, and September 28, 1992, respectively. Sensors within the asphalt concrete were installed in each test cell about one month after construction. Cores were removed to place these sensors. These cores were tested for this research program.

Construction Quality Control Testing

Field bituminous mixture testing and asphalt cement extractions were performed by Braun Intertec. Buffalo Bituminous, Inc., the paving contractor, was responsible for mixture sampling and measuring virgin aggregate gradations. The results of this testing are

summarized in Table 3.4.

The average air void contents for each of the lifts in all four test cells were relatively consistent at around 4 percent. Marshall stability followed the expected trends of increasing stability with increasing compactive effort. VMA were also as expected with the 35 blow mix design having the highest (around 16 percent) and the 75 blow and gyratory mix design showing the lowest (around 14.7 percent for either). The 50 blow mix design VMA was in between these values but close enough to the 75 and gyratory so that the difference may not be statistically significant.

The extracted asphalt contents show that test cell 2, the 35 blow mix design, was constructed with about 5.8 percent (average of all lifts); this was 0.6 percent lower than the design content of 6.4 percent. Test cell 3 (50 blow mix design) showed an asphalt content of 5.6 which was 0.5 percent lower than the mix design recommendation of 6.1 percent. Both test cells 1 and 4, the 75 blow and gyratory designs had binder contents of 5.3 percent which were 0.4 and 0.3 percent lower than the design contents, respectively. While the actual binder contents of the test cells 2, 3, and 1 (35, 50, and 75 blow, respectively) were substantially below the design content, the difference between each consecutive binder content is still 0.3 percent. This matches the intended differences between the design asphalt contents. However, there was no difference between the average 75 blow and the gyratory design asphalt content. The actual differences in the asphalt contents for each test cell will need to be considered in any comparison of mix design and construction material properties.

Table 3.4. Test Results During the Construction of the Mn/ROAD 5-Year Mainline Test Cells (9).

Test	Test Cells					
	1			2		
Asphalt Grade	120/150 pen			120/150 pen		
Course	Base	Base	Wear	Base	Base	Wear
Lift	1st	2nd	3rd	1st	2nd	3rd
Lift Thickness, in.	70 (2.75)	38 (1.50)	38 (1.50)	70 (2.75)	38 (1.50)	38 (1.50)
Mn/DOT Specification	2331 75 blow	2331 75 blow	2331 75 blow	2331 35 blow	2331 35 blow	2331 25 blow
Bulk Specific Gravity	2.361	2.366	2.381	2.346	2.339	2.343
Maximum Specific Gravity	2.473	2.461	2.472	2.453	2.440	2.446
Air Voids, %	4.5	3.9	3.8	4.4	4.2	4.2
VMA, %	14.8	14.9	14.3	15.9	16.4	16.2
Stability, N (lbs)	7553 (1698)	7606 (1710)	8456 (1901)	5658 (1272)	5093 (1145)	5480 (1313)
Flow, 0.25 mm	6.4	7.1	10.3	7.9	7.6	10.8
Extracted Asphalt Content, %	5.3	5.3	5.3	5.5	5.9	5.9
Sieve Analysis After Extraction:						
19 mm (3/4 in)	100	100	100	100	100	100
16 mm (5/8 in)	99	99	99	99	99	99
12.5 mm (1/2 in)	95	94	93	94	94	94
9.0 mm (3/8 in)	87	85	83	85	85	85
4.75 mm (No. 4)	70	68	64	68	69	68
2.0 mm (No. 10)	58	56	52	55	57	56
1.0 mm (No. 20)	43	43	39	42	44	42
0.45 mm (No. 40)	28	27	25	27	28	27
0.25 mm (No. 80)	0	---	---	---	---	---
0.075 mm (No. 200)	4.9	4.8	4.5	4.9	5.0	4.8

Table 3.4 (continued). Test Results During the Construction of the Mn/ROAD 5-Year Mainline Test Cells (9).

Test	Test Cells						
	3			4			
Asphalt Grade	120/150 pen			120/150 pen			
Course	Base	Base	Wear	Base	Base	Wear	Wear
Lift	1st	2nd	3rd	1st	2nd	3rd	3rd
Lift Thickness, in.	70 (2.75)	38 (1.50)	38 (1.50)	70 (2.75)	38 (1.50)	38 (1.50)	38 (1.50)
Mn/DOT Specification	2331 50 blow	2331 50 blow	2331 50 blow	2331 gyratory	2331 gyratory	2331 gyratory	2331 gyratory
Bulk Specific Gravity	2.361	2.359	2.362	2.354	2.364	2.386	2.363
Maximum Specific Gravity	2.467	2.464	2.464	2.479	2.481	2.472	2.469
Air Voids, %	4.3	4.3	4.1	5.1	4.7	3.5	4.3
VMA, %	15.1	15.3	15.3	15.1	14.7	14.1	14.9
Stability, N (lbs)	7036 (1582)	6351 (1428)	7317 (1645)	7797 (1753)	7810 (1756)	8220 (1848)	7957 (1789)
Flow, 0.25 mm	6.0	6.0	10.6	7.0	6.9	6.3	10.6
Extracted Asphalt Content, %	5.5	5.7	5.6	5.3	5.1	5.3	5.4
Sieve Analysis After Extraction:							
19 mm (3/4 in)	100	100	100	100	100	100	100
16 mm (5/8 in)	99	99	100	99	99	99	100
12.5 mm (1/2 in)	94	93	95	93	93	92	95
9.0 mm (3/8 in)	85	84	85	85	84	83	87
4.75 mm (No. 4)	68	68	68	70	68	66	67
2.0 mm (No. 10)	56	55	55	28	56	54	56
1.0 mm (No. 20)	42	42	42	44	42	41	43
0.45 mm (No. 40)	27	27	27	27	28	26	27
0.25 mm (No. 80)	---	---	---	---	---	---	---
0.075 mm (No. 200)	5.0	4.4	4.7	4.4	4.9	4.9	4.7

10-YEAR MAINLINE

Nine of the 10 test cells (14 through 22) were constructed in July, 1993 as the 10-year design life portion of the Mn/ROAD facility. The last test cell, 23, was constructed at the end of September, 1993. Variables for the test cells included asphalt grade and content, layer thicknesses, and base materials (Figure 1.2). Construction control testing included two tests for each lane for aggregate gradation, extracted asphalt content and aggregate gradation, and air void content (rotating base Marshall hammer). These results are shown in Table 3.5.

Additional testing was conducted to determine the moisture content of the individual aggregate stockpiles as each lane of each test cell was constructed. Plant changes to account for the aggregate stockpile moisture content were not made for either the first or second lifts in cells 16 through 22 and the first through third lifts for cells 14 and 15. Computer control inputs were changed every 30 to 45 minutes for the next lift of all cells to account fro moisture content changes. A moving average of three moisture content measurements was used to make plant control adjustments for the last lift and the computerized plant records were obtained for comparisons.

Influence of Aggregate Stockpile Moisture on Mixture Air Voids

The first lifts for test cells 14 and 15 were placed on the first day of paving and this portion of the construction was not included in the analysis. The second and third lifts for cells 14 and 15 and the first and second lifts of the remaining cells were placed on the second and third days of construction. All lifts were placed starting from outside lane in cell 22 and ending with cell 14. Each afternoon, the passing lane was placed, again starting with cell 22 and ending with cell 14. The aggregate stockpile moisture was measured at the beginning of each day, but no changes were made in the mixture proportions. The decision to make no changes was based on both the contractor's and testing laboratory personnel's opinion that since the weather had been consistently clear, there would be major changes in stockpile moisture.

Table 3.5. Test Results During the Construction of the Mn/ROAD 10-Year Mainline Test Cells (9).

Test	Test Cells									
	14					15				
Asphalt Grade	120/150 pen					AC20				
Course	Base	Base	Base	Base	Wear	Base	Base	Base	Base	Wear
Lift	1st	2nd	3rd	4th	5th	1st	2nd	3rd	4th	5th
Lift Thickness, mm (in.)	76 (3.00)	70 (2.75)	50 (2.00)	38 (1.50)	38 (1.50)	76 (3.00)	76 (2.75)	50 (2.00)	38 (1.50)	50 (1.50)
Mn/DOT Specification	2331 75 blow	2331 75 blow	2331 75 blow	2331 75 blow	2331 75 blow	2331 75 blow	2331 75 blow	2331 75 blow	2331 75 blow	2331 75 blow
Bulk Specific Gravity	2.367	2.354	2.366	2.364	2.367	2.351	2.349	2.360	2.365	2.365
Maximum Specific Gravity	2.450	2.453	2.457	2.458	2.460	2.448	2.448	2.454	2.456	2.457
Air Voids, %	3.4	4.0	3.7	3.8	3.8	4.0	4.0	3.8	3.7	3.7
VMA, %	14.8	15.2	14.8	14.8	14.7	15.4	15.4	15.0	14.7	14.7
Stability, N (lbs)	7521 (1691)	7472 (1680)	8193 (1842)	7543 (1696)	7468 (1679)	8691 (1954)	9202 (2069)	9781 (2199)	9074 (2040)	9038 (2032)
Flow, 0.25 mm	9.8	9.5	10.0	10.0	10.2	10.9	10.0	10.2	9.8	10.8
Extracted Asphalt Content, %	5.7	5.5	5.3	5.0	5.2	5.6	5.4	5.5	5.4	5.3
Sieve Analysis After Extraction:										
19 mm (3/4 in)	100	100	100	100	100	100	100	100	100	100
16 mm (5/8 in)	99	99	99	99	98	99	98	99	400	99
12.5 mm (1/2 in)	94	9	95	93	93	94	92	95	94	93
9.0 mm (3/8 in)	86	87	85	84	85	86	85	87	85	85
4.75 mm (No. 4)	70	71	68	70	67	70	70	71	69	68
2.0 mm (No. 10)	58	59	55	58	55	59	57	58	57	56
1.0 mm (No. 20)	45	45	43	44	42	45	44	45	44	43
0.45 mm (No. 40)	26	27	25	27	25	27	26	27	26	25
0.25 mm (No. 80)	8	9	9	10	9	9	8	9	9	9
0.075 mm (No. 200)	3.8	3.9	4.6	4.9	4.2	3.8	3.7	5.0	5.1	4.4

Table 3.5 (continued). Test Results During the Construction of the Mn/ROAD 10-Year Mainline Test Cells (9).

Test	Test Cells							
	16				17			
Asphalt Grade	AC20				AC20			
Course	Base	Base	Base	Wear	Base	Base	Base	Wear
Lift	1st	2nd	3rd	4th	1st	2nd	3rd	4th
Lift Thickness, mm (in)	70 (2.75)	50 (2.00)	38 (1.50)	38 (1.50)	70 (2.75)	50 (2.00)	38 (1.50)	38 (1.50)
Mn/DOT Specification	2331 Gyrator y	2331 Gyratory	2331 Gyratory	2331 Gyratory	2331 75 blow	2331 75 blow	2331 75 blow	2331 75 blow
Bulk Specific Gravity	2.354	2.361	2.351	2.365	2.357	2.365	2.361	2.373
Maximum Specific Gravity	2.461	2.468	2.467	2.4655	2.454	2.453	2.457	2.459
Air Voids, %	4.4	4.3	4.7	4.1	3.9	3.6	3.9	3.5
VMA, %	15.0	14.7	15.0	14.5	15.1	14.8	14.8	14.4
Stability, N (lbs)	9447 (2124)	9896 (2225)	9474 (2130)	8713 (1959)	9398 (2113)	9981 (2244)	9599 (2158)	8780 (1974)
Flow, 0.25 mm	10.2	9.9	9.6	10.2	9.8	10.3	10.5	10.2
Extracted Asphalt Content, %	5.4	5.1	4.8	5.0	9.8	10.3	10.5	10.2
Sieve Analysis After Extraction:								
19 mm (3/4 in)	100	100	100	100	100	100	100	100
16 mm (5/8 in)	99	99	98	99	99	99	100	99
12.5 mm (1/2 in)	94	93	93	93	93	94	94	92
9.0 mm (3/8 in)	86	84	85	83	86	86	87	81
4.75 mm (No. 4)	69	68	69	67	70	70	71	64
2.0 mm (No. 10)	57	56	56	54	57	57	58	53
1.0 mm (No. 20)	43	43	43	42	44	44	45	40
0.45 mm (No. 40)	26	25	26	25	26	26	27	24
0.25 mm (No. 80)	9	8	9	8	8	9	10	8
0.075 mm (No. 200)	4.9	4.4	4.6	4.3	4.1	3.9	4.7	4.2

Table 3.5 (continued). Test Results During the Construction of the Mn/ROAD 10-Year Mainline Test Cells (9).

Test	Test Cells							
	18				19			
Asphalt Grade	AC20				AC20			
Course	Base	Base	Base	Wear	Base	Base	Base	Wear
Lift	1st	2nd	3rd	4th	1st	2nd	3rd	4th
Lift Thickness, mm (in)	70 (2.75)	50 (2.00)	38 (1.50)	38 (1.50)	70 (2.75)	50 (2.00)	38 (1.50)	38 (1.50)
Mn/DOT Specification	2331 50 blow	2331 50 blow	2331 50 blow	2331 50 blow	2331 35 blow	2331 35 blow	2331 35 blow	2331 35 blow
Bulk Specific Gravity	2.346	2.361	2.353	2.360	2.331	2.338	2.341	2.354
Maximum Specific Gravity	2.437	2.442	2.442	2.439	2.421	2.424	2.429	2.432
Air Voids, %	3.8	3.3	3.7	3.2	3.7	3.5	3.6	3.3
VMA, %	15.9	15.4	15.6	15.3	16.8	16.5	16.3	15.8
Stability, N (lbs)	7553 (1698)	7481 (1683)	7686 (1728)	7370 (1657)	6352 (1428)	6281 (1412)	6231 (1401)	6138 (1380)
Flow, 0.25 mm	10.4	10.7	10.3	10.6	9.9	11.1	10.3	10.3
Extracted Asphalt Content, %	6.1	5.8	5.6	5.8	6.2	6.3	5.9	6.0
Sieve Analysis After Extraction:								
19 mm (3/4 in)	100	100	99.7	100	100	100	100	100
16 mm (5/8 in)	98	98	99	99	100	99	99	99
12.5 mm (1/2 in)	93	92	93	93	95	94	94	94
9.0 mm (3/8 in)	86	83	85	84	87	86	85	84
4.75 mm (No. 4)	70	68	70	67	71	70	70	68
2.0 mm (No. 10)	57	55	57	55	59	58	57	56
1.0 mm (No. 20)	44	43	44	43	45	45	44	42
0.45 mm (No. 40)	26	25	27	25	27	27	26	26
0.25 mm (No. 80)	8	8	9	9	9	9	9	9
0.075 mm (No. 200)	4.2	4.3	4.6	4.6	5.2	5.3	4.6	4.7

Table 3.5 (continued). Test Results During the Construction of the Mn/ROAD 10-Year Mainline Test Cells (9).

Test	Test Cells							
	20				21			
Asphalt Grade	120/150 pen				120/150 pen			
Course	Base	Base	Base	Wear	Base	Base	Base	Wear
Lift	1st	2nd	3rd	4th	1st	2nd	3rd	4th
Lift Thickness, mm (in)	70 (2.75)	50 (2.00)	38 (1.50)	38 (1.50)	70 (2.75)	50 (2.00)	38 (1.50)	38 (1.50)
Mn/DOT Specification	2331 35 blow	2331 35 blow	2331 35 blow	2331 35 blow	2331 50 blow	2331 50 blow	2331 50 blow	2331 50 blow
Bulk Specific Gravity	2.338	2.351	2.348	2.351	2.344	2.354	2.351	2.356
Maximum Specific Gravity	2.426	2.433	2.432	2.429	2.442	2.439	2.437	2.439
Air Voids, %	3.7	3.4	3.5	3.2	4.0	3.5	3.5	3.4
VMA, %	16.5	16.0	16.0	15.9	16.0	15.6	15.7	15.5
Stability, N (lb)	5484 (1233)	5747 (1292)	5462 (1228)	4795 (1078)	6405 (1440)	5907 (1328)	6382 (1435)	6454 (1451)
Flow, 0.25 mm	10.3	10.5	10.0	10.7	9.9	10.8	10.0	10.4
Extracted Asphalt Content, %	6.3	6.0	6.1	5.8	5.9	6.0	5.6	5.9
Sieve Analysis After Extraction:								
19 mm (3/4 in)	100	100	100	100	100	100	100	99.7
16 mm (5/8 in)	99	99	99	100	99	99	99	99
12.5 mm (1/2 in)	95	93	93	94	94	95	94	94
9.0 mm (3/8 in)	87	84	85	84	86	86	85	85
4.75 mm (No. 4)	71	68	70	68	70	73	70	69
2.0 mm (No. 10)	58	56	58	56	57	60	58	57
1.0 mm (No. 20)	45	43	44	43	44	45	45	43
0.45 mm (No. 40)	26	25	27	25	26	27	27	26
0.25 mm (No. 80)	9	9	9	9	9	9	9	9
0.075 mm (No. 200)	5.1	4.8	4.8	4.6	4.8	4.6	4.9	4.7

Table 3.5 (continued). Test Results During the Construction of the Mn/ROAD 10-Year Mainline Test Cells (9).

Test	Test Cells								
	22				23				
Asphalt Grade	120/150 pen				120/150 pen				
Course	Base	Base	Base	Wear	Base	Base	Base	Base	Wear
Lift	1st	2nd	3rd	4th	1st	2nd	3rd		4th
Lift Thickness, mm (in)	70 (2.75)	50 (2.00)	38 (1.50)	38 (1.50)	50 (2.00)	38 (1.75)	50 (2.00)	38 (1.50)	38 (1.50)
Mn/DOT Specification	2331 75 blow	2331 75 blow	2331 75 blow	2331 75 blow	2331 50 blow	2331 50 blow	2331 50 blow	2331 50 blow	2331 50 blow
Bulk Specific Gravity	2.359	2.370	2.363	2.367	2.370	2.364	2.353	2.352	2.340
Maximum Specific Gravity	2.451	2.462	2.462	2.459	2.439	2.440	2.444	2.448	2.445
Air Voids, %	3.8	3.8	4.0	3.8	2.9	3.1	3.7	3.9	4.3
VMA, %	15.0	14.6	14.8	14.7	15.0	15.2	15.6	15.5	16.0
Stability, N (lbs)	8162 (1835)	7659 (1722)	7989 (1796)	7437 (1672)	6236 (1402)	6934 (1559)	5551 (1248)	4701 (1057)	5431 (1221)
Flow, 0.25 mm	9.6	10.3	10.2	10.6	11.5	10.1	9.9	10.4	10.3
Extracted Asphalt Content, %	5.8	5.3	5.1	5.2	5.5	5.7	5.6	5.5	5.7
Sieve Analysis After Extraction:									
19 mm (3/4 in)	100	100	100	100	100	100	100	100	100
16 mm (5/8 in)	98	98	99	99	99	98	99	98	100
12.5 mm (1/2 in)	94	95	94	93	92	93	93	93	94
9.0 mm (3/8 in)	8	84	85	84	82	84	85	83	87
4.75 mm (No. 4)	72	69	69	68	64	67	68	67	71
2.0 mm (No. 10)	59	58	57	55	53	55	56	55	59
1.0 mm (No. 20)	45	42	44	42	41	43	43	43	46
0.45 mm (No. 40)	27	25	26	25	25	25	26	26	27
0.25 mm (No. 80)	9	9	9	9	8	8	9	9	10
0.075 mm (No. 200)	4.5	3.9	4.2	4.5	4.1	3.9	4.3	4.9	5.1

Table 3.6 shows that air void contents for a given lane in a test cell varied substantially (e.g. cells 16 and 22, Day 2) for these two days of paving. Minor changes were made to the asphalt contents during the second and third days of paving but the variability in the air voids remained. There was a reluctance to make more than minor changes because of the limited differences in asphalt content between the various test cells. Efforts were made to keep the relative asphalt content differences the same between test cells when changes were made.

Table 3.6. Quality Control Results.

Test Cell	Outside Lane				Passing Lane			
	2nd Day	3rd Day	4th Day	5th Day	2nd Day	3rd Day	4th Day	5th Day
	Air Voids, %							
14	3.6, 4.1	4.3, 3.6	4.4, 3.7	4.0, 4.2	4.0, 4.4	3.4, 3.6	3.7, 3.4	3.5, 3.4
15	3.3, 3.8	4.0, 4.0	3.5, 3.5	4.2, 3.1	4.7, 4.3	3.7, 3.6	4.0, 3.8	3.7, 3.8
16	3.8, 5.1	4.6, 4.1	5.0, 4.6	4.0, 4.2	4.6, 3.9	4.2, 4.1	5.0, 4.3	4.5, 3.5
17	4.3, 4.6	3.5, 3.5	4.0, 3.9	3.3, 3.0	3.7, 3.1	3.7, 3.6	3.7, 4.0	3.6, 4.2
18	3.5, 3.5	3.4, 2.9	3.9, 3.2	3.0, 3.1	3.6, 4.5	3.4, 3.5	4.1, 3.4	3.6, 3.2
19	4.0, 3.6	3.6, 3.7	4.2, 3.7	3.3, 3.0	3.8, 3.5	3.6, 3.2	3.2, 3.4	3.4, 3.3
20	3.9, 3.5	3.7, 2.7	3.9, 3.0	3.0, 3.3	3.0, 4.2	3.6, 3.5	3.5, 3.4	3.3, 3.2
21	4.3, 3.8	3.0, 3.1	3.2, 4.2	3.6, 3.3	4.0, 3.9	3.8, 4.0	3.1, 3.6	3.4, 3.3
22	3.4, 5.0	3.2, 3.8	5.0, 4.0	3.9, 3.6	3.9, 2.7	3.5, 4.5	3.7, 3.4	3.7, 3.9

Other considerations such as stockpile segregation and sampling errors were eliminated as probable sources of variability. Several of the 2 mm (No. 10) gradation results were outside of the target band, but this was not considered enough of a problem to cause the continued erratic air void results. Variability in the stockpile moisture was considered to be the next most likely source of variability.

The next lift was placed on the fourth day of paving, but each aggregate stockpile

moisture content was measured at least one time for every test cell. Plant controls were changed as soon as results were obtained for all three of the stockpiles (Table 3.7, Figure 3.1). This meant that changes were being made at the plant every 30 to 45 minutes but these changes lagged behind the actual stockpile sampling by about a half hour. No significant change in the air void variability was seen. However, this was thought to be because changes were made too often. In other words, frequent changes in the plant controls had the same effect as no change.

Table 3.7. Comparison of Air Voids, Asphalt Cement Content, and the Corresponding Stockpile Moisture Contents.

Time, Hr.	Test Cell	Crow River Fines		Crow River Coarse	CA 50	Air Voids, %
		Moist., %	Grouping & Std. Dev.	Moist., %	Moist., %	
July 28, 1993 (4th Day of Paving)						
9:15	22	6.38	Group A	3.09	0.93	5.0, 4.0
9:55	21	6.22	0.11	3.16	1.58	3.2, 4.2
10:45	19	5.80	Group B	2.97	1.56	4.2, 3.7
11:10	18	6.04	0.15	3.09	1.60	3.9, 3.1
11:15	17	6.07		3.07	1.60	4.0, 3.9
12:25	16	5.93		3.11	1.89	5.0, 4.6
12:40	15	6.18		2.80	1.42	3.8, 4.0
13:35	14	5.66	Group C	2.84	1.19	4.4, 3.7
13:45	22	5.71	0.13	2.84	1.24	3.7, 3.4
15:40	20	5.55		2.90	0.97	3.5, 3.4
16:00	19	5.42		2.44	1.01	3.2, 3.4
16:10	18	6.32	Group D	2.59	0.72	4.1, 3.4
17:30	17	6.06	0.23	2.52	1.03	3.7, 4.0
17:40	16	5.93	Group E	2.54	0.95	5.0, 4.3
18:15	15	5.91	0.02	2.46	0.91	4.0, 3.8
18:45	14	5.95		2.54	0.95	3.7, 3.4

In order to test this hypothesis, the air void and stockpile moisture contents were examined (Table 3.6). Engineering judgement was used to group generally similar moisture contents for the Crow River fine aggregate stockpile (the majority of the aggregate gradation) and average air void values. The standard deviation of moisture content within each group was calculated (Table 3.7); the results indicate an average standard deviation of Crow River fines stockpile moisture content of about 0.1 percent. This information was used to formulate a plan for changing stockpile moisture content inputs for the last day of paving.

A moving average of three values was selected as a reasonable number of data points that would identify significant changes in moisture content while not generating overly frequent adjustments. It was decided to use the one standard deviation value of 0.1 percent moisture as the criterion for when to change the computer inputs. For example, when the moving average of three results differed by more than 0.1 percent moisture from the preceding moving average, the new value was used to adjust the computer input. Also, to prevent continual but gradual incremental changes of less than 0.1 percent, a maximum difference between the current plant settings and the most recent moving average value of 0.2 percent (i.e., two standard deviations) was set.

As a test for the suggested plan, these criteria were applied to that day's results to determine how many changes would have been made if this plan had been used. Using the data shown in Table 3.7, six instead of 16 changes would have been made for the Crow River fines stockpile and only 2 and 6 for the Crow River coarse and CA 50 stockpiles, respectively. All changes would have been made based on the running average of three results exceeding a 0.1 percent change in moisture. No changes would have been made based on a difference of 0.2 percent between the current input values and the latest test results.

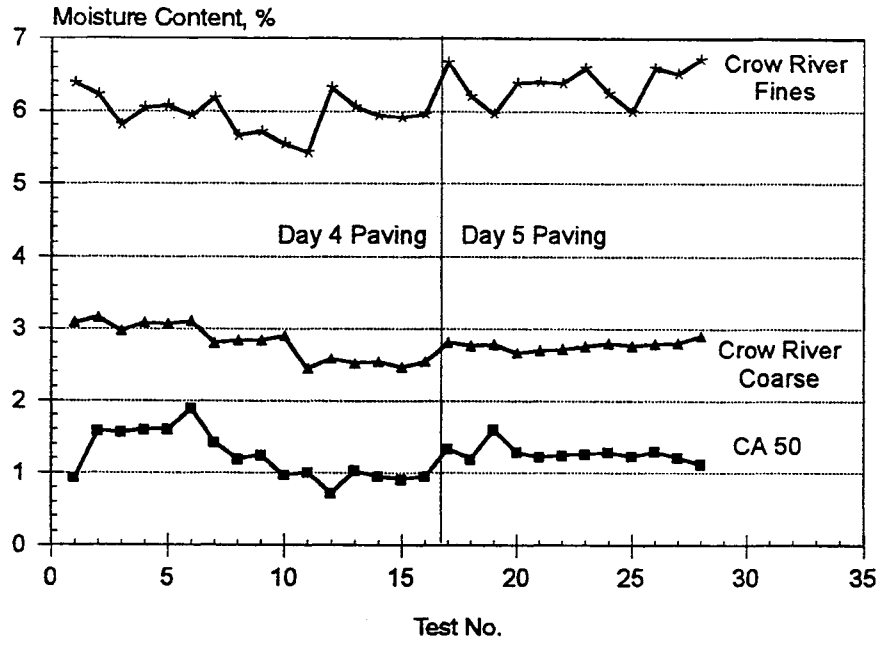

Figure 3.1. Moisture Contents for Each Stockpile.

On the last (fifth) day of paving, the approach outlined above was used to adjust aggregate quantities. The individual stockpile moisture contents and the moving averages are shown in Table 3.7. Test results that triggered a change in the plant control inputs are marked in this table. The plant records indicated that these changes were made about 30 to 45 minutes after the aggregates were sampled (i.e., after the times shown in Table 3.8). Starting values for the day were based on the last three values obtained from previous day. The Crow River fines continued to have a moisture content that varied throughout the day by almost 0.8 percent. Both the Crow River coarse and CA 50 were relatively constant the last day; this consistency was reflected in needing only one change to the plant controls early in the day (Table 3.8).

Table 3.8. Plant Control Changes Based on Running Average of Three Moisture Tests (July 29, 1993, 5th Day of Paving).

Time	Test Cell	Crow River Fines		Crow River Coarse		CA 50	
		Moist., %	Running Average	Moist., %	Running Average	Moist., %	Running Average
Starting Values[1]	NA	NA	5.93	NA	2.51	NA	0.94
7:00	22	6.68	6.18 change	2.81	2.60	1.33	1.06 change
7:10	21	6.20	6.28	2.77	2.71 change	1.19	1.16
7:35	19	5.96	6.28	2.78	2.82	1.26	1.26 change
9:40	17	6.38	6.18	2.67	2.74	1.28	1.24
10:00	16	6.40	6.24	2.70	2.72	1.22	1.25
11:05	14	6.38	6.39	2.72	2.70	1.24	1.25
11:25	22	6.60	6.46 change	2.76	2.73	1.26	1.24
12:35	20	6.25	6.41	2.80	2.76	1.28	1.26
13:05	19	6.00	6.28 change	2.77	2.78	1.23	1.26
13:40	18	6.60	6.28	2.79	2.79	1.29	1.27
14:45	16	6.52	6.37	2.84	2.80	1.21	1.24
15:30	14	6.72	6.61 change	2.90	2.84	1.12	1.21

1: Last values from previous day

Figure 3.2 compares the individual air void results for days 2 through 5. On the second day of paving two test results exceeded the upper limit (5 percent voids) and one results exceeded the lower limit (3 percent voids). Similar problems were seen for both the third (no moisture correction) and fourth (corrections every 30 to 45 min.) days of paving. However, the moving average of three moisture contents used to adjust the plant controls resulted in narrowing the range of air voids on the last day from between 3 and 5 to between 3 and 4.5 percent.

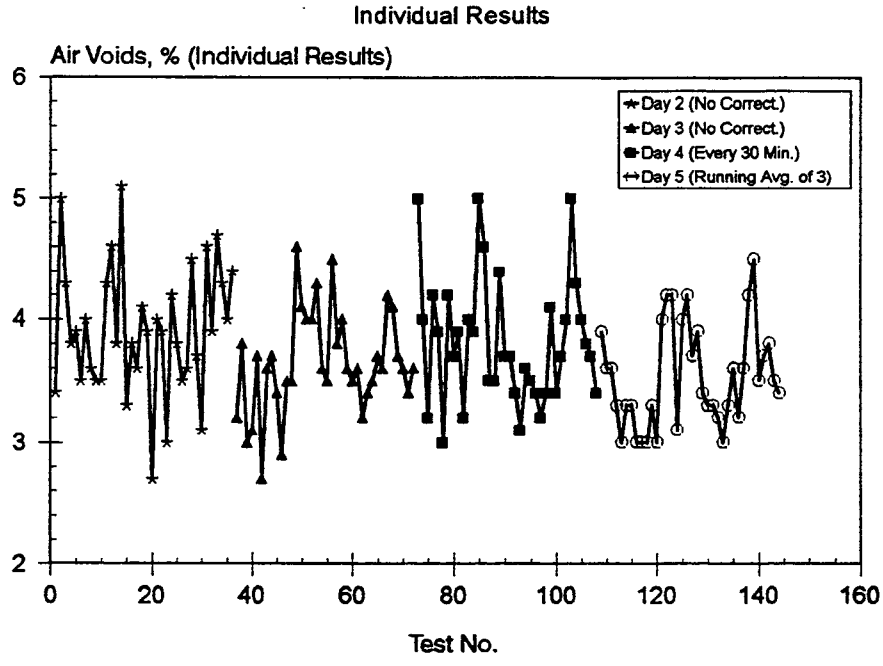

Figure 3.2 . Variability in Individual Air Void Results.

Figure 3.3 presents the air void data shown in the previous figure as a moving average of four test results. Results for both the second and third days were erratic however a distinct oscillating pattern began to emerge for the fourth day's results. This pattern became a relatively smooth sinusoidal-like pattern for the last day of paving. A repeating pattern in a process control is usually an indication of a systematic change in the process rather than random testing variability. A close examination of the data showed that the results for test numbers 110 through 128 closely matched those for test numbers 129 through 147. The first set of tests represent the testing for paving the outside lane and the second set of data for paving the passing lane. This indicated that the pattern was due to the differences in the mixtures between the test cells.

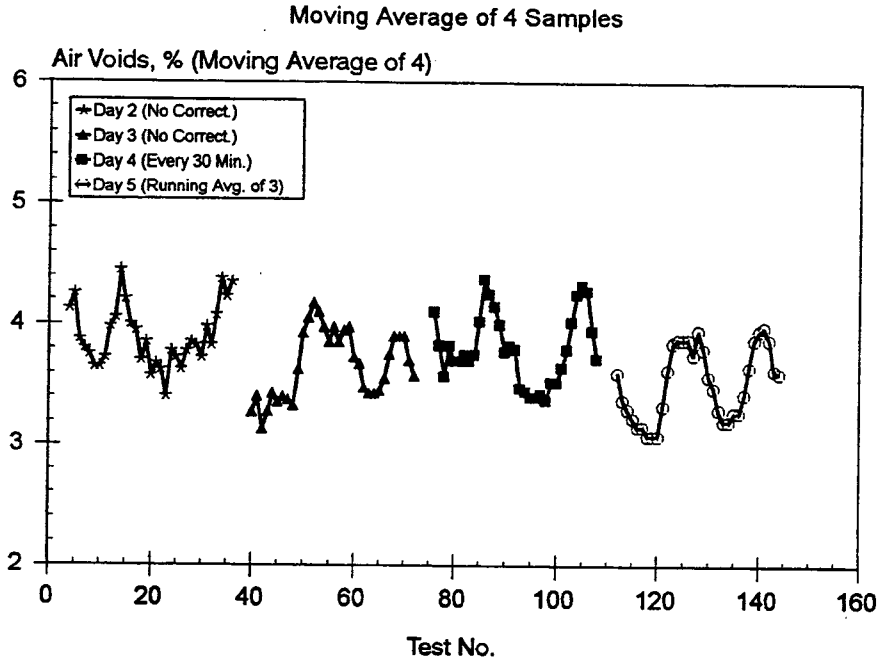

Figure 3.3. Variability in the Moving Average of Four Air Void Results.

When the data are sorted by test cell, Figure 3.4 shows that the air voids within a given cell were very uniform. While there was no relationship between the asphalt grade used in each test cell and the air void pattern, the asphalt content for each of the cells followed the same sinusoidal-like pattern as the moving average of the air voids. As the asphalt content increased, the voids decreased. This dependency on the binder content was unexpected as the content was selected based on a particular mix design method and that method of compaction was used to prepare the quality control samples. For example, 75 blows were used for the 5.9 percent and 35 blows for the 6.3 percent binder contents since these were the mix designs used to select the binder content. Since the binder contents were selected based on 4 percent voids, it was assumed that the mixtures would not have been sensitive to changes in this parameter.

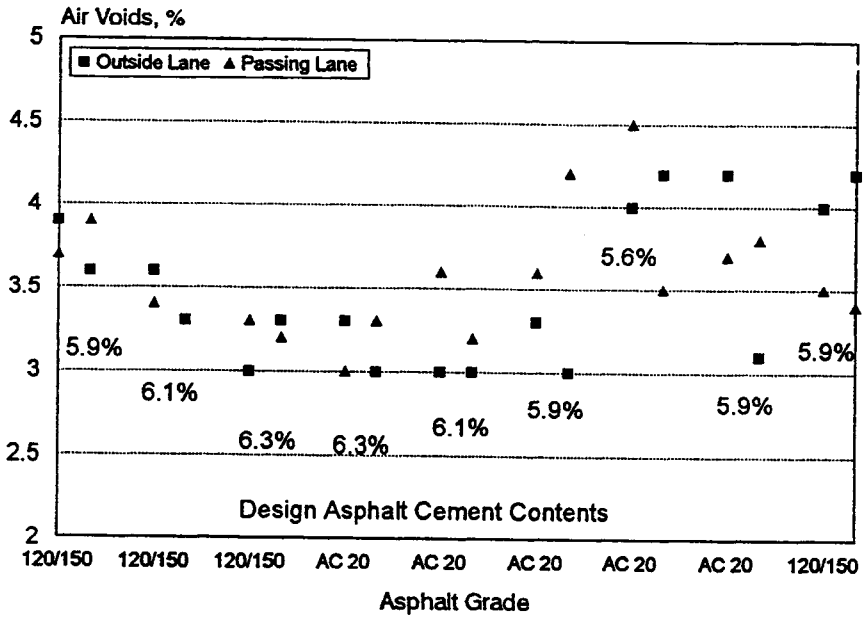

Figure 3.4. Influence of Test Cell Variables on Air Voids.

Typically, a maximum range for the moving average of 4 air void results is 3 to 5 percent. Although the average air voids for the last day of paving was about 0.5 percent below the target of 4 percent, none of the results in Figure 5 had a range of more than 1 percent voids. This suggests that changes in binder content were not sufficient to cause the air voids to exceed this criterion for a uniform mixture. Therefore the assumption of uniform voids for the different mixtures was valid. However, once the cold feed was well controlled, even minor changes in the binder content could be identified. In other words, the sensitivity of the process control data was increased.

Influence of Stockpile Moisture on Aggregate Gradation

The improved consistency in the aggregate proportions can be seen in a comparison of the sieve analysis results. For the 4.75 mm (No. 4) sieve, days 2 through 4 had several values that exceeded the upper and lower ranges of 70 and 64 percent, respectively (Figure 3.5). Only one value exceeded the lower limit when a moving average of 3 moisture test results was used to adjust the plant controls. The mean value also decreased into the middle of the range. Figure 3.6 shows the mean for the 2 mm (No. 10) sieve also moved downward for the last day of paving, but the overall result was that several of the values now exceeded the lower limit of 54 percent.

Results for the 0.45 mm (No. 40) sieve became more uniform with a smaller maximum and minimum range when the aggregate stockpile moisture content was adjusted with a moving average (Figure 3.7). An even greater improvement in the consistency of the 0.075 mm (No. 200) sieve was seen (Figure 3.8). While the results from days 2 through 4 had several results that exceeded the upper limit of 5 percent, the results for the last day of paving were very consistent with none of the values exceeding the limits.

None of the aggregate gradation results showed a pattern in the moving averages. This would substantiate the previous conclusion that the pattern in the air voids was primarily a function of the changes in the binder content and not due to systematic changes in the aggregate gradation.

In general, using a running average of 3 results to adjust the plant controls produced more a uniform gradation with fewer individual tests falling outside of the working range limits. That is, while the moisture content of the stockpile varied throughout the day, the gradation results were more uniform. This indicates that stockpile moisture can be one of the possible causes for non-uniform aggregate gradations. For this particular project, adjustments for stockpile moisture content had the most effect on the finer aggregate gradations.

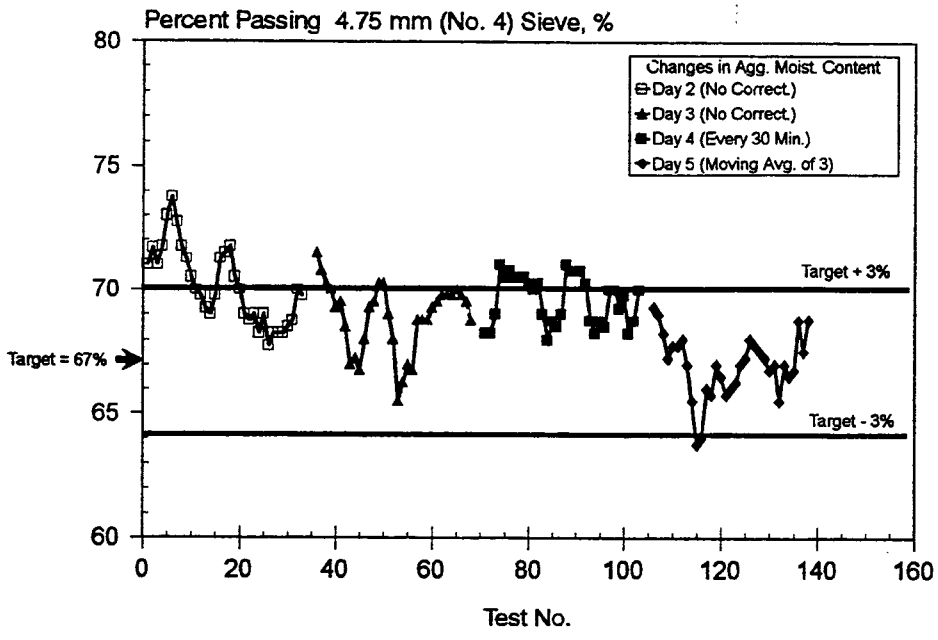

Figure 3.5. Gradation Results for the Percent Passing the 4.75 mm (No. 4) Sieve (Moving Average of Four).

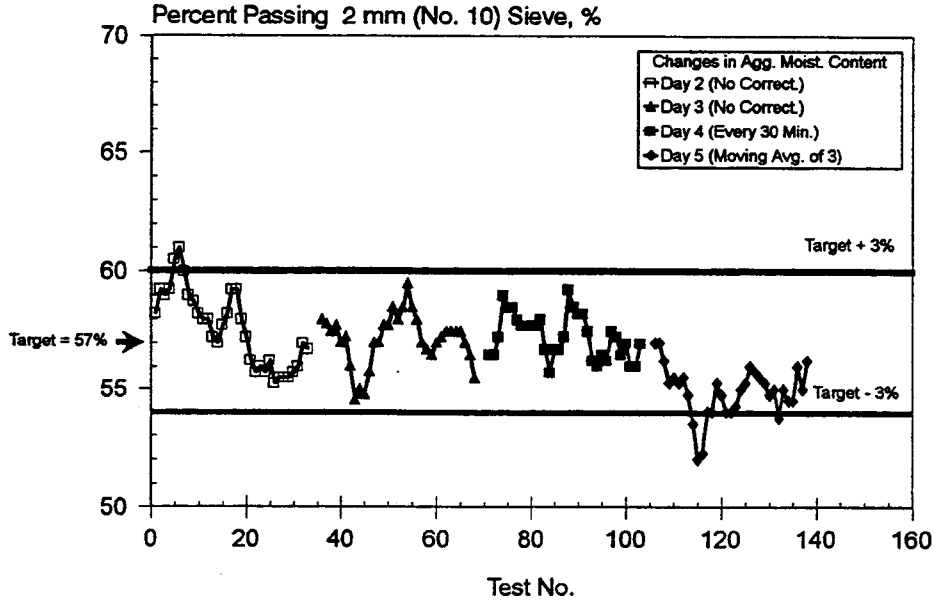

Figure 3.6. Gradation Results for the Percent Passing the 2 mm (No. 10) Sieve (Moving Average of Four).

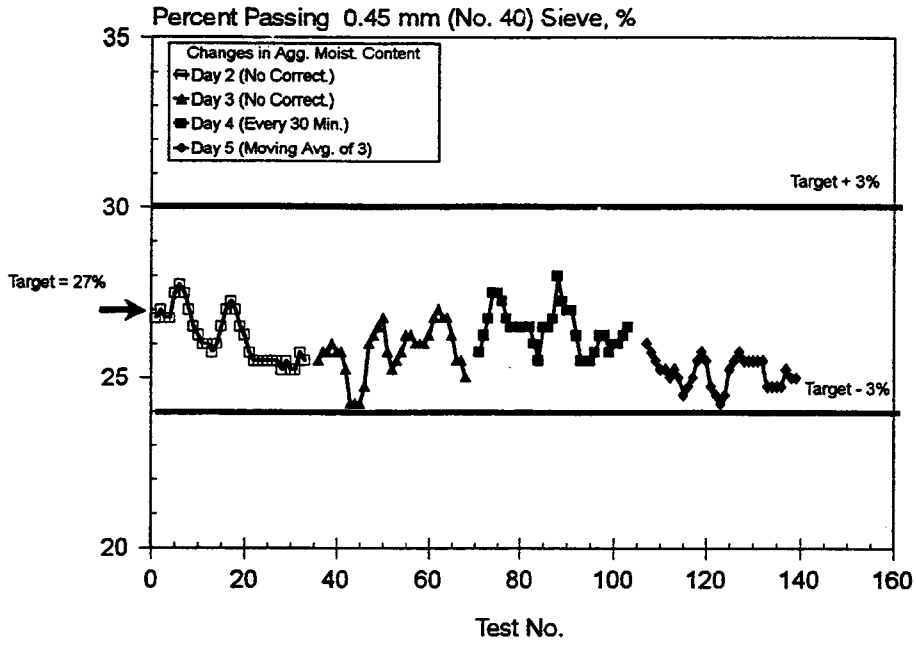

Figure 3.7. Gradation Results for the Percent Passing the 0.45 mm (No. 40) Sieve (Moving Average of Four).

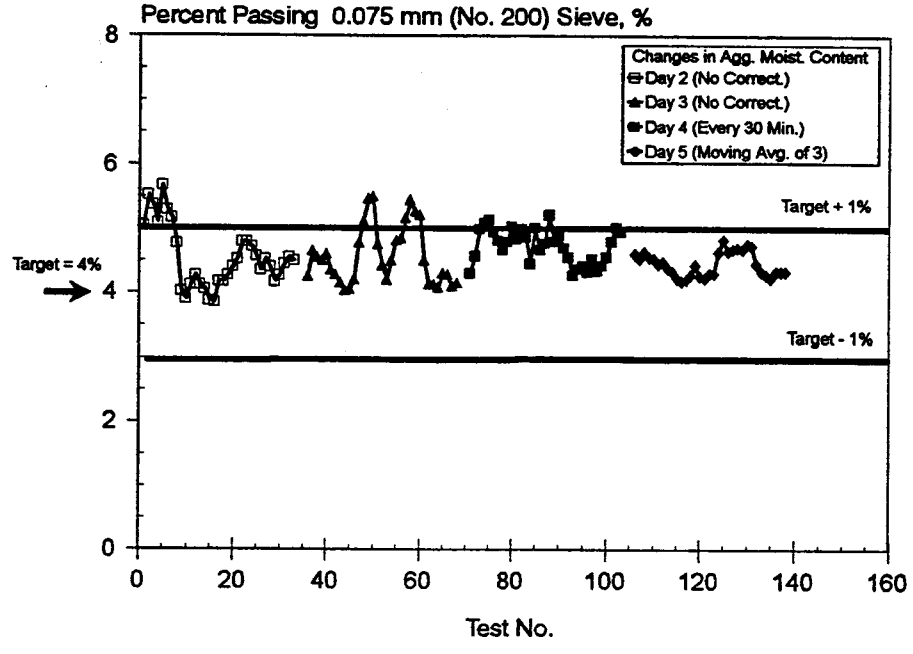

Figure 3.8. Gradation Results for the Percent Passing the 0.075 mm (No. 200) Sieve (Moving Average of Four).

Influence of Stockpile Moisture on Binder Content

Behind-the-paver samples used for determining the extracted asphalt cement content and compacted density were correlated as closely as possible to the point in the construction process where the aggregate was sampled for stockpile moisture content. This was done as follows. The stockpile moisture content samples were taken from the cold-feed belt. Plant records were obtained and the general location of the aggregate within the test cell mix production was established. That is, it was determined whether the mix was being produced at the beginning of the test cell, middle, or end; each test cell being approximately 168 m (550 ft.) long. For comparison purposes, the average binder content on the plant records was used as the target asphalt content because of the minor changes made to the design asphalt contents during construction (Table 3.9).

Figure 3.9 shows that the asphalt content varied substantially for the fourth day of paving (moisture adjusted every 30 to 45 minutes). Extraction results indicated binder contents both above and below those recorded by the plant control by as much as 0.2 and 1.5 percent, respectively. When the cold feed was adjusted based on the moving average of three aggregate stockpile moisture contents, all extracted binder contents were below those indicated by the plant recorder. This is closer to what was expected: the extracted asphalt content should show less asphalt than the plant records due to the retention of some of the binder by the aggregate.

The range of extracted binder contents was also reduced from about 1.7 percent to 0.7 percent. This indicates that there was more consistency in the binder content between design and actual when the aggregate cold feed was well controlled. Again, there was no apparent pattern to these results, indicating that the difference between the two values was not dependent upon the variables between the test cells.

Table 3.9. Extracted and Plant Recorded Binder Contents.

Test Cell	Fourth Day of Paving (July 28, 1993)				Fifth Day of Paving (July 29, 1993)			
	Extracted		Avg. Plant Records		Extracted		Avg. Plant Records	
	Outside Lane	Passing Lane	Outside Lane	Passing Lane	Outside Lane	Passing Lane	Outside Lane	Passing Lane
14	4.6, 5.9	4.2, 5.2	5.6	5.6	5.2, 4.8	5.3, 5.8	5.6	5.6
15	5.4, 5.1	5.4, 5.5	5.6	5.5	5.3, 4.9	5.5, 5.4	5.6	5.6
16	4.8, 4.7	4.8, 4.8	5.2	5.3	4.6, 5.2	5.3, 5.0	5.3	5.3
17	5.4, 5.8	5.2, 5.2	5.6	5.6	5.4, 5.2	5.5, 4.7	5.6	5.6
18	5.6, 5.5	5.9, 5.4	6.0	6.0	5.7, 5.6	5.9, 5.9	6.0	6.0
19	6.0, 5.8	5.8, 6.2	6.4	6.3	6.1, 5.8	5.9, 5.9	6.3	6.4
20	6.0, 6.6	5.9, 5.6	6.4	6.4	6.0, 5.6	6.2, 5.6	6.4	6.4
21	5.4, 5.6	6.0, 5.9	6.2	6.0	5.8, 5.7	5.8, 6.0	6.1	6.1
22	4.6, 5.2	5.3, 5.4	5.6	5.6	5.1, 5.3	4.9, 5.1	5.6	5.6

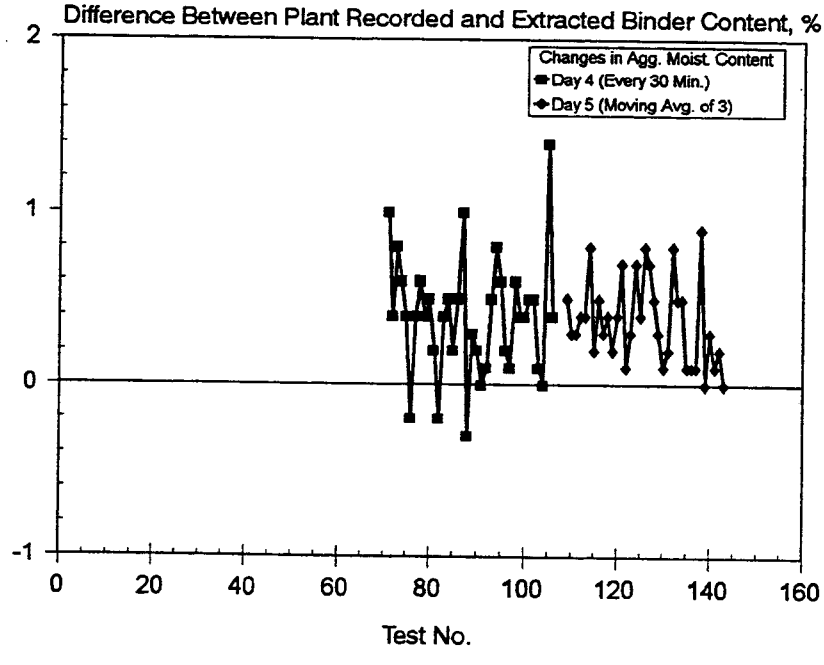

Figure 3.9 Variability in Asphalt Cement Content.

LOW VOLUME ROAD

The eight LVR test cells were constructed August 11, 12, and 16, 1993. One lift was placed each day; lifts were placed starting from 24 and ending with 31. All test cells were constructed with the same rolling patterns used for both the 5-Year and 10-Year Mainline test cells. Based on the stockpile moisture content study conducted during the construction of the 10-Year Mainline cells, a running average of three results were used to adjust the plant controls during the construction of these sections. Table 3.10 shows a summary of the quality control test results for these sections.

With one exception, construction proceeded with few problems. On the afternoon of August 16, 1993, a severe thunderstorm passed over the construction site. Construction was temporarily halted and the truck beds were covered with tarps. However, when work was resumed, the first few truck loads of asphalt concrete placed in the hopper of the paver were drenched with the water accumulated in the tarp as the bed of the truck was raised. The last lift of test cells 30 and 31 were the ones most affected by the rain storm.

Table 3.10. Test Results During the Construction of the Mn/ROAD Low Volume Road Test Cells (9).

Test	Test Cells									
	24		25			26			27	
Asphalt Grade	120/150 pen		120/150 pen			120/150 pen			120/150 pen	
Course	Base	Wear	Base	Base	Wear	Base	Base	Wear	Base	Wear
Lift	1st	2nd	1st	2nd	3rd	1st	2nd	3rd	1st	2nd
Lift Thickness, mm (in)	38 (1.5)	38 (1.5)	50 (2.00)	38 (1.50)	38 (1.50)	76 (3.00)	38 (1.5)	38 (1.50)	38 (1.50)	38 (1.50)
Mn/DOT Specification	2331 35 Blow	2331 35 Blow	2331 50 Blow	2331 50 Blow	2331 50 Blow	2331 50 Blow	2331 50 Blow	2331 50 Blow	2331 35 Blow	2331 35 Blow
Bulk Specific Gravity	2.349	2.343	2.361	2.365	2.349	2.358	2.358	2.360	2.348	2.348
Maximum Specific Gravity	2.436	2.435	2.442	2.444	2.442	2.445	2.435	2.449	2.430	2.429
Air Voids, %	3.6	3.8	3.3	3.2	3.8	3.6	3.2	3.6	3.4	3.3
VMA, %	16.1	16.2	15.3	15.2	15.7	15.4	15.4	15.4	16.1	16.0
Stability, N (lbs)	5306 (1193)	4546 (1022)	5667 (1274)	6281 (1412)	5734 (1289)	5742 (1291)	5817 (1308)	5440 (1223)	5173 (1163)	4662 (1048)
Flow, 0.25 mm	10.4	10.2	10.4	10.8	10.2	10.1	10.0	9.9	10.4	11.3
Extracted Asphalt Content, %	5.9	5.8	5.7	5.6	5.5	5.7	6.0	5.6	6.0	6.0
Sieve Analysis After Extraction:										
19 mm (3/4 in)	100	100	100	100	100	100	100	100	100	100
16 mm (5/8 in)	99	99	99	99	99	99	100	99	98	98
12.5 mm (1/2 in)	93	94	93	94	93	93	94	94	93	94
9.0 mm (3/8 in)	84	85	83	85	84	84	83	86	84	89
4.75 mm (No. 4)	67	69	66	68	69	68	70	70	69	69
2.0 mm (No. 10)	56	57	54	56	57	55	58	58	57	57
1.0 mm (No. 20)	43	43	42	43	44	42	45	44	44	44
0.45 mm (No. 40)	26	26	24	24	26	25	27	26	26	59
0.25 mm (No. 80)	10	9	8	10	9	9	10	9	9	9
0.075 mm (No. 200)	4.9	4.5	3.9	5.1	4.6	4.7	5.0	4.8	4.7	4.8

1: Results Average of 4 Tests Per Lift Per Cell

Table 3.10 (Continued). Test Results During the Construction of the Mn/ROAD Low Volume Road Test Cells (9).

Test	Test Cells[1]									
	28		29			30			31	
Asphalt Grade	120/150 pen		120/150 pen			120/150 pen			120/150 pen	
Course	Base	Wear	Base	Base	Wear	Base	Base	Wear	Base	Wear
Lift	1st	2nd	1st	2nd	3rd	1st	2nd	3rd	1st	2nd
Lift Thickness, mm (in)	38 (1.5)	38 (1.5)	38 (2.00)	38 (1.50)	38 (1.50)	76 (3.00)	38 (1.5)	38 (1.50)	38 (1.50)	38 (1.50)
Mn/DOT Specification	2331 50 Blow	2331 50 Blow	2331 50 Blow	2331 50 Blow	2331 50 Blow	2331 75 Blow	2331 75 Blow	2331 75 Blow	2331 75 Blow	2331 75 Blow
Bulk Specific Gravity	2.359	2.359	2.359	2.369	2.353	2.369	2.375	2.358	2.359	2.360
Maximum Specific Gravity	2.431	2.452	2.439	2.440	2.443	2.458	2.454	2.455	2.452	2.457
Air Voids, %	2.9	3.8	3.3	2.9	3.7	3.6	3.2	4.0	3.8	4.0
VMA, %	15.4	15.4	15.4	15.0	15.6	14.6	14.4	15.0	15.0	14.9
Stability, N (lbs)	6218 (1398)	5933 (1334)	5751 (1293)	5796 (1303)	5800 (1304)	7161 (1610)	7174 (1613)	6841 (1538)	6694 (1505)	7174 (1613)
Flow, 0.25 mm	10.8	10.1	10.4	10.6	10.4	10.0	10.0	10.1	9.9	10.3
Extracted Asphalt Content, %	5.8	5.4	5.8	5.8	5.6	5.2	5.6	4.9	5.2	5.1
Sieve Analysis After Extraction:										
19 mm (3/4 in)	100	100	100	100	100	100	100	100	100	100
16 mm (5/8 in)	99	99	99	99	99	99	99	99	99	99
12.5 mm (1/2 in)	93	94	94	93	94	94	93	9.	94	95
9.0 mm (3/8 in)	85	85	85	84	86	84	86	85	85	87
4.75 mm (No. 4)	69	68	68	68	0	8	70	6	70	71
2.0 mm (No. 10)	58	56	56	56	57	55	57	56	58	59
1.0 mm (No. 20)	44	43	43	43	45	42	44	43	45	45
0.45 mm (No. 40)	27	25	25	26	26	25	26	25	26	27
0.25 mm (No. 80)	9	8	9	9	9	9	9	8	8	9
0.075 mm (No. 200)	4.8	4.1	5.5	5.2	4.6	4.7	4.9	4.1	4.1	5.2

1: Results Average of 4 Tests Per Lift Per Cell

This Page Intentionally Blank

CHAPTER FOUR
TESTING PROGRAM

Mixture properties that are directly related to the ability of an asphalt concrete mixture to perform include temperature susceptibility, moisture sensitivity, low temperature behavior, and permanent deformation. Mixture stiffness over a range of temperatures (i.e., temperature susceptibility) is commonly used as input for the AASHTO pavement design guide as well as in performance models for fatigue cracking. Mixture performance can be adversely affected by the presence of water, and the occupance of freeze/thaw cycles; moisture damaged pavements exhibit excessive raveling and accelerated pavement distress due to lose of cohesion or adhesion. The potential for thermal cracking at colder temperatures is directly related to the mixture's ability to dissipate thermally-induced tensile stresses through viscous flow. However, mixtures that are sufficiently ductile to resist cracking at cold temperatures could also be too soft to resist permanent deformation at warm temperatures.

These considerations led to the development of four testing programs. Specific tests and variables for each of these are listed in Table 4.1. Materials tested included laboratory-prepared loose mixtures (i.e., mix design materials), behind the paver samples, and on a limited basis, cores. Loose mixture sample preparation varied depending upon the test method requirements. Evaluations of the cores were limited by the sample size required for a particular test method. Details of sample preparation techniques and the individual test methods are described in this chapter.

Table 4.1. Test Methods and Testing Variables.

Fundamental Mixture Properties		Test Variables			
Category	Test Method	Load Level & Duration	Frequency or Rate	Confinement	Temperature
Temperature Susceptibility	Resilient Modulus (ASTM D4123)	0.1 sec Variable Load[1]	0.33, 0.5, 1.0 Hz	None	-18, 1, 10, 25, 40°C (0, 34, 50, 77, 104°F)
		1.0 sec Variable Load[1]	0.033, 0.05, 0.1 Hz	None	Same
	Dynamic Modulus	Sinusoidal (Compression Only) Variable Load[1]	0.1, 1.0, and 10.0 Hz	None	1, 10, 25, 40°C (34, 50, 77, 104°F)
Moisture Sensitivity	Modified Lottman (ASTM D4867):				
	Resilient Modulus (ASTM D4123)	0.1 sec Variable Load[1]	0.33, 0.5, 1.0 Hz	None	25°C (77°F)
	Tensile Strength (ASTM D4123)	Not Applicable	50 mm/min (2 in/min)	None	Same
	Net Adsorption	Not Applicable	Not Applicable	Not Applicable	Not Applicable
Low Temperature Behavior	Indirect Tensile Creep (Constant Stress)	Static Load Variable Load[1]	Not Applicable	None	-20, -15, -10, -5, 0°C (-4, 5, 14, 23, 34°F)
	Indirect Tensile Creep (Constant Strain)	Not Applicable	0.025, 0.25, and 2.5 mm/min.	None	-18, 1°C (0, 34°F)
Permanent Deformation Characteristic	Repeated Load Creep	0.1 sec Variable Load[1]	0.33, 0.5, 1.0 Hz	None, 100, 200 kPa (15, 30 psi)	25, 40°C (77, 104°F)
		1.0 sec Variable Load[1]	0.033, 0.05, 0.1 Hz	None, 100, 200 kPa (15, 30 psi)	Same
	Static Load Creep	Variable Load[1]	Static - 1 hour + 15 min. recovery	None, 100, 200 kPa (15, 30 psi)	25, 40°C (77, 104°F)

1: Load selected to obtain a given level of strain at the various test conditions.

SAMPLE PREPARATION

Table 4.2 shows the sample dimensions and procedures used to prepare specimens for individual test methods.

Table 4.2. Sample Sizes Used for Each Test Method.

Category	Test Method	Materials Evaluated	
Temperature Susceptibility		Conventional 100 mm (4 in) diam 60 mm (2.5 in) tall	Cylindrical (uniform) 100 mm (4 in) diam 200 mm (8 in) tall
	Resilient Modulus (ASTM D4123)	Mix Design Behind Paver Cores	---
	Dynamic Modulus	---	Mix Design Behind Paver
Moisture Sensitivity	Modified Lottman (ASTM D4867): Resilient Modulus (ASTM D4123) Tensile Strength (ASTM D4123)	 Mix Design Behind Paver Mix Design Behind Paver Cores (Unconditioned Only)	---
	Net Adsorption	Not Applicable	
Low Temperature Behavior	Indirect Tensile Creep (Constant Stress)	Mix Design Behind Paver	----
	Indirect Tensile Creep (Constant Strain)	Mix Design Behind Paver	---
Permanent Deformation Characteristics	Repeated Load Creep	---	Mix Design Behind Paver
	Static Load Creep	---	Mix Design Behind Paver

Preparation of Loose Mixtures

Bulk laboratory-prepared mixtures were produced in approximately 23 kg (50 lb) batches by the Mn/DOT laboratory and supplied to the University of Minnesota for sample preparation and testing. The same mixing procedure and blending percentages used to prepare the mix design samples were used to prepare these mixtures.

Once the University received the material, it was reheated in a 135°C (275°F) oven for approximately 2 hours. The mixture was stirred to minimize segregation and divided into 1,300 g packages which were wrapped in tin foil and stored at room temperature until needed.

Compaction of Conventional-Size Samples

For compaction of individual samples, the required number of 1,300 g packages were re-heated for 2 hours at 135°C (275°F) and the mixture compacted per the method used during the mix design. That is, 35, 50, or 75 blows per side were used for the Marshall mix design materials and a gyratory compactor using a 1.25° angle of gyration and 100 revolutions was used to compact the rest. The mixture temperature was checked just prior to compaction to insure the compaction temperature of the mixture was between 121 and 135°C (250 and 275°F).

Table 4.3 compares the SHRP Level 1 density requirements at each of three critical numbers of gyrations and the results for AC 20 and 120/150 pen asphalt gyratory mix design materials. These results show that the mix design materials prepared by Mn/DOT for compaction at the University of Minnesota laboratory were generally similar to those originally tested by the Asphalt Institute.

Table 4.3. SHRP Density Requirements and Mn/ROAD Compaction Results.

Materials	Numbers of Gyrations		
	10 (N_{ini})	100 (N_{design})	230 (N_{max})
SHRP Density Requirements	Max. 89%	96 %	Max. 98%
The Asphalt Institute Results (5.7% AC Content)			
Mn/ROAD 1201/50 Pen	91.2	96.2	97.5
University of Minnesota (5.7% AC Content)			
Mn/ROAD 120/150 Pen	91.9	96.8	97.9
Mn/ROAD AC 20	92.8	97.8	98.9

Compaction of Cylindrical Samples

Only one method was used to prepare 200 mm (8 in) high by 100 mm (4 in) diameter samples. A single rotating base, bevel head Marshall hammer for preparing large stone mixtures with a 150 mm (6 in) diameter was adapted so that a single 100 by 200 mm (4 by 8 in) sample could be prepared. The larger hammer was needed because the standard mechanical Marshall hammer did not allow compaction of the taller 200 mm (8 in) specimen. Parts that were redesigned and machined included the mold holder and the hammer release mechanism. The 10 kg (22 lb) mass was kept rather than reducing the mass to the 4.5 kg (10 lb) as is typical on conventional Marshall hammers. The heavier mass was used to compensate for the reduction in the drop height as material was added and because only one side of the sample would be subjected to the impact (i.e., the sample was not rotated). Figure 4.1 shows the modified hammer and parts.

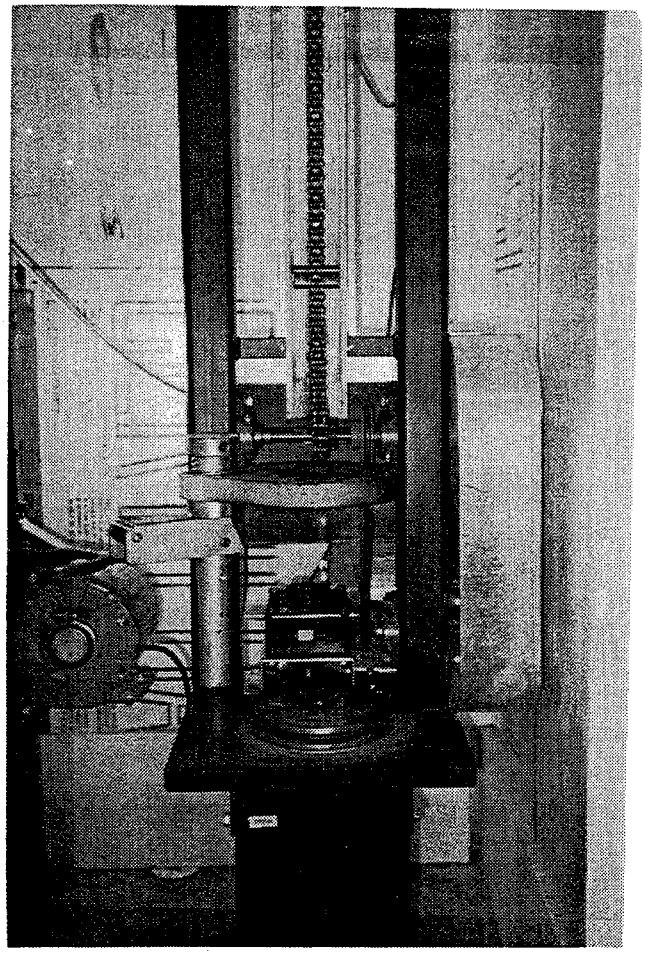

Figure 4.1 Modified Large Stone Mix 150 mm (6 in.) Diameter Rotating Base Hammer.

Mixtures were compacted in a 100 mm (4 in.) diameter by 250 mm (10 in.) tall mold in 3 lifts. The numbers of blows applied varied with each lift. Figure 4.2 shows a relationship between the compactive effort per lift and the individual lift air voids. These relationships were used to select the optimum the compactive effort for each. Table 4.4 shows the numbers of blows per lift that were selected for each of the three Marshall mix design materials. The

compactive effort was selected so that each lift had voids of 4 $\pm$ 0.5 percent. The same numbers of blows were used to prepare behind the paver samples.

Since the maximum height of sample that the gyratory compactor could produce was less that the desired 200 mm (8 in.), these samples were also compacted with the modified hammer.

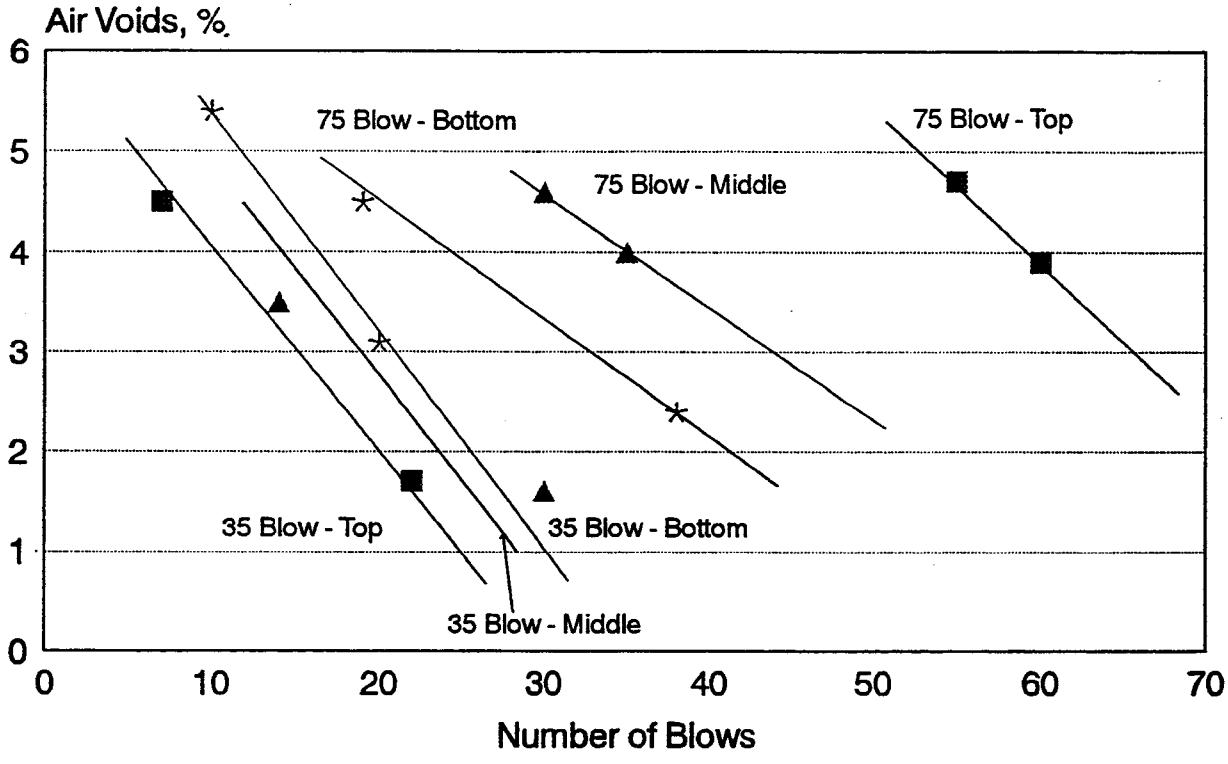

Figure 4.2. Numbers of Blows versus Air Voids (Modified Marshall Hammer) for Conventional 50 Blow Mix Design Materials.

Table 4.4. Numbers of Blows Used to Prepare Uniform Cylindrical Samples with a Modified 150 mm (6 in.) Diameter Rotating Base Marshall Hammer.

Lift	35 Blow Mix Design	50 Blow Mix Design	75 Blow Mix Design	Gyratory
Bottom (First)	7	20	28	24
Middle (Second)	14	35	40	53
Top (Last)	19	55	60	65

TEST METHODS

Temperature Susceptibility

Resilient Modulus - ASTM D4123

The equipment used for this test is shown in Figure 4.3. A sample was placed in an MTS load frame and an extensometer collar fitted with one sensor on either side, attached horizontally across the center of the sample. A sinusoidal load pulse was applied vertically for either 0.1 or 1.0 seconds followed by rest periods of varying durations. The 0.1 second load duration was selected to represent transient traffic loads; the 1.0 second load duration was selected to represent very slow moving loads (**9**). The frequencies, which control the length of the rest period between load pulses, were selected based on the ASTM D4123 recommendations (0.33, 0.5, and 1 Hz). An additional set of three frequencies (0.033, 0.05, and 0.1 Hz) were selected for the 1.0 second load duration condition. These frequencies were selected in order to maintain a consistent ratio of loading time to rest time between the 0.1 and the 1.0 load duration conditions (i.e., load:rest ratios of 1:9, 1:19, and 1:29). The magnitude of the applied load was adjusted for each temperature and mixture type so that the horizontal deformation was kept between 1.25 and 3.75 μm (50 and 150 μ-in). A minimum of 10 preconditioning cycles were used prior to data acquisition.

ASTM D4123 specifies that both horizontal and vertical deformations be measured; these measurements are used to calculate Poisson's ratio. However research has shown that this type of total vertical deformation measurement is unreliable for this calculation (**9**). Therefore all testing using this configuration assumed Poisson's ratio to be: 0.2 for temperatures below 1°C (34°F), 0.3 for 10°C (50°F), 0.35 for 25°C (77°F), and 0.5 for 40°C (104°F) (**10**).

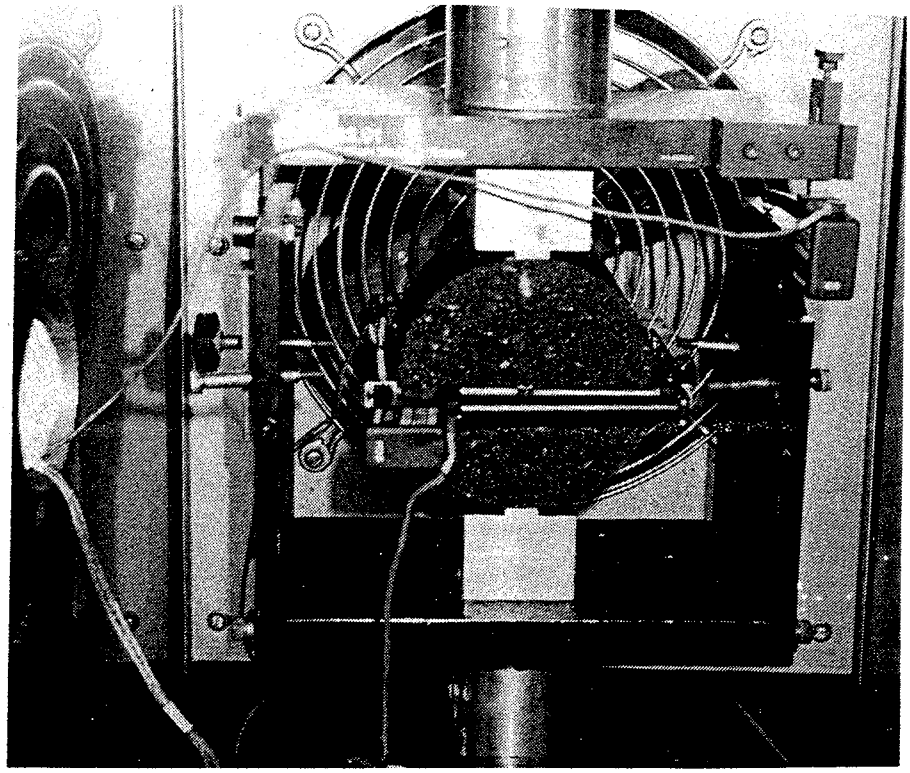

Figure 4.3. Equipment Set Up Used for Determining Resilient Modulus (ASTM D4123).

Dynamic Modulus - Axial

A tall cylindrical sample is subjected to an axially applied sinusoidal load; the corresponding axial strain over the center one-third of the sample is measured. Figure 4.4 shows the equipment set-up. A small capacity load frame (10 kN (2,248 lb.)) was substantially stiffened to remove any frame compliance prior to conducting this test. This frame was used with the MTS Testar control hardware and data acquisition software for both test control and data acquisition. A traditional triaxial cell was used without and with [200 kPa (about 30 psi)] confining pressure. Axial displacement was monitored with a set of three LVDT's mounted across the center one-third of the specimen and spaced at 120° around the sample.

One test cycle consisted of 15 preconditioning cycles of a sinusoidal load followed by an additional 5 cycles over which data were collected at a rate of 50 data points per cycle for both the load and axial displacement. The amplitude of the sinusoidal load was selected so that the center one-third axial displacements were between approximately 1.25 and 3.75 μm (50 and 150 μ-in), similar to those used in the resilient modulus test. The load varied with the test temperature: the load was 276 kPa (40 psi) at 1°C (34°F), 207 kPa (30 psi) at 10°C (50°F), 103 kPa (15 psi) at 25°C (77°F), and 69 kPa (10 psi) at 40°C (104°F).

Prior to testing, samples were conditioned at the test temperature (1, 10, 25, and 40°C (34, 50, 77, and 104°F)) over night. The -18°C (0°F) test temperature used in the ASTM D4123 and SHRP resilient modulus testing was eliminated because the axial loads needed to achieve the appropriate axial strains exceeded the capacity of the load frame. Since the testing could be completed within four minutes of the sample being removed from the conditioning chamber, no environmental chamber was considered necessary.

Results were used to calculate loss modulus, storage modulus, and the phase shift between the applied stress and the corresponding strain response.

Dynamic Modulus - Diametral Compression

The resilient modulus test described above was used with dynamic loading to obtain both the dynamic modulus and horizontal phase angle measurements. Testing was conducted at the same test temperatures as used for the dynamic modulus using the axial method. The loading frequency was 0.1 Hz; the loads used were the same as for resilient modulus testing.

Moisture Sensitivity

The most commonly accepted measure of the loss of mixture strength due to moisture and freeze/thaw damage is defined by the ASTM D 4867, "Standard Test Method for Evaluating the Effect of Moisture on Asphalt Concrete Paving Mixtures" (**11**). The research behind development of this procedure has shown that there is a general correlation between laboratory results and observed moisture damage of in-service pavements. Mixtures with retained strengths less than about 70 percent tend to exhibit moisture related pavement

distresses (**12**).

A second method to evaluate the loss of adhesion at the asphalt-aggregate interface was recently developed by researchers at Auburn University for the SHRP A-003B contract. While this method looks promising, the definition of the test method was not completed at the end of the SHRP contract. The final procedure used to evaluate the Mn/ROAD mixtures was developed under a separate Mn/DOT research project (**13**).

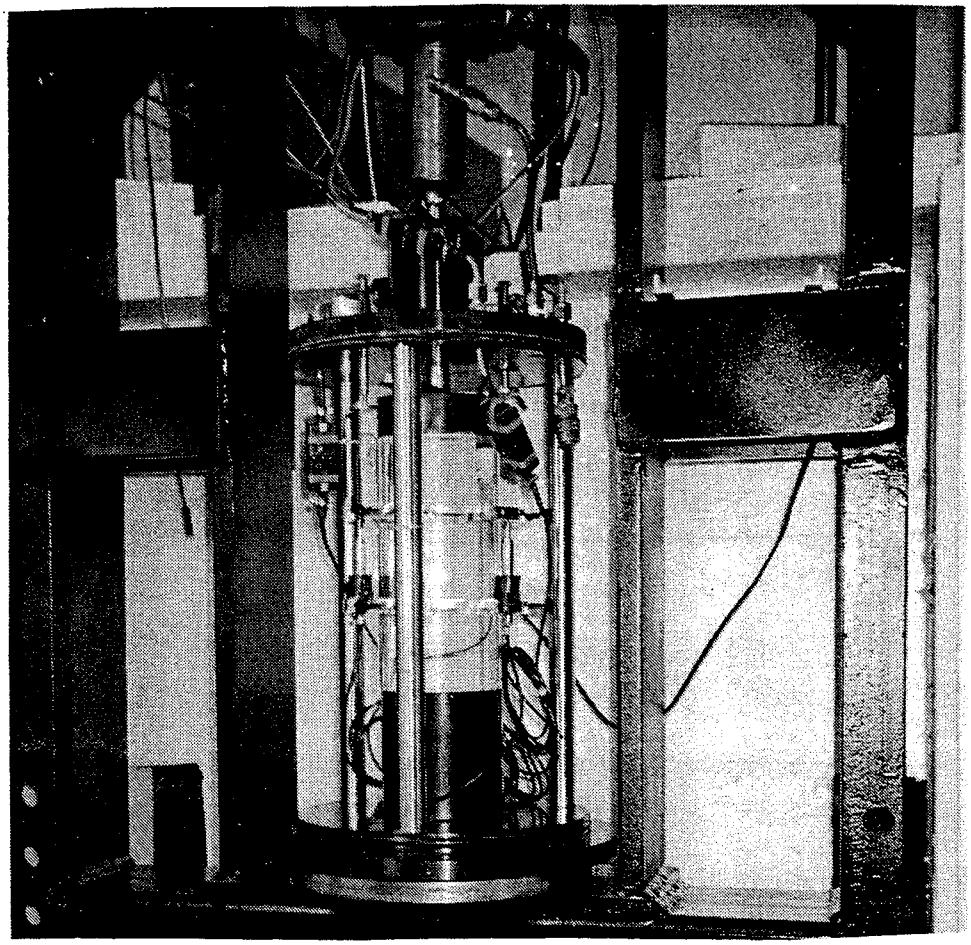

Figure 4.4. Sample and Equipment Set-Up for Dynamic Testing.

ASTM D4867 (Modified Lottman)

A set of six samples were prepared with the design compactive effort rather than reducing the effort in order to increase the air voids per the test method directions. This decision was made based upon a preliminary analysis of in-place air voids obtained for the 5-Year Mainline test sections which indicated that the in-place voids were between about 3 and 7 percent (**14**).

Briefly, the six samples were separated into two sets of three. Air voids, resilient modulus and tensile strengths were determined for the first set designated as the unconditioned set. The second set of samples were partially saturated to a level between 55 and 80 percent, wrapped in plastic, frozen for a minimum of 15 hours, unwrapped and thawed for 24 hours in a 40°C (140°F) water bath. The samples were then brought to the 25°C (77°F) test temperature by storing in a water bath for 2 hours prior to testing. The results from this set of samples were referred as the conditioned values. Moisture sensitivity was evaluated using both the absolute values, before and after conditioning, for resilient modulus and tensile strength as well as the ratios of conditioned to unconditioned values.

Resilient modulus was determined at the 0.1 second load duration with the measurements taken over the full diameter of the sample (ASTM D4123), and test frequencies of 0.33, 0.5, and 1.0 Hz. Tensile strengths were determined at a loading rate of 50 mm/min (2 in/min).

Net Adsorption

A 134 ml sample of a 0.6 g/L concentration solution of asphalt cement in toluene was placed in a large chromatography column and a peristaltic pump was used to continuously circulate the solution. A set of three columns were run simultaneously. Four milliliters of solution were removed from each column for an initial determination of asphalt cement concentration with a spectrophotometer. The spectrophotometer measures the amount of light absorbed by the asphalt suspended in the toluene. Previous research found that a wave length of 410 nm was best for measuring change in asphalt concentration (**16**).

Fifty grams of graded aggregate were then added to each column and the solution circulated through the column for 6 hours. Another 4 ml was removed from each column and the amount of adsorbed asphalt determined with a second spectrophotometer reading. Distilled water (1150 μl) was added, and the solution and water recirculated for another 2 hours. The third and final reading was obtained at this time. The within-laboratory standard deviation was reported by as 0.14 mg/g (**15**) for either washed or unwashed aggregate fractions smaller than 4.75 mm (No. 4). The equipment used in this test is shown in Figure 4.5.

One change was made to the original SHRP procedure. This was to use 50 g of the full aggregate gradation rather than limit the test to only the aggregate fraction smaller than 4.75 mm (No. 4). This change was made in order to assess the influence of the full gradation on moisture sensitivity (**12**).

The amount of asphalt adsorbed from the solution at any given time is calculated by:

$$B_t = \frac{V}{M} C_o \left(\frac{A_o - A_t}{A_o}\right)$$

Where:

B_t = adsorption of asphalt cement by aggregate, mg/g

V = volume of solution in column just prior to obtaining reading, ml

M = mass of aggregate in column, g

A_0 = initial absorbance reading

A_t = absorbance reading at time, t

C_o = initial concentration of asphalt in solution, g/ml

The amount of asphalt cement desorbed is the adsorption value after the water has been added to the column minus the value obtained just prior to adding the water to the column.

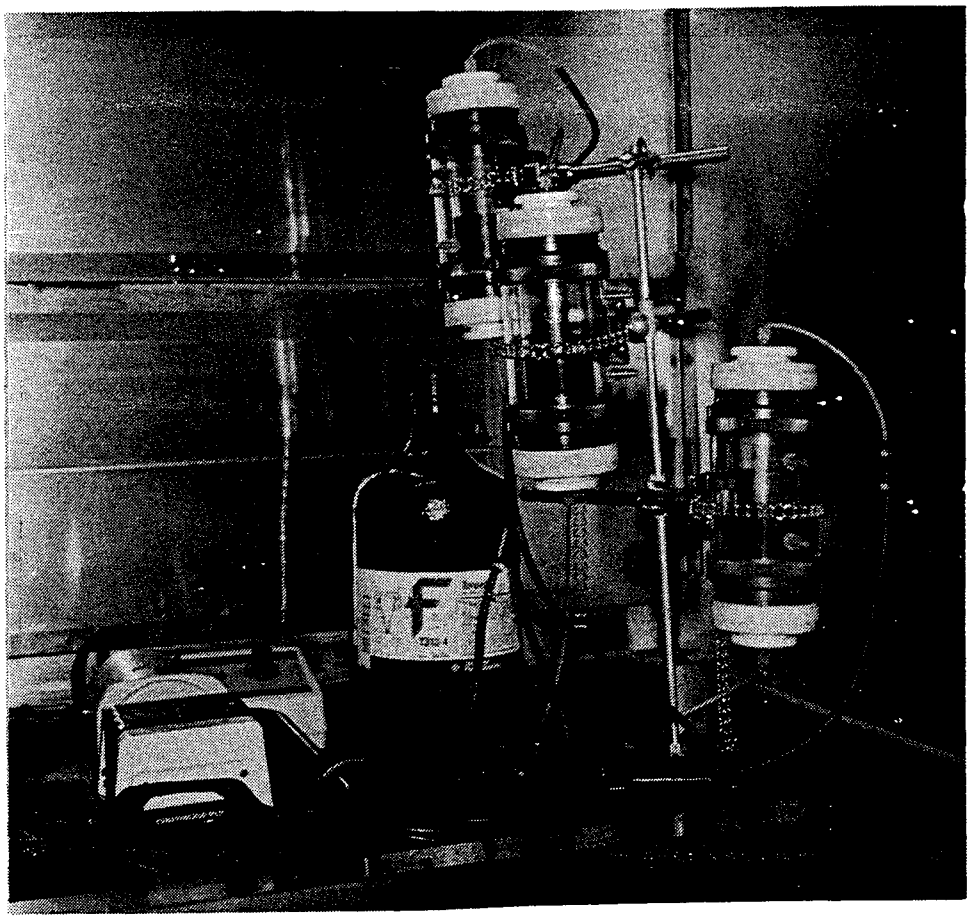

Figure 4.5. Equipment Set-Up for the Net Adsorption Test.

Low Temperature Behavior

Indirect Tensile (NCHRP - Constant Rate of Deformation)

A compacted cylindrical sample was loaded diametrally at a constant rate of vertical displacement, and both the resulting load and the full diameter horizontal displacement were measured (**17**). While it has been (**2**) recommended to 1.25 mm/min (0.05 in/min) rate of displacement a range of deformation rates that encompassed this loading rate was selected for this testing program. Loading rates were 0.025, 0.25, and 2.5 mm/min (0.001, 0.01, and 0.1 in/min). This range was selected in order to evaluate the effect of a wide range of loading rates. Tests were conducted at two temperatures: -18°C (0°F), and 1°C (34°F). Due to the length of time needed to perform each of these tests (approximately 1 to 2 hours per sample), only a set of three replicates were tested. The analysis included an evaluation of the maximum tensile strength and the corresponding full diameter horizontal strain.

SUPERPAVE (SHRP) Indirect Tensile Creep Test

This test is performed using a diametrally loaded sample to determine the creep compliance over a range of times and temperatures. The results are then used to construct a master creep compliance curve. The slope of this curve, m, is then used as a mixture property in the SUPERPAVE performance model.

The SHRP M-005 test method called for mounting both the horizontal and vertical sensors over the center 25 mm (1 in) of the sample (**18**). However, the only sensors available to perform this work were standard MTS extensometers. Horizontal displacements were measured over the full diameter of the sample and the vertical displacements were measured over the center one inch.

Figure 4.6 shows the final configuration used for this test.

Equations to calculate the strain over the center one inch are derived in Appendix A. These equations were then used to calculate the creep compliance reported herein.

A load level for each of the four test temperatures was selected so that about 100 to 500 micro strain in 1,000 seconds was achieved. The strain was then held constant and the stress

was allowed to relax. Typical loads used were: 200 to 275 kPa (30 to 40 psi) at -15°C (5°F), 140 to 200 kPa (10 to 20 psi) at -10°C (14°F), 70 to 140 kPa (10 to 20 psi) at -5°C (23°F), 35 to 70 kPa (5 to 10 psi) at 5°C (41°F), and 35 kPa (5 psi) at 15°C (59°F).

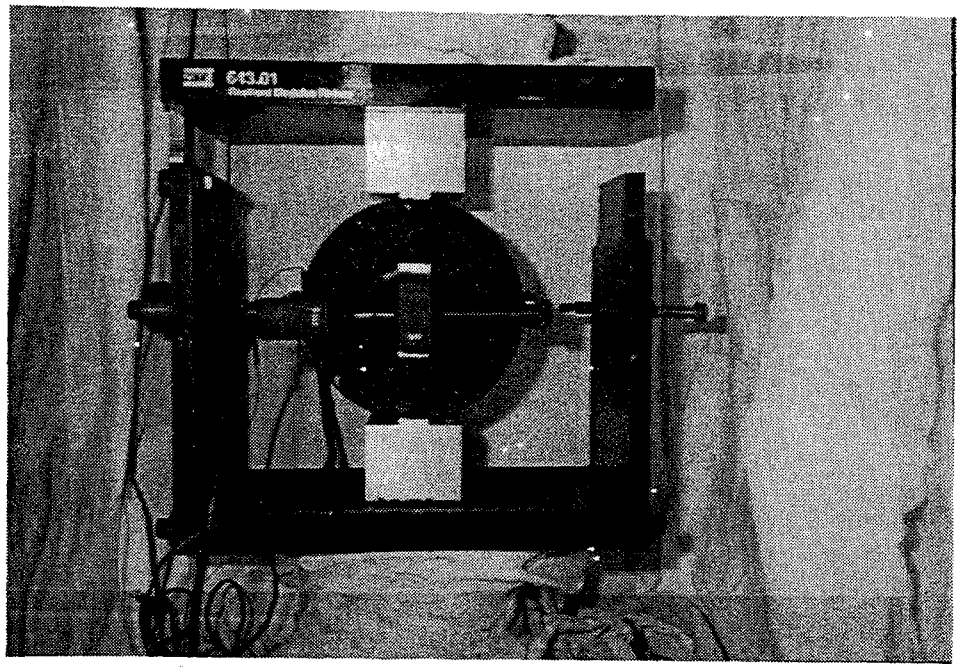

Figure 4.6. Modified SHRP M-005 Indirect Tensile Creep Test Instrumentation.

Permanent Deformation

Repeated Load Axial Creep

Cylindrical samples of 100 mm diameter by 200 mm tall (4 by 8 in) were used for this testing. A rubber membrane (when confining pressure was used) was placed over each sample, and then the sample was conditioned overnight at the test temperature. A collar holding three LVDT's was placed over the center one-third of the sample, and the sample was

placed in a standard triaxial chamber. The exterior plexiglass cylinder was then placed over the cell prior to mounting the entire fixture and sample in the load frame. The following pressures were used: none, 100 kPa (15 psi), and 200 kPa (30 psi).

A repeated load was applied for one hour using a haversine wave form for a specific duration, then removed for a specific rest period. Both the load and rest periods were selected to correspond with those used for resilient modulus testing (ASTM D4123). At a load duration of 0.1 Hz and rest periods of 0.33, 0.5, and 1.0 Hz, the total time the sample was subjected to loading was 2, 3, and 6, minutes, respectively. A load duration of 1.0 second and rest periods of 0.033, 0.05, and 0.1 Hz also loaded the sample for same total time.

Static Axial Creep

Once the repeated load testing was completed, the same samples were used immediately for the static creep test. MTS Testar hardware and control software was used to apply a static preconditioning axial load which was the same as the desired test load for 5 minutes. The load was removed for 2 minutes, and the sample was allowed to recover. The static load was then reapplied for 1 hour; data was collected throughout this time period. At the end of 1 hour, the load was removed and the sample recovery was monitored for 20 minutes. Samples were tested at 25 and 40°C (77 and 104°F). Originally, testing was to be performed at 1°C (34°F) but was dropped in favor of adding the SHRP constant stress test for the evaluation of low temperature creep behavior. The same equipment used for dynamic modulus was used for this testing (Figure 3.6).

Data was used to determine the creep compliance and modulus at 30 minutes, and the elastic, plastic, and viscous components of the material response. The 30 minute time interval for the creep modulus and compliance was selected because most samples survived at least this long at the more extreme ranges of testing conditions (e.g. no confining pressure, warm temperatures).

This Page Intentionally Blank

CHAPTER FIVE
MIX DESIGN MATERIALS

INTRODUCTION

This chapter presents the characterization of the Mn/ROAD asphalt concrete mixtures as they were prepared for the purpose of proportioning the binder and aggregates. The two binders used at Mn/ROAD included a 120/150 penetration grade asphalt and an AC 20 viscosity grade asphalt. The aggregate was a combination of a crushed granite and a river gravel used for both coarse and fine portions of the mixture. The aggregate gradation was held constant for all mixtures. The asphalt content was varied according to whether the mixture design compactive effort was a 35-, 50-, or 75-blow Marshall, or gyratory compaction, according to the SHRP Level 1 criteria.

The mixtures tested in this portion of the research were combined and mixed by the Mn/DOT materials laboratory in Maplewood, Minnesota, and then transported to the University of Minnesota. The mixtures were stored in cloth bags until they were heated and compacted into Marshall briquets for testing.

TEMPERATURE SUSCEPTIBILITY

Resilient Modulus ASTM D4123

The resilient modulus data for the mix design materials are shown in Table 5.1. The data for the 120/150 pen asphalt Marshall mix design materials represent the average of 12 samples. Data for both the AC 20 Marshall mix design and all gyratory-prepared samples are the average of 3 samples. The numbers of samples in a set were reduced based on an evaluation of the larger set of 120/150 pen mixture results. This evaluation is discussed in the following section.

Testing Variability

Previous research indicated variability associated with resilient modulus testing was dependent upon the magnitude of the value, so variability was best expressed in terms of the coefficient of variation (CV) (**15**). This research also showed the moduli to be log-normally distributed. The CV was consistently less than 3 percent for resilient modulus measurements within a set of three samples where the modulus was determined at a 0.1-second load duration and a 2.9-second rest period (0.33 Hz) for mixtures with AR 4000 and AR 8000 grade binders.

In order to compare testing variability the CV of the log transformed data for each set of 12 samples was calculated. A set of typical results are shown in Table 5.2. These moduli have lower CVs (between 1.9 and 2.4 percent) than the previous research indicated for the moderate test temperatures [(i.e., 1, 10, and 25°C (34, 50, and 77°F)]. A slightly greater CV of between 1.5 and 3.5 percent was seen for the longer load duration times. Changes in the rest period duration had little effect on the CV for a given load duration.

The CV generally increased with test temperature. At the -18°C (0°F) the CVs ranged between 3.2 to 5.7 percent and between 5.3 to 8.6 percent for the 40°C (104°F) test temperature. The slightly larger CVs at -18°C (0°F) temperature were most likely the result of thermally induced sensor noise and the small displacements being measured. The higher CVs at the warmer temperature were most likely a function of the binder softening at high temperatures.

The CVs in Table 5.2 were for a set of 12 samples while the previously reported variability was based on a set of 3 samples. In order to evaluate the consequences of the increased number of replicates on testing variability, the CV for a randomly selected set of 3 samples from each set of 12 was calculated. The CVs for a set of 3 versus 12 samples are shown in Table 5.3. No consistent decrease in testing variability was gained by increasing the number of samples from 3 to 12. Therefore, it was suggested that all further ASTM D4123 resilient modulus testing be limited to testing a set of 3 samples since there was no clear statistical advantage to testing a greater number of samples.

Table 5.1. Temperature Susceptibility for a Set of 12 Samples. (ASTM D4123, 120/150 Pen, Marshall Mix Design Materials)

Temperature	Resilient Modulus, MPa (ksi)							
	Load Duration, Seconds							
	0.1			1.0				
	Frequency, Hz							
	0.33	0.5	1.0	0.33	0.5	0.033	0.05	0.1
35 Blow Marshall Mixtures								
-18°C (0°F)	6,766 (981)	7,128 (1,033)	7,781 (1,128)	NA	NA	NA	NA	NA
1°C (34°F)	5,956 (863)	6,122 (888)	6,543 (948)	3,917 (568)	4,311 (625)	3,517 (510)	3,614 (524)	3,670 (536)
10°C (50°F)	3,903 (566)	3,904 (566)	3,944 (572)	3,289 (477)	3,772 (547)	2,800 (406)	3,028 (439)	3,028 (439)
25°C (77°F)	2,082 (302)	1,986 (288)	1,910 (277)	1,125 (163)	1,303 (189)	1,117 (162)	944 (137)	883 (128)
40°C (104°F)	904 (131)	772 (112)	731 (106)	421 (61)	483 (70)	476 (69)	434 (63)	407 (59)
50 Blow Marshall Mixtures								
-18°C (0°F)	4,166 (604)	4,421 (641)	4,648 (674)	5,104 (740)	5,724 (830)	4,144 (601)	4,690 (680)	4,559 (661)
1°C (34°F)	4,166 (604)	4,124 (598)	4,297 (623)	4,441 (644)	4,800 (696)	3,503 (508)	3,903 (566)	3,979 (577)
10°C (50°F)	3,200 (465)	3,193 (463)	3,228 (468)	2,986 (429)	3,283 (476)	2,283 (331)	2,628 (381)	2,676 (388)
25°C (77°F)	2,241 (325)	2,172 (315)	2,103 (305)	1,089 (158)	1,359 (197)	1,379 (200)	1,283 (186)	1,220 (177)
40°C (104°F)	842 (122)	766 (111)	710 (102)	434 (63)	462 (67)	517 (75)	469 (68)	448 (65)
75 Blow Marshall Mixtures								
-18°C (0°F)	6,490 (941)	7,083 (1,027)	7,910 (1,147)	7,607 (1,103)	8,069 (1,170)	5,393 (782)	6,393 (927)	6,959 (1,009)
1°C (34°F)	4,897 (710)	5,324 (772)	5,669 (822)	4,379 (635)	4,814 (698)	3,497 (507)	4,268 (619)	4,490 (651)
10°C (50°F)	4,600 (667)	4,835 (701)	5,055 (733)	3,669 (532)	4,048 (587)	3,131 (454)	3,524 (511)	3,558 (516)
25°C (77°F)	3,055 (443)	3,007 (436)	2,945 (427)	1,517 (220)	1,814 (263)	1,579 (229)	1,572 (228)	1,497 (217)
40°C (104°F)	786 (114)	724 (105)	676 (98)	NA	NA	538 (78)	490 (71)	462 (67)

Table 5.1 (Continued). Temperature Susceptibility for a Set of 3 Samples. (ASTM D4123, AC 20, Marshall Mix Design Materials)

Temperature	Resilient Modulus, MPa (ksi)							
	Load Duration, Seconds							
	0.1			1.0				
	Frequency, Hz							
	0.33	0.5	1.0	0.33	0.5	0.033	0.05	0.1
35 Blow Marshall Mixtures								
-18°C (0°F)	13,200 (1,914)	12,000 (1,740)	14,379 (2,085)	12,421 (1,801)	12,504 (1,813)	9,324 (1,352)	10,497 (1,522)	10,731 (1,556)
1°C (34°F)	7,483 (1,085)	6,648 (964)	7,283 (1,056)	6,186 (897)	6,938 (1,006)	3,738 (542)	5,303 (769)	5,828 (845)
25°C (77°F)	2,538 (368)	2,579 (374)	2,641 (383)	1,462 (212)	1,586 (237)	1,290 (187)	1,421 (206)	1,483 (215)
40°C (104°F)	772 (112)	848 (123)	820 (119)	393 (57)	414 (60)	400 (58)	393 (57)	400 (58)
50 Blow Marshall Mixtures								
-18°C (0°F)	12,062 (1,749)	13,372 (1,939)	15,145 (2,196)	13,641 (1,978)	14,000 (2,030)	9,662 (1,401)	11,683 (1,694)	12,186 (1,767)
1°C (34°F)	6,648 (964)	7,021 (1,018)	7,662 (1,111)	6,159 (893)	6,276 (910)	4,193 (608)	4,821 (699)	6,235 (904)
25°C (77°F)	2,193 (318)	2,441 (354)	2,614 (379)	1,366 (198)	1,483 (215)	1,372 (199)	1,393 (202)	1,389 (197)
40°C (104°F)	703 (102)	800 (116)	717 (104)	366 (53)	338 (49)	345 (50)	345 (50)	345 (50)
75 Blow Marshall Mixtures								
-18°C (0°F)	17,848 (2,588)	15,600 (2,262)	17,613 (2,554)	12,246 (2,199)	18,269 (2,649)	9,786 (1,419)	11,062 (1,604)	13,200 (1,914)
1°C (34°F)	7,283 (1,056)	7,662 (1,111)	8,821 (1,192)	6,448 (935)	7,290 (1,057)	4,503 (653)	5,952 (863)	6,028 (874)
25°C (77°F)	3,186 (462)	3,441 (499)	3,586 (520)	2,028 (294)	2,145 (311)	1,676 (243)	1,938 (281)	2,048 (297)
40°C (104°F)	1,110 (161)	1,048 (152)	1086 (143)	545 (79)	538 (78)	510 (74)	531 (77)	510 (74)

Table 5.1 (Continued). Temperature Susceptibility for a Set of 3 Samples. (ASTM D4123, AC 20 and 120/150 Pen, Gyratory Mix Design Materials)

Temperature	Resilient Modulus, MPa (ksi)							
	Load Duration, Seconds							
	0.1			1.0				
	Frequency, Hz							
	0.33	0.5	1.0	0.33	0.5	0.033	0.05	0.1
120/150 Pen Asphalt (Gyratory)								
-18°C (0°F)	Data Disk Damaged							
1°C (34°F)								
10°C (50°F)								
25°C (77°F)								
40°C (104°F)								
AC 20 Asphalt (Gyratory)								
-18°C (0°F)	10,986 (1,593)	12,482 (1,810	12,986 (1,883)	12,731 (1,846)	12,731 (1,846)	13,282 (1,926)	10,434 (1513)	11,683 (1513)
1°C (34°F)	---	---	---	3,304 (479)	3,421 (496)	3,193 (463)	3,138 (455)	3,345 (485)
25°C (77°F)	3,028 (439)	3,186 (462)	3,269 (474)	1,497 (217)	1,614 (217)	1,542 (223)	1,437 (208)	1,345 (196)
40°C (104°F)	979 (142)	993 (144)	924 (134)	154 (23)	164 (24)	333 (48)	224 (33)	215 (31)

----: Indicates data lost due to computer disk damage.

Table 5.2. Coefficient of Variation for Log Transformed Data (120/150 Pen, 75 Blow Marshall Mix Design Material).

Temperature	Coefficient of Variation, % (Calculated from Log Transformed Data)							
	Load Duration, Seconds							
	0.1			1.0				
	Frequency, Hz							
	0.33	0.5	1.0	0.33	0.5	0.033	0.05	0.1
75 Blow Marshall Mixtures								
-18°C (0°F)	3.22	3.16	3.93	3.10	2.67	4.20	5.66	3.75
1°C (34°F)	2.00	2.12	2.37	3.75	1.50	2.32	2.07	2.42
10°C (50°F)	2.05	1.91	1.88	1.42	1.44	2.56	2.14	1.74
25°C (77°F)	2.22	2.09	2.11	2.89	2.79	3.25	3.54	3.52
40°C (104°F)	8.55	5.30	5.95	NA	NA	4.26	6.04	5.97

Table 5.3. Coefficients of Variation for Selected Sets of 3 and 12 Samples. (75 Blow Marshall Mix Design Material).

Temperature	No. of Samples	Coefficient of Variation, % (Calculated from Log Transformed Data)							
		Load Duration, Seconds							
		0.1			1.0				
		Frequency, Hz							
		0.33	0.5	1.0	0.33	0.5	0.033	0.05	0.1
-18°C (0°F)	3	3.30	3.74	3.91	4.78	4.65	2.60	4.32	2.50
	12	3.22	3.16	3.93	3.10	2.67	4.20	5.66	3.75
1°C (34°F)	3	2.67	2.80	4.81	1.60	3.05	3.00	2.65	0.77
	12	2.00	2.12	2.37	3.75	1.50	2.32	2.07	2.42
10°C (50°F)	3	1.10	1.67	1.64	1.33	5.77	2.18	1.24	1.67
	12	2.05	1.91	1.88	1.42	1.44	2.56	2.14	1.74
25°C (77°F)	3	1.53	2.58	2.89	2.13	1.68	1.57	1.69	3.85
	12	2.22	2.09	2.11	2.89	2.79	3.25	3.54	3.52
40°C (104°F)	3	1.76	6.44	2.24	NA	NA	5.53	3.03	4.50
	12	8.55	5.30	5.95	NA	NA	4.26	6.04	5.97

Influence of Rest Period Duration

Figure 5.1 shows the typical relationship obtained for resilient moduli at different temperatures for a range of rest period durations. No discernable differences could be seen with a 0.1-second load duration and rest periods of either 0.9 (1 Hz), 1.9 (0.5 Hz), and 2.9 (0.33 Hz). Figure 5.2 shows that for load durations of 1.0 seconds, there was some difference in the results with differences in the rest periods. However, these differences did not appear to be not statistically significant.

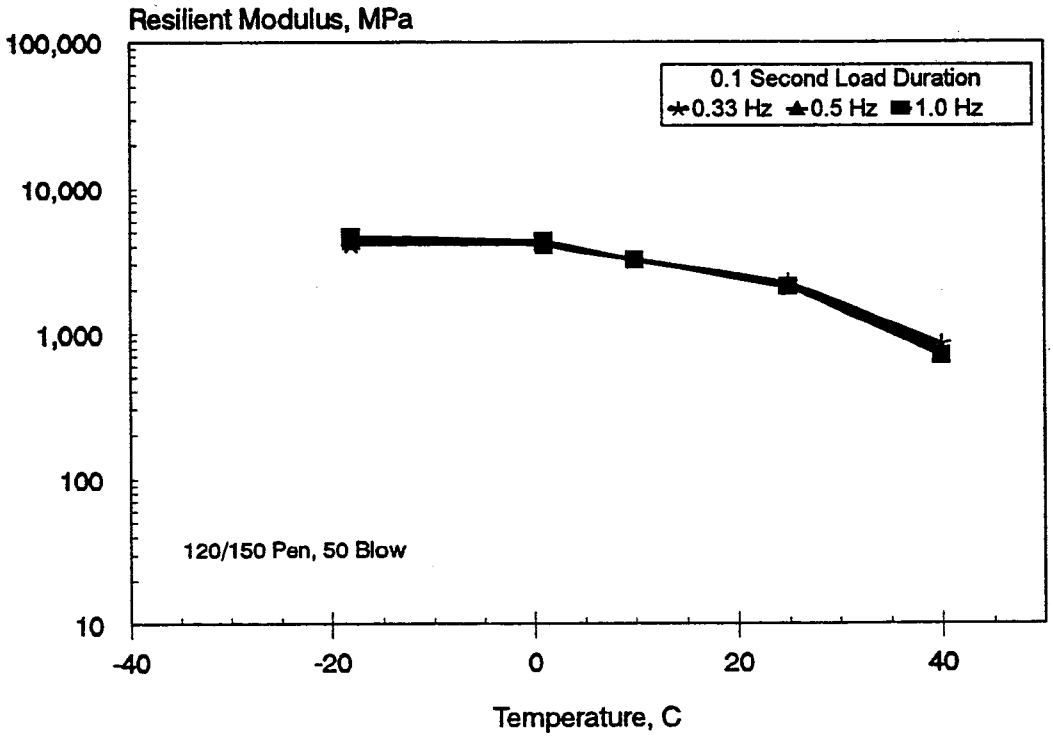

Figure 5.1. Typical Resilient Modulus (ASTM D4123) Relationships Due to Test Frequency (0.1 Second Load Duration) for the 120/150 Pen, 50 Blow Mix Design.

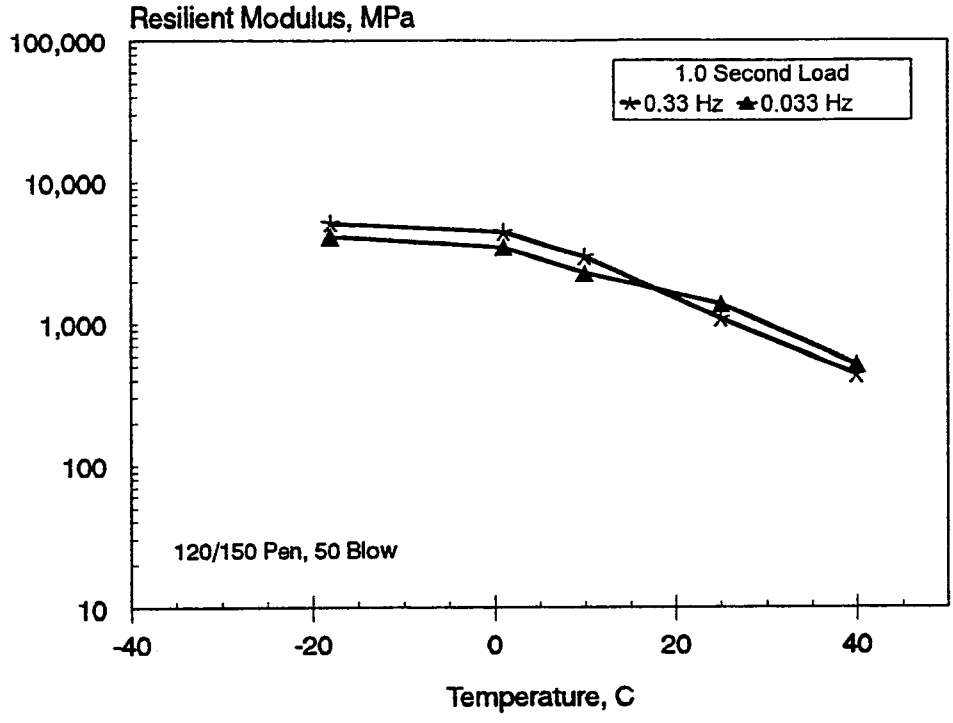

Figure 5.2. Typical Resilient Modulus (ASTM D4123) Relationships Due to Test Frequency (1.0 Second Load Duration) for the 120/150 Pen, 50 Blow Mix Design.

Influence of Load Duration

Figure 5.3 shows a typical relationship between the 0.1 and 1.0 second load durations at approximately the same rest period duration (2 seconds for 1.0 load duration and 2.9 seconds for 0.1 second load duration). This figure indicates that moduli were similar at the colder temperatures. However, there was an increasing difference in moduli with an increasing test temperature above 10°C (50°F). At about 25°C (77°F), there was a loss of apparent stiffness of about 50 percent when the load duration was increased from 0.1 to 1.0 seconds.

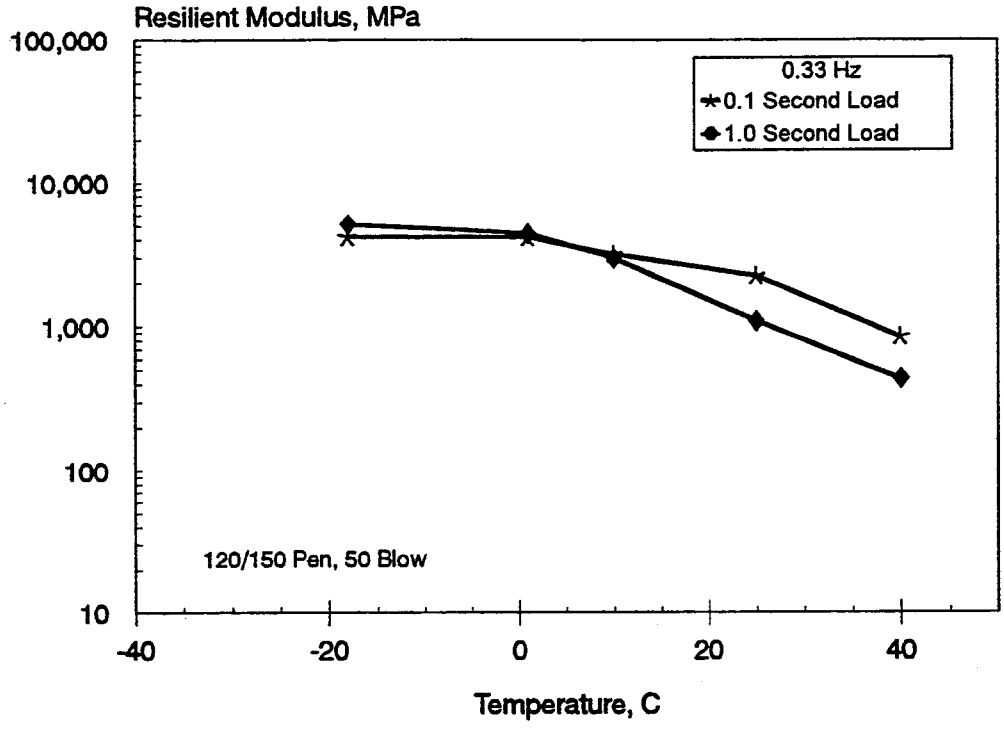

Figure 5.3. Typical Influence of Load Duration on Resilient Modulus.

Influence of Asphalt Grade

Figure 5.4 shows that the there was typically a significant lower modulus for the softer 120/150 pen asphalt mixtures for test temperatures below 25°C (77°F) for the 0.1 second load duration. When the load duration was increased to 1.0 seconds, the 120/150 pen asphalt only had a lower moduli than the AC 20 for temperatures below 1°C (34°F) (Figure 5.5). The apparently lower moduli for the stiffer AC 20 at the 40°C (104°F) test temperature was not statistically significantly lower due to the higher testing variability at this temperature and load duration.

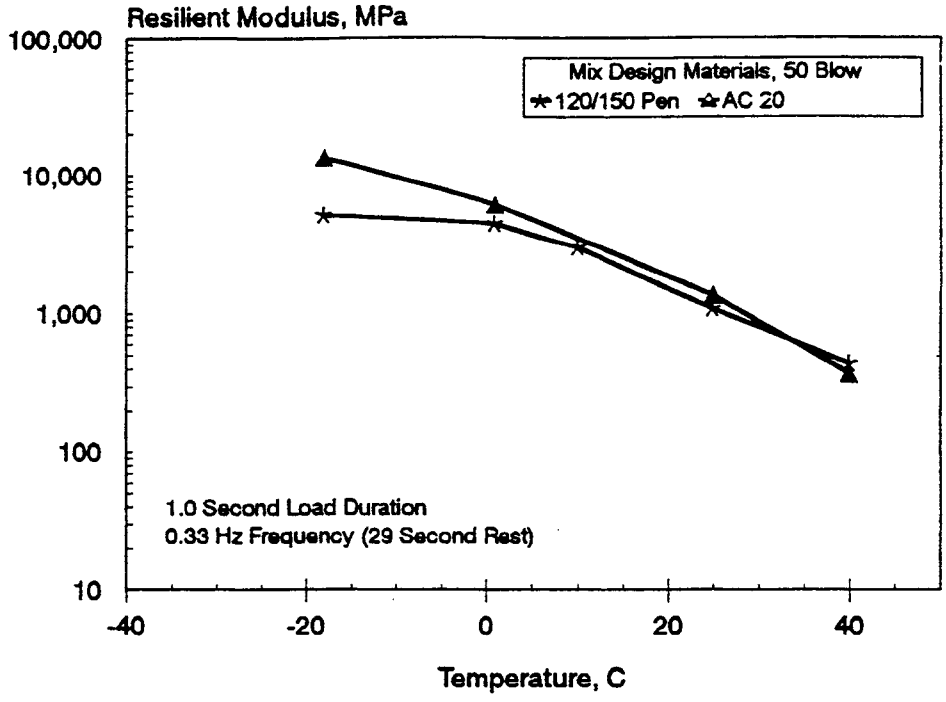

Figure 5.4. Influence of Asphalt Grade on Resilient Modulus (0.1-Second Load Duration, 0.33 Hz).

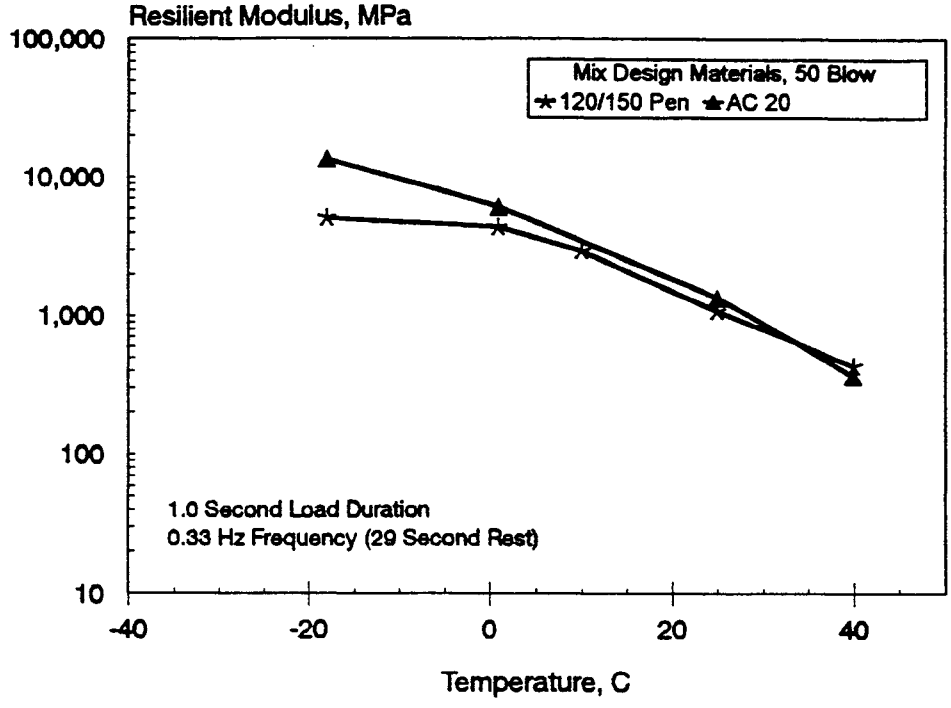

Figure 5.5. Influence of Asphalt Grade on Resilient Modulus (1.0-Second Load Duration, 0.033 Hz).

Comparison of Mixtures

Figure 5.6 compares a typical temperature susceptibility for each of the four mix design materials. Table 5.4 shows the plus and minus one standard deviation range of moduli for each of the 120/150 pen asphalt mix materials around the mean. The standard deviation was calculated based on the CV values developed in Table 5.2. Based on these results, the 50-blow mix design materials appeared to have a slightly lower moduli at the colder test temperatures. There was very little difference between any of the 120/150 pen mixtures at the warmer test temperature.

Figure 5.7 and Table 5.4 show that in general, the lower asphalt cement content mixtures (75 blow and gyratory) had higher moduli at all test temperatures than the higher asphalt cement content mixtures (35- and 50-blow).

Table 5.4. Ranges Plus or Minus One Standard Deviation of Mean for 120/150 Pen and AC 20 Mix Design Mixtures (0.1 second load, 0.33 Hz.)

Test Temperature	+/- One Standard Deviation Range for Resilient Modulus, MPa (ksi)			
	35 Blow Mix Design	50 Blow Mix Design	75 Blow Mix Design	Gyratory Mix Design
120/150 Pen Mixtures				
-18°C (0°F)	5,093 - 8,988 (785 - 1,224)	3,191 - 5,439 (492 - 741)	4,892 - 8,610 (755 - 1,173)	Not Available
0°C (34°F)	5,005 - 7,087 (754 - 987)	3,526 - 4,921 (531 - 687)	4,132 - 5,804 (622 - 809)	
10°C (50°F)	3,308 - 4,605 (499 - 643)	2,723 - 3760 (411 - 526)	3,886 - 5,445 (585 - 760)	
25°C (77°F)	1,787 - 2,426 (269 - 338)	1,921 - 2,615 (289 - 364)	2,602 - 3,587 (392 - 500)	
40°C (104°F)	600 - 1,360 (98 - 175)	562 - 1,261 (92 - 163)	527 - 1,173 (85 - 151)	
AC 20 Mixtures				
-18°C (0°F)	10,821 - 14,021 (1,569 -2,033)	11,973 - 15,310 (1,736 - 2220)	14,748 - 15,593 (2,137 - 2,261)	6,421 - 15,538 (931 - 2,253)
0°C (34°F)	5,986 - 8,979 (868 - 1,302)	6,203 - 7,014 (911 - 1,017)	6,393 - 8,175 (927 - 1,185)	---
10°C (50°F)	NT	NT	NT	NT
25°C (77°F)	2,421 - 2,655 (351 - 1,302)	2,007 - 2,379 (291 - 345)	2,407 - 3,966 (349 - 575)	2,703 - 3,369 (392 - 532)
40°C (104°F)	662 - 883 (96 - 128)	517 - 889 (75 - 129)	879 - 1,345 (127 - 195)	919 - 1,041 (133 - 151)

--- : Data disk damaged. NT: Not tested at this temperature.

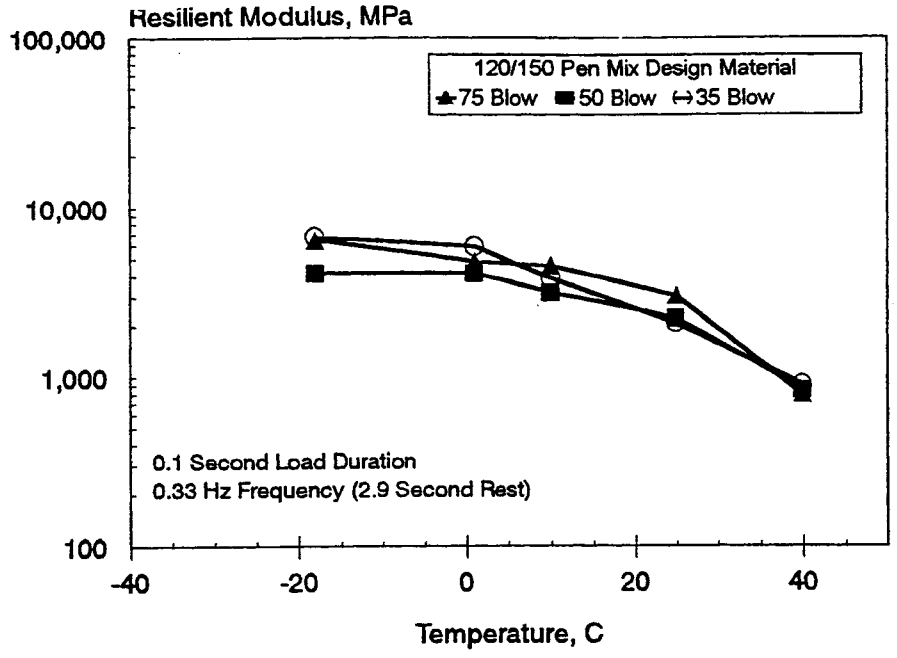

Figure 5.6. Typical Resilient Modulus Relationships (ASTM D4123) for 120/150 Pen Asphalt.

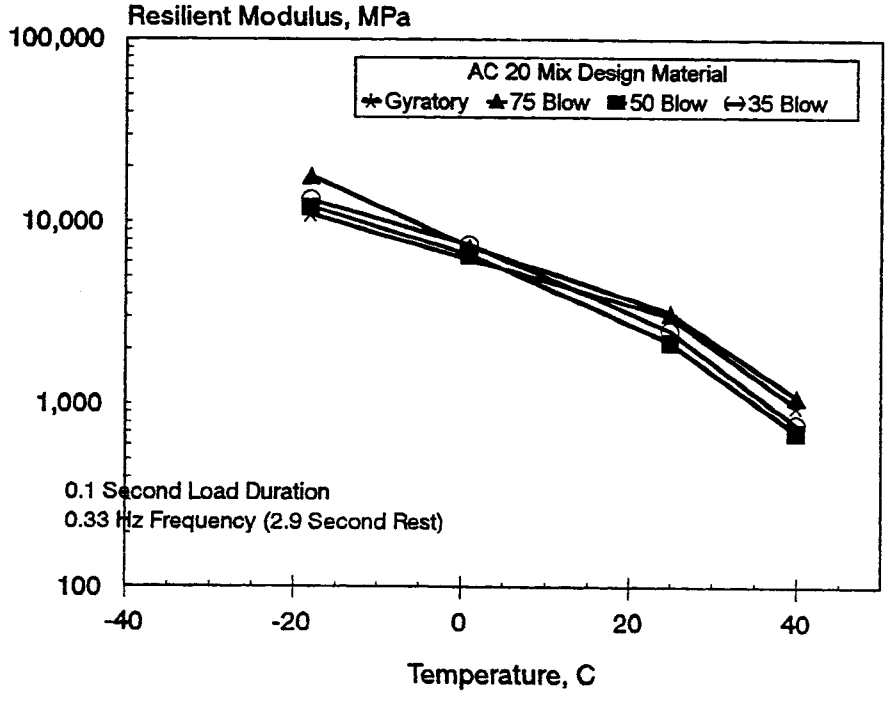

Figure 5.7. Typical Resilient Modulus Relationships (ASTM D4123) for AC 20 Asphalt

Dynamic Modulus

Axial Loading Configuration

Data Reduction: Preliminary tests were conducted with a set of 120/150 pen asphalt mixture samples at room temperature to evaluate the sensor response at each of three frequencies (0.1, 1.0, and 10 Hz). Electronic noise was present at all frequencies, however, a clear sinusoidal wave form could be identified at 0.1 and 1.0 Hz. Data obtained from the 10 Hz sequence had too much noise and a distinct wave form was difficult to identify. This was attributed to the inability of the spring loaded LVDT's to respond quickly and smoothly to the loading rate. Also, at 10 Hz, a measurable displacement was difficult to obtain due to equipment load and frame compliance limitations.

Strain amplitude (ϵ) and the average phase shift (δ) were measured from the last 5 loading cycles of a 15 cycle testing sequence. While a fair response was obtained from the 0.1 and 1.0 Hz tests, it was noted that some adjustment was needed to be made to smooth the strain curves. Therefore, a moving average of 12 data points was used to smooth the raw data curves. This adjustment shifted the smoothed curve to the right; the curve was manually shifted back so that it was properly in phase. This process was used for all data discussed in the following sections.

Test Method Precision: Table 5.5 shows typical standard deviations and coefficients of variation associated with measuring the strain amplitude over the center one-third of the sample for both the last five cycles used to report results for one sample and a set of six samples. This table shows that the standard deviation of the last five cycles of data obtained for one sample was constantly less than 6 μmm/mm, regardless of test temperature or frequency. However, there was a consistent increase in the standard deviation within a set of six samples and a corresponding increase in temperature. Standard deviations were below 10 μmm/mm for the 1 and 10°C (34 and 50°F) test temperatures. The variability approximately doubled for the unconfined samples at 40°C (104°F).

These results indicate that the displacement measurements were very consistent for a given sample, regardless of test temperature, loading frequency, and confining pressure.

However, mix variables such as sample preparation, air voids, etc. had a significantly increasing influence on the precision of the test results as the test temperature was increased above 10°C (50°F).

Table 5.6 shows the standard deviations and coefficients of variation associated with the determination of the phase shift, δ. Standard deviations for the phase angle were much more variable than for those for determining strain amplitudes. This can be seen by comparing the coefficients of variation: between 9 to 22 percent and between 1 to 8 percent for the phase angle (0.1 Hz) and strain amplitude, respectively. The coefficient of variation increased to between 16 and 51 percent when the frequency was increased to 1 Hz. A comparison of the statistics for the last five cycles of the same sample and a set of six samples shows little increase in standard deviation. This indicates that the variability associated with determining the phase angle was primarily a function of the measurement system and/or the data reduction process.

Complex Modulus: Tables 5.7 and 5.8 show the complex modulus values for the 0.1 and 1.0 Hz loading frequencies, respectively, for the 120/150 pen and AC 20 asphalt mixtures. In general the modulus decreased with increasing temperature, regardless of loading frequency. Also as expected, a higher loading frequency resulted in an increase in modulus. Increasing the frequency from 0.1 to 1.0 Hz resulted in an increase in stiffness of approximately 100 percent for these materials, regardless of test temperature. Differences in asphalt content did not have a noticeable influence on the complex modulus for the 120/150 pen mixtures. The modulus was similar for all of these mixtures for any given loading condition and test temperature. The AC 20 showed slightly higher modulus values at the warmer temperatures and decreasing asphalt cement content.

Confining pressure only appears to significantly increase the modulus at the 40°C (104°F) test temperature. Figure 5.8 shows typical results for complex modulus behavior over a range of temperatures. Figure 5.9 shows that the faster 1.0 Hz loading frequency results in a relatively uniform increase in complex modulus over the entire temperature range. This is generally true with or without confining pressure.

Table 5.5. Precision of Strain Amplitude Measurements (120/150 Pen Asphalt Mix Design Mixtures).

Mixture	Confining Press., psi	Strain Amplitude Statistics, μin/in for 0.1 Hz					Strain Amplitude Statistics, μin/in for 1 Hz				
		Mean	Last 5 Cycles		Set of 6 Samples		Mean	Last 5 Cycles		Set of 6 Samples	
			Stand. Dev.,	CV, %	Stand. Dev.,	CV, %		Stand. Dev.,	CV, %	Stand. Dev.,	CV, %
1°C (34°F)											
35	0	61	1.15	1.9	6.26	10.3	36	1.65	4.6	5.06	14.1
	30	57	0.90	1.6	6.23	11.0	37	3.09	8.4	4.88	13.2
75	0	52	1.82	3.5	3.80	7.3	32	3.89	12.3	4.28	13.5
	30	56	1.40	2.5	5.75	10.4	34	4.13	12.2	6.68	19.7
10°C (50°F)											
35	0	95	1.95	2.1	9.62	10.2	42	4.33	10.2	7.54	17.8
	30	89	1.42	1.6	9.00	10.1	42	5.02	12.0	6.59	15.8
75	0	72	5.83	8.1	8.41	11.7	33	2.87	8.8	5.22	16.0
	30	69	2.56	3.7	5.56	8.0	33	3.31	9.9	4.97	14.9
25°C (77°F)											
35	0	116	3.40	2.9	13.36	11.6	47	4.70	10.1	7.07	15.2
	30	108	3.10	2.9	10.96	10.2	44	4.27	9.8	9.40	21.5
75	0	120	2.42	2.0	12.86	10.8	46	2.77	6.1	6.49	14.2
	30	90	1.92	2.1	14.09	15.6	39	3.51	8.9	8.96	22.8
40°C (104°F)											
35	0	282	4.15	1.6	24.53	8.71	128	3.56	2.8	10.8	8.42
	30	210	4.61	2.2	45.63	21.69	105	4.26	4.1	23.5	22.3
75	0	277	4.72	1.7	25.63	9.2	114	3.35	2.9	11.52	10.1
	30	167	2.31	1.4	50.77	30.4	86	4.77	5.5	22.47	26.0

Table 5.6. Precision for Phase Angle Measurements (120/150 Pen Asphalt Mix Design Mixtures).

Mixture	Confining Press., psi	Phase Angle Statistics, 0.1 Hz					Phase Angle Statistics ,1 Hz				
		Mean	Last 5 Cycles		Set of 6 Samples		Mean	Last 5 Cycles		Set of 6 Samples	
			Stand. Dev., °	CV, %	Stand. Dev.,°	CV, %		Stand. Dev., °	CV, %	Stand. Dev., °	CV, %
1°C (34°F)											
35	0	33.5	4.34	13.0	6.26	10.3	3.78	6.27	16.5	5.06	14.1
	30	31.9	4.76	14.9	6.23	11.0	5.56	5.53	99.5	4.88	13.2
75	0	26.1	5.16	19.8	6.44	224.7	13.9	6.67	48.0	6.90	49.6
	30	29.4	4.67	15.9	6.37	21.7	4.69	4.79	102.0	**	**
10°C (50°F)											
35	0	38.8	4.98	12.8	5.43	14.0	20.4	10.30	50.5	10.78	52.8
	30	37.4	5.62	15.0	5.45	14.6	24.8	8.21	33.1	9.71	39.2
75	0	43.3	6.93	16.0	9.30	21.5	27.3	6.74	24.7	7.30	26.7
	30	37.9	8.26	21.8	8.40	22.2	22.3	5.89	26.5	7.70	34.6
25°C (77°F)											
35	0	46.4	7.02	15.1	7.66	16.5	37.8	16.2	42.8	16.83	44.5
	30	41.1	9.14	22.2	9.50	23.1	44.0	13.05	29.6	16.05	36.5
75	0	47.5	3.92	8.3	4.61	9.7	47.6	8.61	18.1	12.88	27.1
	30	41.3	4.09	9.9	5.55	13.4	41.3	9.72	23.5	17.05	41.3
40°C (104°F)											
35	0	34.5	3.54	10.3	3.86	11.2	35.0	7.77	22.3	8.17	23.4
	30	34.5	3.15	9.2	6.02	17.4	29.0	6.32	21.8	7.42	25.6
75	0	34.5	5.13	14.5	25.63	9.2	35.7	7.81	21.9	11.52	10.1
	30	32.1	4.12	12.8	50.77	30.4	27.0	7.44	27.6	22.47	26.0

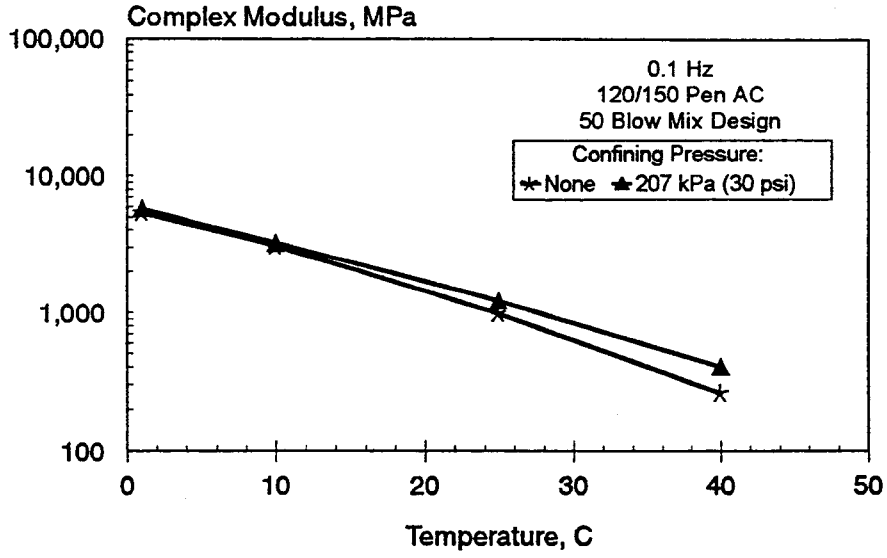

Figure 5.8. Influence of Confining Pressure and Test Temperature on Complex Modulus (120/150 Pen Asphalt, 50 Blow Mix Design Mixtures, Frequency = 0.1 Hz).

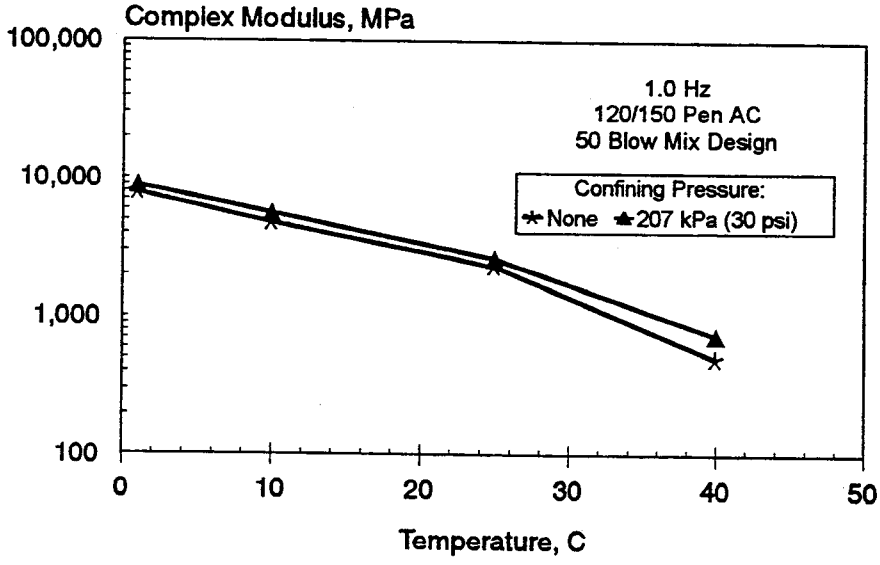

Figure 5.9. Influence of Confining Pressure and Test Temperature on Complex Modulus (120/150 Pen Asphalt, 50 Blow Mix Design Mixtures, Frequency = 1.0 Hz).

Figure 5.10 compares typical complex modulus test results (1.0 Hz) and the more commonly used resilient modulus test results [0.1 load duration, 0.9 second rest period (1.0 Hz)]. As mentioned before, there is little difference between the complex modulus due to changes in asphalt percent asphalt contents. Resilient modulus values were consistently higher at the warmest temperature and lower at the colder temperatures than the complex modulus. These trends generally agree with those reported by Tayebali, et. al (20). Since these moduli are not theoretically equivalent, it was not expected that the values should be similar. This analysis was included as a frame of reference for reviewing the data and relative magnitudes of moduli.

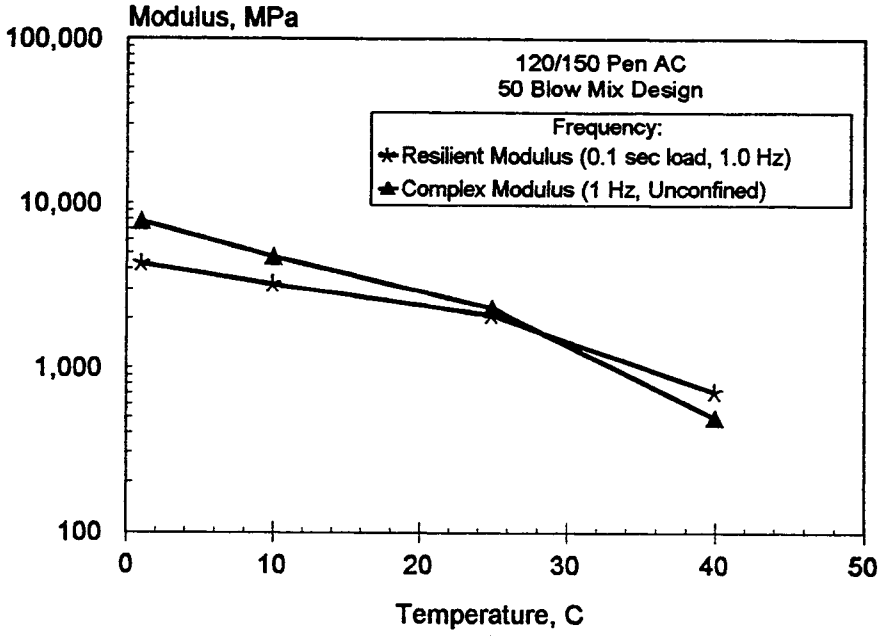

Figure 5.10. Comparison of Resilient and Complex Moduli Values over a Range of Test Temperatures (120/150 Pen Asphalt Mix Design Mixtures).

Phase Angle: Tables 5.7 and 5.8 also show the mean phase angles and strain response. The average phase angle increased with increasing test temperature up to 25°C (77°F). It either leveled off at this temperature or decreased slightly as the test temperature was increased. The AC 20 mixtures showed a continual increase in the phase angle above 25° C(77°F). The faster 1.0 Hz loading frequency resulted in a decrease in the phase angle at both the 1 and 10°C (34 and 50°F) test temperatures for both grades of asphalt.

Diametral Loading Configuration

A thorough theoretical evaluation of the complicated stresses and strains associated with the diametral testing configuration was conducted and the results are discussed in Appendix A. This analysis approach was used to calculate the dynamic modulus and phase angle.

Table 5.9 shows the typical horizontal strain amplitude standard deviations associated with testing a set of three samples. This table shows that results for the 0.1 Hz testing frequency had generally high coefficients of variation. The coefficient of variation values were erratic with no obvious trends in the data. Variability of results obtained at the faster 1.0 Hz was both lower and more consistent than those for the 0.1 Hz. No test results could be obtained at the warmer 40°C (104°F) test temperature because the expoxied knife edges used to mount the sensors moved as the asphalt softened at the mixture-knife edge interface.

Complex Modulus: Tables 5.10 and 5.11 show the results for the 0.1 Hz and 1.0 Hz dynamic loading, respectively. The variability in the strain amplitude measurements can be seen in the typically large standard deviations shown in these tables. These large standard deviations prevent conclusive statements regarding differences between mixtures. There appears to be a tendency for the gyratory samples to have consistently higher complex moduli values at all test temperatures. This difference could reflect real difference in mixture properties such as a lower asphalt cement content. It could also, however, reflect mixture differences induced by changing the method of compaction. A thorough investigation into the influence of method of compaction on test results is needed before any conclusion can be drawn. The expected mixture stiffer response with a faster loading time was seen only at the faster 1.0 Hz loading frequency when samples are tested at 40°C (104°F).

Table 5.7. Axially Loaded Complex Modulus and Phase Shift Data Collected at 0.1 Hz

Mix Design Mixtures	120/150 Pen				AC 20	
	Unconfined		207 kPa (30 psi)		Unconfined	
	Complex Modulus, MPa (ksi)	Mean Phase Angle, °	Complex Modulus, MPa (ksi)	Mean Phase Angle, °	Complex Modulus, MPa (ksi)	Mean Phase Angle, °
1°C (34°F)						
35 Blow	3991 (578)	29.7	4,274 (620)	30.9	9,766 (1,416)	24.4
50 Blow	5,379 (780)	26.1	5,792 (840)	21.9	8,954 (1,298)	24.2
75 Blow	4,697 (681)	25.8	4,356 (631)	27.3	9,269 (1,344)	24.9
Gyratory*	Not Tested Due to Limited Materials					
10°C (50°F)						
35 Blow	1,696 (246)	36.6	1,795 (260)	36.9	3,850 (588)	33.1
50 Blow	3,070 (445)	28.7	3,244 (470)	24.0	4,248 (615)	36.6
75 Blow	2,214 (321)	39.2	2,262 (328)	38.7	4,133 (599)	34.5
Gyratory*	Not Tested Due to Limited Materials					
25°C (77°F)						
35 Blow	869 (126)	44.5	908 (132)	43.1	774 (112)	48.5
50 Blow	981 (142)	37.3	1,215 (176)	37.8	887 (129)	43.6
75 Blow	817 (119)	43.1	1,060 (154)	40.4	1,078 (156)	47.5
Gyratory*	Not Tested Due to Limited Materials					
40°C (104°F)						
35 Blow	211 (31)	33.2	290 (42)	34.0	255 (37)	44.4
50 Blow	259 (38)	35.2	401 (58)	32.8	308 (45)	46.1
75 Blow	210 (31)	33.1	368 (53)	31.0	310 (45)	46.1
Gyratory*	Not Tested Due to Limited Materials					

Table 5.8. Axially Loaded Complex Modulus and Phase Shift Data Collected at 1.0 Hz

Mix Design Mixture	120/150 Pen				AC 20	
	Unconfined		207 kPa (30 psi)		Unconfined	
	Complex Modulus, MPa (ksi)	Mean Phase Angle, °	Complex Modulus, MPa (ksi)	Mean Phase Angle, °	Complex Modulus, MPa (ksi)	Mean Phase Angle,
1°C (34°F)						
35 Blow	6,540 (948)	7.1	6,546 (949)	3.5	10,692 (1,550)	27.7
50 Blow	7,798 (1,130)	16.3	8,811 (1,278)	10.9	10,098 (1,464)	25.7
75 Blow	7,757 (1,124)	12.3	7,053 (1,023)	3.7	10,245 (1,485)	31.3
Gyratory*	Not Tested Due to Limited Materials					
10°C (50°F)						
35 Blow	3.667 (532)	21.6	3,734 (541)	26.2	5,694 (825)	25.1
50 Blow	4,752 (689)	17.7	5,581 (809)	18.4	6,542 (949)	35.8
75 Blow	4,725(685)	28.9	4,627(671)	22.1	5,550 (805)	34.7
Gyratory*	Not Tested Due to Limited Materials					
25°C (77°F)						
35 Blow	2,075 (301)	36.0	2,176 (316)	42.7	2,079 (301)	44.7
50 Blow	2,311(335)	33.9	2,634 (382)	34.2	2,235 (324)	36.2
75 Blow	2,043 (296)	40.0	2,388 (346)	38.6	2,576 (373)	39.8
Gyratory*	Not Tested Due to Limited Materials					
40°C (104°F)						
35 Blow	435 (63)	36.7	571 (83)	29.6	677 (98)	47.1
50 Blow	496 (72)	38.7	730 (106)	33.4	807 (117)	46.5
75 Blow	471 (68)	35.7	700 (102)	27.9	792 (115)	50.5
Gyratory*	Not Tested Due to Limited Materials					

Table 5.9. Typical Precision of Strain Amplitude Measurements for Diametral Dynamic Modulus (Mix Design Materials).

Mixture	120/150 Pen			AC 20		
	Mean x 10^6	Stand. Dev. x 10^6	CV, %	Mean x 10^6	Stand. Dev. x 10^6	CV, %
Testing Frequency of 0.1 Hz						
-18°C (0°F)						
35 Blow	4.79	1.34	27.93	2.52	0.83	32.82
75 Blow	3.63	1.08	29.67	3.77	0.20	7.93
1°C (34°F)						
35 Blow	7.87	1.21	15.38	3.08	1.03	33.40
75 Blow	7.48	0.85	11.34	4.86	1.17	24.00
25°C (77°F)						
35 Blow	25.05	5.19	20.75	14.40	1.63	11.32
75 Blow	23.60	3.80	16.08	14.70	3.26	22.18
Testing Frequency of 1.0 Hz						
-18°C (0°F)						
35 Blow	3.31	0.27	8.06	1.78	0.11	6.00
75 Blow	2.15	0.32	14.77	2.40	0.33	13.71
1°C (34°F)						
35 Blow	5.36	0.36	6.78	2.25	0.22	9.67
75 Blow	4.29	0.26	6.08	3.82	0.58	15.18
25°C (77°F)						
35 Blow	10.8	2.05	18.99	6.10	0.69	11.31
75 Blow	8.91	1.34	15.08	6.74	1.16	17.16

Table 5.10. Diametral Complex Modulus and Phase Shift Data (0.1 Hz).

Mix Design Mixtures	120/150 Pen		AC 20	
	Complex Modulus, MPa (ksi)	Phase Angle, °	Complex Modulus, MPa (ksi)	Phase Angle, °
-18°C (0°F)				
35 Blow	18,023 ± 6,646 (2,613 ± 964)	15.38 ± 9.4	25,748 (3,733)	16.63 ± 11.0
50 Blow	9,188 (1,322)	15.71 ± 7.7	17,741 (2,572)	15.21 ± 7.4
75 Blow	25,472 ± 17,499 (3,693 ± 2,537)	33.57 ± 42.2	Disk Damaged Data Lost	
Gyratory	28,390 (4,117)	3.39 ± 1.3		
1°C (34°F)				
35 Blow	5,149 ± 1,040 (747 ± 151)	22.27 ± 5.1	94,97 ± 2,467 (1,377 ± 358)	25.38 ± 5.6
50 Blow	4,963 ± 575 (720 ± 83)	20.01 ± 4.8	10,901 ± 2,177 (1,81 ± 316)	17.03 ± 6.2
75 Blow	6,335 ± 1,331 (919 ± 193)	21.71 ± 3.6	14,475 ± 3,186 (2,099 ± 462)	14.20 ± 8.4
Gyratory	12,204 ± 6,356 (1,770 ± 921)	26.00 ±7.6	19,744 (2,863)	15.68 ± 2.3
25°C (77°F)				
35 Blow	1,163 ± 444 (169 ± 64)	36.55 ± 3.1	1,281 ± 324 (1,377 ± 47)	37.78 ± 3.9
50 Blow	961 ± 138 (139 ± 20)	40.43 ± 1.7	1,603 ± 306 (232 ± 44)	38.11 ± 1.6
75 Blow	1,036 ± 110 (150 ± 16)	37.30 ± 5.4	1,719 ± 509 (249 ± 74)	37.17 ± 1.8
Gyratory	1,211 ± 339 (176 ± 49)	34.44 ± 4.3	2,679 ± 198 (388 ± 29)	32.90 ± 1.8
40°C (104°F)				
35 Blow	Testing Difficulties			
50 Blow				
75 Blow				
Gyratory				

Table 5.11. Diametral Complex Modulus and Phase Shift Data (1.0Hz).

Mix Design Mixtures	120/150 Pen		AC 20	
	Complex Modulus, MPa (ksi)	Phase Angle, °	Complex Modulus, MPa (ksi)	Phase Angle, °
-18°C (0°F)				
35 Blow	21,752 ± 5,897 (3,154 ± 855)	6.67 ± 3.0	16,284 (2,352)	5.59 ± 2.4
50 Blow	15,457 ±4,904 (2,241 ± 711)	3.75 ± 2.2	21,945 ± 5,252 (3,182 ± 762)	4.86 ± 2.0
75 Blow	27,613 ± 28,535 (4,004 ± 4,138)	20.67 ± 30.4	30,852 ± 14,267 (4,473 ± 2,069)	5.34 ± 2.0
Gyratory	NA	NA	55,617 (8,064)	2.27 ± 2.2
1°C (34°F)				
35 Blow	8,090 ± 1,529 (1,173 ± 222)	17.46 ± 3.3	13,519 ± 1,423 (1,960 ± 206)	9.54 ± 4.0
50 Blow	7,929 ± 1,451 (1,150 ± 210)	15.13 ± 0.8	15,325 ± 2,960 (2,222 ± 429)	9.58 ± 2.2
75 Blow	10,140 ± 2,257 (1,470 ± 371)	14.99 ± 1.0	19,514 ± 3,395 (2,830 ± 492)	9.20 ± 2.2
Gyratory	12,351 ± 5,383 (1,791 ± 781)	14.05 ± 2.4	36,441 (5,284)	6.36 ± 0.4
25°C (77°F)				
35 Blow	2,696 ± 1,051 (391 ± 152)	34.43 ± 2.8	2,833 ± 530 (411 ± 77)	30.97 ± 2.9
50 Blow	2,359 ± 383 (342 ± 55)	35.94 ± 4.0	3,615 ± 545 (524 ± 79)	29.58 ± 1.6
75 Blow	2,381 ± 324 (345 ± 47)	34.41 ± 1.5	3,614 ± 915 (524 ± 133)	27.87 ± 2.0
Gyratory	2,530 ± 735) (367 ± 107)	30.05 ± 3.4	5,193 ± 337 (753 ± 337)	24.66 ± 1.2
40°C (104°F)				
35 Blow	Testing Difficulties			
50 Blow				
75 Blow				
Gyratory				

Phase Angle: Because of the standard deviations associated with phase angle measurements, only general conclusions can be made. The phase angle increases with test temperature and appears to be independent of the grade of asphalt when mixtures were tested at a loading frequency of 0.1 Hz. However, when the mixtures were tested at a loading frequency of 1.0 Hz, mixtures with the stiffer AC 20 asphalts had consistently lower phase angles than mixtures with the softer 120/150 pen asphalt.

MOISTURE SENSITIVITY

Net Adsorption

Table 5.12 shows the results for this test method. Since the net adsorption test uses only individual component materials to evaluate the attraction of the asphalt for the aggregate, neither the asphalt content nor the method of compaction are represented in these results. The data indicate little difference between the asphalt cements. This agrees with the original SHRP research which indicated that only small changes in test results were obtained by varying the asphalt cement grade and/or source in a given mixture (**15**).

While not specifically stated in the final SHRP report, results indicated that asphalt-aggregate pairs with net adsorption values less than 0.700 mg/g (washed aggregate) could be expected to show moisture-related pavement distresses while pairs with net absorptions greater than approximately 0.900 mg/g (washed aggregates) were associated with mixtures that did not have a history of moisture sensitivity (**16**). Data between 0.700 and 0.900 was not presented in the final SHRP report. Given these results, neither Mn/ROAD mixture would be expected to exhibit moisture sensitivity due to the loss of adhesion at the asphalt-aggregate interface.

Table 5.12. Net Adsorption Results

Test Time	Test Results, mg of asphalt cement/ gram of aggregate[1]	
	120/150	AC 20
Adsorption	1.350 ± 0.090	1.457 ± 0.098
Desorption	0.209 ± 0.083	0.177 ± 0.093
Net Adsorption	1.141 ± 0.077	1.280 ± 0.100

1: Average of three columns.

ASTM D4867 - Modified Lottman

The moisture sensitivity of the compacted mixtures was evaluated and the test results are shown in Table 5.13. High tensile strengths are most likely due to the lower than usual 6 to 8 percent sample air voids being lower than specified for this test. The tensile strength ratios appear to be acceptable (i.e., > 70%), however higher air voids would be expected to decrease this ratio. The gyratory compacted samples appear to have consistently higher values of both resilient modulus and tensile strength ratios.

Figure 5.11 shows that the tensile strengths for the 120/150 pen asphalt mixtures are lower than for the AC 20 mixtures. There was only a slight influence from the asphalt content on the tensile strengths for the 120/150 pen asphalt mixtures. Figure 5.12 shows that both the resilient modulus and the tensile strength ratios were similar for both grades of asphalt cement.

LOW TEMPERATURE BEHAVIOR

Indirect Tensile (Constant Rate of Deformation)

Table 5.14 shows both the results and the testing variability for the low-temperature indirect tension test. The variability is shown as plus or minus one standard deviation. This table shows that the precision associated with determining tensile strength decreased with increasing rates of displacement. This was true for either test temperature. The precision of corresponding horizontal displacement measurements was not dependent upon the load rate but upon the test temperature. The variability for the 120/150 pen asphalt mixtures increased from approximately 80 to between 200 to 800 μm for the -18°C (0°F) and 1°C (34°F) test

Table 5.13. Assessment of Moisture Sensitivity for Compacted Samples (Mix Design Materials).

Project	Air Voids, %	Resilient Modulus MPa (ksi)			Tensile Strength, kPa (psi)		
		Dry 25°C (77°F)	Wet 25°C (77°F)	Ratio, %	Dry 25°C (77°F)	Wet 25°C (77°F)	Ratio, %
120/150 Pen Asphalt							
35 Blow	3.1	2,413 ± 282 (350 ± 41)	1,703 ± 310 (237 ± 45)	71	863 ± 48 (111 ± 7)	766 ± 14 (125 ± 2)	112
50 Blow	4.1	2,172 ± 231 (315 ± 34)	1,475 ±68 (214 ± 10)	68	745 ± 62 (135 + 9)	931 ± 62 (108 ± 9)	80
75 Blow	3.4	2,372 ± 131 (344 ± 19)	1,662 ± 79 (241 ± 11)	70	917 ± 13 (156 ± 2)	1,076 ± 21 (133 ± 3)	86
Gyratory	4.3	1,772 ± 227 (257 ± 33)	1,751 ± 69 (254 ± 10)	99	952 ± 21 (132 ± 3)	910 ± 14 (138 ± 2)	105
AC 20							
35 Blow	3.7	2,537 ± NA[1] (368)	1,613 ± 159 (234 ± 23)	64	1,090 ± NA[1] (190)	76 ± 14 (125 ± 2)	83
50 Blow	3.2	3,075 ± 303 (446 ± 44)	2,427 ± 331 (352 ± 48)	79	1,193 ± 83 (196 ± 12)	1,351 ± 145 (173 ± 21)	88
75 Blow	4.0	2,241 ± 200 (325 ± 29)	1,648 ± 482 (239 ± 70)	74	1,158 ± 49 (205 ± 7)	1,413 ± 97 (168 ± 14)	82
Gyratory	4.6	2,634 ± 296 (382 ± 43)	2,359 ± 344 (342 ± 50)	90	1,200 ± 145 (208 ± 21)	1,435 ± 331 (174 ± 48)	84

1: these values were obtained from the temperature series samples

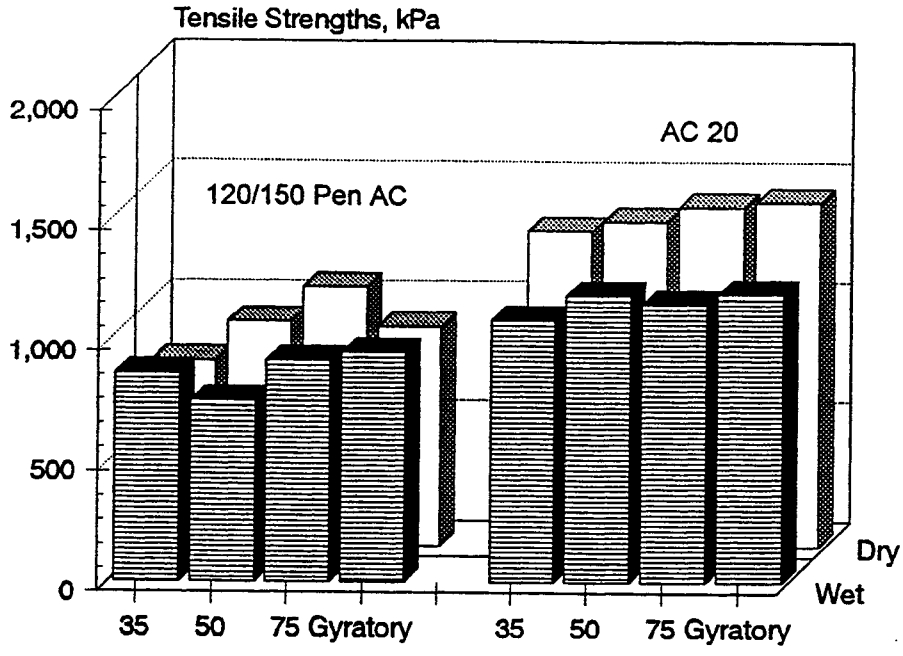

Figure 5.11. Tensile Strengths Before and After Moisture Conditioning.

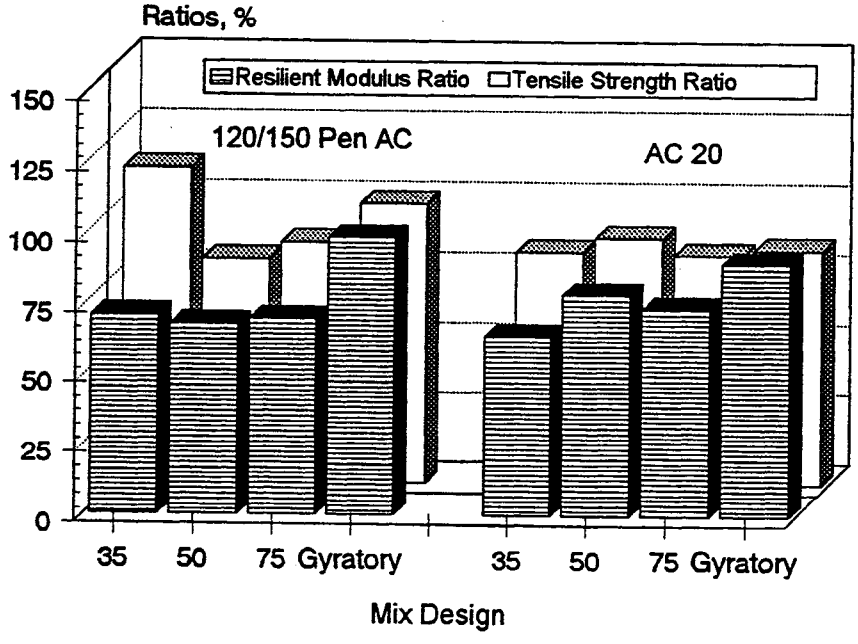

Figure 5.12. Resilient Modulus and Tensile Strength Ratios.

temperatures, respectively. These precision estimates indicate that most tensile strengths were significantly different while the horizontal displacements were only significantly different at the colder test temperature.

The results show that faster displacement rates result in higher tensile strength values. However, it appears that the magnitude of this increase at the colder -18°C (0°F) test temperature was also dependent to some extent on the binder content for the softer 120/150 pen asphalt mixtures. As the test temperature increased, changes in the 120/150 pen mixture stiffness became more dependent on the loading rate than the asphalt content. There was no significant difference in the tensile strengths for the AC 20 mixtures due to different asphalt cement contents.

At the colder -18°C (0°F) test temperature the horizontal displacements of the 120/150 pen mixtures increased with decreasing tensile strength. This was expected as a more ductile material will have a greater ability to strain. The AC 20 mixtures all showed approximately similar horizontal strains regardless of deformation rate or asphalt content at the same test temperature. While the tensile strength of both the 120/150 pen and AC 20 mixtures were similar, the horizontal strains for the AC 20 mixtures were substantially lower than the 120/150 pen mixtures for all but the 2.5 mm/min (0.1 in/min) rate. This would indicate that the AC 20 mixture could be expected to have a similar stiffness but much less ability to resist thermal cracking than the 120/150 pen mixtures.

At the warmer 1°C (34°F) test temperature, similar trends of increasing stiffness with increasing deformation rate were seen for both the 120/150 pen and AC 20 mixtures. The AC 20 mixtures had significantly higher tensile strengths at this temperature than the 120/150 pen mixtures. This increased tensile strength was also accompanied by a significant decrease in the horizontal strain measurements.

Table 5.14. Low Temperature Behavior at Constant Rate of Deformation (Mix Design Materials).

Constant Rate of Vertical Deformation mm/min (in/min)	Test Temperature, °C (°F)			
	-18°C (0°F)		1°C (34°F)	
	Maximum Tensile Strength kPa (psi)	Corresponding Horizontal Strain $\mu\epsilon$	Maximum Tensile Strength kPa (psi)	Corresponding Horizontal Strain $\mu\epsilon$
120/150 Pen Asphalt, 35 Blow Marshall Mixtures				
0.025 (0.001)	2,862 (415) ± 66 (10)	970 ± 80	663 (96) ± 18 (3)	3,852 ± 300
0.25 (0.01)	3,262 (473) ± 129 (19)	820 ± 30	1,131 (164) ± 15 (2)	3,794 ± 600
2.5 (0.1)	3,545 (514) ± 230 (33)	783 ± 70	1,897 (275) ± 45 (7)	2,704 ± 700
120/150 Pen Asphalt, 50 Blow Marshall Mixtures				
0.025 (0.001)	3,296 (478) ± 82 (12)	694 ± 80	717 (104) ± 41 (6)	3,673 ± 700
0.25 (0.01)	3,897 (565) ± 175 (25)	450 ± 50	1,103 (160) ± 54 (8)	3,951 ± 800
2.5 (0.1)	3,993 (579) ± 508 (74)	232 ± 70	2,303 (334) ± 88 (13)	2,664 ± 200
120/50 Pen Asphalt, 75 Blow Marshall Mixtures				
0.025 (0.001)	3,510 (509) ± 35 (5)	694 ± 50	772 (112) ± 26 (4)	3,527 ± 100
0.25 (0.01)	3,770 (547) ± 107 (16)	602 ± 30	1,276 (185) ± 131 (18)	3,188 ± 500
2.5 (0.1)	3,620 (525) ± 344 (50)	323 ± 10	1,993 (289) ± 188 (27)	2,817 ± 400
120/150 Pen Asphalt, Gyratory Mixtures				
0.025 (0.001)	3,268 (474) ± 372 (54)	655 ± 58		
0.25 (0.01)	3,227 (468) ± 166 (24)	696 ± 12		
2.5 (0.1)	Not Tested			

Table 5.14 (Continued). Low Temperature Behavior at Constant Rate of Deformation (Mix Design Materials).

Constant Rate of Vertical Deformation mm/min (in/min)	Test Temperature, °C (°F)			
	-18°C (0°F)		1°C (34°F)	
	Maximum Tensile Strength kPa (psi)	Corresponding Horizontal Strain $\mu\epsilon$	Maximum Tensile Strength kPa (psi)	Corresponding Horizontal Strain $\mu\epsilon$
AC 20 Asphalt, 35 Blow Marshall Mixtures				
0.025 (0.001)	3,248 (471) ± 234 (34)	258 ± 160	1,021 (148) ± 69 (10)	1,870 ± 380
0.25 (0.01)	3,241 (470) ±317 (46)	449 ± 80	1,813 (263) ± 58 (8)	1,850 ± 40
2.5 (0.1)	3,490 (506) ± 235 (34)	188 ± 18	2,393 (347) ± 317 (46)	1,480 ± 150
AC 20 Asphalt, 50 Blow Marshall Mixtures				
0.025 (0.001)	3,310 (480) ± 110 (16)	190 ± 77	1,069 (155) ±35 (5)	1,390 ± 260
0.25 (0.01)	3,407 (494) ± 207 (30)	516 ± 206	1,848 (268) ± 83 (12)	1,640 ± 150
2.5 (0.1)	3,855 (529) ± 166 (24)	206 ± 51	2,758 (400) ± 179 (26)	1,310 ± 320
AC 20 Asphalt, 75 Blow Marshall Mixtures				
0.025 (0.001)	3,317 (481) ± 269 (39)	256 ± 79	1,097 (159) ± 35 (5)	1,890 ± 130
0.25 (0.01)	3,538 (513) ±166 (24)	212 ± 35	1,828 (265) ± 117 (17)	1,600 ± 250
2.5 (0.1)	3,600 (522) ± 96 (14)	230 ± 34	2,655 (385) ±256 (37)	1,710 ± 200
AC 20 Asphalt, Gyratory Mixtures				
0.025 (0.001)	3,014 (437) ± 297 (43)	360 ±129	972 (141) ± 55 (8)	2,639 ±227
0.25 (0.01)	3,207 (465) ± 393 (57)	651 ± 183	2,524 ±(366) ±117 (17)	1,652 ± 67
2.5 (0.1)	Not Tested			

Indirect Tensile Creep (SHRP - Constant Stress)

Table 5.15 shows the creep compliance values after 1,000 seconds of loading. The compliance increases with temperature and is uniformly less for the higher viscosity AC 20 as compared to the 120/150 pen asphalt. Figures 5.13 through 5.20 show the average creep compliance curves for 120/150 pen and AC 20 asphalt mixtures, respectively. As expected, the slope of the compliance curves increase with increasing test temperature.

Table 5.15. Indirect Tensile Creep Test Results for Mix Design Materials.

Mixture	Creep Compliance at 1,000 sec, 1/MPa				
	Test Temperature				
	0°C (-18°F)	-5°C (-21°F)	-10°C (-23°F)	-15°C (-26°F)	-20°C (-29°F)
120/150 Pen Asphalt Mix Design Mixtures					
35 Blow	0.0259	0.0118	0.0060	0.0020	0.0010
50 Blow	0.0207	0.0120	0.0058	0.0019	0.00095
75 Blow	No Data	No Data	0.0045	0.0018	0.00076
Gyratory	0.0226	0.0114	0.0059	0.0025	0.0010
AC 20 Asphalt Mix Design Mixtures					
35 Blow	0.0069	0.0039	0.0018	0.00090	0.00052
50 Blow	0.0126	0.0062	0.0022	0.00100	0.00050
75 Blow	0.0085	0.0042	0.0018	0.00069	0.00049
Gyratory	0.0134	0.0062	0.0020	0.00086	0.00051

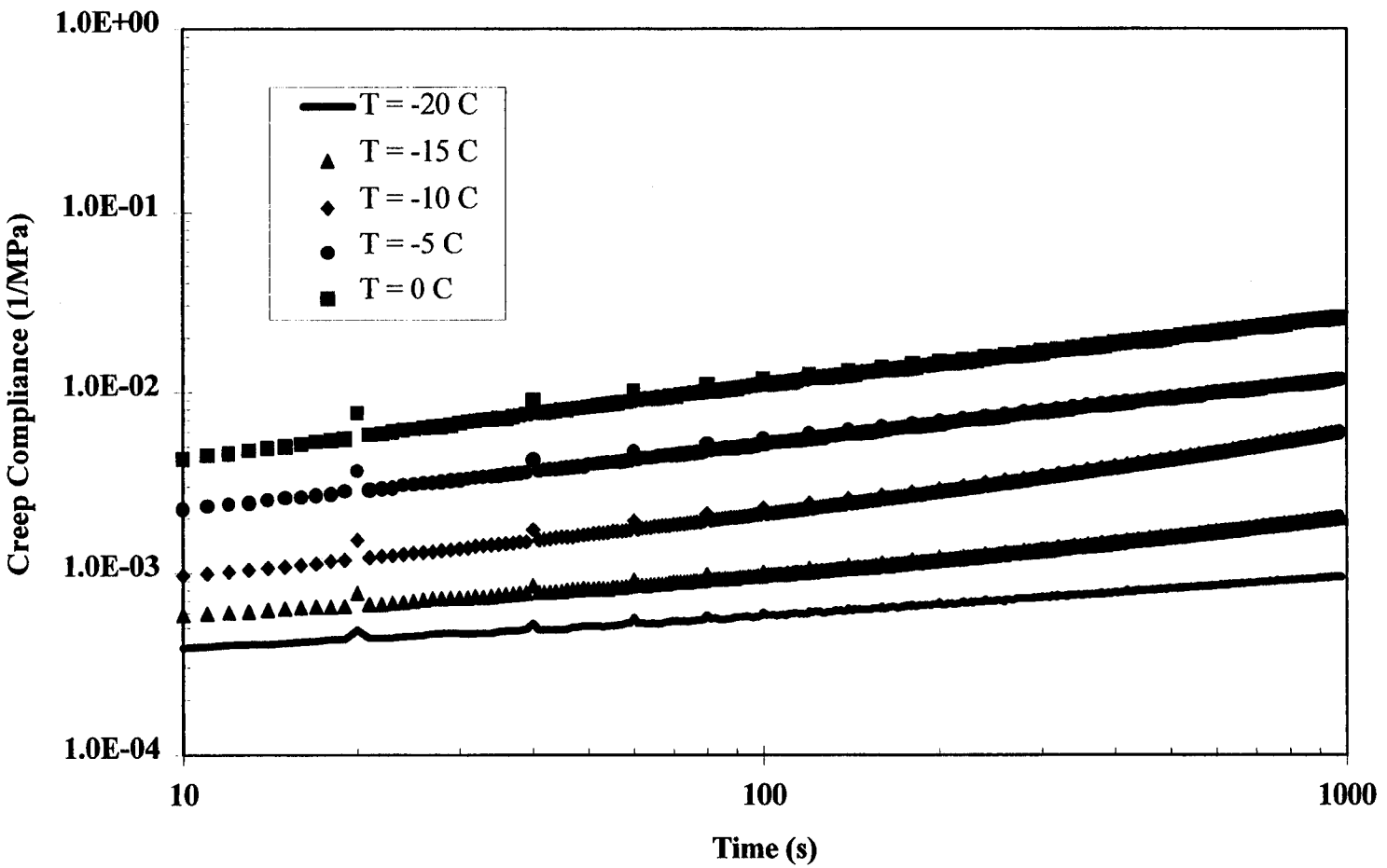

Figure 5.13. Creep Compliance Curves
35 Blow Mix Design, 120/150 pen asphalt

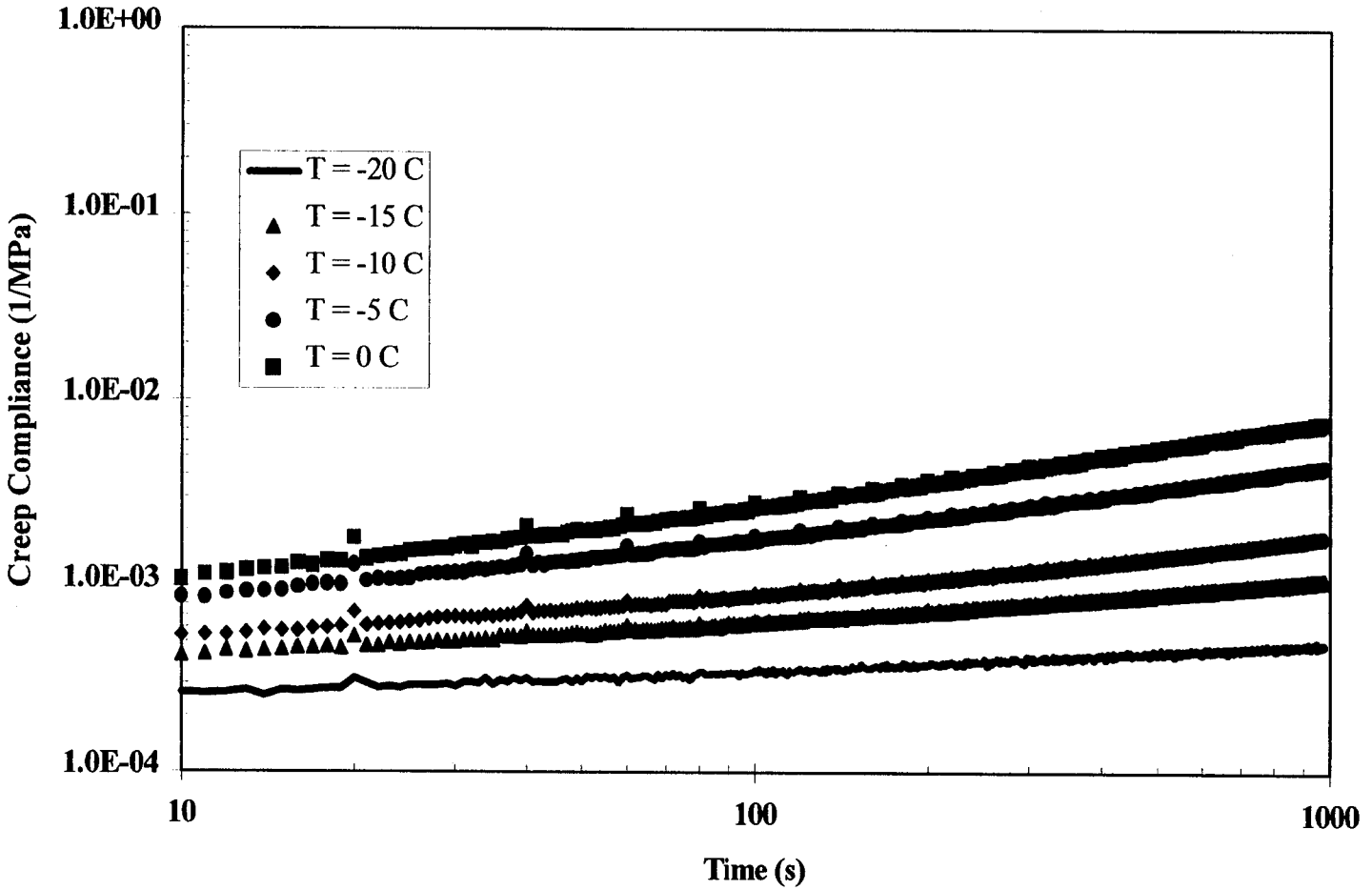

Figure 5.14. Creep Compliance Curves
35 Blow Mix Design, AC 20 asphalt

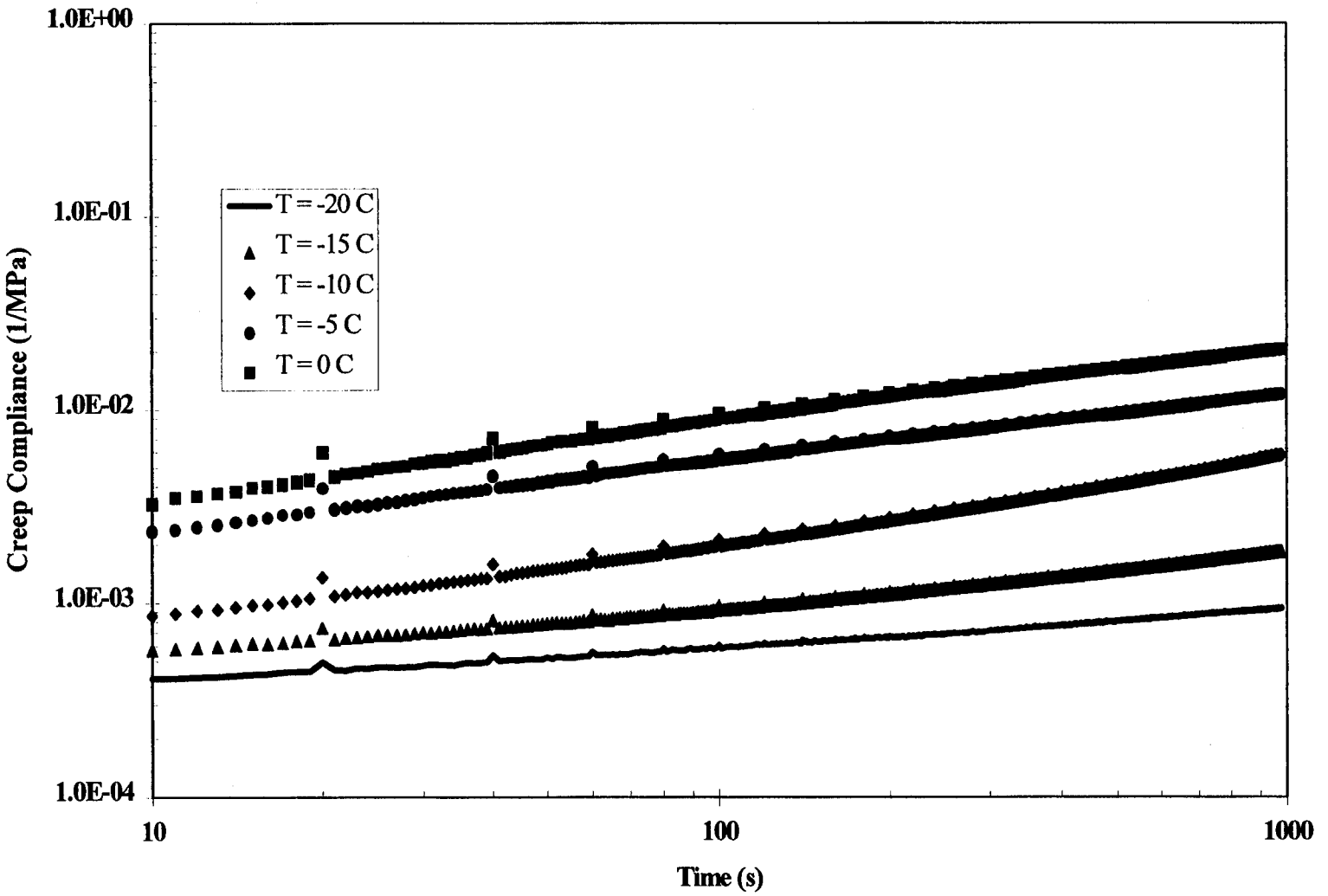

Figure 5.15. Creep Compliance Curves
50 Blow Mix Design, 120/150 pen asphalt

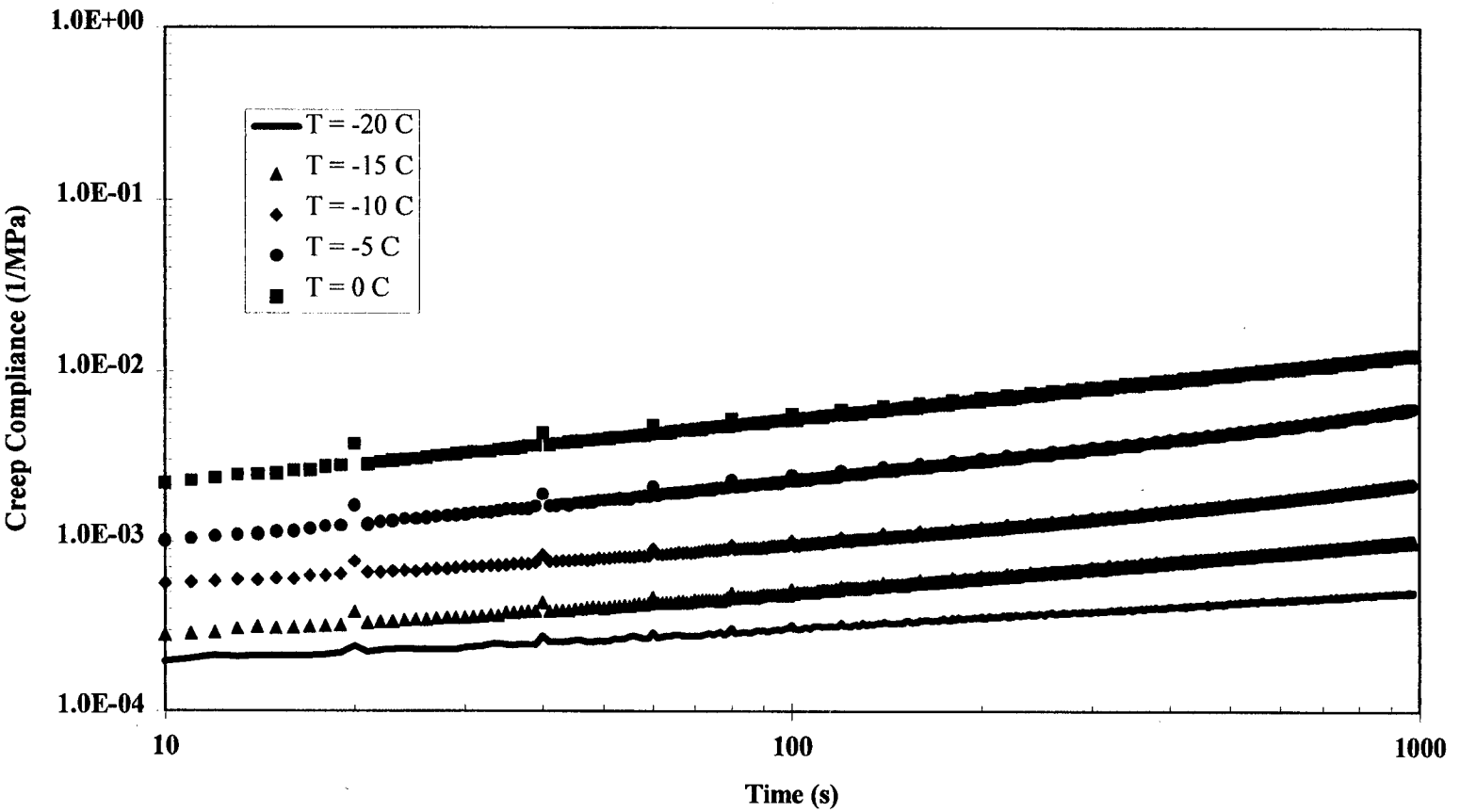

Figure 5.16. Creep Compliance Curves
50 Blow Mix Design, AC 20 asphalt

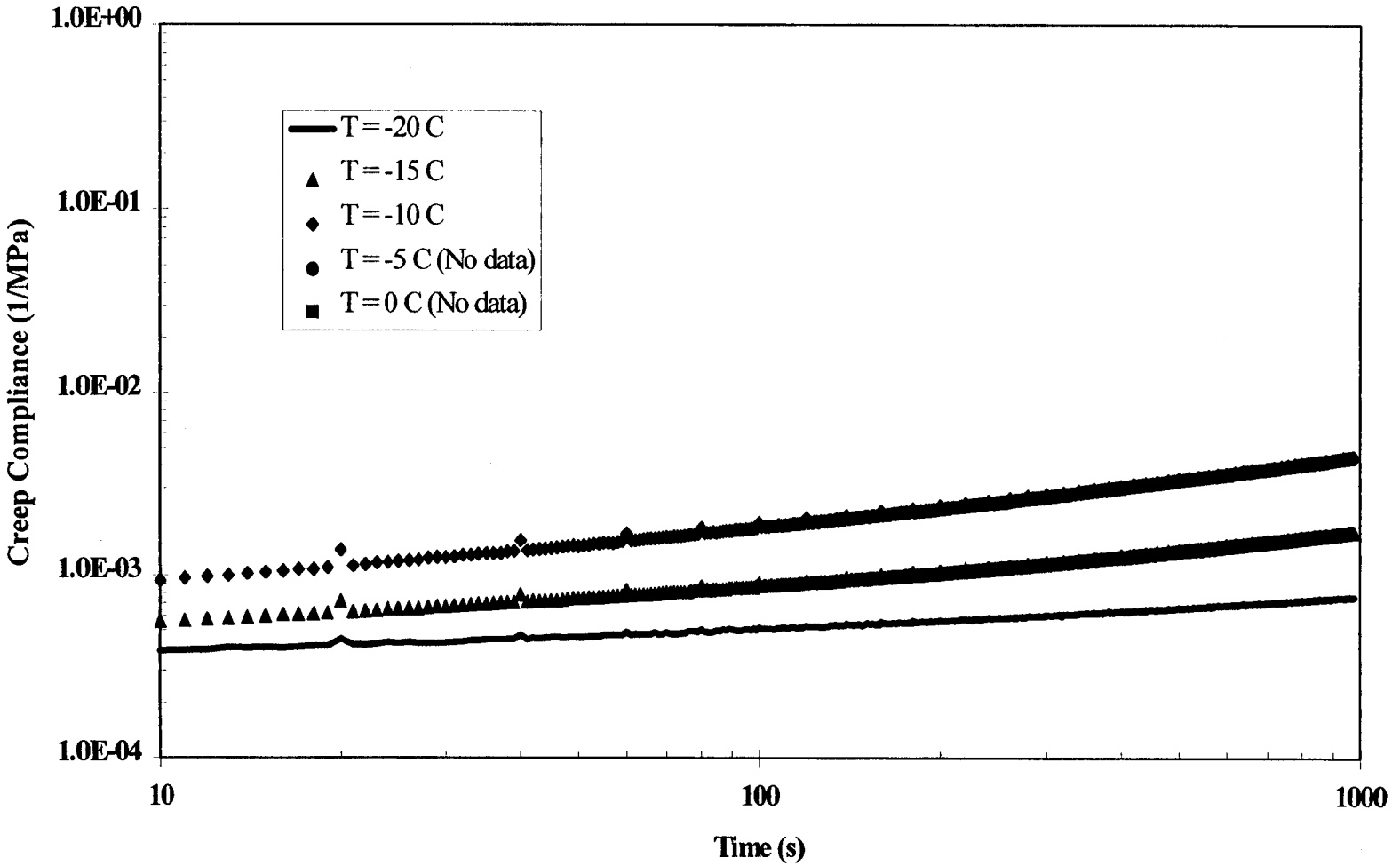

Figure 5.17. Creep Compliance Curves
75 Blow Mix Design, 120/150 pen asphalt

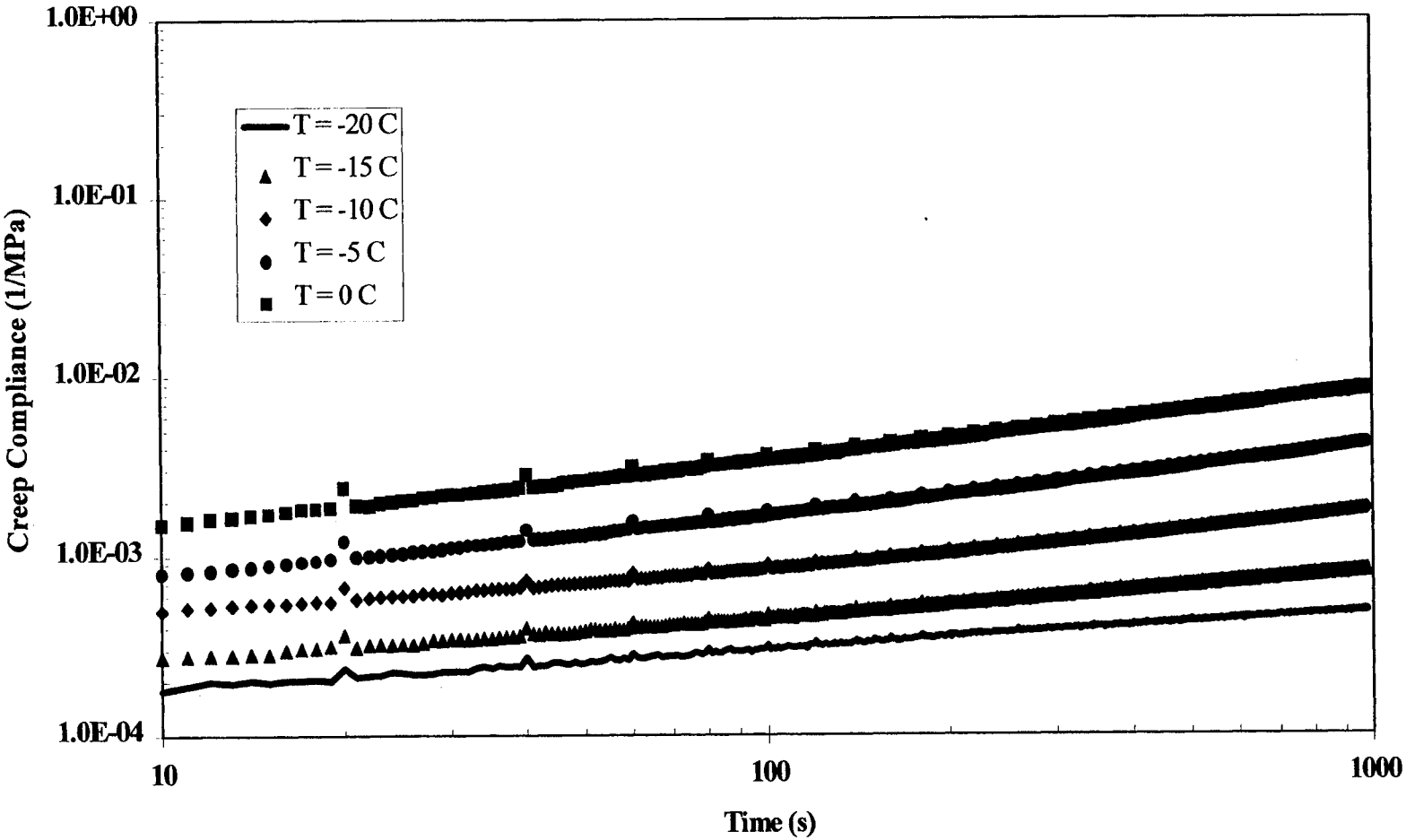

Figure 18. Creep Compliance Curves
75 Blow Mix Design, AC 20 asphalt

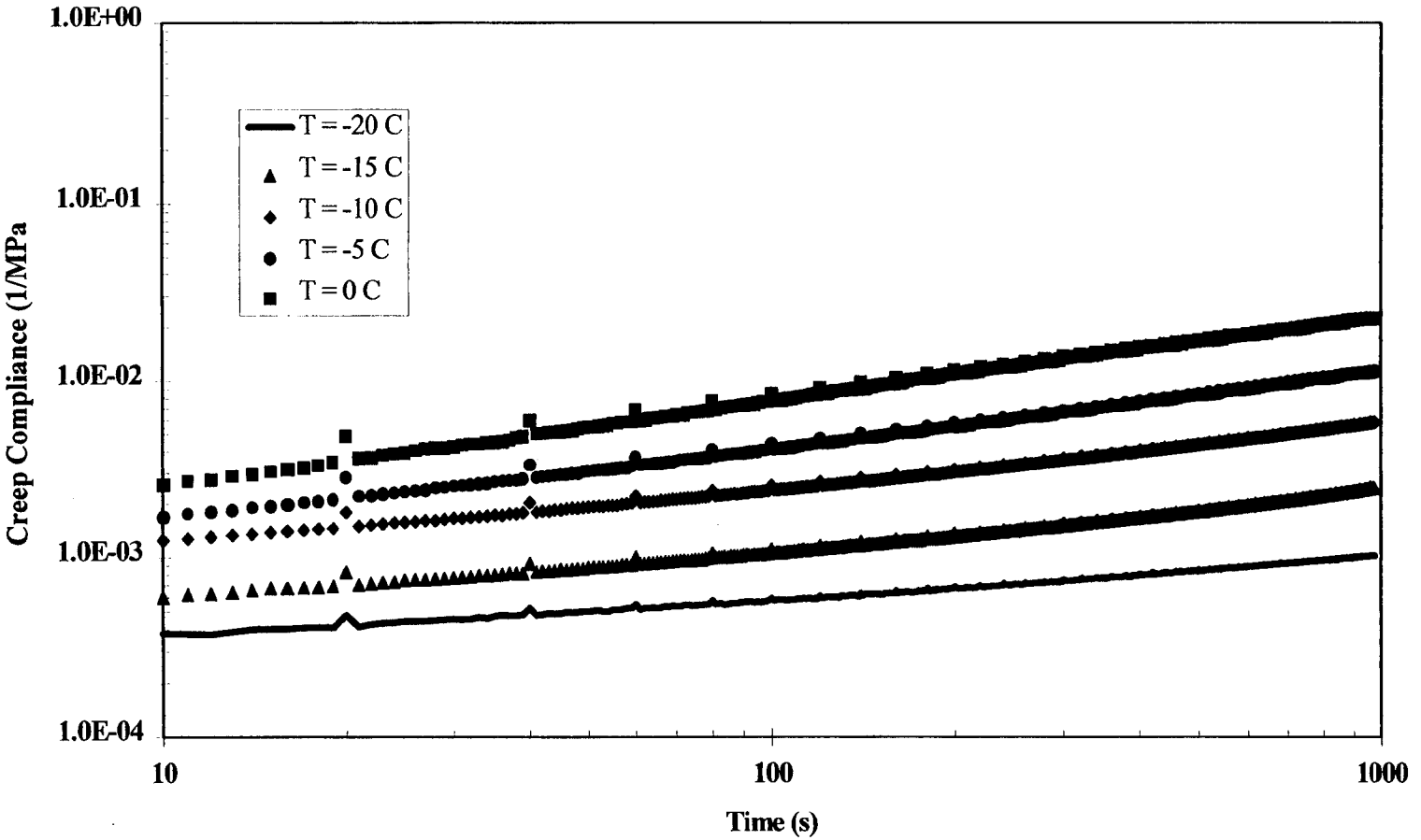

Figure 5.19. Creep Compliance Curves
Gyratory Mix Design, 120/150 pen asphalt

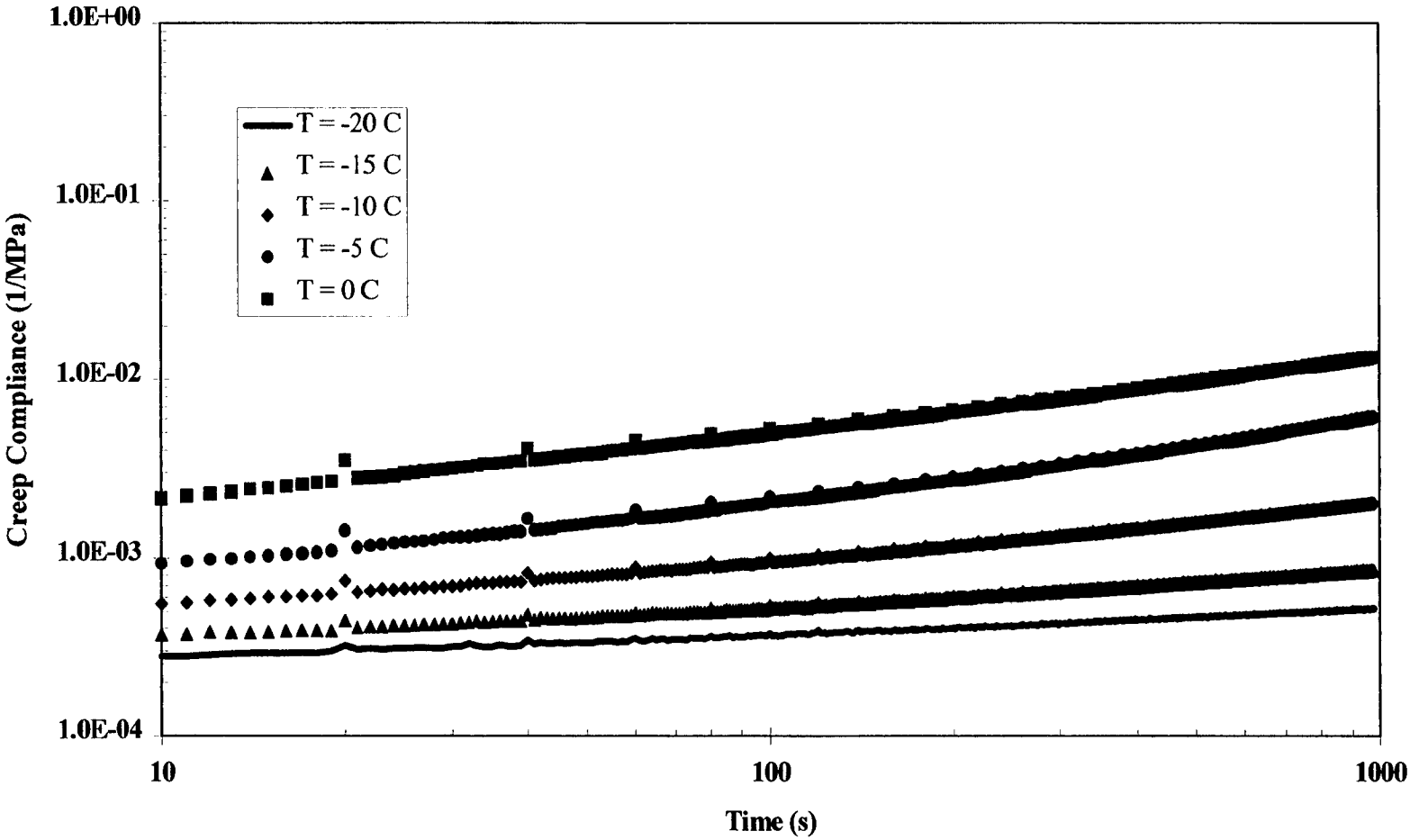

Figure 5.20. Creep Compliance Curves
Gyratory Mix Design, AC 20 asphalt

PERMANENT DEFORMATION

Repeated Load Creep

Tables 5.16 and 5.17 show the repeated load creep test results obtained with both a 0.1- and 1.0-second load duration, respectively. The 0.1-second load duration test results for either temperature show a general trend of increasing creep modulus with decreasing asphalt content for the 120/150 pen asphalt mixtures. This same trend can be seen in the results for the AC 20 at 25°C (77°F). At 40°C (104°F), there is little difference in the creep modulus with asphalt content. Similar trends are seen when the load duration is increased to 1.0 second.

When the loading frequency is increased, the total time a load is applied to the sample during a 1-hour test is increased. The data shows the longer the load is applied to the sample (i.e., the higher the frequency), the higher the compliance calculated at the end of a 1-hour test. This is as expected since the longer the load is applied, the more the sample deforms (i.e., material is more compliant). This is consistent for all of the data, regardless of load duration, test temperature, or confining pressure.

The data indicate that the standard deviation associated with the average creep modulus for a set of three samples increased when confining pressure was used. This was true for either the 25 or 40°C (77 or 104°F) test temperature. Figure 5.21 shows that the creep modulus standard deviation was consistency less than 50 MPa for the 0.1-second load duration [25°C (77°)] test conditions with no confining pressure. When confining pressure was used, the standard deviation increased to about 100 to 250 MPa. There was a clear trend of increasing standard deviation with increasing creep modulus values which would indicate that the coefficient of variation would be a more appropriate statistic. Similar conclusions apply to the results for the 1.0-Hz loading frequency data.

Static Creep

Static creep testing was conducted on the same samples as used for the repeated load testing. This means that the samples were subjected to a total of 11 minutes of preconditioning

load prior to static testing. It was assumed that since the total load duration was the same for both the 0.1-and 1.0-second load duration testing, then these sample sets should be replicates. Since the creep moduli were similar between the two sets of samples (Figures 5.22 and 5.23), it was concluded that this was a reasonable assumption. The results for each set of samples tested at 25°C (77°F) and 40°C (104°F) are shown in Tables 5.18 and 5.19, respectively.

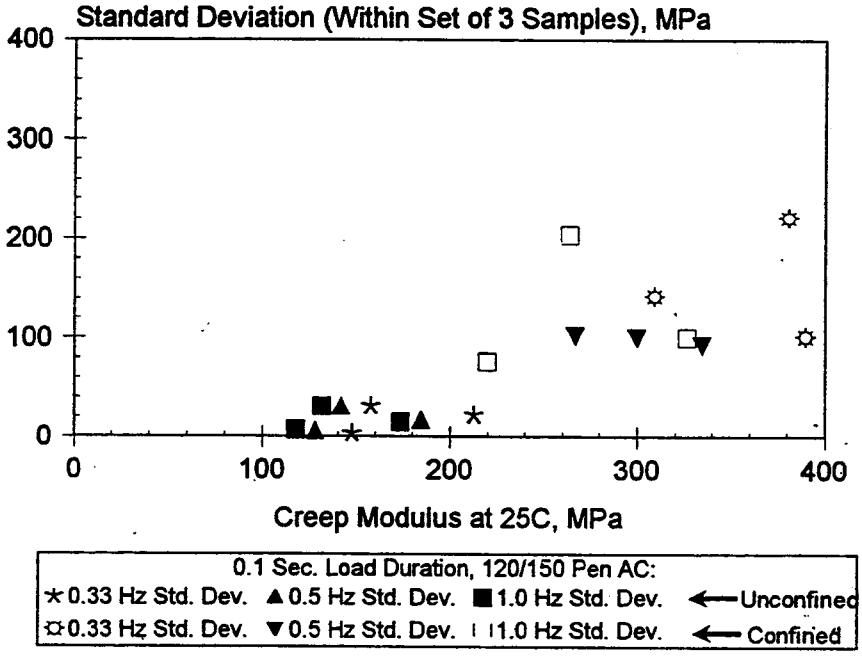

Figure 5.21. Comparison of Creep Modulus for 120/150 Pen AC (0.1 Second Load Duration, 25°C)

Table 5.16. Repeated Load (0.1 Second) Creep Test Results at 25°C After 1 Hr. (120/150 Pen Asphalt).

Test Temp. °C (°F)	Confining Pressure kPa (psi)	Frequency, Hz					
		0.33 Hz		0.5 Hz		1.0 Hz	
		Creep Modulus MPa (ksi)	Creep Compliance MPa^{-1} (ksi^{-1})	Creep Modulus MPa (ksi)	Creep Compliance MPa^{-1} (ksi^{-1})	Creep Modulus MPa (ksi)	Creep Compliance MPa^{-1} (ksi^{-1})
25 (77)	35 Blow Marshall Mixtures						
	None	158 ± 31 (23 ± 5)	0.006 (0.04)	142 ± 31 (21 ± 5)	0.007 (0.05)	132 ± 31 (19 ± 4)	0.008 (0.05)
	207 (30)	309 ± 142 (45 ± 21)	0.003 (0.02)	300± 100 (44 ± 14)	0.003 (0.02)	264± 204 (38 ± 30)	0.004 (0.03)
	50 Blow Marshall Mixtures						
	None	148 ± 4 (22 ± 0.6)	0.007 (0.05)	128 ± 6 (19± 0.9)	0.008 (0.05)	118 ± 7 (17 ± 1)	0.009 (0.06)
	207 (30)	381 ± 221 (55 ± 32)	0.003 (0.02)	267± 102 (39 ± 15)	0.004 (0.03)	220 ± 76 (32 ± 11)	0.005 (0.03)
	75 Blow Marshall Mixtures						
	None	213 ± 22 ((31 ± 3)	0.005 (0.03)	185 ± 17 (27 ± 3)	0.005 (0.04)	174 ± 15 (25 ± 2)	0.006 (0.04)
	207 (30)	390 ± 101 (57 ± 15)	0.003 (0.02)	335 ± 92 (49 ± 13)	0.003 (0.02)	327± 101 (47 ± 15)	0.003 (0.02)
	Gyratory Mix Design[1]						
	None	173 ± 81 (25 ± 12)	0.006 (0.04)	148 ± 79 (22 ± 12)	0.007 (0.05)	138 ± 79 (20 ± 11)	0.007 (0.05)
	207 (30)	251 ± 25 (36 ± 4)	0.004 (0.03)	200 ± 21 (29 ± 30	0.005 (0.03)	171 ± 22 (25 ± 3)	0.006 (0.04)

1: Used Modified Marshall compactor to fabricate samples. Numbers of blows based on obtaining 4% voids.

Table 5.16 (Continued). Repeated Load (0.1 Second) Creep Test Results at 40°C After 1 Hr. (120/150 Pen Asphalt)

Test Temp. °C (°F)	Confining Pressure kPa (psi)	Frequency, Hz					
		0.33 Hz		0.5 Hz		1.0 Hz	
		Creep Modulus MPa (ksi)	Creep Compliance MPa^{-1} (ksi^{-1})	Creep Modulus MPa (ksi)	Creep Compliance MPa^{-1} (ksi^{-1})	Creep Modulus MPa (ksi)	Creep Compliance MPa^{-1} (ksi^{-1})
40 (104)	35 Blow Marshall Mixtures						
	None	39 ± 11 (6 ± 2)	0.025 (0.18)	23 ± 6 (3 ± 0.8)	0.044 (0.30)	12 ± 3 (2 ± 0.4)	0.081 (0.56)
	207 (30)	42 ± 12 (6 ± 2)	0.023 (0.16)	32 ± 12 (5 ± 2)	0.031 (0.21)	23 ± 8 (3 ± 1)	0.044 (0.30)
	50 Blow Marshall Mixtures						
	None	50 ± 10 (7 ± 2)	0.020 (0.14)	40 ± 8 (6 ± 1)	0.024 (0.17)	35 ± 5 (5 ± 0.8)	0.029 (0.20)
	207 (30)	87 ± 39 (13 ± 6)	0.011 (0.08)	65 ± 33 (9 ± 5)	0.015 (0.11)	58 ± 36 (9 ± 5)	0.017 (0.12)
	75 Blow Marshall Mixtures						
	None	58 ± 14 (8 ± 2)	0.017 (0.12)	47 ± 11 (7 ± 2)	0.021 (0.15)	44 ± 11 (6 ± 2)	0.023 (0.16)
	207 (30)	55 ± 23 (8 ± 3)	0.018 (0.13)	40 ± 12 (6 ± 2)	0.025 (0.17)	34 ± 10 (5 ± 1)	0.029 (0.20)
	Gyratory Mix Design[1]						
	None	23 ± 3 (3 0.5)	0.043 (0.30)	18 ± 2 (3 ± 0.3)	0.055 (0.38)	17 ± 3 (2 ± 0.4)	0.060 (0.42)
	207 (30)	86 ± 46 (13 ± 7)	0.012 (0.08)	68 ± 32 (10 ± 5)	0.015 (0.10)	57 ± 26 (8 ± 4)	0.018 (0.12)

1: Used Modified Marshall compactor to fabricate samples. Numbers of blows based on obtaining 4% voids.

Table 5.16 (Continued). Repeated Load (0.1 Second) Creep Test Results at 25°C After 1 Hr. (AC 20 Asphalt)

Test Temp. °C (°F)	Confining Pressure kPa (psi)	Frequency, Hz					
		0.33 Hz		0.5 Hz		1.0 Hz	
		Creep Modulus MPa (ksi)	Creep Compliance MPa^{-1} (ksi^{-1})	Creep Modulus MPa (ksi)	Creep Compliance MPa^{-1} (ksi^{-1})	Creep Modulus MPa (ksi)	Creep Compliance MPa^{-1} (ksi^{-1})
25 (77)	35 Blow Marshall Mixtures						
	None	204 ± 128 (30 ± 19)	0.005 (0.03)	170± 104 (25 ± 15)	0.006 (0.04)	170 ± 72 (25 ± 10)	0.006 (0.04)
	207 (30)	573 ± 235 (83 ± 35)	0.002 (0.01)	496± 230 (72 ± 33)	0.002 (0.01)	421± 357 61 ± 52)	0.002 (0.02)
	50 Blow Marshall Mixtures						
	None	222 ± 36 (32 ± 5)	0.005 (0.03)	150 ± 34 (22 ± 5)	0.007 (0.05)	130 ± 24 (19 ± 3)	0.008 (0.05)
	207 (30)	407 ± 286 (59 ± 42)	0.003 (0.02)	418± 321 (61 ± 47)	0.002 (0.02)	445± 435 (65 ± 63)	0.002 (0.02)
	75 Blow Marshall Mixtures						
	None	92 ± 38 (14 ± 6)	0.010 (0.07)	73 ± 41 (11 ± 6)	0.014 (0.09)	69 ± 32 (10 ± 5)	0.015 (0.10)
	207 (30)	513 ± 166 (74 ± 24)	0.002 (0.01)	499± 174 72 ± 25)	0.002 (0.01)	488± 129 (71 ± 20)	0.002 (0.01)
	Gyratory Mix Design						
	None	Insufficient Material to Complete this Test					
	207 (30)						

Table 5.16 (Continued). Repeated Load (0.1 Second) Creep Test Results 40°C After 1 Hr. (AC 20 Asphalt)

Test Temp. °C (°F)	Confining Pressure kPa (psi)	Frequency, Hz					
		0.33 Hz		0.5 Hz		1.0 Hz	
		Creep Modulus MPa (ksi)	Creep Compliance MPa^{-1} (ksi^{-1})	Creep Modulus MPa (ksi)	Creep Compliance MPa^{-1} (ksi^{-1})	Creep Modulus MPa (ksi)	Creep Compliance MPa^{-1} (ksi^{-1})
40 (104)	35 Blow Marshall Mixtures						
	None	43 ± 3 (6 ± 0.4)	0.023 (0.16)	35 ± 4 (5 ± 0.5)	0.029 (0.09)	34 ± 7 (5 ± 1)	0.030 (0.20)
	207 (30)	145 ± 11 (21 ± 2)	0.007 (0.05)	108 ± 13 (16 ± 2)	0.009 (0.06)	111 ± 23 (16 ± 2)	0.009 (0.06)
	50 Blow Marshall Mixtures						
	None	46 ± 11 (7 ± 2)	0.022 (0.15)	47 ± 18 (7 ± 3)	0.021 (0.15)	35 ± 7 (5 ± 2)	0.029) (0.20)
	207 (30)	146 ± 32 (21± 5)	0.007 (0.05)	113 ± 36 (17 ± 5)	0.009 (0.06)	115 ± 30 (17 ± 4)	0.009 (0.06)
	75 Blow Marshall Mixtures						
	None	42 ± 10 (6 ± 1)	0.024 (0.16)	40 ± 3 (6 ± 0.4)	0.025 (0.17)	48 ± 3 (7 ± 0.5)	0.009 (0.06)
	207 (30)	84 ± 19 (12 ± 3)	0.012 (0.08)	64 ± 16 (9 ± 2)	0.016 (0.11)	57 ± 15 (8 ± 2)	0.018 (0.12)
	Gyratory Mix Design						
	None	Insufficient Material to Complete this Test					
	207 (30)						

Table 5.17. Repeated Load (1.0 Second) Creep Test Results 25°C After 1 Hr. (120/150 Pen Asphalt)

Test Temp. °C (°F)	Confining Pressure kPa (psi)	Frequency, Hz					
		0.033 Hz		0.05 Hz		0.1 Hz	
		Creep Modulus MPa (ksi)	Creep Compliance MPa^{-1} (ksi^{-1})	Creep Modulus MPa (ksi)	Creep Compliance MPa^{-1} (ksi^{-1})	Creep Modulus MPa (ksi)	Creep Compliance MPa^{-1} (ksi^{-1})
25 (77)	35 Blow Marshall Mixtures						
	None	87 ± 17 (13 ± 3)	0.011 (0.08)	69 ± 15 (10 ± 2)	0.015 (0.10)	58 ± 14 (8 ± 2)	0.017 (0.12)
	207 (30)	364 ± 163 (53 ± 24)	0.003 (0.02)	314± 144 (46 ± 21)	0.003 (0.02)	309± 148 (45 ± 22)	0.003 (0.02)
	50 Blow Marshall Mixtures						
	None	89 ± 17 (13 ± 3)	0.011 (0.08)	75 ± 18 (11 ± 3)	0.013 (0.09)	72 ± 23 (10 ± 3)	0.014 (0.10)
	207 (30)	192 ± 46 (28 ± 7)	0.005 (0.04)	165 ± 50 (24 ± 7)	0.006 (0.04)	156 ± 55 (23 ± 8)	0.006 (0.04)
	75 Blow Marshall Mixtures						
	None	186 ± 38 (27 ±6)	0.005 (0.04)	143 ± 27 (21 ± 4)	0.007 (0.04)	123 ± 22 (18 ± 3)	0.008 (0.06)
	207 (30)	388 ± 98 (56 ± 14	0.003 (0.02)	324 ± 82 (47 ± 12)	0.003 (0.02)	315 ± 79 (46 ± 11)	0.003 (0.02)
	Gyratory Mix Design[1]						
	None	112 ± 37 (16 ± 5)	0.009 (0.06)	85 ± 21 (12 ± 3)	0.004 (0.03)	74 ± 14 (11 ± 2)	0.014 (0.09)
	207 (30)	252 ± 30 (37 ± 4)	0.005 (0.03)	209 ± 53 (30 ± 8)	0.005 (0.03)	187 ± 60 (27 ± 9)	0.005 (0.04)

1: Used Modified Marshall compactor to fabricate samples. Numbers of blows based on obtaining 4% voids.

Table 5.17 (Continued). Repeated Load (1.0 Second) Creep Test Results 40°C After 1 Hr. (120/150 Pen Asphalt)

Test Temp. °C (°F)	Confining Pressure kPa (psi)	Frequency Between Loads, Hz					
		0.033 Hz		0.05 Hz		0.1 Hz	
		Creep Modulus MPa (ksi)	Creep Compliance MPa^{-1} (ksi^{-1})	Creep Modulus MPa (ksi)	Creep Compliance MPa^{-1} (ksi^{-1})	Creep Modulus MPa (ksi)	Creep Compliance MPa^{-1} (ksi^{-1})
40 (104)	35 Blow Marshall Mixtures						
	None	24 ± 2 (3 ± 0.3)	0.042 (0.29)	15 ± 0 (2 ± 0)	0.066 (0.45)	7 ± 1 (1 ± 0.2)	0.135 (0.91)
	207 (30)	35 ± 8 (5 ± 1)	0.029 (0.20)	25 ± 4 (4 ± 0.6)	0.041 (0.28)	19 ± 3 (4 ±0.6)	0.054 (0.37)
	50 Blow Marshall Mixtures						
	None	33 ± 4 (5 ± 0.6)	0.030 (0.21)	30 ± 5 (4 ± 0.8)	0.034 (0.23)	27 ± 6 (4 ± 0.9)	0.036 (0.25)
	207 (30)	67 ± 8 (10 ± 1)	0.015 (0.10)	47 ± 4 (7 ± 0.5)	0.021 (0.15)	39 ± 5 (6 ± 0.7)	0.026 (0.18)
	75 Blow Marshall Mixtures						
	None	35 ± 3 (5 ± 0.4)	0.029 (0.20)	28 ± 1 (4 ± 0.2)	0.036 (0.25)	27 ± 2 (4 ± 0.2)	0.037 (0.26)
	207 (30)	50 ± 21 (7 ± 3)	0.020 (0.14)	34 ± 7 (5 ±1)	0.029 (0.20)	28 ± 4 (4 ± 0.6)	0.036 (0.25)
	Gyratory Mix Design[1]						
	None	24 ± 4 (3 ± 0.5)	0.042 (0.29)	20 ± 4 (3 ± 0.5)	0.051 (0.35)	16 ± 3 (2 ± 0.5)	0.063 (0.43)
	207 (30)	68 ± 1 (10 ± 0.1)	0.015 (0.10)	53 ± 1 (8 ± 0.1)	0.019 (0.13)	51 ± 2 (7 ± 0.3)	0.020 (0.14)

1: Used Modified Marshall compactor to fabricate samples. Numbers of blows based on obtaining 4% voids.

Table 5.17 (Continued). Repeated Load (1.0 Second) Creep Test Results 25°C After 1 Hr. (AC 20 Asphalt)

Test Temp. °C (°F)	Confining Pressure kPa (psi)	Frequency Between Loads, Hz					
		0.033 Hz		0.05 Hz		0.1 Hz	
		Creep Modulus MPa (ksi)	Creep Compliance MPa^{-1} (ksi^{-1})	Creep Modulus MPa (ksi)	Creep Compliance MPa^{-1} (ksi^{-1})	Creep Modulus MPa (ksi)	Creep Compliance MPa^{-1} (ksi^{-1})
25 (77)	35 Blow Marshall Mixtures						
	None	97 ± 14 (14 ± 2)	0.010 (0.07)	78 ± 18 (11 ± 3)	0.013 (0.09)	71 ± 21 (10 ± 3)	0.014 (0.10)
	207 (30)	400 ± 12 (58 ± 2)	0.003 (0.02)	303 ± 28 (44 ± 4)	0.003 (0.02)	298 ± 29 (43 ± 4)	0.003 (0.02)
	50 Blow Marshall Mixtures						
	None	341 ± 106 (50 ± 15)	0.003 (0.02)	216 ± 31 (31 ± 5)	0.005 (0.03)	229 ± 34 (33 ± 5)	0.004 (0.03)
	207 (30)	242 ± 55 (35 ± 8)	0.004 (0.03)	194 ± 22 (28 ± 3)	0.005 (0.04)	172 ± 10 (25 ± 1)	0.006 (0.04)
	75 Blow Marshall Mixtures						
	None	94 ± 10 (14 ± 2)	0.011 (0.07)	70 ± 8 (10 ± 1)	0.014 (0.10)	59 ± 9 (9 ± 1)	0.017 (0.12)
	207 (30)	270 ± 90 (39 ± 13)	0.004 (0.03)	233 ± 85 (34 ± 12)	0.004 (0.03)	228 ± 97 (33 ± 14)	0.004 (0.03)
	Gyratory Mix Design						
	None	Insufficient Material to Complete this Test					
	207 (30)						

Table 5.17 (Continued). Repeated Load (1.0 Second) Creep Test Results 40°C After 1 Hr. (AC 20 Asphalt)

Test Temp. °C (°F)	Confining Pressure kPa (psi)	Frequency Between Loads, Hz					
		0.033 Hz		0.05 Hz		0.1 Hz	
		Creep Modulus MPa (ksi)	Creep Compliance MPa^{-1} (ksi^{-1})	Creep Modulus MPa (ksi)	Creep Compliance MPa^{-1} (ksi^{-1})	Creep Modulus MPa (ksi)	Creep Compliance MPa^{-1} (ksi^{-1})
40 (104)	35 Blow Marshall Mixtures						
	None	31 ± 5 (5 ± 0.7)	0.032 (0.22)	20 ± 10 (3 ± 1)	0.051 (0.34)	22 ± 2 (3 ±0.2)	0.047 (0.32)
	207 (30)	36 ± 8 (5 ± 1)	0.028 (0.19)	24 ± 4 (4 ± 0.6)	0.042 (0.29)	14 ± 2 (2 ± 0.2)	0.071 (0.48)
	50 Blow Marshall Mixtures						
	None	27 ± 0 (4 ± 0)	0.037 (0.26)	21 ± 0 (3 ± 0)	0.047 (0.32)	18 ± 0 (3 ± 0)	0.057 (0.38)
	207 (30)	52 ± 23 (8 ± 3)	0.019 (0.13)	44 ± 26 (6 ± 4)	0.023 (0.16)	37 ± 23 (5 ± 3)	0.027 (0.19)
	75 Blow Marshall Mixtures						
	None	45 ± 3 (7 ± 0.4)	0.022 (0.15)	52 ± 13 (8 ± 2)	0.019 (0.13)	56 ± 22 (8 ± 3)	0.018 (0.12)
	207 (30)	58 ± 5 (8 ± 0.7)	0.017 (0.12)	46 ± 1 (7 ± 0.2)	0.022 (0.15)	38 ± 1 (6 ± 0.2)	0.026 (0.18)
	Gyratory Mix Design						
	None	Insufficient Material to Complete This Test					
	207 (30)						

As with the repeated load creep testing, there was a slight increase in the creep modulus with decreasing asphalt cement content. The creep modulus and compliance for the 120/150 pen mixtures shown in the tables were calculated at 30 minutes rather than at the end of the test (i.e., at 60 minutes) because several of the mixtures failed after 30 but before 60 minutes. The selection of the 30 minute time allowed a more complete comparison of test results. These show that the test method variability was exceptionally high; the standard deviations ranged from 12 to around 50 percent of the mean value (i.e., coefficient of variation). Trends were as expected: the creep modulus increased with confining pressure and decreased with increasing test temperature. Again, as anticipated, the creep modulus increased and the creep compliance of the AC 20 asphalt mixtures decreased when confining pressure was used. However, creep modulus for the AC 20 mixtures was similar to the 120/150 pen asphalt mixtures with the same asphalt content when there was no confining pressure. In general, there was a slight increase in the creep modulus of the higher viscosity AC 20 asphalt mixtures when compared to the 120/150 pen asphalt mixtures when confining pressure was used.

Table 5.18. Static Creep Results (25°C).

Test Temp. °C (°F)	Confining Pressure kPa (psi)	Creep Modulus MPa (ksi)		Creep Compliance MPa^{-1} (ksi^{-1})	
		120/150 Pen	AC 20	120/150 Pen	AC 20
25 (77)	35 Blow Marshall Mixtures				
	None	55 (8) ± 17 (3) 38 (6) ± 2 (0.2)	56 (8) ± 8 (1) 39 (6) ± 10 (2)	0.018 (0.13) 0.027 (0.18)	0.018 (0.12) 0.025 (0.17)
	207 (30)	67 (10) ± 1 (0.1) 63 (9) ± 26 (4)	93 (13) ± 34 (5) 103 (15) ± 8 (1)	0.015 (0.10) 0.016 (11)	0.011 (0.08) 0.010 (0.07)
	50 Blow Marshall Mixtures				
	None	58 (8) ± 2 (0.2) 45 (7) ± 11 (2)	54 (8) ± 13 (2) 67 (10) ± 6 (0.8)	0.017 (0.12) 0.022 (0.15)	0.019 (0.13) 0.015 (0.10)
	207 (30)	60 (9) ± 3 (0.5) 69 (10) ± 14 (2)	107 (16) ± 36 (5) 84 (12) ±9 (1)	0.017 (0.09) 0.014 (0.10)	0.009 (0.06) 0.012 (0.08
	75 Blow Marshall Mixtures				
	None	70 (10) ± 4 (0.6) 59 (9) ± 2 (0.3)	38 (6) ± 9 (1) 35 (5) ± 6 (0.9)	0.014 (0.10) 0.017 (0.12)	0.027 (0.18) 0.029 (0.200)
	207 (30)	78 (11) ± 9 (1) 99 (14) ± 17 (3)	118 (17) ± 16 (2) 97 (14) ± 27 (4)	0.013 (0.09) 0.010 (0.07)	0.009 (0.06) 0.010 (0.07)
	Gyratory				
	None	71 ± 46 (10 ± 7)	Not Available	0.014 (0.10)	Not Available
	207 (30)	69 ± 17 (10 ± 3)		0.015 (0.10)	

NA: indicates only one sample survived testing.

Table 5.19. Static Creep Results (40°C)

Test Temp. °C (°F)	Confining Pressure kPa (psi)	Creep Modulus MPa (ksi)		Creep Compliance MPa^{-1} (ksi^{-1})	
		120/150 Pen	AC 20	120/150 Pen	AC 20
40 (104)	35 Blow Marshall Mixtures				
	None	Failed Failed	23 (3) ± 6 (0.8) 16 (2) ± 0.8 (0.1)	Failed Failed	0.043 (0.30) 0.064 (0.44)
	207 (30)	Failed 11 (2) ± 3 (0.5)	52 (8) ± 7 (1) Failed	Failed 0.089 (0.59)	0.019 (0.06) Failed
	50 Blow Marshall Mixtures				
	None	16 (2) ± 11 (2) 19 (3) ± 4 (0.6)	10 (1) ± NA 38 (5) ± NA	0.065 (0.043) 0.053 (0.37)	0.105 (0.71) 0.027 (0.19)
	207 (30)	21 (3) ± 3 (0.4) 25 (4) ± 4 (0.6)	60 (9) ± 19 (3) 14 (2) ± 3 (0.5)	0.048 (0.33) 0.040 (0.28)	0.017 (0.22) 0.071 (0.48)
	75 Blow Marshall Mixtures				
	None	26 (4) ± 7 (1.0) 21 (3) ± 1 (0.2)	24 (4) ± NA 10 (1) ± NA	0.038 (0.26) 0.047 (0.32)	0.041 (0.28) 0.105 (0.71)
	207 (30)	20 (3) ± 5 (0.8) 21 (3) ± (0.2)	31 (5) ± 8 (1) 28 (4) ± 0.7 (0.1)	0.050 (0.34) 0.047 (0.32)	0.032 (0.22) 0.036 (0.25)
	Gyratory				
	None	11 ± 1 (2 ± 0.2)	Not Available	0.092 (0.63)	Not Available
	207 (30)	31 ± 11 (5 ± 2)		0.032 (0.22)	

NA: indicates only one sample survived testing.

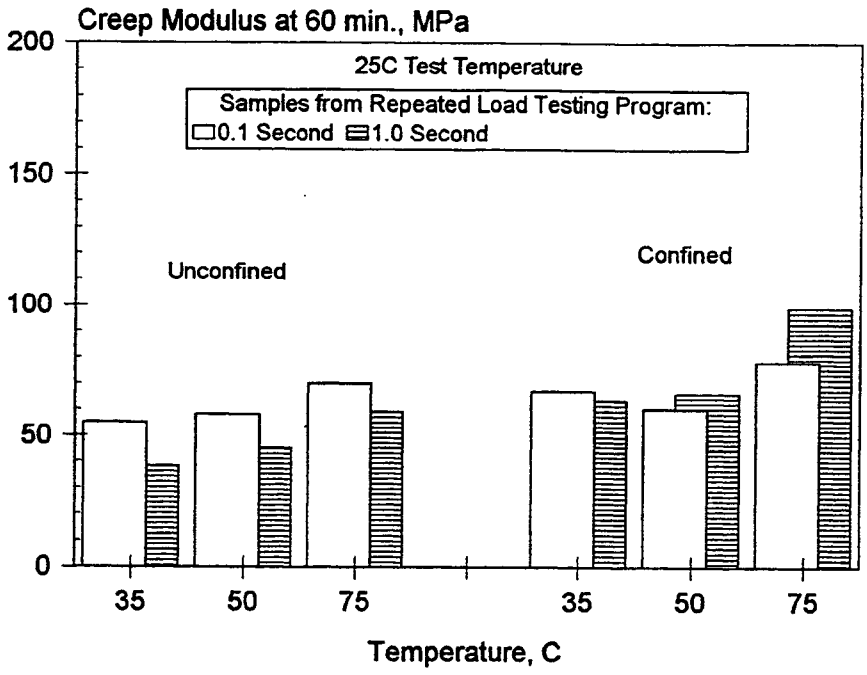

Figure 5.22. Comparison of Static Creep Sample Sets (25°C).

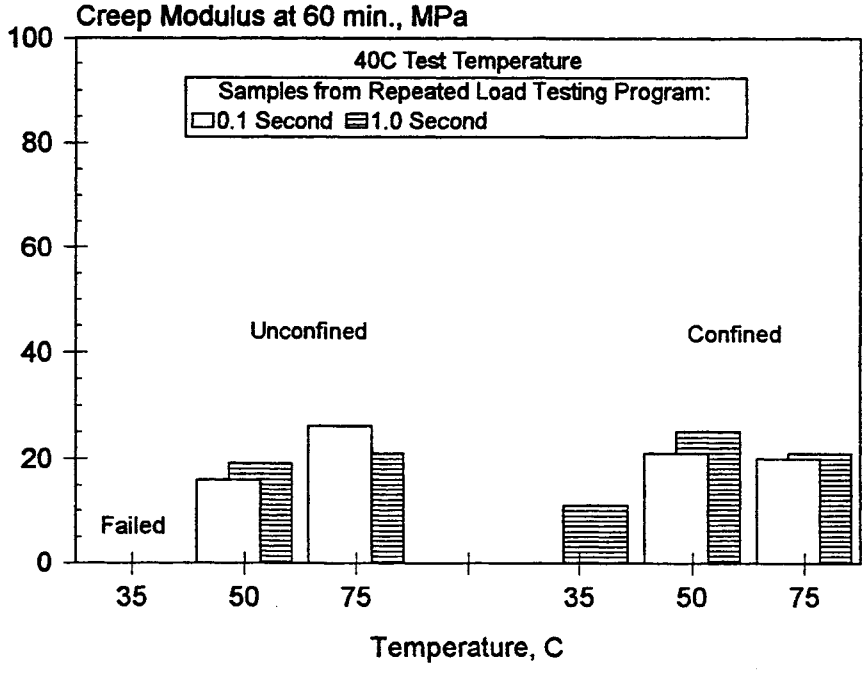

Figure 5.23. Comparison of Static Creep Sample Sets (40°C).

CHAPTER SIX
BEHIND-THE-PAVER MATERIAL PROPERTIES

INTRODUCTION

This chapter presents the characteristics of the asphalt mixtures as they occurred in material which has been processed through the hot-mix plant, but not yet compacted. The samples were taken from random locations within the test cells by shoveling material from behind the paver into buckets, and then sealing the buckets. The labeled samples were then stored for testing at a later date.

At the time of testing, the buckets were heated to loosen the asphalt mixtures. The mixtures were placed into heated molds, and compacted with the appropriate amount of effort using either the Marshall or gyratory devices.

PRELIMINARY INVESTIGATION

Material from test cell 2 was selected for a study of the anticipated material variability between lifts throughout a given test cell. If the material showed that properties were acceptably uniform (i.e., within the test method variabilities established in the previous chapter), then the testing of the remaining cells could be reduced. The materials used for this analysis are shown in Table 6.1.

Prior to any testing, the air voids were determined for all samples used in this study. Samples were compacted using the numbers of blows used in the mix design. These results are shown in Table 6.2. These results are fairly consistent between both the stations and the lifts. The range was typically less than 1.5 percent voids for either a given lift or location. These variations are similar to those reported by Braun Intertec, Inc. (8).

Table 6.1. Behind-the-paver Material Tested for Test Cell 2 (35 Blow).

Sample Date	Course	Lift	Station	Offset
9-28-93	Wear	3rd	1108+87	Left
	Base	2nd	1108+67	Left
	Base	1st	1108+78	Left
9-28-93	Wear	3rd	1111+08	Right
	Base	2nd	1111+02	Right
	Base	1st	1110+73	Right
9-28-93	Wear	3rd	1112+11	Left
	Base	2nd	1111+77	Left
	Base	1st	1111+71	Left
9-28-93	Wear	3rd	1113+89	Right
	Base	2nd	1113+05	Right
	Base	1st	1113+54	Right

Table 6.2. Percent Air Voids for Test Cell 2 (35 Blow).

General Sampling Station Location	Lift		
	Top	Middle	Bottom
1108	3.7	5.8	4.7
1110	5.1	5.1	3.7
1111	4.3	4.8	4.9
1113	4.9	4.2	4.6
Average	4.5	5.0	4.5

Temperature Susceptibility

Resilient Modulus ASTM D4123

The average resilient modulus test results from a set of three samples are shown in Table 6.3; the loading conditions were limited to the 0.1 second-load duration and 0.33, 0.5 and 1.0 Hz frequencies. The variability was found to be statistically similar to that obtained for the mix design materials in the previous chapter. Therefore, all comparisons of results assumed coefficients of variability of 3.2, 2.1, and 6.0 (log transformed data) for test temperatures of -18, 0 through 25, and 40°C (0, 34 through 77, and 104°F), respectively, to determine if results were statistically different.

Table 6.3 and Figure 6.1 show that there was very good agreement between the values obtained for each lift. This indicated that material properties could be assumed uniform throughout the test cell. Based on these data, future testing of the Mn/ROAD behind-the-paver materials was limited to randomly selecting one sample per lift. One specimen was prepared from each behind-the-paver sample and this composite set of samples was considered representative of the material properties of the test cell. If the variability of this set of specimens exceeded the acceptable testing variability criteria (i.e., coefficients of variation), then the individual values were examined to determine if a more thorough investigation of each lift was warranted.

Table 6.3. Temperature Susceptibility (Resilient Modulus Testing) for Each Lift of Test Cell 2 (35 Blow) Behind-the-Paver Material.

Temperature	Resilient Modulus at Various Temperatures, MPa (ksi)								
	Lift								
	Top			Middle			Bottom		
	Frequency, Hz								
	0.33	0.5	1.0	0.33	0.5	1.0	0.033	0.05	0.1
-18°C (0°F)	15,714 (2,279)	16,403 (2,378)	15,914 (2,308)	16,071 (2,330)	15,550 (2,255)	16,478 (2,390)	14,380 (2,085)	14,431 (2,093)	14,135 (2,137)
1°C (34°F)	9,150 (1,237)	9,74 (1,316)	9,303 (1,349)	8,695 (1,261)	8,619 (1,249)	9,101 (1,319)	8,452 (1,225)	8,752 (1,269)	19,070 (1,315)
25°C (77°F)	2,633 (288)	2,558 (371)	2,495 (362)	2,465 (358)	2,336 (338)	2,298 (333)	2,557 (371)	2,476 (359)	2,469 (349)
40°C (104°F)	821 (119)	779 (113)	732 (106)	779 (113)	730 (106)	657 (96)	821 (119)	731 (106)	699 (101)

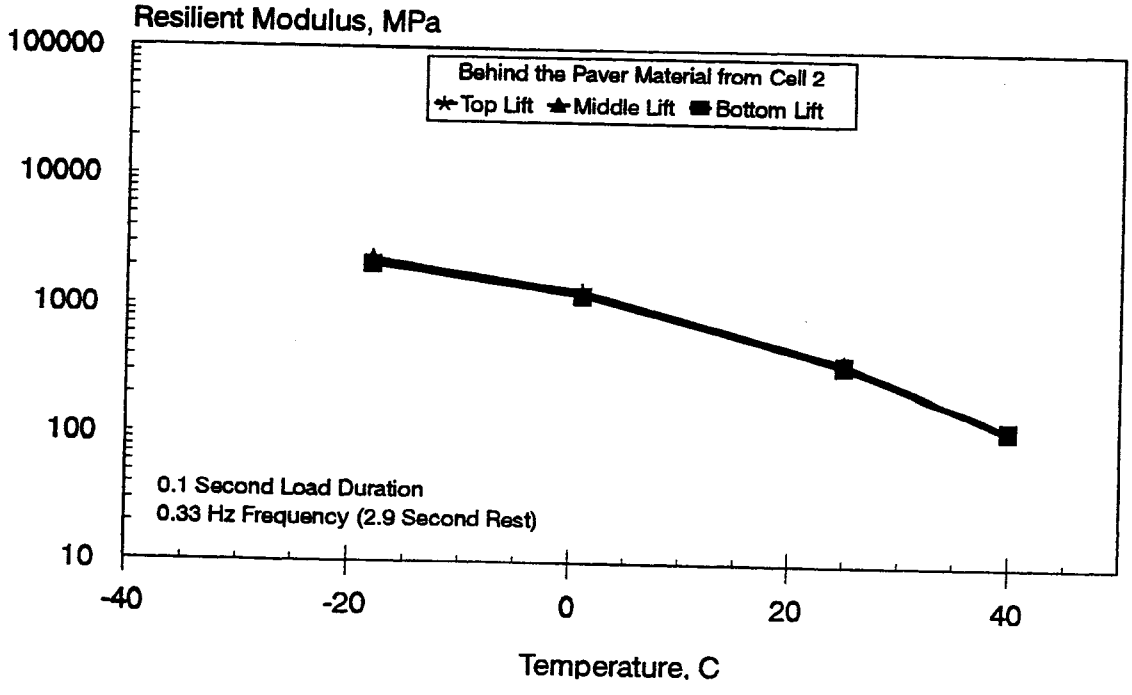

Figure 6.1. Comparison of Resilient Moduli versus Temperature for Each Lift in Test Cell 2 (35 Blow).

Low Temperature Susceptibility

Indirect Tensile (Constant Rate of Deformation)

Only the colder -18°C (0°F) test temperature was used for this evaluation in order to limit testing time. The test results, shown in Table 6.4, indicate that both the tensile strength and corresponding horizontal displacement for each lift were statistically similar between the lifts. This confirms the previous conclusion that there was no statistical difference in material properties between the lifts.

5-YEAR MAINLINE

Since there did not appear to be significant differences between the lifts, test results presented in this section were developed for a set of three samples, with each sample within a set randomly selected from a different lift and station within the cell.

Resilient Modulus (ASTM D4123)

Table 6.5 shows the results for each of the four test cells. There appears to be a limited dependence of modulus on asphalt content with the modulus increasing slightly as the asphalt content decreases. As noted in the previous section, longer load durations correspond to lower moduli values.

Moisture Sensitivity (ASTM D4687)

Moisture sensitivity testing was not completed for these test cells as the initial comparison of the mixture properties for the same type of mixtures from the 5- and 10-Year Mainline test cells appeared to have similar properties. Therefore, the full testing matrix was completed for only the 10-Year Mainline test cells.

Table 6.4. Low Temperature Behavior (120/150 Pen Asphalt Mixtures).

Constant Rate of Vertical Deformation mm/min (in/min)	Test Temperature, -18°C (0°F)	
	Maximum Tensile Strength kPa (psi)	Corresponding Horizontal Strain $\mu\epsilon$
Top Lift		
0.025 (0.001)	2,663 ± 166 (386 ± 24)	694 ± 141
0.25 (0.01)	3,303 ± 213 (479 ± 31)	427 ± 109
Middle Lift		
0.025 (0.001)	2,564 ± 90 (372 ± 13)	687 ± 175
0.25 (0.01)	3,051 ± 103 (443 ± 15)	400 ± 199
Bottom Lift		
0.025 (0.001)	2,386 ± 358 (346 ± 52)	639 ± 285[1]
0.25 (0.01)	3,337 ± 182 (484 ± 27)	294 ± 56[1]

1: One data point removed from data base prior to calculation of statistics due to unreasonable results.

Low Temperature Behavior

Table 6.6 shows the results for each of the four test cells. The strains at -18°C (0°F) for test cell 2 (35 blow mix design) are substantially lower than strains for any other test cells. Since the test cell 2 material was tested about 4 months earlier than the other three test cells, this difference may reflect slow changes in the mixtures with storage time. It may also reflect operator variability as different technicians tested the test cells 2 and test cells 1, 3, and 4 mixtures. All equipment, sensors, and computer programs were the same for all mixtures.

The data in Table 6.6 shows an increase in the maximum tensile strength with increasing deformation rate while the corresponding horizontal deformation varies only slightly with the deformation rate. Tensile strengths decreased with increasing test temperatures, however the corresponding horizontal strains showed only a slight increase with the change in test temperature.

Table 6.5. Temperature Susceptibility (Resilient Modulus Testing) for the 5-Year Mainline Behind-the-Paver Material.

Temperature, °C (°F)	Resilient Modulus, MPa (ksi)							
	Frequency, Hz							
	0.1 Second Load Duration			1.0 Second Load Duration				
	0.33	0.5	1.0	0.33	0.5	0.033	0.05	0.1
Test Cell 1 (120/150 Pen AC, 75 Blow)								
-18 (0)	19,270 (2,751)	21,670 (3,143)	20,856 (3,025)	18,488 (2,725)	17,120 (2,483)	12,059 (1,749)	14,927 (2,165)	15.575 (2,259)
1 (34)	8,301 (1,204)	8,914 (1,293)	9,121 (1,323)	6,908 (1,002)	7,080 (1,027)	6,136 (890)	6,736 (977)	7,081 (1,027)
10 (50)	6784 (984)	6,887 (999)	7,074 (1,026)	4,764 (691)	5,122 (743)	4,006 (581)	4,420 (641)	4,523 (656)
25 (77)	2,923 (424)	2,834 (411)	2,806 (407)	1,351 (196)	1,344 (195)	1,268 (184)	1,172 (170)	1,137 (165)
40 (104)	922 (144)	896 (130)	848 (123)	337 (49)	324 (47)	345 (50)	338 (49)	234 (47)
Test Cell 2 (120/150 Pen AC, 35 Blow)								
-18 (0)	15,714 (2,279)	16,403 (2,378)	15,914 (2,308)	Data Not Available				
1 (34)	9,150 (1,237)	9,74 (1,316)	9,303 (1,349)					
10 (50)	NA	NA	NA					
25 (77)	2,633 (288)	2,558 (371)	2,495 (362)					
40 (104)	821 (119)	779 (113)	732 (106)					

Table 6.5. (Continued) Temperature Susceptibility (Resilient Modulus Testing) for the 5-Year Mainline Behind-the-paver Material.

Temperature, °C (°F)	Resilient Modulus, MPa (ksi)							
	Frequency, Hz							
	0.1 Second Load Duration			1.0 Second Load Duration				
	0.33	0.5	1.0	0.33	0.5	0.033	0.05	0.1
Test Cell 3 (120/150 Pen AC, 50 Blow)								
-18 (0)	15,782 (2,289)	15,734 (2,282)	15,809 (2,293)	15,403 (2,234)	17,140 (2,486)	12,266 (1,779)	13,851 (2,009)	14,638 (2,123)
1 (34)	7,736 (1,122)	7,798 (1,131)	8,142 (1,181)	6,323 (917)	7,398 (1,073)	4,909 (712)	5,674 (823)	5,784 (839)
10 (50)	5,585 (810)	5,453 (791)	5,647 (819)	3,923 (569)	4,475 (649)	3,392 (492)	3,709 (538)	3,730 (541)
25 (77)	2,213 (321)	2,227 (323)	2,185 (317)	1,027 (149)	1,061 (154)	1,096 (159)	958 (139)	917 (133)
40 (104)	896 (130)	792 (115)	730 (106)	345 (50)	386 (56)	Samples too Soft to Test		
Test Cell 4 (120/150 Pen AC, Gyratory)								
-18 (0)	17,099 (2,480)	17,264 (2,504)	17,899 (2,596)	16,623 (2,411)	16,851 (2,444)	12,617 (1,830)	14,927 (2,165)	16,051 (2,328)
1 (34)	9,825 (1,425)	10,121 (1,468)	10,528 (1,527)	7,666 (1,112)	8,046 (1,167)	6,150 (892)	6,895 (1,000)	7,384 (1,071)
10 (50)	6,219 (902)	6,633 (962)	6,998 (1,015)	4,888 (709)	4,950 (718)	3,613 (524)	4,240 (615)	4,302 (624)
25 (77)	2,840 (412)	2,737 (397)	2,758 (400)	1,324 (192)	1,544 (224)	1,324 (192)	1,165 (169)	1,165 (169)
40 (104)	1,144 (166)	965 (140)	931 (135)	393 (57)	359 (52)	303 (44)	283 (41)	290 (42)

Permanent Deformation

Permanent deformation testing was not completed for these test cells as the initial comparison of the mixture properties for the same type of mixtures from the 5- and 10-Year Mainline test cells appeared to have similar properties. Therefore, the full testing matrix was completed for only the 10-Year Mainline test cells.

Table 6.6. Low Temperature Behavior for the 5-Year Mainline Behind-the-Paver Materials.

Rate of Vertical Displacement mm/min (in/min)	Test Temperature,-18°C (0°F)		Test Temperature, 1°C (34°F)	
	Maximum Tensile Strength kPa (psi)	Corresponding Horizontal Strain 10^{-6} $\mu\epsilon$	Maximum Tensile Strength kPa (psi)	Corresponding Horizontal Strain 10^{-6} $\mu\epsilon$
Test Cell 1 (120/150 Pen AC, 75 Blow)				
.025 (0.001)	2,875 ± 144 (417 ± 21)	824 ± 138	910 ± 83 (132 ± 12)	1,104 ± 27
0.25 (0.01)	3,447 ± 379 (500 ± 55)	1,102 ± 136	1,303 ± 76 (189 ± 11)	1,171 ±124
Test Cell 2 (120/150 Pen AC, 35 Blow)				
.025 (0.001)	2,537 ± 140 (368 ± 20)	673 ± 30	Not Available	
0.25 (0.01)	3,230 ± 156 (469 ± 23)	374 ± 70		
Test Cell 3 (120/150 Pen AC, 50 Blow)				
.025 (0.001)	2,916 ± 69 (423 ± 10)	1,008 ± 103	717 ± 35 (104 ± 5)	1,353 ± 260
0.25 (0.01)	3,675 ± 69 (533 ± 10)	1,065 ±27	1,158 ± 131 (168 ± 19)	1,286 ± 187
Test Cell 4 (120/150 Pen AC, Gyratory)				
.025 (0.001)	2,885 ± 234 (433 ± 34)	969 ± 169	861 ± 42 (125 ± 6)	1,288 ± 139
0.25 (0.01)	3,592 ± 310 (521 ± 45)	1,019 ± 308	1,378 ± 69 (200 ± 10)	1,237 ± 97

1: One data point removed from data base prior to calculation of statistics due to unreasonable results.

10 YEAR MAINLINE

As with the 5-Year Mainline test cells, the data presented in this section is based on the average of three samples tested. Each sample for a given set was randomly selected from a different lift and station within the cell.

Resilient Modulus (ASTM D4123)

Table 6.7 shows the results for each of the ten test cells. Figure 6.2 shows that while there is some difference between the 120/150 Pen and AC 20 asphalt at the warmer test temperatures, there was no statistical difference between the results for different test cells with the same mixture. This suggests that mixture properties for a given binder content and grade of asphalt are similar regardless of test cell.

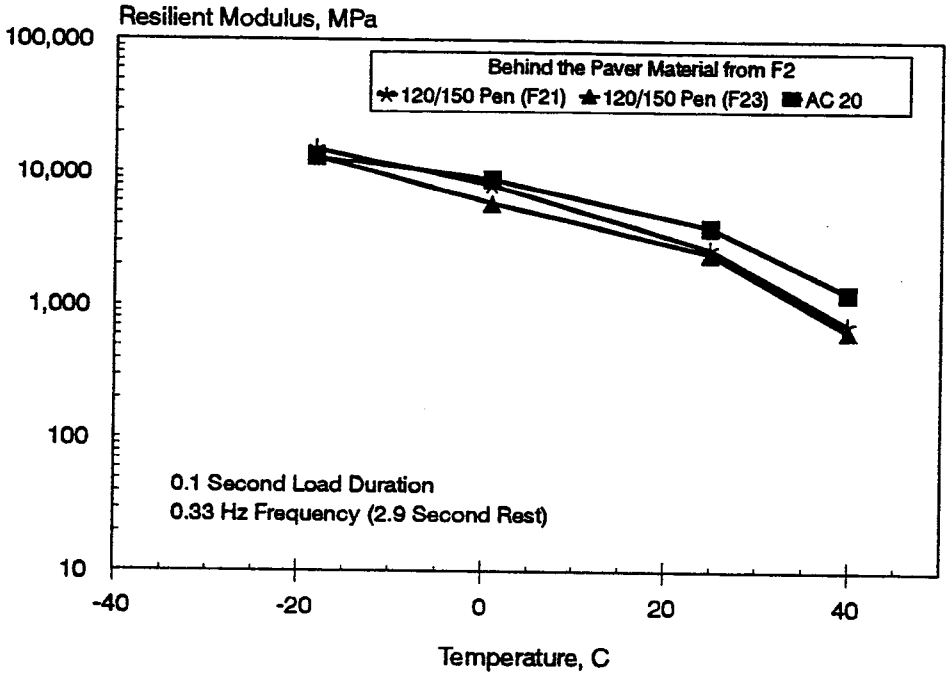

Figure 6.2. Resilient Modulus at Various Temperatures (10-Year Mainline).

Table 6.7. Resilient Modulus at Various Temperatures for the 10-Year Mainline (0.1 Second Load Duration, Various Frequencies)

Temperature, °C (°F)	Resilient Modulus, MPa (ksi)		
	0.33 Hz	0.5 Hz	1.0 Hz
Cell 14, 120/150 Pen AC (75 Blows)			
-18 (0)	10,421 (1,511)	10,945 (1,587)	11,007 (1,596)
1 (34)	7,455 (1,081)	7,808 (1,132)	8,200 (1,189)
25 (77)	3,207 (465)	3,614 (524)	3,834 (556)
40 (104)	848 (123)	772 (112)	738 (107)
Cell 15, AC 20 (75 Blows)			
-18 (0)	14,020 (2,033)	14,848 (2,153)	15,628 (2,266)
1 (34)	8,386 (1,245)	8,752 (1,269)	9,186 (1,332)
25 (77)	3,683 (534)	3,586 (520)	3,593 (521)
40 (104)	1,055 (153)	972 (141)	952 (138)
Cell 16, AC 20 (Gyratory)			
-18 (0)	15,561 (2,256)	17,223 (2,497)	18,457 (2,676)
1 (34)	10,839 (1,572)	11,002 (1,595)	11,002 (1,595)
25 (77)	3,600 (522)	3,683 (534)	3,678 (533)
40 (104)	1,211 (176)	1,092 (158)	1,064 (154)
Cell 17, AC20 (75 Blows)			
-18 (0)	15,151 (2,197)	15,683 (2,274)	16,290 (2,362)
1 (34)	10,986 (1,593)	10,066 (1,590)	11,731 (1,701)
25 (77)	4,441 (644)	4,407 (639)	4,428 (642)
40 (104)	1,303 (189)	1,186 (172)	1,138 (165)
Cell 18, AC20 (50 Blows)			
-18 (0)	13,262 (1,923)	12,828 (1,860)	13,310 (1,930)
1 (34)	8,993 (1,304)	9,228 (1,338)	9,586 (1,361)
25 (77)	3,886 (563)	4,055 (588)	4,186 (607)
40 (104)	1,248 (181)	1,138 (165)	1,062 (154)

Table 6.7 (Continued). Resilient Modulus at Various Temperatures for the 10-Year Mainline (0.1 Second Load Duration, Various Frequencies)

Temperature, °C (°F)	Resilient Modulus, MPa (ksi)		
	0.33 Hz	0.5 Hz	1.0 Hz
Cell 19, AC20 (35 Blows)			
-18 (0)	13,221 (1,917)	13,517 (1,960)	14,260 (2,059)
1 (34)	8,303 (1,204)	8,352 (1,211)	8,717 (1,264)
25 (77)	3,786 (549)	4,021 (583)	4,138 (600)
40 (104)	572 (83)	579 (84)	579 (84)
Cell 20, 120/150 Pen AC (35 Blows)			
-18 (0)	12,372 (1,1794)	13,786 (1,999)	13,869 (2,011)
1 (34)	7,469 (1,083)	7,469 (1,083)	7,738 (1,132)
25 (77)	2,993 (434)	3,007 (426)	2,979 (432)
40 (104)	855 (124)	869 (126)	786 (114)
Cell 21, 120/150 Pen AC (50 Blows)			
-18 (0)	15,159 (2,198)	15,99 (2,317)	16,021 (2,323)
1 (34)	8,159 (1,183)	8421 (1,221)	8,779 (1,273)
25 (77)	2,683 (389)	2,614 (379)	2,579 (374)
40 (104)	724 (114)	697 (101)	662 (96)
Cell 22, 120/150 Pen AC (75 Blows)			
-18 (0)	14,966 (2,170)	15,848 (2,298)	16,510 (2,394)
1 (34)	7,710 (1,118)	7,717 (1,119)	8,007 (1,161)
25 (77)	2,379 (345)	2,352 (341)	2,317 (336)
40 (104)	786 (114)	697 (101)	662 (96)
Cell 23, 120/150 Pen AC (50 Blows)			
-18 (0)	13,172 (1,910)	13,083 (1,879)	13,172 (1,910)
1 (34)	5,924 (859)	6,076 (881)	6,234 (904)
25 (77)	2,469 (358)	2,476 (359)	2,510 (364)
40 (104)	648 (94)	662 (96)	621 (90)

Moisture Sensitivity (ASTM D4867)

Table 6.8 shows the results for each of the ten 10-Year Mainline test cells. Figures 6.3 and 6.4 show both the unconditioned (dry) and conditioned (wet) resilient modulus and tensile strengths, respectively. These figures show data grouped first by asphalt grade and then by decreasing asphalt content. In general, the 120/150 pen asphalt mixtures have lower tensile strengths than the AC 20 mixtures. No clear trends in resilient modulus values are evident due to changes in asphalt content. However, the unconditioned (dry) tensile strengths appear to decrease with asphalt content. This trend is more obvious with the AC 20 mixtures. It is this lower initial strength that appears to contribute to the high retained strength ratios seen in Figure 6.5 for the gyratory mixtures.

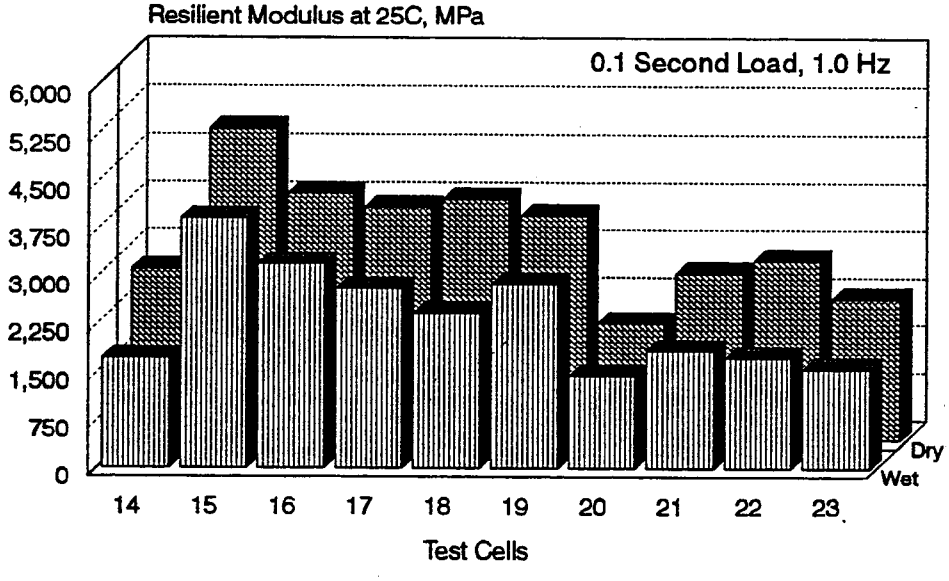

Figure 6.3. Unconditioned and Conditioned Resilient Modulus Values (10-Year Mainline).

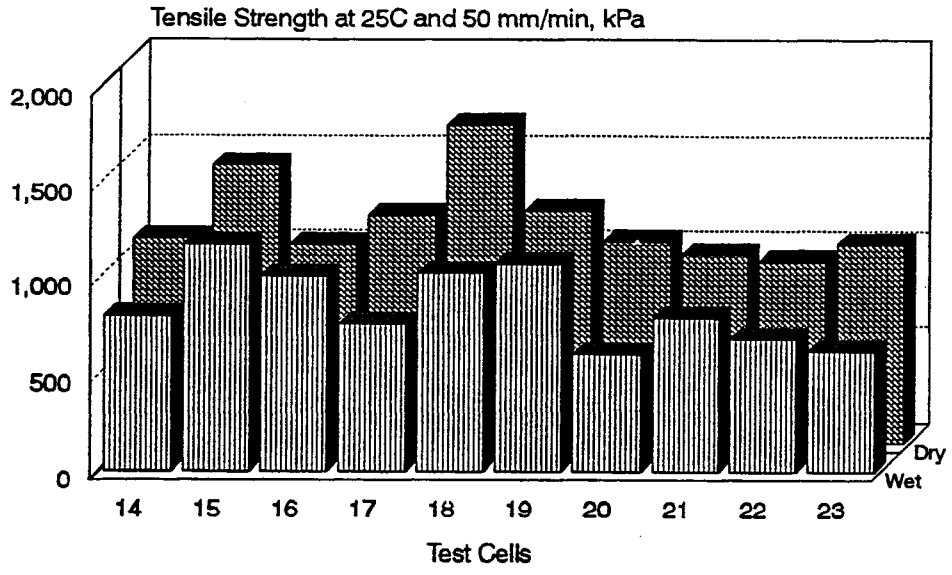

Figure 6.4. Unconditioned and Conditioned Tensile Strengths (10-Year Mainline).

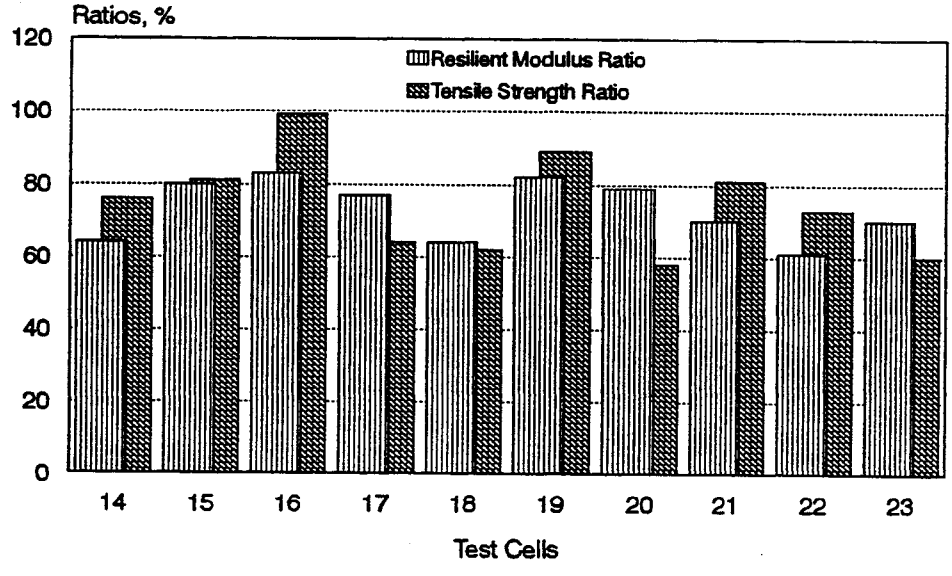

Figure 6.5. Resilient Modulus and Tensile Strength Ratios (10-Year Mainline).

Table 6.8. Moisture Sensitivity Test Results for 10-Year Mainline Mixtures.

Mn/ROAD Test Cell	Air Voids, %	Resilient Modulus, MPa (ksi) 0.1 Sec. Load, 1 Hz.			Tensile Strength, kPa (psi)		
		Dry 25°C (77°F)	Wet 25°C (77°F)	Ratio, %	Dry 25°C (77°F)	Wet 25°C (77°F)	Ratio, %
Cell 14, 120/150 Pen 75 Blows	4.5	2,676 (388)	1,724 (250)	64	1,058 (153)	800 (116)	76
Cell 15, AC20 75 Blows	4.4	4,891 (709)	3,936 (571)	80	1,450 (210)	1,178 (171)	81
Cell 16, AC20 Gyratory	4.1	3,876 (562)	3,207 (465)	83	1,028 (149)	1,014 (147)	99
Cell 17, AC20 75 Blows	4.1	3,661 (531)	2,827 (410)	77	1,188 (173)	761 (110)	64
Cell 18, AC20 50 Blows	4.0	3,786 (549)	2,434 (353)	64	1,660 (241)	1,028 (149)	62
Cell 19, AC 20 35 Blows	3.9	3,529 (512)	2,897 (420)	82	1,208 (175)	1,074 (156)	89
Cell 20, 120/150 Pen 35 Blows	4.0	1,825 (265)	1,446 (210)	79	1,046 (152)	604 (88)	58
Cell 21, 120/150 Pen 50 Blows	4.1	2,621 (380)	1,841 (267)	70	977 (142)	793 (115)	81
Cell 22, 120/150 Pen 75 Blows	4.2	2,822 (409)	1,732 (251)	61	942 (137)	684 (99)	73
Cell 23, 120/150 Pen 50 Blows	3.9	2,215 (321)	1,558 (226)	70	1,034 (150)	622 (90)	60

Low Temperature Behavior

Table 6.9 shows the results for each of the ten test cells. Testing was limited to the 1°C (34°F) due to time constraints. Only the two slower loading rates were used as these were considered more representative of the slow build-up of thermal stresses in the pavement.

Table 6.9. Low Temperature Behavior (Constant Rate of Deformation, 1°C (34°F).

Mn/ROAD Test Cell	0.025 mm/min (0.001 in/min)		0.25 mm/min (0.010 in/min)	
	Maximum Tensile Strength, kPa (psi)	Corresponding Horizontal Strain, $\mu\epsilon$	Maximum Tensile Strength, kPa (psi)	Corresponding Horizontal Strain, $\mu\epsilon$
Cell 14, 120/150 Pen 75 Blows	697 (101)	2,615	1,145 (166)	2,632
Cell 15, AC20 75 Blows	959 (139)	1,868	1,572 (228)	1,534
Cell 16, AC20 Gyratory	892 (129)	1,751	1,552 (226)	2,467
Cell 17, AC20 75 Blows	986 (143)	1,796	1,559 (226)	2,034
Cell 18, AC20 50 Blows	945 (137)	1,862	1,559 (226)	2,354
Cell 19, AC 20 35 Blows	828 (120)	2,380	1,179 (171)	3,023
Cell 20, 120/150 Pen 35 Blows	668 (97)	2,971	1,036 (150)	2,923
Cell 21, 120/150 Pen 50 Blows	710 (103)	3,097	1,110 (161)	3,089
Cell 22, 120/150 Pen 75 Blows	752 (109)	2,635	1,145 (166)	2,580
Cell 23, 120/150 Pen 50 Blows	641 (93)	2,402	1,152 (167)	3,123

Permanent Deformation

The results from both the repeated load and static creep tests are shown in Table 6.10. Because the preceding results indicated that the AC20 and 75 blow mix design materials used in cells 15 and 17 were similar, only one set of three samples was prepared and tested for these two cells. Cells 14 and 22 were also combined (120/150 pen asphalt, 75 blow). Because the trends in creep behavior for the 1-second loading were similar to those for the 0.1-second loading conditions, testing was limited to the latter load duration for the repeated load creep test. At 40°C (104°F), the statistics were similar for the 0.1 and 1.0 second load durations. This was also the most severe test temperature as several samples failed at this temperature.

LOW VOLUME ROAD

The data for both the 5 and 10-Year Mainline test cells showed that there was no statistically significant difference in test results for a given asphalt content and grade of binder. Therefore, a set of three samples was prepared for each mixture variable with materials for each sample within a set being randomly selected from different lifts and different test cells.

Resilient Modulus (ASTM D4123)

Table 6.11 shows the results for each of the mixtures used in the Low Volume Road facility.

Moisture Sensitivity (ASTM D4687)

The moisture sensitivity testing was not completed for the Low Volume Road facilities due to time and available material constraints. However, the original tensile strengths of the mixtures at 25°C (77°F) and a deformation rate of 50 mm/min (2 in/min) were determined for the purpose of comparing the Low Volume Road materials with those from the 5- and 10-Year Mainline. These results are shown in Table 6.12.

Table 6.10. Repeated Load Creep and Static Creep Test Results for the 10-Year Mainline.

Frequency, Hz	Creep Modulus, MPa (ksi)	Creep Compliance MPa^{-1} (ksi^{-1})
Cells 14 and 22 (120/150 Pen AC, 75 Blow)		
0.33	63 (9) ± 22 (3)	0.016 (0.11)
0.5	47 (7) ± 45 (6)	0.021 (0.15)
1.0	17 (3) ± 10 (1)	0.058 (0.40)
Static	Failed	
Cells 15 and 17 (AC20, 75 Blow)		
0.33	33 (5) ± 2 (0.3)	0.031 (0.21)
0.5	28 (4) ± 4.5 (0.7)	0.035 (0.24)
1.0	28 (4) ± 10 (1.4)	0.036 (0.25)
Static	18 (3) ± 6 (0.9)	0.054 (0.37)
Cells 16 (AC20, Gyratory)		
0.33	47 (7) ± 15 (2)	0.021 (0.15)
0.5	40 (6) ± 16 (2)	0.025 (0.17)
1.0	39 (6) ± 18 (3)	0.025 (0.18)
Static	21 (3) ± 13 (2)	0.047 (0.32)
Cells 18 (AC20, 50 Blow)		
0.33	81 (12) ± 48 (7)	0.012 (0.08)
0.5	70 (10) ± 42 (6)	0.014 (0.10)
1.0	66 (10) ± 42 (6)	0.015 (0.10)
Static	37 (5) ± NA	0.027 (0.19)

NA: Only one sample survived testing

Table 6.10 (Continued). Repeated Load Creep and Static Creep Test Results for the 10-Year Mainline.

Frequency, Hz	Creep Modulus, MPa (ksi)	Creep Compliance MPa^{-1} (ksi^{-1})
Cell 19 (AC20, 35 Blow)		
0.33	52 (8) ± NA	0.019 (0.13)
0.5	47 (7) ± NA	0.021 (0.15)
1.0	36 (5) ± NA	0.028 (0.19)
Static	Failed	
Cell 20 (120/150 Pen AC, 35 Blow)		
0.33	14 (2) ± 9 (1)	0.070 (0.48)
0.5	Failed	
1.0	Failed	
Static	Failed	
Cells 21 and 23 (120/150 Pen AC, 50 Blow)		
0.33	52 (8) ± 14 (2)	0.019 (0.13)
0.5	40 (6) ± 8 (1)	0.025 (0.18)
1.0	17 (3) ± 10 (1)	0.058 (0.40)
Static	Failed	

Table 6.11. Resilient Modulus at Various Temperatures for the Low Volume Road. (0.1 Second Load Duration, Various Frequencies)

Temperature, °C (°F)	Resilient Modulus, MPa (ksi)		
	0.33 Hz	0.5 Hz	1.0 Hz
Cell 24 (120/150 Pen AC, 35 blow)			
-18 (0)	12,245 ± 1,041 (1,776 ± 151)	13,335 ± 1,048 (1,937 ± 152)	14,817 ± 786 (2,149 ± 114)
1 (34)	7,171 ± 241 (1,040 ± 35)	7,688 ± 207 (1,115 ± 30)	7,564 ± 117 (1,097 ± 17)
25 (77)	2,668 ± 331 (387 ± 48)	2,744 ± 310 (398 ± 45)	2,861 ± 379 (415 ±55)
40 (104)	538 ± 48 (78 ± 7)	496 ± 28 (72 ± 4)	469 ± 41 (68 ± 8)
Cell 25 (120/150 Pen AC, 50 Blow)			
-18 (0)	11,501 ± 1,034 (1,668 ± 150)	11,873 ± 648 (1,722 ± 94)	12,259 ± 627 (1,778 ± 91)
1 (34)	7,460 ± 172 (1,082 ± 25)	7,997 ± 69 (1,160 ± 10)	8,184 ± 241 (1,187 ± 35)
25 (77)	2,551 ± 407 (370 ± 59)	2,496 ± 379 (362 ± 55)	2,503 ± 400 (363 ± 58)
40 (104)	752 ± 76 (109 ± 11)	718 ± 76 (104 ± 11)	669 ± 69 (97 ± 10)
Cell 26 (120/150 Pen AC, 50 Blow)			
-18 (0)	10,535 ± 228 (1,528 ± 33)	11,927 ± 579 (1,730 ± 84)	12,831 ± 821 (1,861 ± 119)
1 (34)	7,729 ± 352 (1,121 ± 51)	8,329 ± 731 (1,208 ± 106)	8,488 ± 462 (1,231 ± 67)
25 (77)	2,534 ± 338 (382 ± 49)	2,696 ± 276 (391 ± 40)	2,758 ± 345 (400 ± 50)
40 (104)	758 ± 112 (110 ± 20)	758 ± 117 (110 ± 17)	689 ± 97 (100 ± 14)

Table 6.11 (Continued). Resilient Modulus at Various Temperatures for the Low Volume Road.(0.1 Second Load Duration, Various Frequencies)

Temperature, °C (°F)	Resilient Modulus, MPa (ksi)		
	0.33 Hz	0.5 Hz	1.0 Hz
Cell 27 (120/150 Pen AC, 35 blow)			
-18 (0)	10,100 ± 1,096 (1,465 ± 159)	11,190 ± 676 (1,623 ± 98)	11,997 ± 200 (1,740 ± 29)
1 (34)	7,874 ± 214 (1,142 ± 31)	8,136 ± 276 (1,180 ± 40)	8,397 ± 593 (1,218 ± 86)
25 (77)	2,551 ± 482 (370 ± 70)	2,517 ± 496 (365 ± 72)	2,544 ± 469 (369 ± 68)
40 (104)	1,076 ± 28 (156 ± 4)	952 ± 110 (138 ± 16)	889 ± 69 (129 ± 10)
Cell 28 (120/150 Pen AC, 50 Blow)			
-18 (0)	9.356 ± 565 (1,357 ± 82)	9,673 (1,403 ± 24)	10,649 ± 117 (1,546 ± 17)
1 (34)	7,757 ± 352 (1,125 ± 51)	7,646 ± 234 (1,109 ± 34)	8,136 ± 428 (1,180 ± 62)
25 (77)	2,551 ± 83 (370 ± 12)	2,689 ± 41 (390 ± 6)	2,826 ± 69 (410 ± 10)
40 (104)	689 ± 62 (100 ± 9)	641 ± 28 (93 ± 4)	586 ± 62 (85 ± 9)
Cell 29 (120/150 Pen AC, 50 Blow)			
-18 (0)	9,232 ± 1,172 (1,339 ± 170)	9,184 ± 159 (1,332 ± 23)	10,597 ± 683 (1,537 ± 99)
1 (34)	6,061 ± 559 (879 ± 81)	6,585 ± 407 (955 ± 59)	6,874 ± 703 (997 ± 102)
25 (77)	2,937 ± 207 (426 ± 30)	2,986 ± 200 (433 ± 29)	2,034 ± 166 (440 ± 24)
40 (104)	683 ± 69 (99 ± 10)	600 ± 35 (87 ± 5)	572 ± 35 (83 ± 5)

Table 6.11 (Continued). Resilient Modulus at Various Temperatures for the Low Volume Road.(0.1 Second Load Duration, Various Frequencies)

Temperature, °C (°F)	Resilient Modulus, MPa (ksi)		
	0.33 Hz	0.5 Hz	1.0 Hz
Cell 30 (120/150 Pen AC, 75 blow)			
-18 (0)	12,652 ± 1,565 (1,835 ± 227)	12,955 ± 1,331 (1,897 ± 193)	13,638 ± 200 (1,978 ± 145)
1 (34)	8,667 ± 1,951 (1,257 ± 283)	9,556 ± 2,841 (1,386 ± 412)	9,791 ± 3,137 (1,420 ± 455)
25 (77)	3,468 ± 552 (503 ± 80)	3,365 ± 579 (488 ± 84)	3,358 ± 579 (487 ± 84)
40 (104)	1,138 ± 241 (165 ± 35)	910 ± 166 (132 ± 24)	869 ± 166 (126 ± 24)
Cell 31 (120/150 Pen AC, 75 Blow)			
-18 (0)	12,507 ± 1,172 (1,814 ± 170)	12,513 ± 1,110 (1,815 ± 161)	12,451 ± 772 (1,806 ± 112)
1 (34)	7,626 ± 552 (1,106 ± 80)	7,805 ± 607 (1,132 ± 88)	8,026 ± 393 (1,164 ± 57)
25 (77)	2,792 ± 62 (405 ± 9)	2,772 ± 179 (402 ± 26)	2,834 ± 221 (411 ± 32)
40 (104)	1,096 ± 90 (159 ± 13)	938 ± 69 (136 ± 10)	924 ± 76 (134 ± 11)

Table 6.12 Tensile Strength Values for the Low Volume Road.

Test Cell	Tensile Strength kPa (psi) 25°C (77°F), 50 mm/min (2 in/min)
	1.0 Hz
Cell 24 (35 Blow)	814 (118) ±48 (7)
Cell 25 (50 Blow)	965 (140) ± 5.8 (0.7)
Cell 26 (50 Blow)	959 (139) ± 21 (3)
Cell 27 (35 Blow)	841 (122) ± 41 (6)
Cell 28 (50 Blow)	869 (126) ± 21 (3)
Cell 29 (50 Blow)	917 (133) ±21 (3)
Cell 30 (75 Blow)	1,103 (160) ± 90 (13)
Cell 31 (75 Blow)	1,007 (146) ± 21 (3)

Low Temperature Behavior

Low temperature testing was not completed for these test cells as the initial comparison of the mixture properties for the same type of mixtures from the LVR and 10-Year Mainline test cells appeared to have similar properties. Therefore, the full testing matrix was completed for only the 10-Year Mainline test cells.

Permanent Deformation

Permanent deformation testing was not completed for these test cells as the initial comparison of the mixture properties for the same type of mixtures from the LVR and 10-Year Mainline test cells appeared to have similar properties. Therefore, the full testing matrix was completed for only the 10-Year Mainline test cells.

This Page Intentionally Blank

CHAPTER SEVEN
IN-PLACE PROPERTIES

INTRODUCTION

The materials were characterized as they existed in-place immediately after field compaction by testing the separated lifts of field cores. It is often believed that the properties of the asphalt mixtures in the field are the most important in terms of predicting the performance of the upper layer of the pavement.

All the cores used for testing the in-place characteristics were obtained at the time of sensor placement. Therefore, these data represent material obtained from within the test cells rather than from the areas reserved for coring in the transition areas. All cores were obtained prior to any traffic loadings.

Testing of the cores was limited to the temperature susceptibility, ASTM D4123 (0.1-sec. load and 0.3, 0.5 and 1.0 Hz), tensile strengths at 25°C (77°F) and 25 mm/min (2 in.), and low-temperature behavior at a constant rate of displacement. Moisture sensitivity testing was eliminated because of the storage history of the cores which could be assumed to influence test results. Creep testing was eliminated because the height of most of the cores was less than the needed 200 mm (8 in.).

5-YEAR MAINLINE

Table 7.1 presents the location and testing program for all cores tested for the 5-Year Mainline portion of Mn/ROAD.

In-Place Density

One of the most important mixture characteristics that influences pavement performance is the in-situ air void content of the asphalt mixtures. Therefore, every effort was made to ensure accurate measurement of the in-place voids. A comparison of test results between the University of Minnesota and Mn/DOT laboratories was conducted and a separate report was prepared. A full discussion of this comparison can be found in Appendix A. Briefly, it indicated that the

University void calculations for the Mn/ROAD cores were consistently lower than those reported by Mn/DOT. This difference was attributed to differences in the sample preparation of the cores prior to determining the maximum specific gravity. The University results are shown in Table 7.2, and with the exception of test cell 2 (35-blow), were around anticipated values.

Table 7.1. Location of Cores and Scheduled Testing Programs (5-Year Mainline).

Sample Date	Cell	Station	Offset	Field I.D.	Testing
10-22-93	1	1103+98	8' Rt.	1	Temp. susc., ITS @ 25°C
		1103+98	6' Rt.	2	Low temp. behavior, 1°C, 0.25 mm/min
		1104+00	8' Rt.	3	Low temp. behavior, -18°C, 0.25 mm/min
		1105+39	2' Rt.	5	Temp. susc., ITS @ 25°C
		1105+39	1' Lt.	6	Low temp. behavior, 1°C, 0.025 mm/min
		1106+71	8' Rt.	9	Temp. susc., ITS @ 25°C
		1106+71	6' Rt.	10	Low temp. behavior, -18°C, 0.025 mm/min
10-22-93	2	1109+70	3' Rt.	13	Temp. susc., ITS @ 25°C
		1109+70	1'Rt.	14	Low temp. behavior, 1°C, 0.25 mm/min
		1109+72	3' Rt.	15	Low temp. behavior, -18°C, 0.25 mm/min
		1111+32	5' Lt.	17	Temp. susc., ITS @ 25°C
		1111+32	7' Lt.	18	Low temp. behavior, 1°C, 0.025 mm/min
		1113+25	2' Lt.	21	Temp. susc., ITS @ 25°C
		1113+25	4' Lt.	22	Low temp. behavior, -18°C, 0.025 mm/min

Table 7.1. (Continued) Location of Cores and Scheduled Testing Programs (5-Year Mainline).

Sample Date	Cell	Station	Offset	Field I.D.	Testing
10-22-93	3	1114+89	1' Rt.	25	Temp. susc., ITS @ 25°C
		1114+89	1' Lt.	26	Low temp. behavior, 1°C, 0.25 mm/min
		1114+91	1' Rt.	27	Low temp. behavior, -18°C, 0.25 mm/min
		1117+53	3' Rt.	29	Temp. susc., ITS @ 25°C
		1117+53	1' Rt.	30	Low temp. behavior, 1°C, 0.025 mm/min
		1118+63	10' Rt.	33	Temp. susc., ITS @ 25°C
		1118+63	8' Rt.	34	Low temp. behavior, -18°C, 0.025 mm/min
10-22-93	4	1121+18	3' Rt.	37	Temp. susc.
		1121+18	1'Rt.	38	Static creep
		1121+20	3' Rt.	39	Low temp. behavior, 1°C, 0.25 mm/min
		1121+20	1' Lt.	40	Dynamic creep and modulus
		1123+34	1' Rt.	41	Static creep
		1123+34	1' Lt.	42	Temp. susc.
		1123+36	1' Rt.	43	Low temp. behavior, -18°C, 0.025 mm/min
		1123+36	1' Lt.	44	Dynamic creep and modulus
		1124+03	6' Rt.	45	Static creep
		1124+03	4' Rt.	46	Dynamic creep and modulus
		1124+05	6' Rt.	47	Temp. susc.
		1124+05	4' Rt.	48	Low temp. behavior, 1°C, 0.025 mm/min

Table 7.2. In-Place Density Results (5-Year Mainline).

Mn/ROAD Cell	Lift	Thickness[1] mm (in.)	Bulk Specific Gravity	Theoretical Max. Sp. Gr.	Air Voids, %
1 (75-blow)	Wear	37.64 (1.482)	2.260	2.444	7.5
	Base 1	39.09 (1.539)	2.275	2.417	5.9
	Base 2	69.60 (2.740)	2.307	2.452	5.9
2 (35-blow)	Wear	37.67 (1.483)	2.282	2.370	3.7
	Base1	41.02 (1.615)	2.301	2.380	3.3
	Base 2	61.70 (2.429)	2.302	2.390	3.7
3 (50-blow)	Wear	42.27 (1.664)	2.265	2.456	7.8
	Base 1	47.68 (1.877)	2.293	NA	---
	Base 2	57.68 (2.271)	2.285	2.437	5.9
4 (Gyratory)	Wear	37.16 (1.463)	2.273	2.462	7.7
	Base 1	44.45 (1.750)	2.297	2.451	6.3
	Base 2	58.72 (2.312)	2.285	2.458	7.0
	Base 3	60.60 (2.386)	2.310	2.461	6.1

1. Lift thickness was measured after separating lifts with wet saw.

Temperature Susceptibility

Resilient Modulus (ASTM D4123)

The testing variability was similar to that reported in the previous sections. The coefficients of variation for the -18 and 0 through 25°C (0 and 34 through 77°F) were within 3.2 percent, and 2.4 percent, respectively. No data were available for the 40°C (104°F) temperature as the samples were too soft to be tested without permanent damage. This indicated that any between-lift variability was not statistically significant. Therefore, the results for each core represent the average results from all lifts. The values shown in the following tables represent the average of three cores.

All the cores were too soft to test at the 40°C (104°F) test temperature. This may be due

to damage during coring, separating the lifts or storage problems. Cores were individually sealed in plastic cylinders used in portland cement concrete testing. However, since they were sealed shortly (within hours) after coring, the samples were most likely wet. They were then placed in long-term storage in a -18°C (0°F) freezer. This may have resulted in some freeze-thaw damage which was reflected as a softer material. Figure 7.1 shows that there was little difference in the resilient modulus due to changes in the asphalt content.

Tensile Strength

Table 7.4 shows the unconditioned (dry) tensile strength for cores. This table presents the average results for each lift in a given test cell. While the 120/150 penentration asphalt and 35-blow mixtures (test cell 2) show a higher tensile strength than the other test cells, the testing variability was also much larger. The difference between the means is not statistically significant.

Low-Temperature Behavior

Indirect Tensile Test (Constant Displacement Rate)

Both test temperatures, -18 and 0°C (0 and 34°F) were used for this evaluation. The test results, shown in Table 7.5, indicate the standard deviation associated with tensile strength was between 100 and 400 kPa (about 15 and 55 psi), regardless of the loading rate for the colder test temperature. The range decreased to between 10 and 66 kPa (1 and 10 psi) for the warmer (1°C (34°F)) test temperature. The horizontal strain measurements had a standard deviation of between 100 and 400 microstrain, and between 300 and 2000 micostrain for the -18 and 1°C (0 and 34°F) test temperatures, respectively.

Figure 7.2 compares the tensile strength results for both test temperatures. There was no significant difference between any of the test cells for either temperature when the slower displacement rate of 0.025 mm/min (0.001 in./min) was used. There were some differences in tensile strengths at the faster 0.25 mm/min (0.01 in./min) displacement rate. There was a consistent trend for test cell 2, the mixture with the highest asphalt content, to have the highest

tensile strength, while test cell 4, with the lowest asphalt content had the lowest tensile strength when tested at 0.25 mm/min. These differences are most likely a function of binder content and air void content.

Figure 7.3 compares the horizontal strains at the maximum tensile strengths. A decrease in tensile strength did not always result in corresponding increase in the horizontal tensile strains. This could indicate that there was a loss of strength with decreasing asphalt content. Due to the large variability in the results, it was not possible to draw any firm conclusions.

10-YEAR MAINLINE

Table 7.6 indicates the specfic locations and testing program for cores taken from the 10-Year Mainline portion of Mn/ROAD.

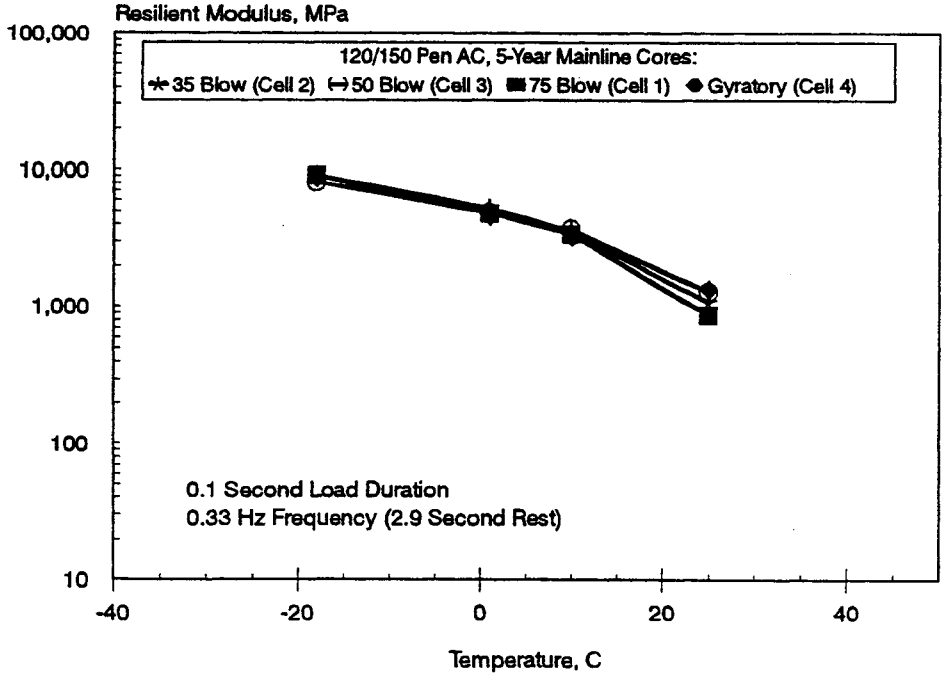

Figure 7.1. Comparision of Resilient Modulus for the 5-Year Mainline Core Mixtures.

Table 7.3. Temperature Susceptibility (Resilient Modulus ASTM D4123).

Temperature, °C (°F)	Resilient Modulus, MPa (ksi) Average of All Lifts Per Test Cell					
	Load Duration, sec.					
	0.1			1.0		
	Frequency, Hz					
	0.33	0.5	1.0	0.033	0.05	0.1
1 (120/150 Pen AC, 75 Blow)						
-18 (0)	9,057 (1,313)	4,795 (1,275)	9,514 (1,380)	5,069 (735)	6,384 (926)	6,919 (1,003)
1 (34)	4,797 (696)	5,044 (731)	5,274 (765)	3,424 (497)	3,624 (525)	3.606 (525)
10 (50)	3,390 (491)	3,352 (486)	2,854 (414)	2,127 (308)	1,972 (286)	1,840 (267)
25 (77)	861 (124)	908 (131)	874 (127)	Samples Too Soft To Test		
40 (104)	Samples Too Soft To Test					
2 (120/150 Pen AC, 35 Blow)						
-18 (0)	9,122 (1,323)	9,390 (1,361)	9,731 (1,410)	6,889 (999)	8,221 (1,192)	9,271 (1,344)
1 (34)	5,206 (755)	5,102 (740)	5,219 (757)	3,237 (469)	3,295 (478)	3,325 (482)
10 (50)	3,560 (560)	3,407 (494)	3,305 (492)	1,973 (286)	1,777 (258)	1,601 (232)
25 (77)	1,070 (155)	1,356 (197)	1,244 (180)	Samples Too Soft To Test		
40 (104)	Samples Too Soft To Test					
3 (120/150 Pen AC, 50 Blow)						
-18 (0)	8,108 (1,176)	8,259 (1,198)	8,894 (1,290)	5,429 (787)	6,653 (965)	7,155 (1,037)
1 (34)	4,842 (702)	4,881 (708)	4,996 (724)	3,252 (471)	3,409 (494)	3,390 (491)
10 (50)	3,652 (530)	3,535 (511)	3,485 (505)	2,207 (320)	2,116 (306)	2,025 (294)
25 (77)	1,281 (186)	1,619 (235)	1,361 (197)	Samples Too Soft To Test		
40 (104)	Samples Too Soft To Test					
4 (120/150 Pen AC, Gyratory)						
-18 (0)	8,621 (1,250)	9,566 (1,387)	10,466 (1,518)	5,923 (829)	8,031 (1,165)	7,479 (1,084)
1 (34)	4,651 (674)	4,730 (686)	4,841 (702)	2,085 (433)	3,174 (460)	3,376 (489)
10 (50)	3,263 (473)	3,217 (467)	3,174 (460)	1,947 (282)	1,803 (261)	1,728 (251)
25 (77)	1,329 (193)	1,336 (194)	1,249 (181)	Samples Too Soft To Test		
40 (104)	Samples Too Soft To Test					

Table 7.4. Tensile Strength Results for the 5-Year Mainline Cores.

Mn/ROAD Cell	Lift	Tensile Strength, kPa (psi) ± 1σ
1 (75 Blow)	Wear	423 (61) ± 53 (8)
	Base 1	412 (60) ± 66 (10)
	Base 2	480 (70) ± 13 (2)
2 (35 Blow)	Wear	566 (82) ± 345 (50)
	Base 1	497 (72) ± 83 (12)
	Base 2	503 (73) ± 21 (3)
3 (50 Blow)	Wear	380 (55) ± 32 (5)
	Base 1	471 (68) ± 44 (6)
	Base 2	471 (68) ± 19 (3)
4 (Gyratory)	Wear	385 (56) ± 43 (6)
	Base 1	469 (68) ± 66 (10)
	Base 2	403 (59) ± 15 (2)
	Base 3	371 (54) ± 126 (18)

In-Place Density

Table 7.7 shows the average in-place air voids for each lift in each test cell as well as the specific gravity and average lift thickness (after cutting into lifts). With the exception of cell 23, most of the in-place voids were below 8 percent. These differences in air voids reflect the influence of the aggregate stockpile moisture study in Chapter 3.

The in-place voids were calculated using the maximum specific gravity obtained for each core. The procedure was discussed at the beginning of this chapter and is presented in Appendix A of this report.

Table 7.5. Low Temperature Behavior (5-Year Mainline).

Constant Rate of Vertical Displacement mm/min (in/min)	-18°C (0°F)		1°C (34°F)	
	Maximum Tensile Strength kPa (psi)	Corresponding Horizontal Strain με	Maximum Tensile Strength kPa (psi)	Corresponding Horizontal Strain με
F1 (120/150 Pen AC, 75 Blow)				
0.025 (0.001)	1,862 ± 279 (270 ± 41)	1,107 ± 100	221 ± 21 (32 ± 3)	7,945 ± 2,058
0.25 (0.01)	1,910 ± 117 (277 ± 17)	854 ± 117	540 ± 92 (78 ± 13)	6.673 ± 1,606
F2 (120/150 Pen AC, 35 Blow)				
0.025 (0.001)	1,901 ± 106 (277 ± 15)	1,029 ± 106	276 ± 66 (40 ± 10)	5,870 ± 336
0.25 (0.01)	2,306 ± 370 (334 ± 54)	698 ± 102	632 ± 51 (92 ± 8)	6,057 ± 515
F3 (120/150 Pen AC, 50 Blow)				
0.025 (0.001)	1,636 ± 379 (237 ± 55)	1,377 ± 254	274 ± 50 (40 ± 7)	6,777 ± 445
0.25 (0.01)	1,903 ± 133 (276 ± 19)	1,004 ± 413	430 ± 60 (62 ± 9)	8,277 ± 1,695
F4 (120/150 Pen AC, Gyratory)				
0.025 (0.001)	1,772 ± 73 (257 ± 11)	1,148 ± 216	290 ± 28 (42 ± 4)	6,953 ± 2,266
0.25 (0.01)	Data Not Available		207 ± 10 (30 ± 1.4)	5,680 ± 990

1: One data point removed from data base prior to calculation of statistics due to unreasonable results.

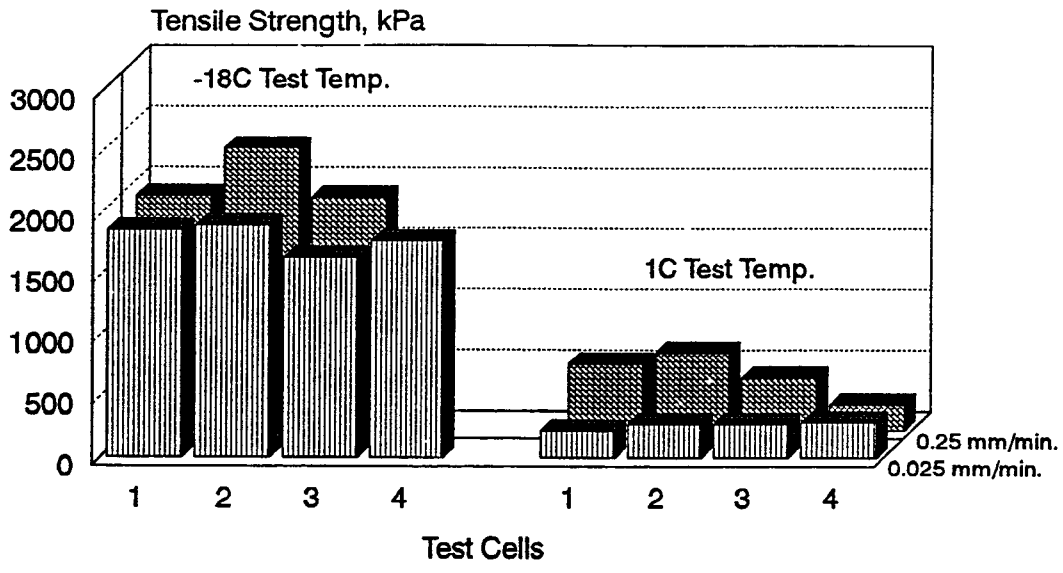

Figure 7.2. Comparison of Low Temperature Tensile Strengths (5-Year Mainline).

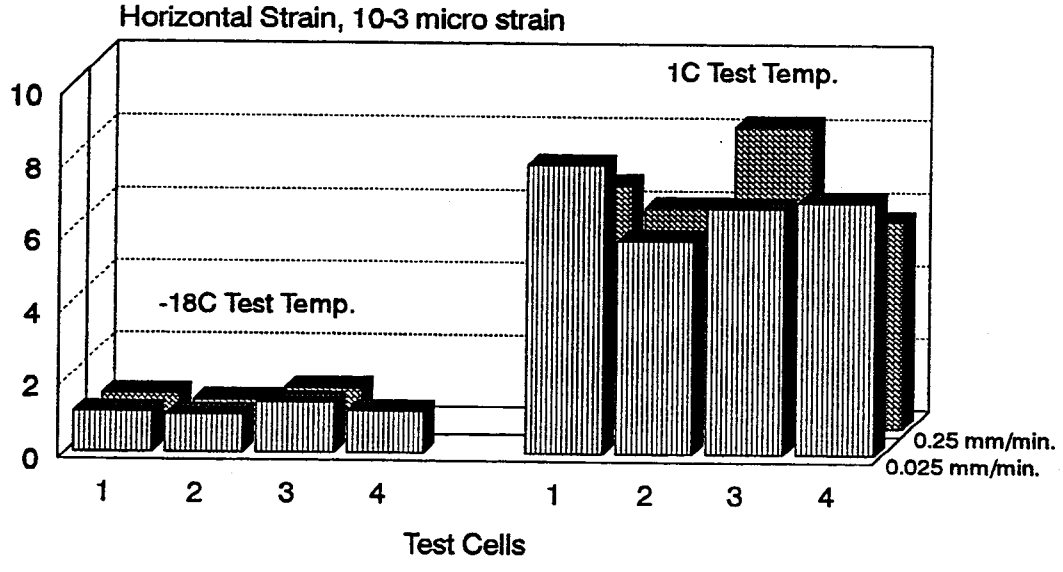

Figure 7.3. Comparison of Corresponding Horizontal Strains for Low Temperature Tensile Strength (5-Year Mainline).

Temperature Susceptibility

Resilient Modulus ASTM D4123

Table 7.8 shows the resilient moduli of the in-situ material. As with the 5-Year Mainline cores, the 10-Year Mainline cores were also too soft to test at 40°C (104°F). In general, there was little difference in moduli values at a given test temperature for mixtures prepared with the same grade of asphalt cement. As with the mix design and the behind-the-paver materials, higher moduli were obtained for the AC 20 mixtures compared to the 120/150 pen asphalt mixtures. A typical comparison is shown in Figure 7.4.

Note that cell 23 has lower moduli values than the cell 21 which has an identical mixture. It is possible that this is related to the higher in-place air voids for this test cell or the fact that this test cell was not constructed at the same time as the other nine 10-Year Mainline cells.

Tensile Strengths

Table 7.9 presents the tensile strengths for each lift in each test cell; Figure 7.5 compares these results. The tensile strengths for cell 23 clearly show that the in-place mixture is significantly weaker than other 120/150 pen asphalt mixtures.

Low Temperature Behavior

Testing included both the -18°C (0°F) and the 1°C (34°F) test temperatures. The slower 0.025 and 0.25 mm/min (0.001 and 0.01 in/min) displacement rates were used. The results are shown in Table 7.10. Figures 7.6 and 7.7 compare the maximum tensile strength and corresponding horizontal strain. The softer 120/150 pen asphalt mixtures had lower tensile strengths and higher strains than the AC 20 mixtures. While tensile strengths differed according to displacement rate, the horizontal strains were not significantly affected. Test cell 23 had the lowest tensile strengths and highest strains. This test cell also had the highest in-place air voids.

Table 7.6. Location of Cores and Scheduled Testing Programs (10-Year Mainline).

Sample Date	Cell	Station	Offset	Field ID.	Testing
9-16-93	14	118918	1	51	Temperature susceptibility Tensile strength, 25°C
		118918	-6	55	
		119424	-8	58	
9-16 and 9-17-93	15	119468	6	64	Temperature susceptibility Tensile strength, 25°C
		119974	-7	70	
		119972	-5	71	
9-17-93	16	120063	3	75	Temperature susceptibility Tensile strength, 25°C
		120063	-10	80	
		120567	-4	84	
9-17-93	17	120611	-10	86	Temperature susceptibility Tensile strength, 25°C
		120613	5	92	
		121119	-6	94	
9-17-93	18	121181	-10	101	Temperature susceptibility Tensile strength, 25°C
		121183	-8	104	
		121687	9	107	
9-17-93	19	121751	-11	110	Temperature susceptibility Tensile strength, 25°C
		121753	3	115	
		122259	-6	117	
9-17-93	20	122301	-7	121	Temperature susceptibility Tensile strength, 25°C
		122809	-5	129	
		122807	-5	131	

Table 7.6 (Continued). Location of Cores and Scheduled Testing Programs (10-Year Mainline).

Sample Date	Cell	Station	Offset	Field ID.	Testing
9-17-93	21	122891	9	134	Temperature susceptibility Tensile strength, 25°C
		122893	-10	139	
		123397	8	144	
9-17-93	22	123473	4	147	Temperature susceptibility Tensile strength, 25°C
		123471	-7	149	
		123979	-3	153	
9-17-93	23	124	-11	157	Temperature susceptibility Tensile strength, 25°C
		124053	10	163	
		124559	-5	166	

Table 7.7. Test Results Associated with In-Place Density Measurements (10-Year Mainline)

Mn/ROAD Cell	Lift	Height of Lift[1] mm (in)	Bulk Specific Gravity	Theoretical Maximum Specific Gravity	Air Voids, %
14 (120/150 Pen AC, 75 Blow)	Wear	42.85 (1.687)	2.301	2.442	5.8 ± 0.3
	Base 4	35.56 (1.400)	2.266	2.444	7.3 ± 0.3
	Base 3	55.70 (2.193)	2.278	2.434	6.6 ± 1.0
	Base 2	64.69 (2.547)	2.332	2.445	4.6 ± 2.2
	Base 1	63.17 (2.487)	2.284	2.427	5.9 ± 0.9
15 (AC20, 75 Blow)	Wear	39.12 (1.540)	2.295	2.457	2.5 ± 0.3
	Base 4	40.06 (1.577)	2.258	2.446	7.7 ± 1.3
	Base 3	54.16 (2.150)	2.251	2.444	7.9 ± 1.1
	Base 2	69.67 (2.743)	2.268	2.440	7.1 ± 0.2
	Base 1	61.54 (2.423)	2.292	2.440	6.1 ± 1.7
16 (AC20, Gyratory)	Wear	40.56 (1.597)	2.261	2.453	7.8 ± 0.8
	Base 3	38.02 (1.497)	2.234	2.459	9.1 ± 3.0
	Base 2	52.32 (2.060)	2.259	2.452	7.9 ± 0.6
	Base 1	53.85 (2.120)	2.265	2.2457	7.8 ± 0.2
17 (AC20, 75 Blow)	Wear	41.26 (1.563)	2.298	2.469	6.9 ± 0.6
	Base 3	38.02 (1.440)	2.262	2.467	8.3 ± 0.5
	Base 2	52.88 (2.003)	2.244	2.442	8.1 ± 1.3
	Base 1	50.50 (1.913)	2.266	2.448	7.5 ± 0.5
18 (AC20, 50 Blow)	Wear	39.52 (1.497)	2.295	2.432	5.5 ± 1.2
	Base 3	41.18 (1.560)	2.290	2.434	5.9 ± 1.1
	Base 2	55.52 (2.103)	2.287	2.434	6.0 ± 0.4
	Base 1	62.49 (2.367)	2.283	2.417	4.9 ± 0.0

Table 7.7. (Continued) Test Results Associated with In-Place Density Measurements (10-Year Mainline)

Mn/ROAD Cell	Lift	Height of Lift[1] mm (in)	Bulk Specific Gravity	Theoretical Maximum Specific Gravity	Air Voids, %
19 (AC20, 35 Blow)	Wear	41.90 (1.587)	2.272	2.439	6.8 ± 2.1
	Base 3	37.49 (1.420)	2.278	2.439	6.6 ± 1.1
	Base 2	53.67 (2.033)	2.242	2.421	7.4 ± 0.8
	Base 1	61.17 (2.317)	2.287	2.408	5.0 ± 1.3
20 (120/150 Pen AC, 35 Blow)	Wear	39.52 (1.497)	2.301	2.433	5.4 ± 0.0
	Base 3	33.71 (1.277)	2.252	2.434	7.5 ± 0.2
	Base 2	55.07 (2.110)	2.277	2.434	6.5 ± 0.6
	Base 1	57.29 (2.170)	2.298	2.434	5.6 ± 1.2
21 (120/150 Pen AC, 50 Blow)	Wear	38.02 (1.440)	2.301	2.435	5.5 ± 1.1
	Base 3	37.83 (1.433)	2.300	2.453	6.2 ± 1.5
	Base 2	48.58 (1.773)	2.307	2.428	5.0 ± 0.8
	Base 1	57.46 (2.097)	2.304	2.420	4.3 ± 0.6
22 (120/150 Pen AC, 75 Blow)	Wear	41.29 (1.507)	2.304	2.455	6.2 ± 0.8
	Base 3	40.87 (1.390)	2.265	2.455	7.8 ± 0.2
	Base 2	63.95 (2.175)	2.298	2.421	5.1 ± 0.6
	Base 1	63.89 (2.173)	2.279	2.442	6.7 ± 1.2
23 (120/150 Pen AC, 50 Blow)	Wear	49.10 (1.670)	2.2207	2.445	9.6 ± 1.2
	Base 4	41.75 (1.420)	2.242	2.433	7.9 ± 0.8
	Base 3	50.36 (1.713)	2.235	2.429	8.0 ± 2.0
	Base 2	56.45 (1.920)	2.211	2.428	9.0 ± 0.4
	Base 1	57.24 (1.947)	2.293	2.425	5.5 ± 0.7

Table 7.8. Temperature Susceptibility (Resilient Modulus ASTM D4123) (10-Year Mainline).

Temperature, °C (°F)	Resilient Modulus, MPa (ksi) ± 1σ 0.1-sec load/1.0 Hz				
	Lift				
	Wear	Base 4	Base 3	Base 2	Base 1
14 (120/150 Pen AC, 75 Blow)					
-18 (0)	17,040 (2,473) ± 1,739 (252)	14,254 (2,069) ± 663 (96)	12,957 (1,880) ± 666 (97)	12,082 (1,753) ± 1,768 (257)	10,876 (1,578) ± 2,965 (430)
1 (34)	6,494 (942) ± 232 (34)	4,930 (715) ± 496 (72)	4,916 (713) ± 892 (129)	4,799 (696) ± 580 (85)	5,238 (760) ± 301 (44)
25 (77)	1,595 (232) ± 184 (27)	1,439 (209) ± 131 (19)	1,182 (172) ± 336 (49)	998 (145) ± 190 (28)	1,099 (160) ± 111 (16)
40 (104)	Samples Too Soft				
15 (AC 20, 75 Blow)					
-18 (0)	16,916 (2,455) ± 953 (138)	15,215 (2,208) ± 2,144 (256)	12,066 (1,882) ± 2,139 (310)	12,615 (1,831) ± 956 (139)	13,384 (1,942) ± 925 (133)
1 (34)	7,845 (1,138) ± 396 (57)	7,121 (1,033) ± 459 (67)	6,212 (901) ± 807 (117)	5,865 (851) ± 95 (14)	6,431 (933) ± 341 (50)
25 (77)	2,098 (305) ± 207 (30)	1,876 (272) ± 143 (21)	1,818 (264) ± 124 (18)	1,673 (242) ± 54 (8)	1,784 (359) ± 211 (32)
40 (104)	Samples Too Soft				
16 (AC 20, 75 Blow)					
-18 (0)	15,281 (2,218) ± 1,030 (149)	---	13,480 (1,956) ± 2,172 (315)	14,776 (2,114) ± 1,481 (215)	13,141 (1,907) ± 1,345 (195)
1 (34)	7,470 (1,084) ± 472 (68)	---	7,011 (1,107) ± 896 (377)	7,075 (1,027) ± 1,260 (183)	6,823 (990) ± 272 (40)
25 (77)	2,130 (309) ± 144 (17)	---	2,066 (300) ± 138 (20)	1,860 (270) ± 244 (35)	1,892 (274) ± 76 (11)
40 (104)	Samples Too Soft				
17 (AC 20, 75 Blow)					
-18 (0)	16,402 (2,380) ± 5,504 (800)	---	15,141 (2,197) ± 1,740 (252)	15,258 (2,214) ± 2,637 (382)	16,411 (2,382) ± 4,857 (705)
1 (34)	7,316 (1,061) ± 1,069 (155)	---	8,910 (1,293) ± 2,172 (315)	6,120 (888) ± 1,093 (159)	7,627 (1,107) ± 806 (117)
25 (77)	2,117 (307) ± 317 (46)	---	2,015 (293) ± 224 (33)	1,775 (258) ± 206 (30)	2,073 (301) ± 162 (23)
40 (104)	Samples Too Soft				

Table 7.8. (Continued) Temperature Susceptibility (Resilient Modulus ASTM D4123) (10-Year Mainline).

Temperature, °C (°F)	Resilient Modulus, MPa (ksi) ± 1σ 0.1-sec load/1.0 Hz				
	Lift				
	Wear	Base 4	Base 3	Base 2	Base 1
18 (AC 20, 50 Blow)					
-18 (0)	16,760 (2,432) ± 725 (105)	---	16,675 (2,420) ± 1,531 (222)	15,550 (2,257) ± 2,241 (267)	13,469 (1,955) ± 706 (102)
1 (34)	7,946 (1,153) ± 582 (84)	---	7,323 (1,063) ± 1,690 (245)	6,701 (972) ± 859 (125)	7,126 (1,041) ± 736 (107)
25 (77)	2,365 (343) ± 205 (30)	---	2,278 (331) ± 222 (32)	1,864 (271) ± 82 (12)	1,912 (278) ± 226 (33)
40 (104)	Samples Too Soft				
19 (AC 20, 35 Blow)					
-18 (0)	15,802 (2,293) ± 2,183 (317)	---	15,936 (2,313) ± 205 (30)	13,021 (1,890) ± 2,201 (319)	11,268 (1,617) ± 357 (52)
1 (34)	6,992 (1,105) ± 283 (133)	---	6,885 (999) ± 827 (120)	6,747 (979) ± 1,450 (211)	6,480 (940) ± 590 (86)
25 (77)	1,795 (261) ± 283 (41)	---	1,699 (247) ± 181 (26)	1,579 (229) ± 181 (26)	1,848 (268) ± 464 (67)
40 (104)	Samples Too Soft				
20 (120/150 Pen AC, 35 Blow)					
-18 (0)	15,143 (2,980) ± 1,034(150)	---	13,388 (1,943) ± 840 (122)	12,998 (1,886) ± 777 (113)	13,033 (1891) ± 2,168 (315)
1 (34)	6,039 (876) ± 356 (52)	---	5,792 (840) ± 685 (99)	5,497 (798) ± 243 (35)	5,778 (841) ± 971 (141)
25 (77)	1,203 (175) ± 55 (8)	---	1,159 (168) ± 74 (11)	1,147 (167) ± 45 (7)	927 (135) ± 160 (23)
40 (104)	Samples Too Soft				
21 (120/150 Pen AC, 50 Blow)					
-18 (0)	16,241 (2,226) ± 720 (105)	---	14,319 (2,078) ± 1,211 (176)	14,319 (2,078) ± 1,730 (251)	13, 401 (2,031) ± 1,494 (217)
1 (34)	5,504 (799) ± 815 (118)	---	5,973 (867) ± 285 (41)	6,140 (891) ± 771 (112)	5,440 (789) ± 917 (133)
25 (77)	1,101 (160) ± 149 (22)	---	1,129 (164) ± 161 (23)	1,209 (176) ± 201 (29)	1,017 (148) ± 157 (23)
40 (104)	Samples Too Soft				

Table 7.8. (Continued) Temperature Susceptibility (Resilient Modulus ASTM D4123) (10-Year Mainline).

Temperature, °C (°F)	Resilient Modulus, MPa (ksi) ± 1σ 0.1-sec load/1.0 Hz				
	Lift				
	Wear	Base 4	Base 3	Base 2	Base 1
22 (120/150 Pen AC, 75 Blow)					
-18 (0)	17,586 (2,552) ± 2,026 (439)	---	14,792 (2,147) ± 336 (49)	14,220 (2,064) ± 946 (137)	12,941 (1,878) ± 1,775 (258)
1 (34)	5,720 (830) ± 596 (86)	---	5,495 (797) ± 286 (41)	5,684 (825) ± 321 (47)	5,137 (745) ± 615 (89)
25 (77)	1,166 (169) ± 123 (18)	---	1,122 (163) ± 60 (9)	1,088 (158) ± 121 (2)	966 (140) ± 175 (25)
40 (104)	Samples Too Soft				
23 (120/150 Pen AC, 50 Blow)					
-18 (0)	NA	NA	NA	NA	NA
1 (34)	4,535 (658) ± 1,063 (154)	NA	NA	NA	NA
25 (77)	815 (118) ± 69 (10)	683 (99) ± 33 (5)	844 (123) ± 183 (27)	940 (136) ± 4 (1)	925 (134) ± 176 (24)
40 (104)	Samples Too Soft				

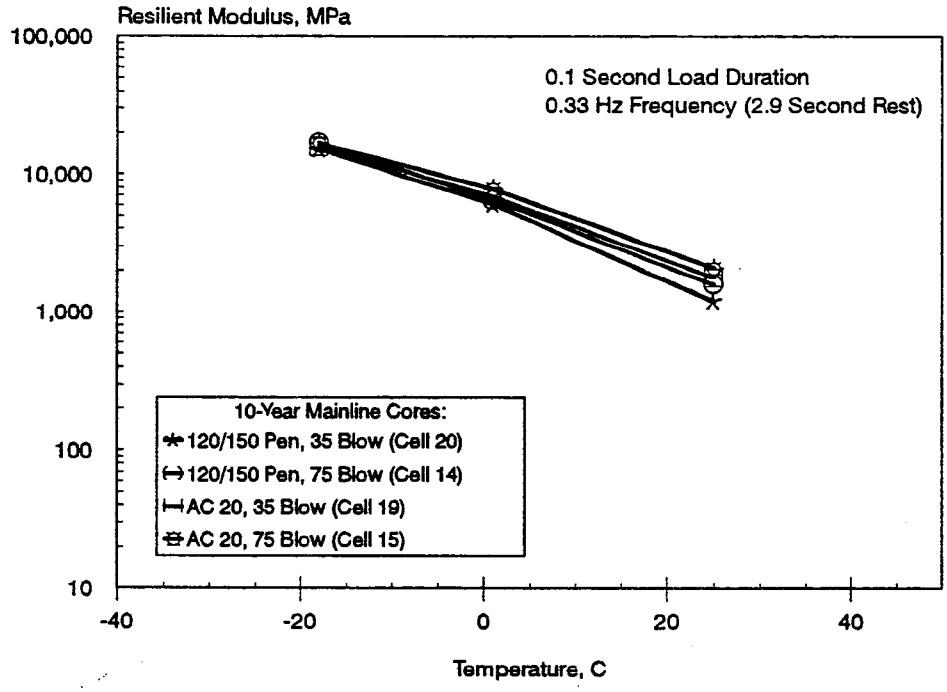

Figure 7.4. Typical Resilient Modulus vs. Temperature for 10-Year Mainline Cores.

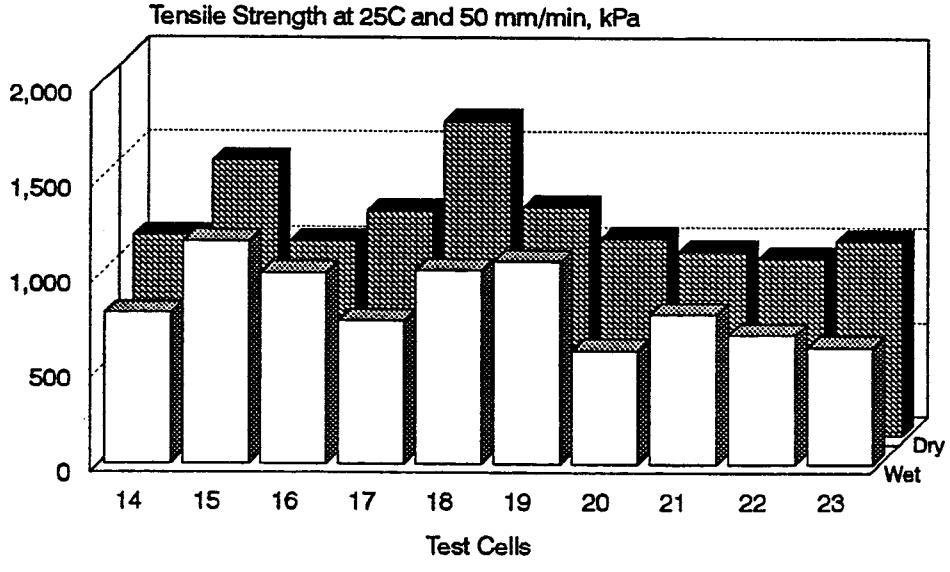

Figure 7.5 Comparison of Unconditioned and Conditioned Tensile Strengths for 10-Year Mainline Cores.

Table 7.9. Tensile Strengths for 10-Year Mainline Cores.

Test Cell	Tensile Strength, kPa (psi) ± 1σ @25°C (77°F), 25 mm/min (2 in/min)				
	Wear	Base 4	Base 3	Base 2	Base 1
14 (120/150, 35 Blow)	462 (67) ± 28 (4)	428 (62) ± 28 (4)	393 (57) ± 55 (8)	455 (66) ± 90 (13)	393 (57) ± 83 (12)
15 (AC 20, 75 Blow)	635 (92) ± 35 (5)	572 (83) ± 21 (3)	593 (86) ± 35 (5)	669 (97) ± 103 (15)	607 (88) ± 103 (15)
16 (AC 20, Gyratory)	627 (91) ± 69 (10)	531 (77) ± 76 (11)	641 (93) ± 28 (4)	628 (91) ± 69 (10)	---
17 (AC 20, 75 Blow)	648 (94) ± 90 (13)	573 (82) ± 97 (14)	641 (93) ± 48 (7)	655 (95) ± 69 (10)	---
18 (AC 20, 50 Blow)	697 (101) ± 21 (3)	655 (95) ± 48 (7)	738 (107) ± 41 (6)	703 (102) ± 48 (7)	---
19 (AC 20, 35 Blow)	641 (93) ± 90 (13)	586 (85) ± 96 (14)	641 (93) ± 62 (9)	620 (90) ± 41 (6)	---
20 (120/150, 35 Blow)	421 (61) ± 28 (4)	359 (52) ± 35 (5)	462 (67) ± 48 (7)	441 (64) ± 7 (1)	---
21 (120/150, 50 Blow)	421 (61) ± 35 (5)	435 (63) ± 49 (7)	497 (72) ± 21 (3)	435 (63) ± 21 (3)	---
22 (120/150, 75 Blow)	462 (67) ± 42 (6)	428 (62) ± 28 (4)	538 (78) ± 41 (6)	441 (64) ± 62 (9)	---
23 (120/150, 50 Blow)	269 (39) ± 14 (2)	220 (32) ± 62 (9)	227 (33) ± 70 (10)	277 (40) ± 7 (1)	352 (51) ± 28 (4)

Table 7.10. Low-Temperature Test Results (10-Year Mainline).

Test Temperature, °C (°F)	Test Cell	Displ. Rate mm/min (in/min)	Tensile Strength, kPa (psi) ± 1σ	Horiz. Strain, με± 1σ
-18 (0)	14 (120/150, 35 Blow)	0.025 (0.001)	1,950 ± 92 (283 ± 14)	9,040 ± 1,530
		0.25 (0.01)	2,260 ± 180 (327 ± 26)	10,400 ± 1,230
	15 (AC 20, 75 Blow)	0.025 (0.001)	2,170 ± 195 (315 ± 28)	7,610 ± 864
		0.25 (0.01)	2,520 ± 289 (365 ± 43)	8,730 ± 1,760
	16 (AC 20, Gyratory)	0.025 (0.001)	2,170 ± 110 (314 ± 16)	7,320 ± 1,180
		0.25 (0.01)	2,190 ± 200 (318 ± 35)	8,360 ± 897
	17 (AC 20, 75 Blow)	0.025 (0.001)	2,430 ± 220 (353 ± 32)	8,040 ± 289
		0.25 (0.01)	2,380 ± 211 (346 ± 30)	8,590 ± 661
	18 (AC 20, 50 Blow)	0.025 (0.001)	2,270 ± 164 (329 24)	6,600 ± 1,210
		0.25 (0.01)	2,250 ± 76 (326 ± 17)	8,590 ± 496
	19 (AC 20, 35 Blow)	0.025 (0.001)	2,520 ± 290 (365 ± 42)	8,240 ± 184
		0.25 (0.01)	2,800 ± 298 (406 ± 44)	7,440 ± 127
	20 (120/150, 35 Blow)	0.025 (0.001)	1,940 ± 76 (280 ± 11)	12,100 ± 2,190
		0.25 (0.01)	2,630 ± 337 (381 ± 49)	10,200 ± 2,330
	21 (120/150, 50 Blow)	0.025 (0.001)	2,230 ± 116 (323 ± 17)	14,800 ± 1,760
		0.25 (0.01)	2,400 ± 227 (348 ± 32)	11,190 ± 451
	22 (120/150, 75 Blow)	0.025 (0.001)	1,810 ± 283 (262 ± 42)	10,100 ± 396
		0.25 (0.01)	2,390 ± 176 (347 ± 25)	9,610 ± 332
	23 (120/150, 50 Blow)	0.025 (0.001)	1,610 (234)	18,200
		0.25 (0.01)	1,790 (259)	14,000

Table 7.10. (Continued) Low-Temperature Test Results (10-Year Mainline).

Test Temperature, °C (°F)	Test Cell	Displ. Rate mm/min (in/min)	Tensile Strength, kPa (psi) ± 1σ	Horiz. Strain, με± 1σ
1 (34)	14 (120/150, 35 Blow)	0.025 (0.001)	404 ± 24 (59 ± 4)	23,500 ± 3,270
		0.25 (0.01)	688 ± 30 (100 ± 5)	9,040 ± 1,530
	15 (AC 20, 75 Blow)	0.025 (0.001)	508 ± 129 (74 ± 19)	21,800 ± 1,470
		0.25 (0.01)	872 ± 157 (126 ± 23)	17,900 ± 764
	16 (AC 20, Gyratory)	0.025 (0.001)	501 ± 19 (73 ± 3)	19,500 ± 1,760
		0.25 (0.01)	814 ± 25 (118 ± 4)	18,800 ± 2,830
	17 (AC 20, 75 Blow)	0.025 (0.001)	562 ± 10 (82 ± 2)	18,400 ± 1,260
		0.25 (0.01)	871 ± 80 (126 ± 12)	19,400 ± 1,760
	18 (AC 20, 50 Blow)	0.025 (0.001)	554 ± 82 (80 ± 12)	23,800 ± 2,310
		0.25 (0.01)	892 ± 77 (129 ± 11)	18,000 ± 1,260
	19 (AC 20, 35 Blow)	0.025 (0.001)	565 ± 41 (82 ± 6)	23,000 ± 2,040
		0.25 (0.01)	885 ± 129 (128 ± 19)	19,700 ± 2,950
	20 (120/150, 35 Blow)	0.025 (0.001)	378 ± 31 (55 ± 5)	20,700 ± 3,450
		0.25 (0.01)	733 ± 85 (106 ± 12)	21,500 ± 2,460
	21 (120/150, 50 Blow)	0.025 (0.001)	379 ± 37 (55 ± 6)	23,300 ± 2,410
		0.25 (0.01)	686 ± 70 (100 ± 10)	24,500 ± 2,030
	22 (120/150, 75 Blow)	0.025 (0.001)	383 ± 32 (55 ± 5)	23,500 ± 2,200
		0.25 (0.01)	643 ± 95 (93 ± 14)	23,100 ± 2,980
	23 (120/150, 50 Blow)	0.025 (0.001)	288 (42)	26,100
		0.25 (0.01)	548 (80)	30,000

LOW VOLUME ROAD

Cores were obtained during the sensor placement operations. However, there were only a limited number of appropriate sized cores available for testing as some of the cells were cored with a large 150-mm (6-in) outside diameter barrel. These cores were used to determine density, but they would not fit in the apparatus for resilient modulus testing since the core diameter was about 6 mm (0.25 in) smaller than the core barrel diameter.

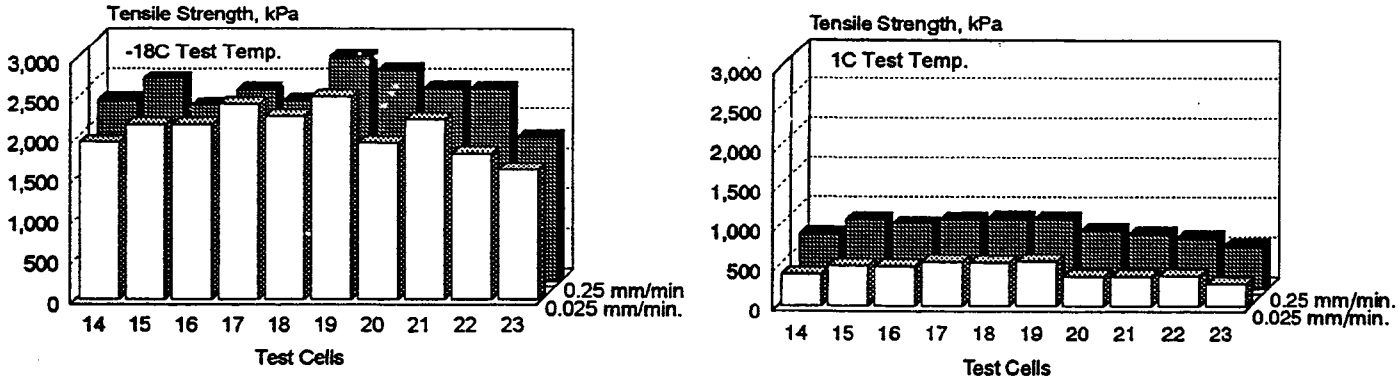

Figure 7.6. Comparison of Low Temperature Tensile Strengths (10-Year Mainline Cores).

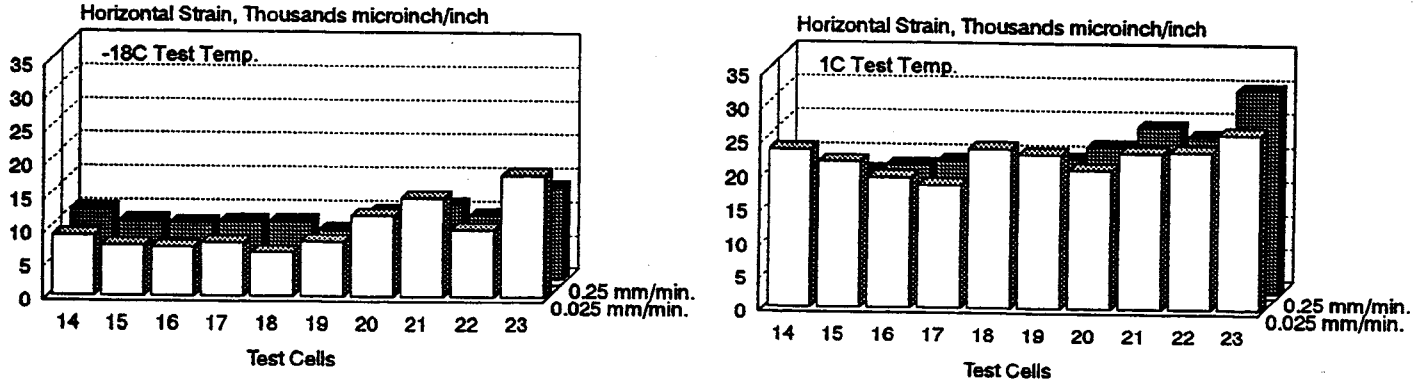

Figure 7.7. Comparison of Horizontal Strains at Fracture for Low Temperature Tensile Strength (10-Year Mainline Cores).

As with the cores for the 5-Year and 10-Year Mainline sections, these were wet-cored and then stored in sealed containers. Upon opening the containers, there was evidence of damage for several of the samples.

In-Place Density and Air Voids

Table 7.11 shows the average in-place air voids for each lift in each test cell as well as specific gravity and the average lift thicknesses (after sawing into lifts). The in-place voids were calculated using the maximum specific gravity reported by Braun Intertec, Inc. For the behind-the-paver materials. This was because of the limited number of cores available for testing.

The air void contents were generally between 5 and 8 percent. The exceptions were the wear courses in cells 30 and 31 with void contents of 9.9 and 9.8 percent, respectively. These test cells were paved during a thunderstorm noted in the Low Volume Road construction section.

Temperature Susceptibility

Resilient Modulus ASTM D 4123

Table 7.12 shows the resilient modulus values over a range of temperatures for the Low Volume Road test cells. Moduli values are very consistent between lifts of the same test cell as well as between different test cells. This suggests that the variations in asphalt content did not significantly influence the moduli values.

Tensile Strengths

Table 7.13 shows the tensile strength results obtained for the Low Volume Road cores. Tensile strength values were consistent between both lifts and test cells. However, all values are lower than would normally be expected, most likely because of damage incurred by storing wet samples and then freezing for long-term storage.

Table 7.11. Test Results Associated with In-Place Density Measurements (Low Volume Road)

Mn/ROAD Cell	Lift	Height of Lift[1] mm (in)	Bulk Specific Gravity	Theoretical Maximum Specific Gravity[1]	Air Voids, %
24 (120/150 Pen AC, 35 Blow)	Wear	No Cores Available			
	Base 2				
	Base 1				
25 (120/150 Pen AC, 50 Blow)	Wear	43.61 (1.717)	2.223	2.442	9.0 ± 0.4
	Base 2	43.05 (1.695)	2.273	2.444	7.0 ± 0.2
	Base 1	48.56 (1.912)	2.280	2.442	7.4 ± 3.6
26 (120/150 Pen AC, 50 Blow)	Wear	41.02 (1.615)	2.219	2.449	9.4 ± 2.1
	Base 2	37.44 (1.474)	2.210	2.435	9.5 ± 1.0
	Base 1	67.69 (2.665)	2.259	2.445	7.3 ± 0.9
27 (120/150 Pen AC, 35 Blow)	Wear	39.37 (1.550)	2.236	2.439	9.1
	Base 2	Lifts Either Missing or Damaged			
	Base 1				
28 (120/150 Pen AC, 50 Blow)	Wear	Unable to Test			
	Base 2				
	Base 1				
29 (120/150 Pen AC, 50 Blow)	Wear	41.05 (1.616)	2.253	2.443	7.7 ± 0.8
	Base 2	37.74 (1.486)	2.283	2.440	8.3 ± 1.0
	Base 1	47.68 (1.877)	2.273	2.439	6.8 ± 0.7
30 (120/150 Pen AC, 75 Blow)	Wear	37.85 (1.490)	2.253	2.443	7.7 ± 0.8
	Base 2	37.49 (1.476)	2.234	2.454	8.8 ± 0.1
	Base 1	54.48 (2.145)	2.247	2.458	8.2 ± 0.1
31 (120/150 Pen AC, 75 Blow)	Wear	43.18 (1.700)	2.216	2.457	9.8 ± 0.8
	Base 1	37.31 (1.469)	2.237	2.452	8.8 ± 1.1

1: Max. sp. gr. from behind-the-paver samples tested by Braun Intertec.

Table 7.12. Resilient Modulus of Low Volume Road Cores.

Temperature, °C (°F)	Resilient Modulus, MPa (ksi) ± 1σ 0.1-sec load/1.0 Hz		
	Lift		
	Wear	Base 2	Base 1
24 (120/150 Pen AC, 35 Blow)			
	No Cores Available		
25 (120/150 Pen AC, 50 Blow)			
-18 (0)	8,018 (1,163) ± 1,163 (160)	9,604 (1,393) ± 2,399 (348)	8,808 (1,305) ± 841 (122)
1 (34)	3,383 (491) ± 916 (133)	3,640 (470) ± 528 (68)	3,503 (508) ± 427 (62)
25 (77)	741 (108) ± 119 (17)	722 (104) ± 203 (29)	710 (103) ± 151 (22)
40 (104)	Samples Too Soft		
26 (120/150 Pen AC, 50 Blow)			
-18 (0)	8,243 (1,196) ± 1,501(218)	9,516 (1,380) ± 1,484 (215)	9,186 (1,332) ± 1,875 (215)
1 (34)	2,444 (355) ± 1,128 (164)	3,603 (523) ± 520 (76)	4,068 (590) ± 511 (74)
25 (77)	758 (110) ± 216 (31)	969 (141) ± 253 (37)	808 (117) ± 106 (15)
40 (104)	Samples Too Soft		
27 (120/150 Pen AC, 35 Blow)			
-18 (0)	Unable to Test		8,956 (1,296)
1 (34)			3,530 (512)
25 (77)			607 (88)
40 (104)	Samples Too Soft		
28 (120/150 Pen AC, 50 Blow)			
	Unable to Test		

Table 7.12. (Continued) Resilient Modulus of Low Volume Road Cores.

Temperature, °C (°F)	Resilient Modulus, MPa (ksi) ± 1σ 0.1-sec load/1.0 Hz		
	Lift		
	Wear	Base 2	Base 1
29 (120/150 Pen AC, 50 Blow)			
	Unable to Test		
30 (120/150 Pen AC, 75 Blow)			
-18 (0)	8,019 (1,163) ± 1,523 (221)	11,089 (1,608) ± 1,486 (216)	11,083 (1,608) ± 1,695 (246)
1 (34)	2,744 (398) ± 876 (127)	3,164 (459) ± 666 (97)	2,769 (402) ± 370 (54)
25 (77)	639 (98) ± 90 (13)	818 (119) ± 86 (13)	712 (103) ± 131 (19)
40 (104)	Samples Too Soft		
31 (120/150 Pen AC, 75 Blow)			
	Unable to Test		

Table 7.13. Tensile Strength Values for Low Volume Road.

Test Cell	Tensile Strength, kPa (psi) ± 1σ @25°C (77°F), 25 mm/min (2 in/min)		
	Wear	Base 2	Base 1
24 (120/150 Pen AC, 35 Blow)	No Cores Available		
25 (120/150 Pen AC, 50 Blow)	241 (35) ± 35 (5)	248 (36) ± 28 (4)	193 (28) ± 41 (6)
26 (120/150 Pen AC, 50 Blow)	283 (41) ± 14 (2)	269 (39) ± 28 (4)	200 (29) ± 21 (3)
27 (120/150 Pen AC, 35 Blow)	Lifts Missing or Damaged		235 (34)
28 (120/150 Pen AC, 50 Blow)	Unable to Test		
29 (120/150 Pen AC, 50 Blow)	Unable to Test		
30 (120/150 Pen AC, 75 Blow)	269 (39) ± 21 (3)	283 (41) ± 7 (1)	200 (29) ± 28 (4)
31 (120/150 Pen AC, 75 Blow)	Unable to Test		

CHAPTER EIGHT
COMPARISON OF RESULTS

TESTING VARIABILITY

Any comparison of data requires an understanding of the testing variability associated with the test results. Table 8.1 summarizes the average standard deviation or coefficient of variation for all testing used to characterize the Mn/ROAD mixtures.

Resilient and Dynamic Modulus Tests

The resilient modulus testing variability was consistent between all sample sources (i.e., mix design, behind-the-paver, and cores); the coefficient of variation (CV) for this test was determined for the log transformed data.

The coefficient of variation for the untransformed data from the axially loaded dynamic modulus testing was approximately 10 percent (with one exception) for all test temperatures, with or without confining pressure, at a loading frequency of 0.1 Hz. The exception was that using confining pressure significantly increased the CV at the warm 40°C (104°F) test temperature. The CV also increased to about 15 percent when the loading frequency increased to 1.0 Hz. The CV for the phase angle measurements were approximately 16.9 percent for all test temperatures, with or without confining pressure, and the 0.1 Hz loading frequency. This CV also increased with loading frequency to 30.7 percent. The consistency of the CV with increasing magnitude of measurements indicate that the standard deviation is magnitude dependent for both the strain and phase angle measurements.

The strain measurements for the diametrally loaded dynamic modulus measurements showed the opposite trend. That is, the faster the loading frequency the lower the CV. For 0.1 Hz, the average CV was 21.1 percent and decreased to 11.9 percent at the 1.0 Hz frequency. The phase angle measurements were highly variable at the cold test temperature. The coefficient of variability decreased with increasing temperature. These phase angle measurements were not dependent upon the loading frequency.

Moisture Sensitivity Tests

The standard deviations for the adsorption, desorption, and net adsorption results were similar with the average standard deviation being 15 mg/g. The testing variability for the unconditioned resilient modulus portion of the moisture testing was the same as reported in the previous section. The tensile strength coefficient of variation for the unconditioned samples was 5.2 percent, which was slightly less than the 7.9 percent for testing after freeze/thaw conditioning. Testing of both mix design and behind-the-paver samples had similar variability.

Low Temperature Tests

The standard deviations for the indirect tensile testing at various rates of deformation increased with increasing rates. Similar trends were seen for all sample sources and test temperatures. However, the standard deviations at the warmer 1°C (34°F) test temperature were significantly lower than for colder -18°C (0°F) which also corresponds to a decrease in tensile strength with increasing temperature. This suggests that the standard deviation will be dependent upon the magnitude of the tensile strength. The corresponding horizontal strains were not only dependent upon the deformation rate and test temperature but also on the sample source. The faster the rate of deformation, the greater the horizontal strain variability. When the test temperature increased from -18°C (0°F) to 1°C (34°F), the horizontal strain standard deviation increased by an order of magnitude. The standard deviations associated with testing cores were 200 to 400 percent greater than those for the corresponding mix design materials.

The modified indirect tensile creep test showed the coefficient of variation of the creep compliance to be 21.1 percent and independent of test temperature. The CV for measuring the slope of the creep compliance curves was 23.1 percent and also apparently independent of test temperature.

Permanent Deformation Tests

The testing variability for the static and repeated load creep tests increased when confining pressure was used. The standard deviations decreased with increasing test temperatures, but since this is also accompanied by a decrease in creep modulus, it is most

likely that the standard deviation is a function of the magnitude of the modulus. Therefore, the coefficient of variation may be a more appropriate expression of creep testing variability. Since only a limited amount of testing was completed for the behind-the-paver materials, no conclusions regarding the influence of sample source on testing variability can be made.

COMPARISON OF RESULTS FOR THE VARIOUS SAMPLE SOURCES

Temperature Susceptibility

Figures 8.1a through 8.1c show the typical results obtained for the mix design and behind-the paver material sources of the 35-, 50-, and 75-blow 120/150 pen asphalt mixtures. In general, the mix design materials had lower moduli than the behind-the-paver materials below test temperatures of 25°C (77°F) and similar moduli above this temperature. Figures 8.2a through 8.2c show the same comparisons for the AC 20 mixtures. The mix design and behind-the-paver moduli were similar at the colder temperatures and were variable at the warm temperatures. This suggests that the temperature susceptibility of softer grade asphalt may be significantly altered during production while the higher viscosity AC 20 may be relatively unaffected.

Figure 8.3 shows that erratic results were obtained for the gyratory compacted samples. In general, both mix design and behind-the-paver materials had similar moduli values at a given test temperature. Differences in the influence of asphalt content on mixture properties between these data and the previous data shown in Figure 8.2 may be due to the different aggregate structure formed during gyratory shear compaction versus impact compaction with the Marshall hammer.

Table 8.1. Comparison of Test Method Variability.

Test Method	Variability		
	Mix Design	Behind Paver	Cores
Temperature Susceptibility			
Resilient Modulus ASTM D4123	CV for log transformed data: 3.5 at -18°C 2.00 at 1 to 25°C 6.60 at 40°C	Same as Mix Design	Same as Mix Design
Dynamic Modulus (Axial) 1°C (34°F) 10°C (50°F) 25°C (77°F) 40°C (104°F) without confine with confine Phase Angle (CV, %): 1°C (34°F) 10°C (50°F) 25°C (77°F) 40°C (104°F)	Strain (CV, %): 0.1 Hz / 1.0 Hz 9.8 / 15.1 10.0 / 16.1 12.1 / 18.4 9.0 / 9.3 26.0 / 24.2 Phase Angle (CV, %): 0.1 Hz / 1.0 Hz 16.8 / 25.6 18.1 / 38.3 15.7 / 37.4 17.1 / 21.3	Same as for Mix Design	Not Applicable
Dynamic Modulus: (Diametral) -18°C (0°F) 1°C (34°F) 25°C (77°F) Phase Angle (CV, %): -18°C (0°F) 1°C (34°F) 25°C (77°F)	Strain (CV, %): 0.1 Hz / 1.0 Hz 24.6 / 10.6 21.0 / 9.4 17.6 / 15.6 Phase Angle (CV, %): 0.1 Hz / 1.0 Hz 64.7 / 64.1 28.1 / 19.0 8.1 / 7.7	Not Applicable	Not Applicable
Moisture Sensitivity			
Net Adsorption[1]	Standard Deviation: Adsorption: 0.13 mg/g Desorption: 0.18 mg/g Net Adsorpt.:0.14 mg/g	Not Applicable	
ASTM D4867 (Modified Lottman)	Resilient Modulus: Same as ASTM D4123 Tensile Strength (CV, %): Dry: 5.2 Wet: 7.9	Same as Mix Design	Not Applicable

Table 8.1 (Continued). Comparison of Test Method Variability.

Test Method	Variability		
	Mix Design	Behind Paver	Cores
Low Temperature Behavior			
Indirect Tensile, Rate of Displacement Tensile Strength	Std. Dev. at -18°C kPa (psi):	Std. Dev. at -18°C kPa (psi):	Std. Dev. at -18°C kPa (psi):
0.025 mm/min.	156 (22)	147 (21)	210 (31)
0.25 mm/min.	213 (31)	229 (33)	210 (31)
2.5 mm/min.	230 (33)	NA	NA
	Std. Dev. at 1°C kPa (psi):	Std. Dev. at 1°C kPa (psi):	Std. Dev. at 1°C kPa (psi):
0.025 mm/min.	40 (6)	53 (8)	41 (6)
0.25 mm/min.	74 (11)	92 (13)	54 (8)
2.5 mm/min	172 (25)	NA	NA
Horizontal Strain	Std. Dev. -18°C, με:	Std. Dev. at -18°C, με:	Std. Dev. -18°C, με:
0.025 mm/min.		No Testing at This	169
0.25 mm/min.	37	Temperature	211
2.5 mm/min	50		NA
	Std. Dev. at 1°C, με:	Std. Dev. at 1°C, με:	Std. Dev. at 1°C, με:
0.025 mm/min.	367	200	1,276
0.25 mm/min.	633	121	1,202
2.5 mm/min	433	NA	NA
Indirect Tensile, Constant Stress	Compliance CV, %:		
-20°C (-4°F)	20.4		
-15°C (5°F)	17.8		
-10°C (14°F)	22.3	Not Applicable	Not Applicable
-5°C (23°F)	22.3		
0°C (32°F)	22.5		

Table 8.1 (Continued). Comparison of Test Method Variability.

Test Method	Variability		
	Mix Design	Behind Paver	Cores
Permanent Deformation Characteristics			
Static Creep 25°C (77°F) 40°C (104°F)	Creep Mod. Std. Dev. MPa (ksi) No Confine. With Confine 8 (1.4) 17 (2) Too Many Samples Failed to Obtain Testing Variability	Not Available	Not Available
Repeated Load Creep	Creep Mod. Std. Dev. MPa (ksi) No Confine. With Confine	Creep Mod. Std. Dev. MPa (ksi) No Confine. With Confine	
	0.1 sec load, 25°C (77°F):	0.1 sec load, 25°C (77°F):	
0.33 Hz	43 (6) 192 (28)	29 (4) NA	
0.50 Hz	39 (6) 170 (25)	23 (3) NA	Not Available
1.00 Hz	30 (4) 217 (32)	18 (3) NA	
	0.1 sec load, 40°C (104°F):		
0.33 Hz	10 (1.4) 23 (3)		
0.50 Hz	8 (1.2) 20 (3)	Not Available	Not Available
1.00 Hz	6 (0.9) 20 (3)		
	1.0 sec load, 25°C (77°F):		
0.33 Hz	34 (5) 77 (11)		
0.50 Hz	20 (3) 69 (10)	Not Available	Not Available
1.00 Hz	21 (3) 70 (10)		
	1.0 sec load, 40°C (104°F):		
0.33 Hz	3 (0.4) 12 (2)		
0.50 Hz	5 (0.7) 8 (1.2)	Not Available	Not Available
1.00 Hz	6 (0.8) 6 (0.8)		

Figure 8.4 shows that changes in the asphalt content did not significantly influence the temperature susceptibility of the mixtures. The low moduli value for the 35 blow AC 20 mixture from test cell 19 (Figure 8.4d) may be due to sampling problems during construction.

Figure 8.5 shows that there was some difference in cold temperature moduli values for the 5-Year Mainline materials (120/150 pen asphalt) when compared to those from the 10-Year Mainline. Note that the mix design results under-predicted the cold temperature moduli of the 10-Year Mainline 120/150 pen asphalt test cells while over-predicting the moduli at the warmer temperatures (Figure 8.5a) for the same cells. However, the AC 20 behind-the-paver mixtures moduli were reasonably similar to those for the mix design materials.

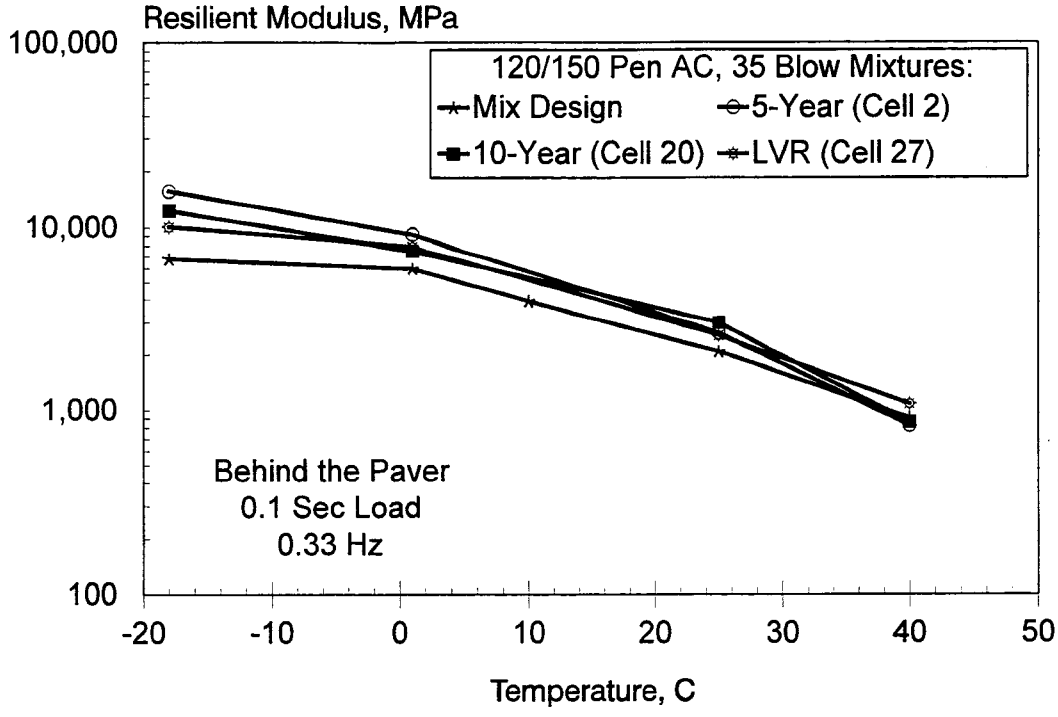

(a) 35-Blow, 120/150 Pen AC

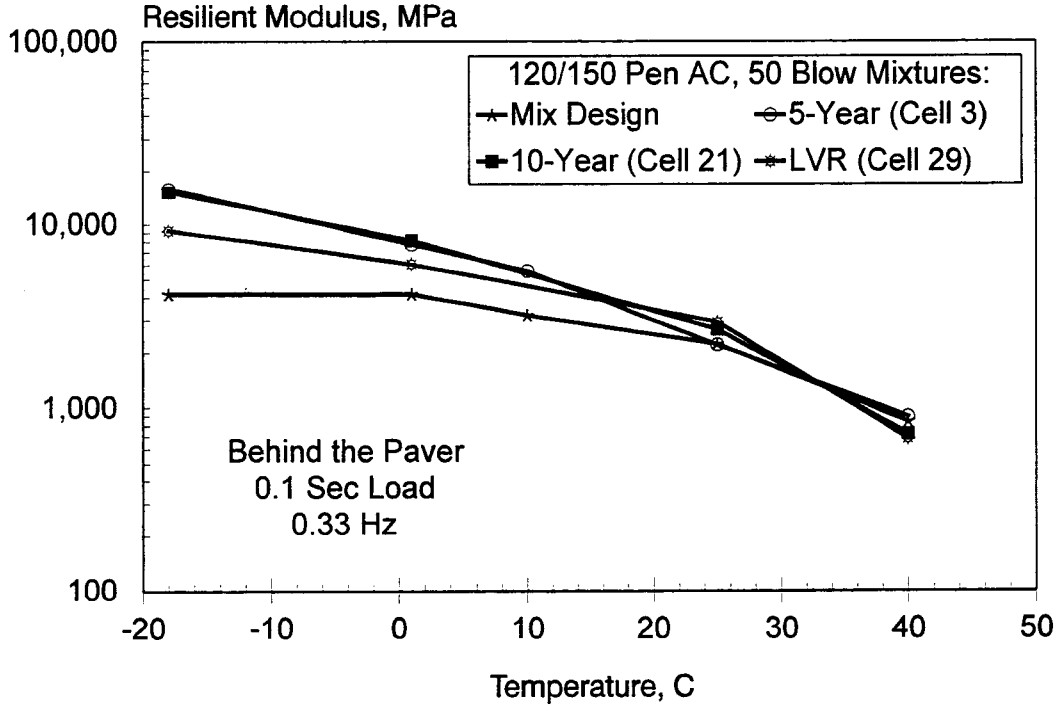

(b) 50-Blow, 120/150 Pen AC

Figure 8.1. Comparison of Mix Design and Behind the Paver Mixtures. (120/150 Pen AC)

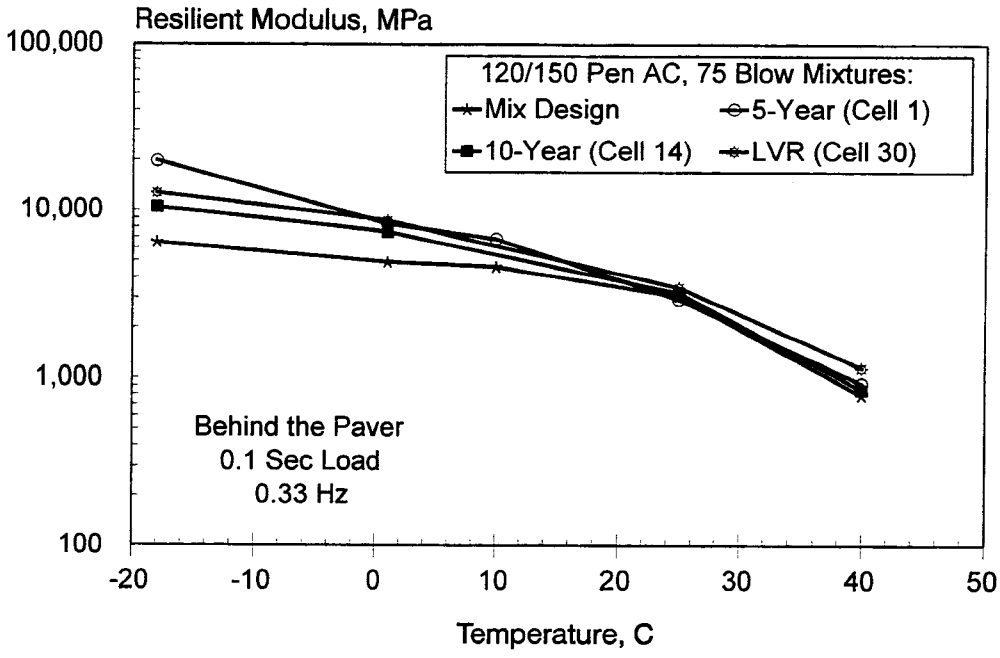

(c) 75-Blow, 120/150 Pen AC

Figure 8.1. (Continued) Comparison of Mix Design and Behind the Paver Mixtures. (120/150 Pen AC)

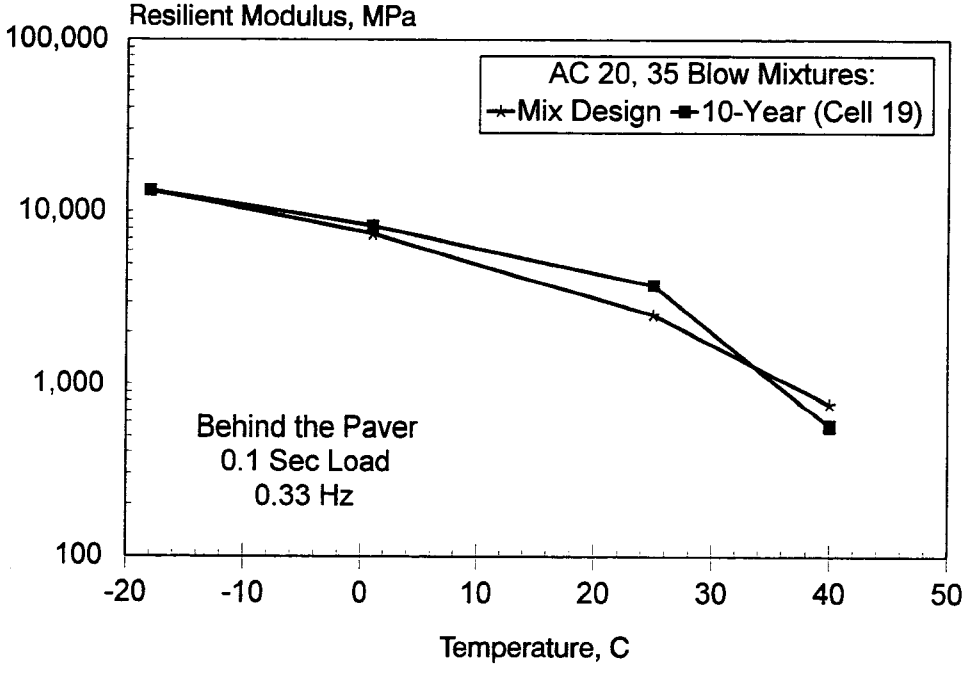

(a) 35-Blow, AC 20

Figure 8.2. Comparison of Mix Design and Behind the Paver Mixtures. (AC 20)

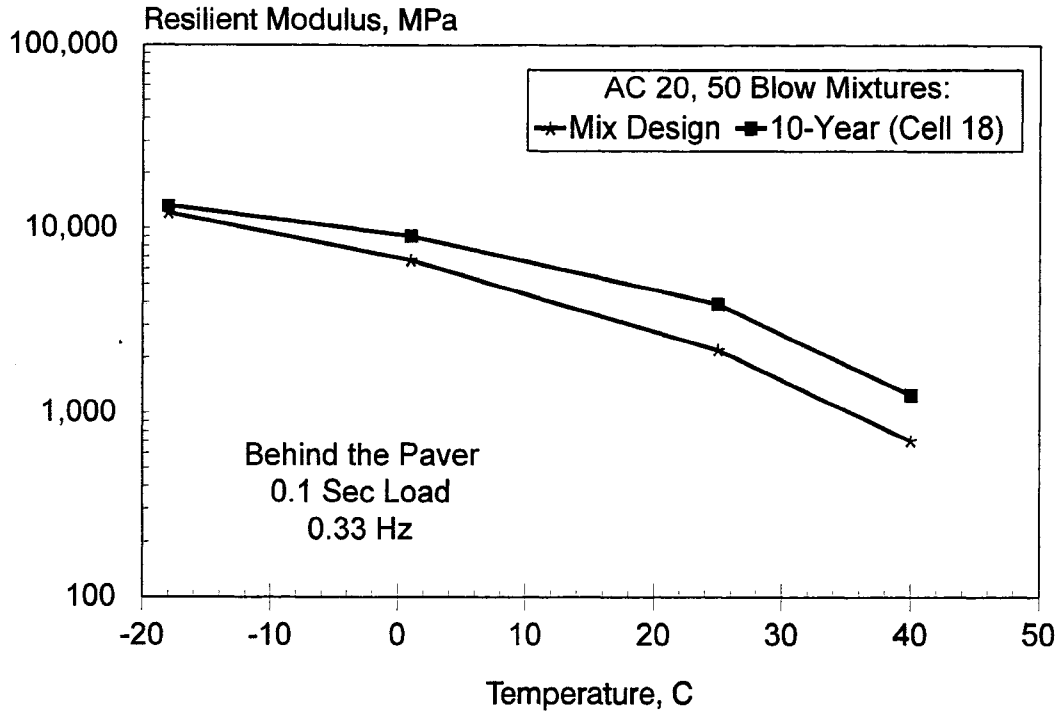

(b) 50-Blow, AC 20

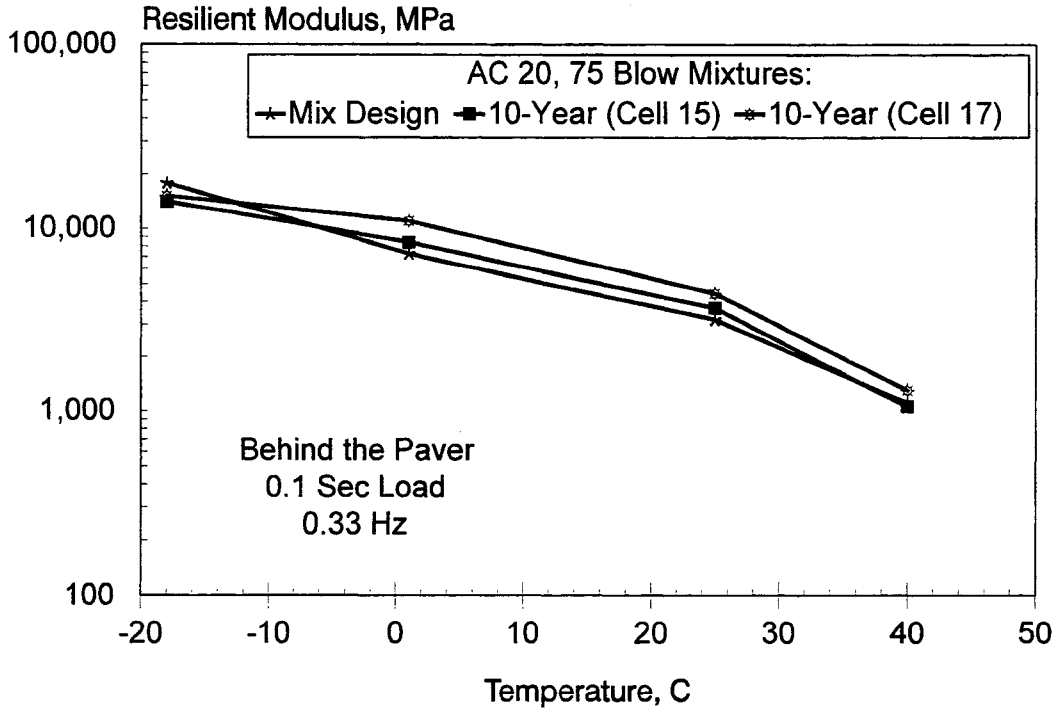

(c) 75-Blow, AC 20

Figure 8.2. (Continued) Comparison of Mix Design and Behind the Paver Mixtures. (AC 20)

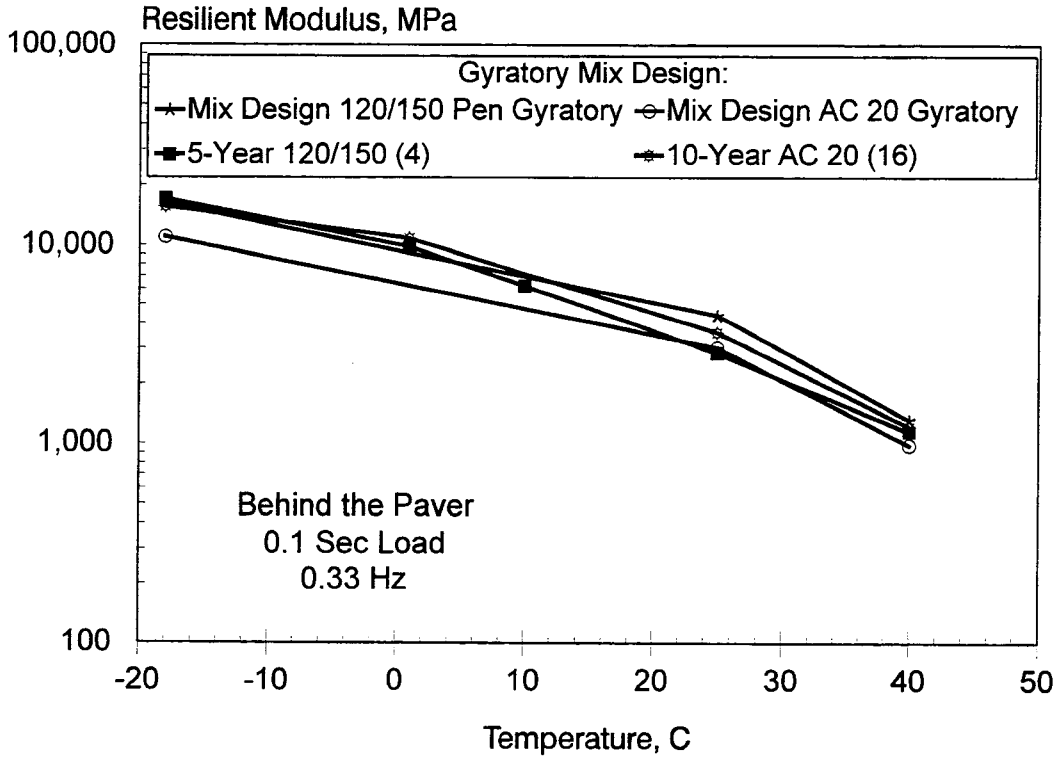

Figure 8.3. Comparison of Mix Design and Behind the Paver Mixtures (Gyratory Mix Design)

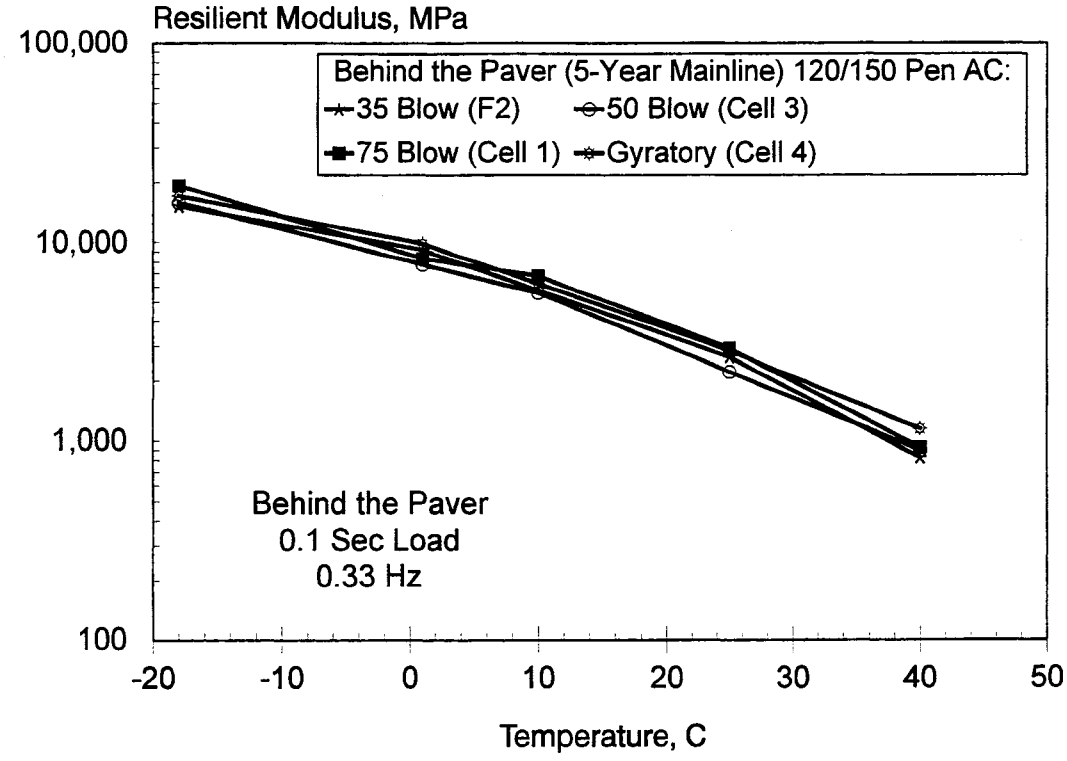

(a) 120/150 Pen AC Mixtures, 5-Year Mainline

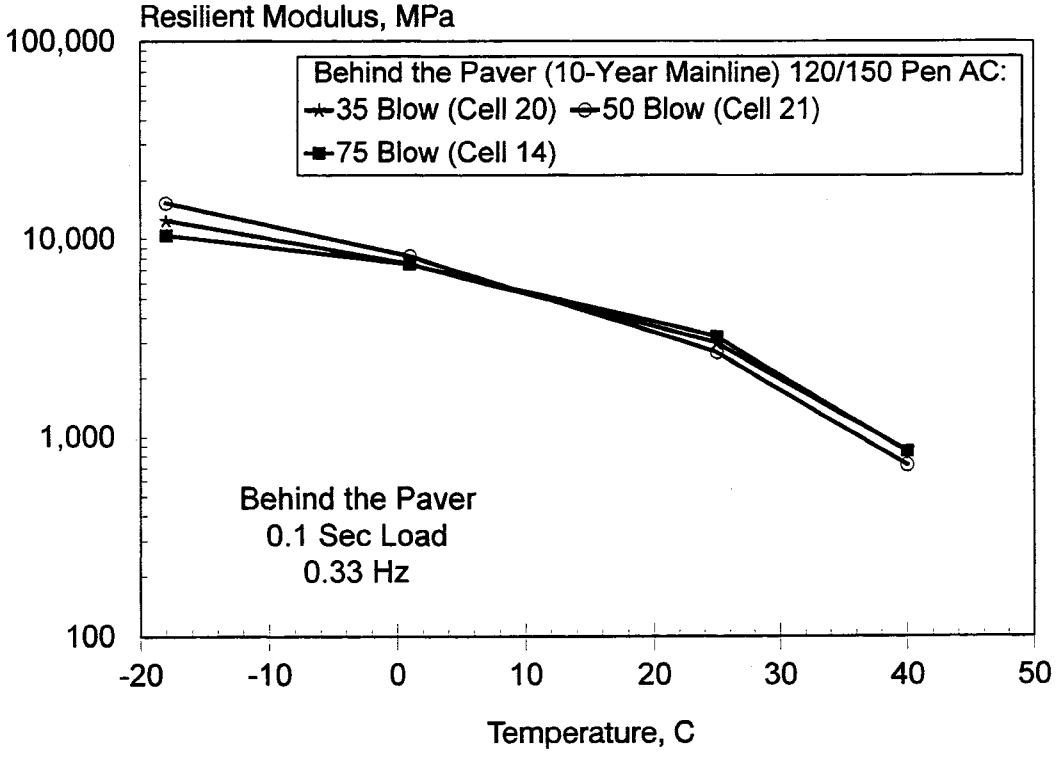

(b) 120/150 Pen AC Mixtures, 10-Year Mainline

Figure 8.4. Influence of Asphalt Content on Moduli Values.

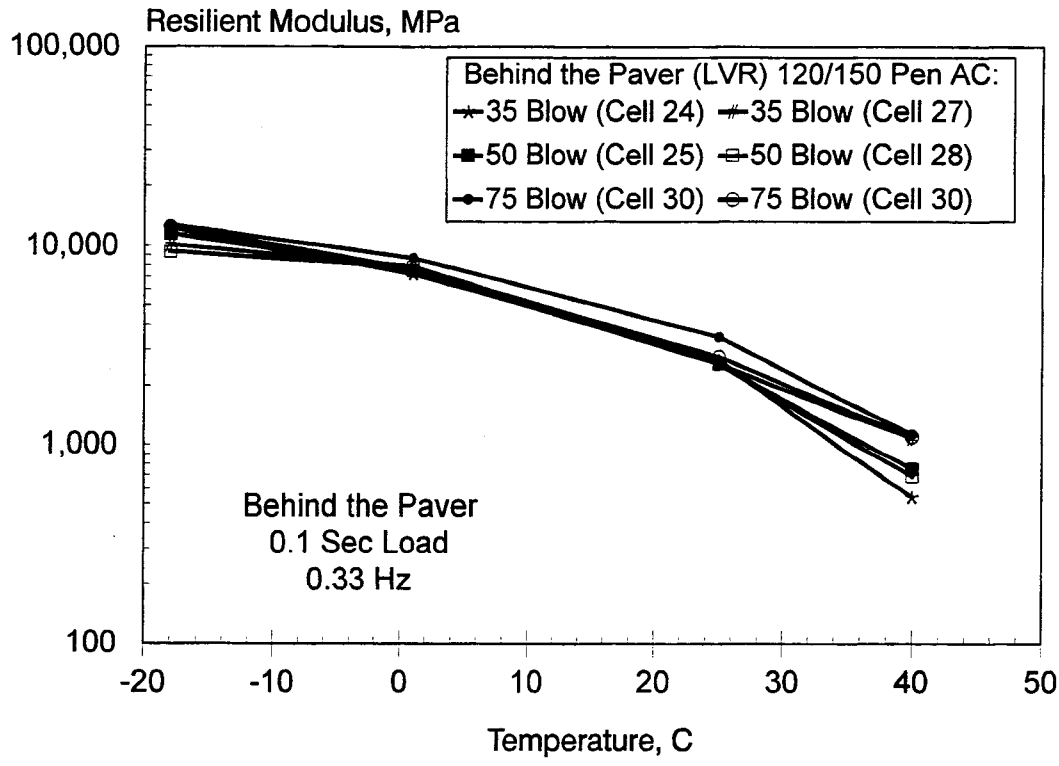

(c) 120/150 Pen AC Mixtures, LVR

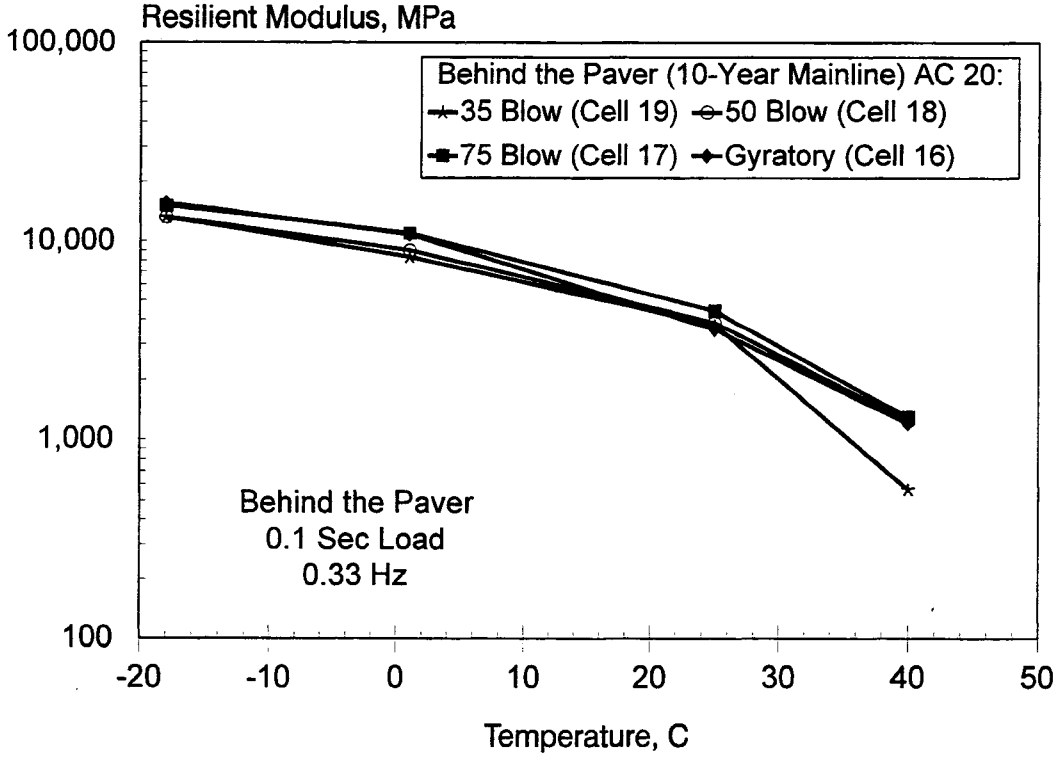

(d) AC Mixtures, 10-Year Mainline

Figure 8.4. (Continued) Influence of Asphalt Content on Moduli Values.

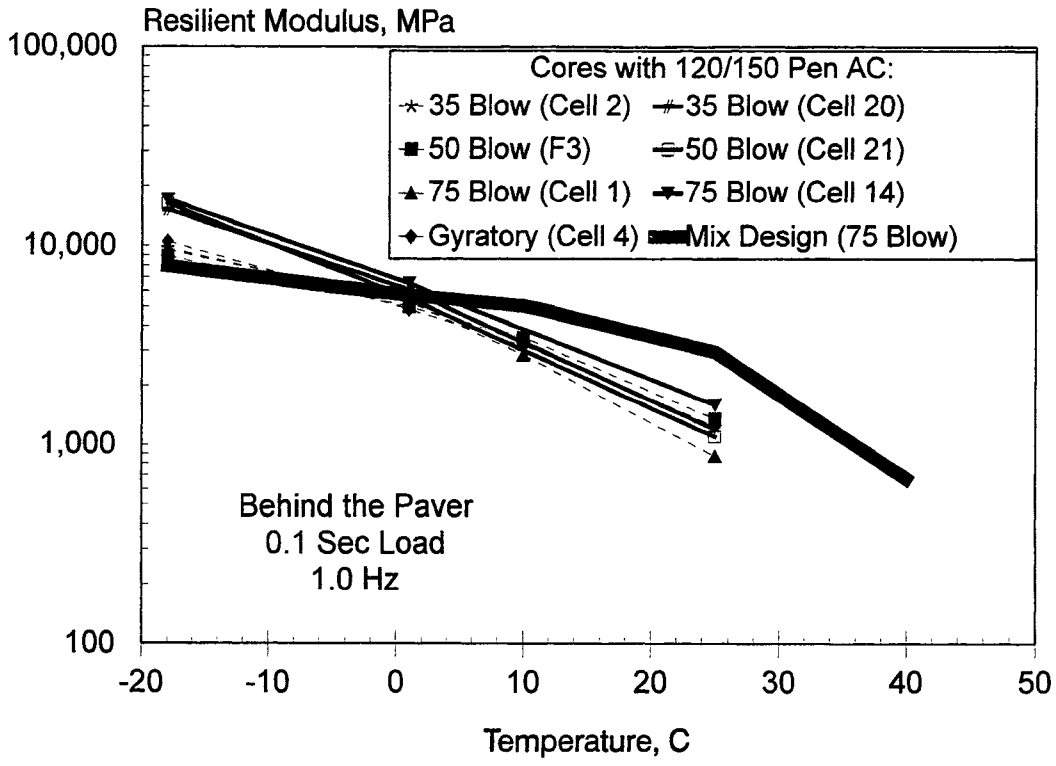

(a) 120/150 Pen AC Mixtures

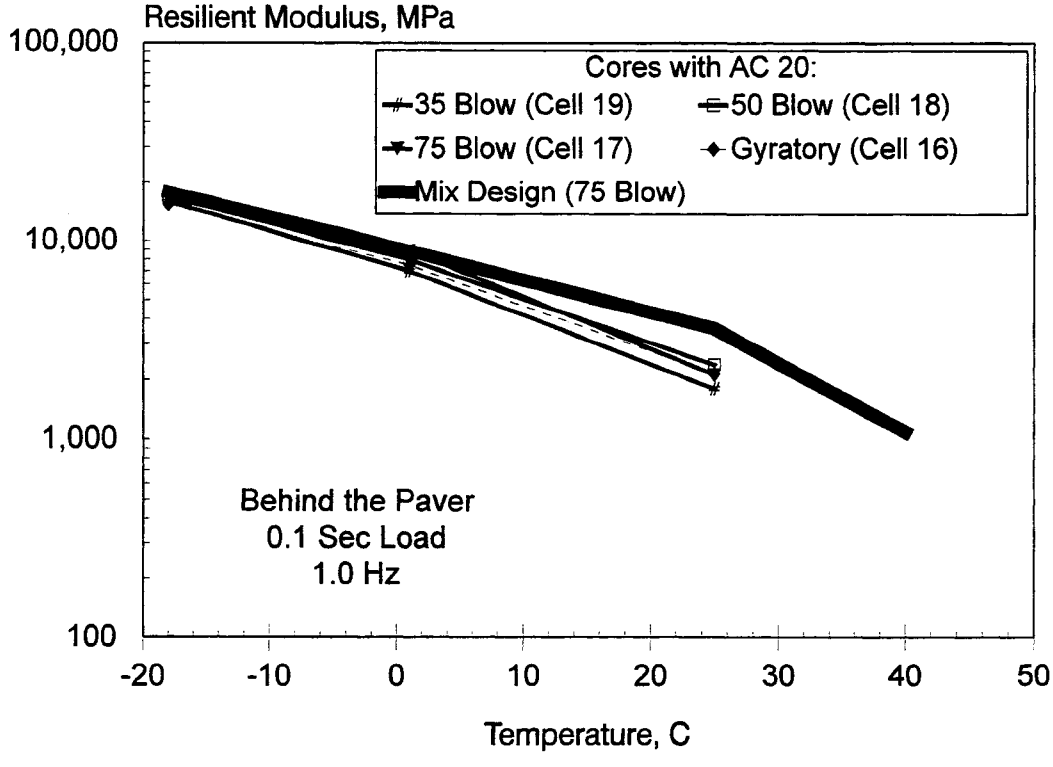

(b) AC 20 Mixtures

Figure 8.5. Comparison of Moduli Values for Cores and Representative Mix Design Materials.

Moisture Sensitivity

Figure 8.6 compares the mix design and behind-the-paver unconditioned tensile strengths and tensile strength ratios. In general, the behind-the-paver materials had either similar or greater tensile strengths than the mix design samples. The tensile strengths of the AC 20 mixtures from either sample source were about 20 percent higher than those for the 120/150 pen asphalt mixtures (Figures 8.6a and 8.6b). There was no consistent trend in tensile strength ratio results (Figures 8.6c and 8.6d).

Low Temperature Testing

Figure 8.7 compares the tensile strengths and corresponding horizontal strains for the 0.025 mm/min deformation rate at 1°C (34°F) of the mix design, behind-the-paver materials, and cores. The tensile strengths for the 120/150 pen asphalt behind-the-paver mixtures were similar to those for the mix design mixtures. They were approximately 50 percent higher than the mix design material results for the AC 20 mixtures. The tensile strengths of the cores were only about half of those for the mix design materials. This is most likely a function of the differences in air voids between the sample sets. Mix design samples generally had around 4 percent air voids while the voids in the cores were between 6 and about 7 percent.

The corresponding horizontal strains for the mix design and behind-the-paver mixtures were similar, regardless of asphalt grade. However, the strains for the cores were approximately 5 times those for the mix design mixtures. This difference is also most likely due to the difference in air voids.

Permanent Deformation

The creep compliance for the behind-the-paver mixtures were all consistently higher than for the corresponding mix design materials (Figure 8.8). While there were limited differences in creep compliance between the mix design 120/150 pen and AC 20 asphalt mixtures, there was a significant difference due to the asphalt grades in the behind-the-paver creep compliances. Note that all of the 120/150 pen asphalt behind-the-paver mixtures failed before 60 minutes of loading, while the AC 20 mixtures survived the testing program.

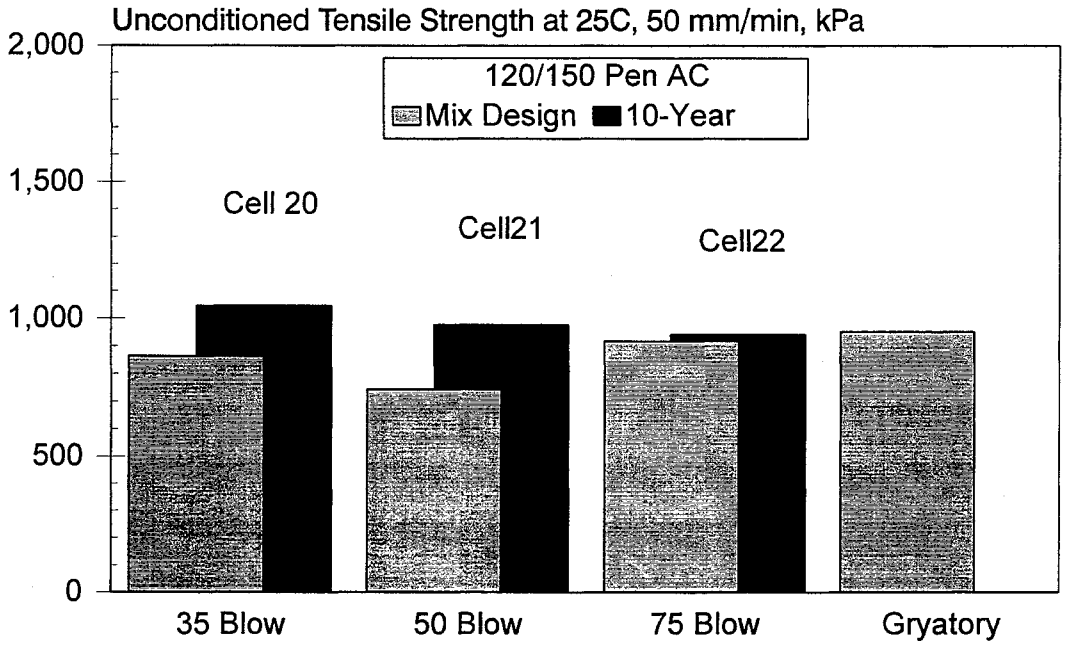

(a) 120/150 Pen AC Mixtures

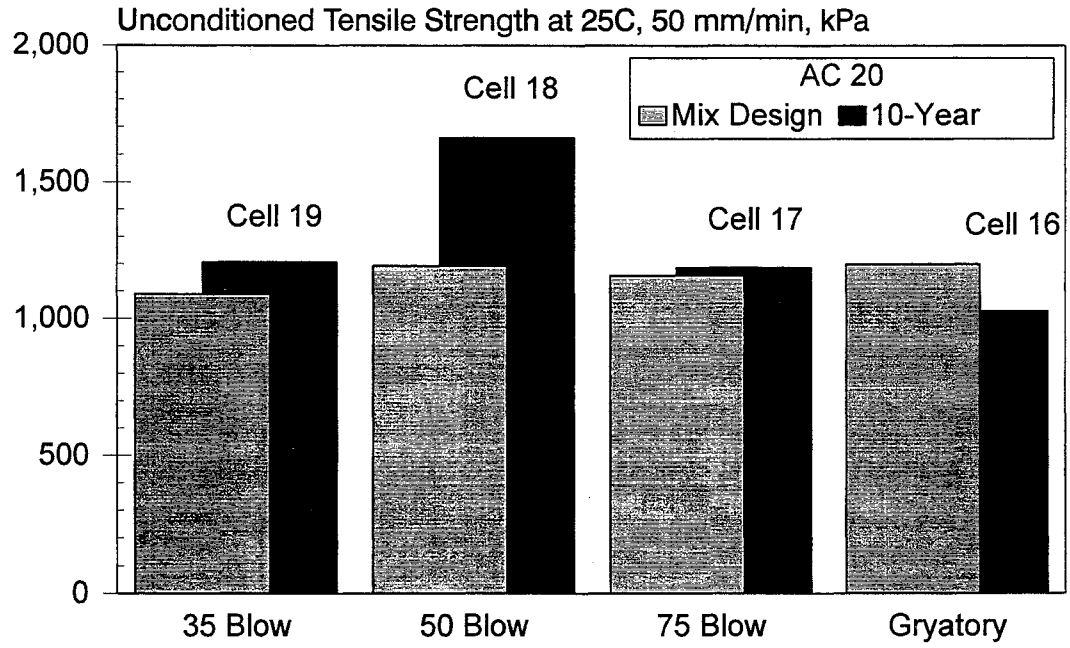

(b) AC 20 Mixtures

Figure 8.6. Unconditioned Tensile Strengths.

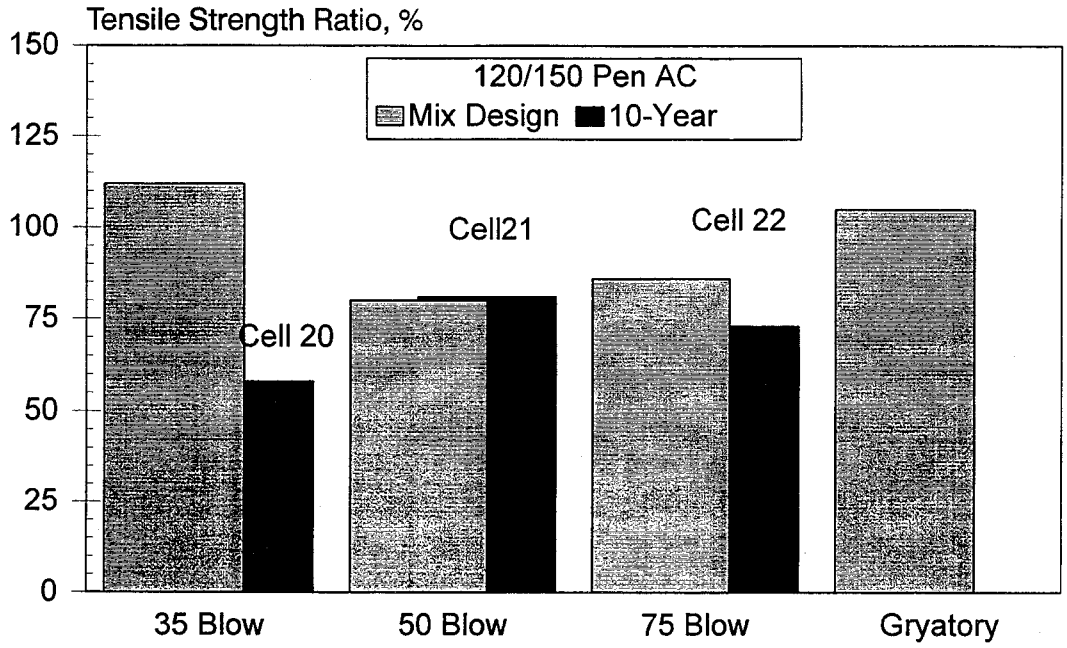

(c) 120/150 Pen AC Mixtures

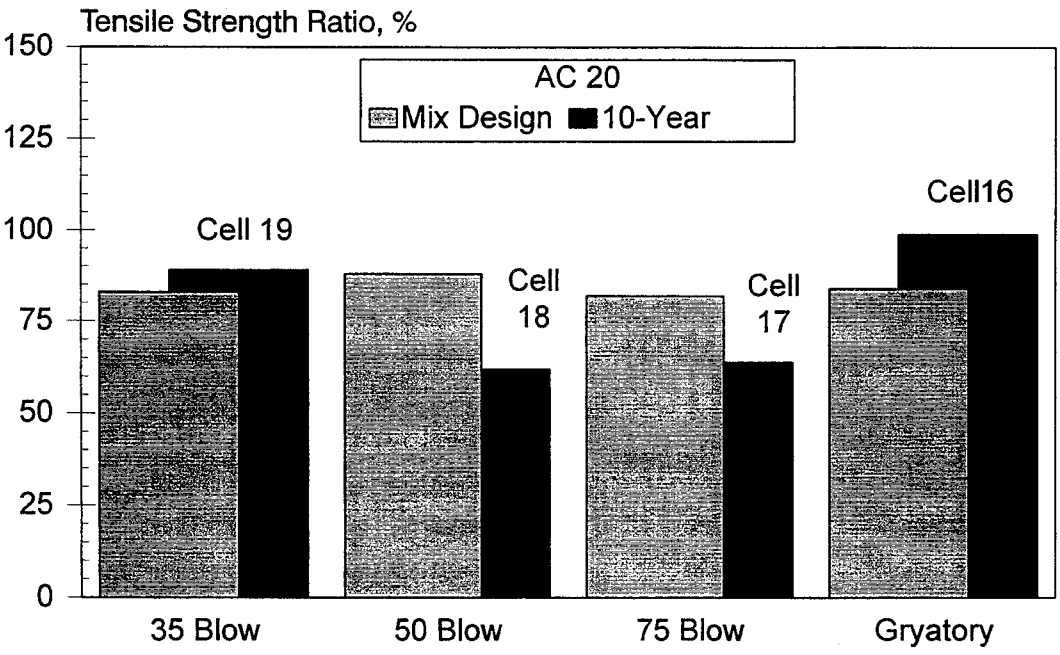

(d) AC 20 Mixtures

Figure 8.6. (Continued) Tensile Strength Ratios.

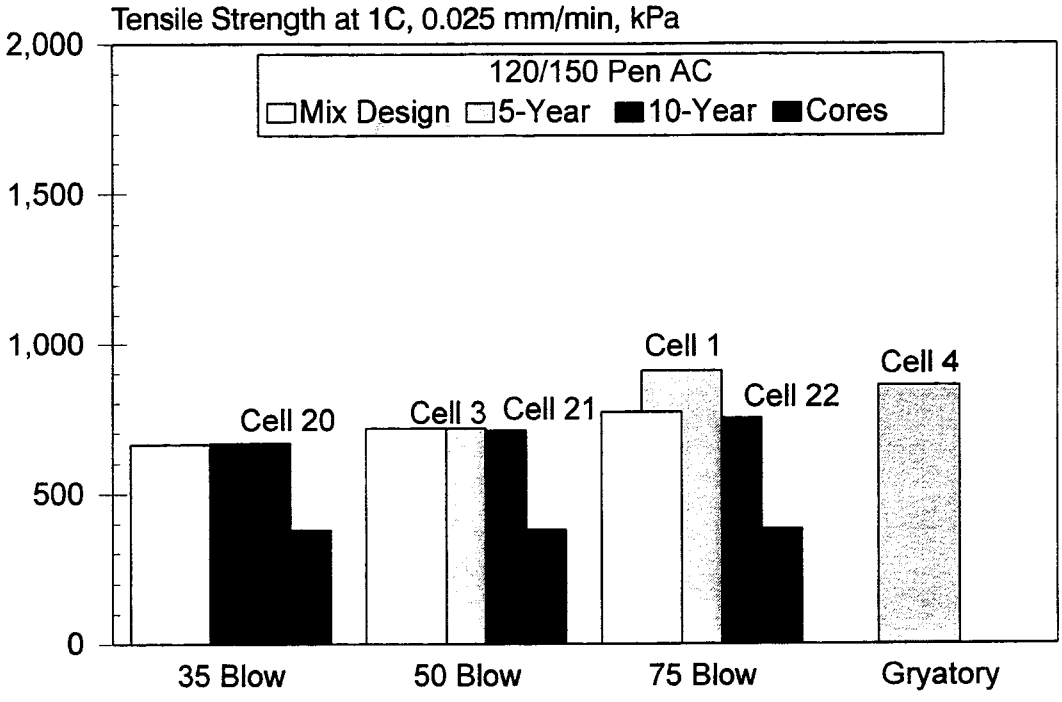

(a) 120/150 Pen AC Mixtures

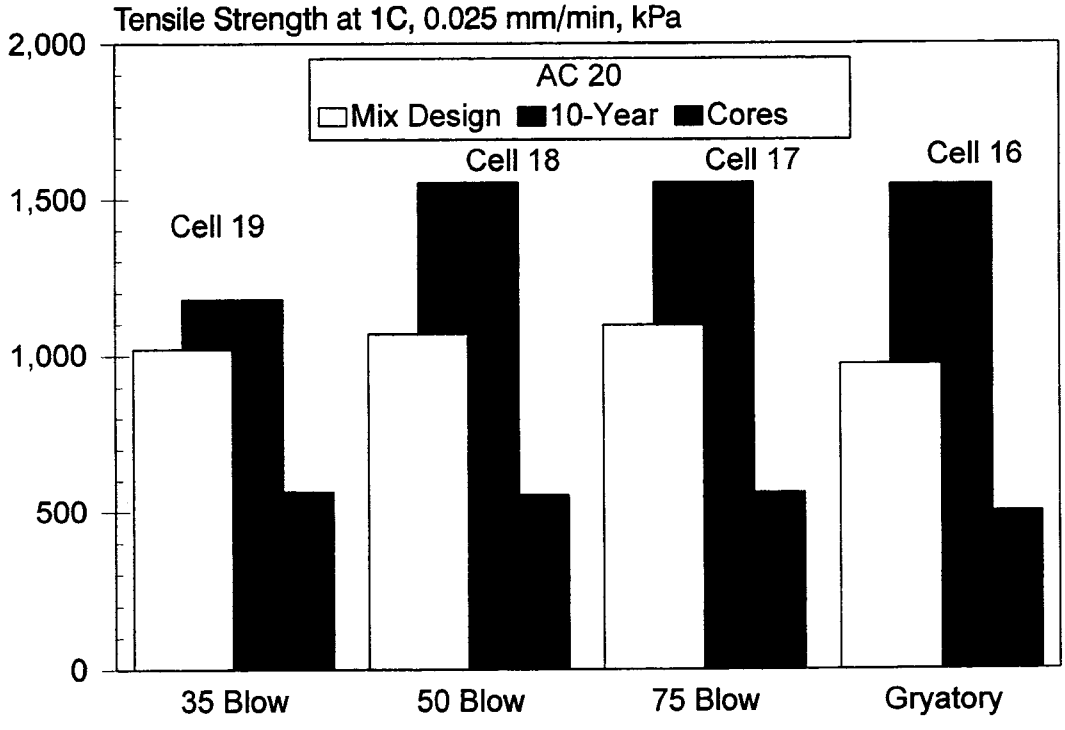

(b) AC 20 Mixtures

Figure 8.7. Low Temperature Tensile Strengths and Horizontal Strains.

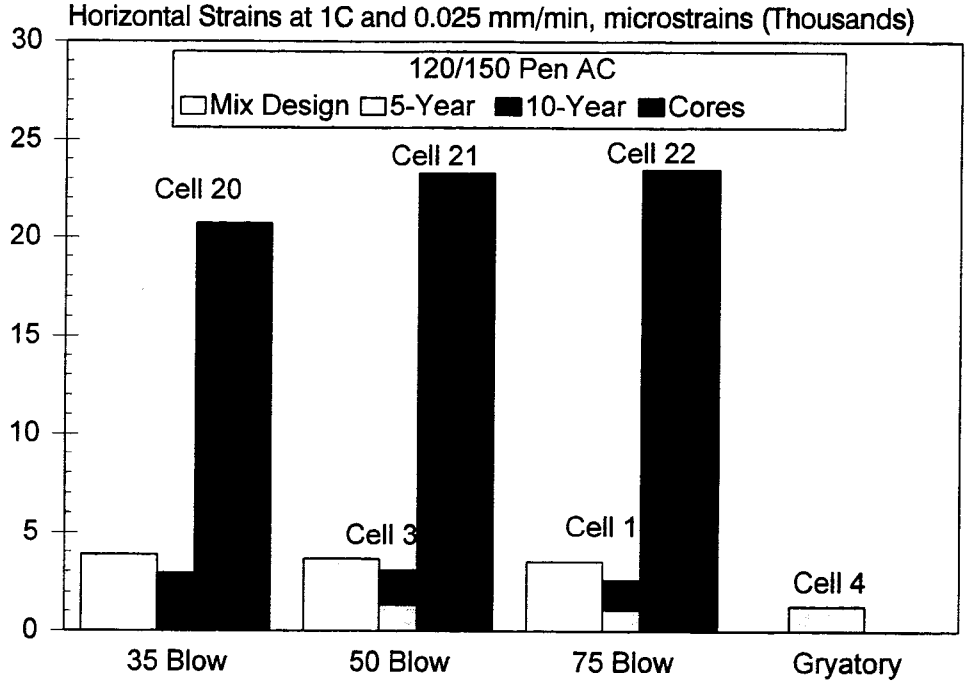

(c) 120/150 Pen AC Mixtures

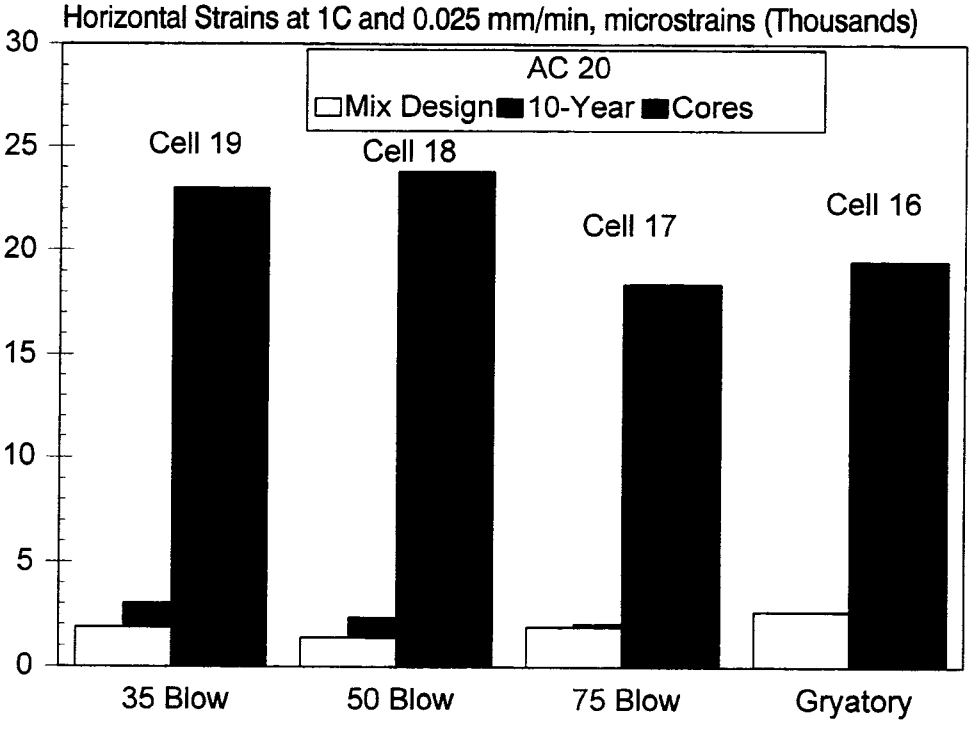

(d) AC 20 Mixtures

Figure 8.7. (Continued) Low Temperature Tensile Strengths and Hori Strains.

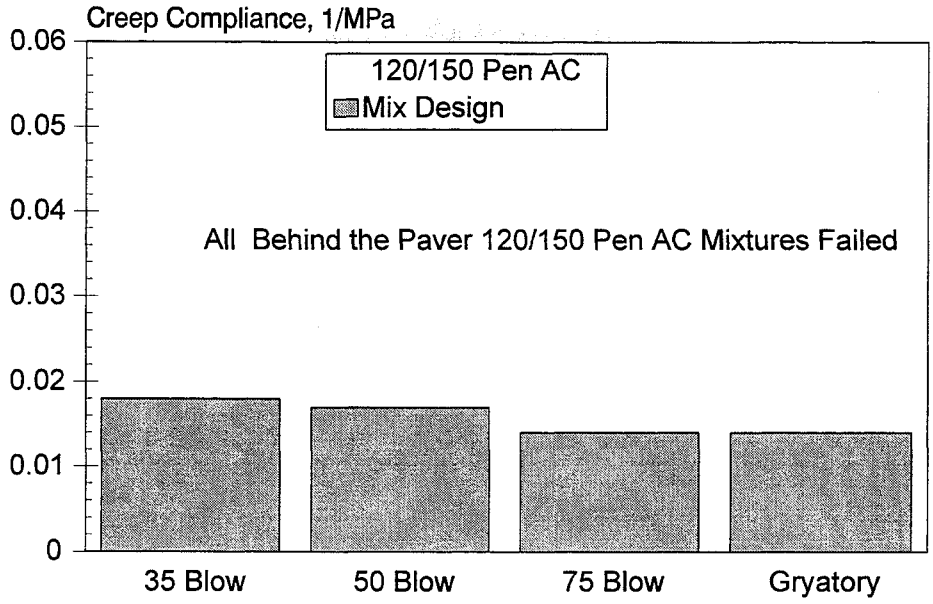

(a) 120/150 Pen Mixtures

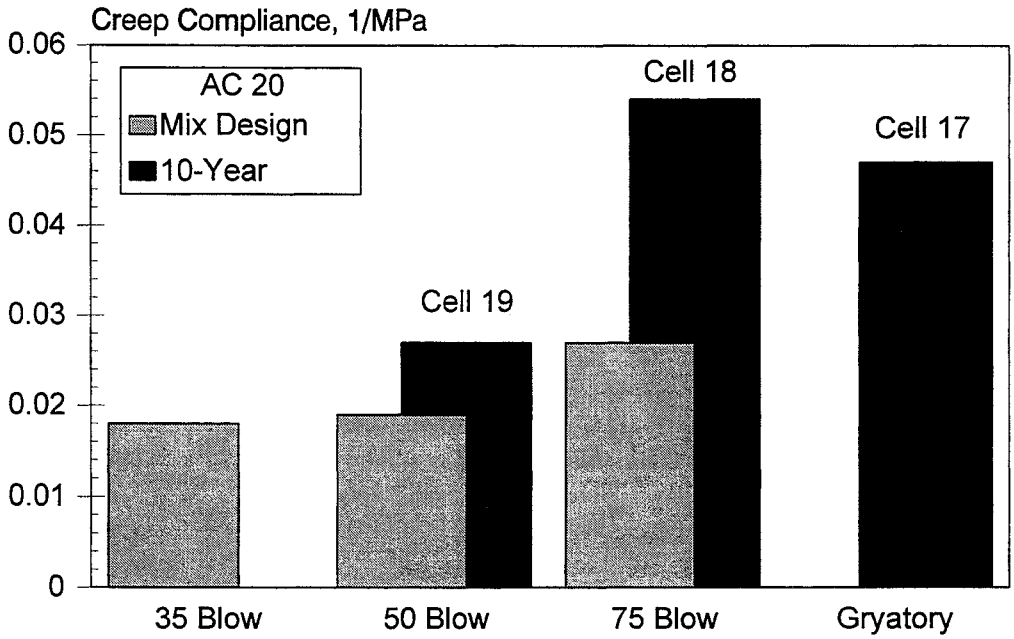

(b) AC 20 Mixtures

Figure 8.8. Comparison of Creep Compliance.

SUMMARY

Some general observations that can be made about the Mn/ROAD mixtures are as follows:

1. Temperature susceptibility, using resilient modulus testing (ASTM D4123) over a range of test temperatures, showed that mix design materials significantly under-predicted the moduli of the 120/150 pen asphalt mixtures when compared to the behind-the-paver materials. However, the higher viscosity AC 20 mix design moduli were generally similar to those obtained for behind-the-paver materials. This suggests that the lower viscosity asphalt may be more susceptible to aging (i.e., an increase in moduli) during production than the higher viscosity asphalt.

2. Resilient moduli values for mix design materials significantly under-predicted the cold temperature moduli for the cores from the 120/150 pen asphalt 10-Year Mainline test cells and over-predicted the warm temperature moduli. However, it should be noted that wet cores were sealed in plastic containers immediately after coring and then placed in cold storage until testing. This resulted in unplanned moisture conditioning of the cores and may be a significant factor in these comparisons.

3. Asphalt cement content did not have a significant influence on either temperature susceptibility or the magnitude of resilient moduli for a given asphalt grade.

4. Gyratory compaction of materials produced mixtures with similar moduli values at a given test temperature for both the 120/150 pen asphalt and the AC 20. There was also no significant difference between mix design and behind-the-paver materials.

5. The tensile strength of mixtures prepared with the AC 20 asphalt were approximately 20 percent greater than those prepared with the 120/150 pen asphalt. The tensile strengths of the behind-the-paver materials were either similar to or greater than the tensile strengths

for mix design materials.

6. There was no clear trend between tensile strength ratios for mix design and behind-the-paver materials.

7. Low temperature [1°C (34°F)] tensile strengths at slow rates of deformation (0.025 mm/min) were similar for the mix design and behind-the-paver materials. The tensile strength of the cores was approximately half of those for either the mix design or behind-the-paver materials. The horizontal strains for cores were about 5 times greater than those for either of the other two sources of materials. The most likely reason for this difference is a difference in air voids between the sample sets (approximately 4 percent for mix design and behind-the-paver, and between 6 and 8 percent for cores).

8. The creep compliance determined from unconfined static creep testing at 25°C (77°F) was similar for both the 120/150 pen and AC 20 mix design mixtures. However, there was a significant difference in the compliance for the behind-the-paver materials with the 120/150 pen asphalt mixtures showing a much greater compliance (i.e, failed) than the AC 20 mixtures.

This Page Intentionally Blank

REFERENCES

1. Lytton, R.L., Uzan, J., Fernando, E., Roque, R., Hiltunen, D., Stoffels, S., "Development and Validation of Performance Prediction Models and Specifications for Asphalt Binders and Paving Mixtures," Strategic Highway Research Program Report SHRP A357, National Research Council, 1993.

2. Von Quintas, H., Scherocman, J., Von Quintas, H., Hughes, C.S., Kennedy, T.W., "Procedural Manual for Mixture Design and AAMAS Volume I, Preliminary Draft Final Report," NCHRP 9-6(1), May, 1990.

3. Federal Highway Administration, Technical Advisory, 1989.

4. ---, Standard Specifications for Construction, Minnesota Department of Transportation, 1987.

5. ---, "Mix Design Methods for Asphalt Concrete and Other Hot-Mix Types," The Asphalt Institute Manual Series No. 2 (MS-2), 1988.

6 --, "Draft of SHRP Gyratory Compaction Method Procedures," The Asphalt Institute, 1992.

7. ---, "Recommended CRPRTF Base and Road Surface Aggregate Classes-Mn/DOT I-94 Cold Regions Pavement Research Test Facility (CRPRTF)," Version No. 1, Part III, DAMA, Inc., May 1988.

8. ---, "Bituminous Testing Report - Minnesota Road Research Project SP 8680-123 (TH-63), Monicello, Minnesota," Braun Intertec Engineering, Inc., 6801 Washington Ave. South, PO Box 39108, Minneapolis, Minnesota 55439-0108, November, 1993.

9. ---, "Test Procedures of Characterizing Dynamic Stress-Strain Properties of Pavement Materials, TRB Special Report 162, 1975.

10. American Society of Testing and Materials, Road and Paving Materials; Paving Management Technologies, Vol. 04.3, 1993.

11. Tunnicliff, D.G., Root, R.E., "Use of Anti-Stripping Additives in Asphaltic Concrete Mixtures," NCHRP Report 274, Transporation Researc Board, 1984.

12. Stroup-Gardiner, M., Newcomb, D., "Moisture Sensitivity of Minnesota Asphalt Concrete Mixtures,", Draft Report for Minnesota Department of Transportation, February, 1994.

13. Stroup-Gardiner, M., Newcomb, D., "Determination of Maximum Specific Gravity for Cores," Draft Report for Minnesota Department of Transportation, January, 1994.

14. Stroup-Gardiner, M., Krutz, N., Newcomb, D., "Data Distributions for Asphalt Concrete Resilient Modulus and Tensile Strengths," Strategic Highway Research Program and Traffic Safety on Two Continents, Gothenburg, Sweden, Sept. 27-29, 1989.

15. Curtis, C., Ensly, K., Epps, J., "Fundamental Properties of Asphalt-Aggregate Interactions Including Adhesion and Absorption," Strategic Highway Research Program Report SHRP A341, National Research Council, 1993.

16. Robl, T., Milburn, P., Thomas, G., Groppo, J., O'Hara, K., Haak, A., "The SHRP Materials Reference Library Aggregate: Chemical, Mineralogical, and Sorption Analyses," Strategic Highway Research Program Report SHRP UIR-91-509, National Research Council, 1991.

17. Stroup-Gardiner, M., Newcomb, D., Crow, B., "Physio-Chemical Evaluation of Asphalt-Aggregate Interactions," Mn/DOT Draft Report, February, 1994.

Appendix A

Theoretical Discussion of Diametral Compression

Theory of Diametral Tension Test

Most research samples, except the creep samples, were tested using the indirect tension apparatus. The theory of indirect tension test done on a Marshall sample is based on elastic Theory. The stresses σ_{xx} and σ_{yy} along the X and Y axes for the loading configuration shown in Figure A-1 were derived by Hondros (20). According to Hondros' solution:

$$\sigma_{xx}(0,y) = \frac{2P}{\pi at}\left[\frac{(1-\frac{y^2}{R^2})\sin 2\alpha}{(1-2\frac{y^2}{R^2}\cos 2\alpha+\frac{y^4}{R^4})} - \operatorname{atan}\left(\frac{1+\frac{y^2}{R^2}}{1-\frac{y^2}{R^2}}\tan\alpha\right)\right]$$

$$\sigma_{yy}(0,y) = -\frac{2P}{\pi at}\left[\frac{(1-\frac{y^2}{R^2})\sin 2\alpha}{(1-2\frac{y^2}{R^2}\cos 2\alpha+\frac{y^4}{R^4})} + \operatorname{atan}\left(\frac{1+\frac{y^2}{R^2}}{1-\frac{y^2}{R^2}}\tan\alpha\right)\right]$$

$$\sigma_{xx}(x,0) = \frac{2P}{\pi at}\left[\frac{(1-\frac{x^2}{R^2})\sin 2\alpha}{(1+2\frac{x^2}{R^2}\cos 2\alpha+\frac{x^4}{R^4})} - \operatorname{atan}\left(\frac{1-\frac{x^2}{R^2}}{1+\frac{x^2}{R^2}}\tan\alpha\right)\right] \qquad \text{(A-1)}$$

$$\sigma_{yy}(x,0) = -\frac{2P}{\pi at}\left[\frac{(1-\frac{x^2}{R^2})\sin 2\alpha}{(1+2\frac{x^2}{R^2}\cos 2\alpha+\frac{x^4}{R^4})} + \operatorname{atan}\left(\frac{1-\frac{x^2}{R^2}}{1+\frac{x^2}{R^2}}\tan\alpha\right)\right]$$

Where:

P = Applied load, kN (psi)

a = Width of the loading strip, mm (in)

t = Thickness of the sample, mm (in)

R = Radius of the sample, mm (in)

2α = Angle as shown in Figure A-1, radians

Since $a = 2R \sin\alpha$, Equation(A-1) can be rewritten as:

$$\sigma_{xx}(0,y) = \frac{P}{\pi Rt}\frac{1}{\sin\alpha}\left[\frac{(1-\frac{y^2}{R^2})\sin 2\alpha}{(1-2\frac{y^2}{R^2}\cos 2\alpha+\frac{y^4}{R^4})} - \operatorname{atan}\left(\frac{1+\frac{y^2}{R^2}}{1-\frac{y^2}{R^2}}\tan\alpha\right)\right]$$

$$\sigma_{yy}(0,y) = -\frac{P}{\pi Rt}\frac{1}{\sin\alpha}\left[\frac{(1-\frac{y^2}{R^2})\sin 2\alpha}{(1-2\frac{y^2}{R^2}\cos 2\alpha+\frac{y^4}{R^4})} + \operatorname{atan}\left(\frac{1+\frac{y^2}{R^2}}{1-\frac{y^2}{R^2}}\tan\alpha\right)\right]$$

$$\sigma_{xx}(x,0) = \frac{P}{\pi Rt}\frac{1}{\sin\alpha}\left[\frac{(1-\frac{x^2}{R^2})\sin 2\alpha}{(1+2\frac{x^2}{R^2}\cos 2\alpha+\frac{x^4}{R^4})} - \operatorname{atan}\left(\frac{1-\frac{x^2}{R^2}}{1+\frac{x^2}{R^2}}\tan\alpha\right)\right] \qquad \text{(A-2)}$$

$$\sigma_{yy}(x,0) = -\frac{P}{\pi Rt}\frac{1}{\sin\alpha}\left[\frac{(1-\frac{x^2}{R^2})\sin 2\alpha}{(1+2\frac{x^2}{R^2}\cos 2\alpha+\frac{x^4}{R^4})} + \operatorname{atan}\left(\frac{1-\frac{x^2}{R^2}}{1+\frac{x^2}{R^2}}\tan\alpha\right)\right]$$

Define the dimensionless stress components as

$$\sigma' = \frac{\sigma}{\frac{P}{\pi R t}} \tag{A-3}$$

Equation (A-2) becomes

$$\sigma'_{xx}(0,y) = \frac{1}{\sin\alpha}\left[\frac{(1-\frac{y^2}{R^2})\sin 2\alpha}{(1-2\frac{y^2}{R^2}\cos 2\alpha+\frac{y^4}{R^4})} - \operatorname{atan}(\frac{1+\frac{y^2}{R^2}}{1-\frac{y^2}{R^2}}\tan\alpha)\right]$$

$$\sigma'_{yy}(0,y) = -\frac{1}{\sin\alpha}\left[\frac{(1-\frac{y^2}{R^2})\sin 2\alpha}{(1-2\frac{y^2}{R^2}\cos 2\alpha+\frac{y^4}{R^4})} + \operatorname{atan}(\frac{1+\frac{y^2}{R^2}}{1-\frac{y^2}{R^2}}\tan\alpha)\right]$$

$$\sigma'_{xx}(x,0) = \frac{1}{\sin\alpha}\left[\frac{(1-\frac{x^2}{R^2})\sin 2\alpha}{(1+2\frac{x^2}{R^2}\cos 2\alpha+\frac{x^4}{R^4})} - \operatorname{atan}(\frac{1-\frac{x^2}{R^2}}{1+\frac{x^2}{R^2}}\tan\alpha)\right] \tag{A-2a}$$

$$\sigma'_{yy}(x,0) = -\frac{1}{\sin\alpha}\left[\frac{(1-\frac{x^2}{R^2})\sin 2\alpha}{(1+2\frac{x^2}{R^2}\cos 2\alpha+\frac{x^4}{R^4})} + \operatorname{atan}(\frac{1-\frac{x^2}{R^2}}{1+\frac{x^2}{R^2}}\tan\alpha)\right]$$

Figures A-2 and A-3 show the corresponding stress distribution. At the center of the specimen, where $x = y = 0.0$, the stresses along the horizontal and vertical axes are:

$$\sigma'_{xx}(0,0) = \frac{\sin 2\alpha - \alpha}{\sin\alpha}$$

$$\sigma'_{yy}(0,0) = -\frac{\sin 2\alpha + \alpha}{\sin\alpha} \tag{A-4}$$

Both plane stress and plane strain loading conditions can be considered from this set of solution and some useful guidelines can be obtained from such analysis.

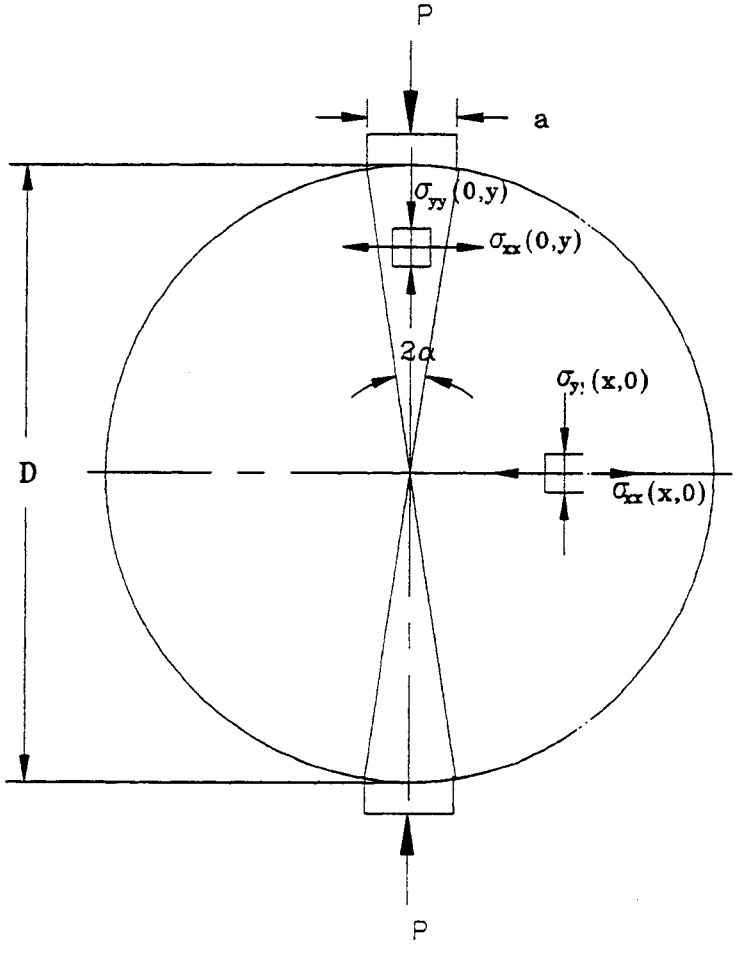

Figure A-1. Loading Configuration of Indirect Tension Test (20)

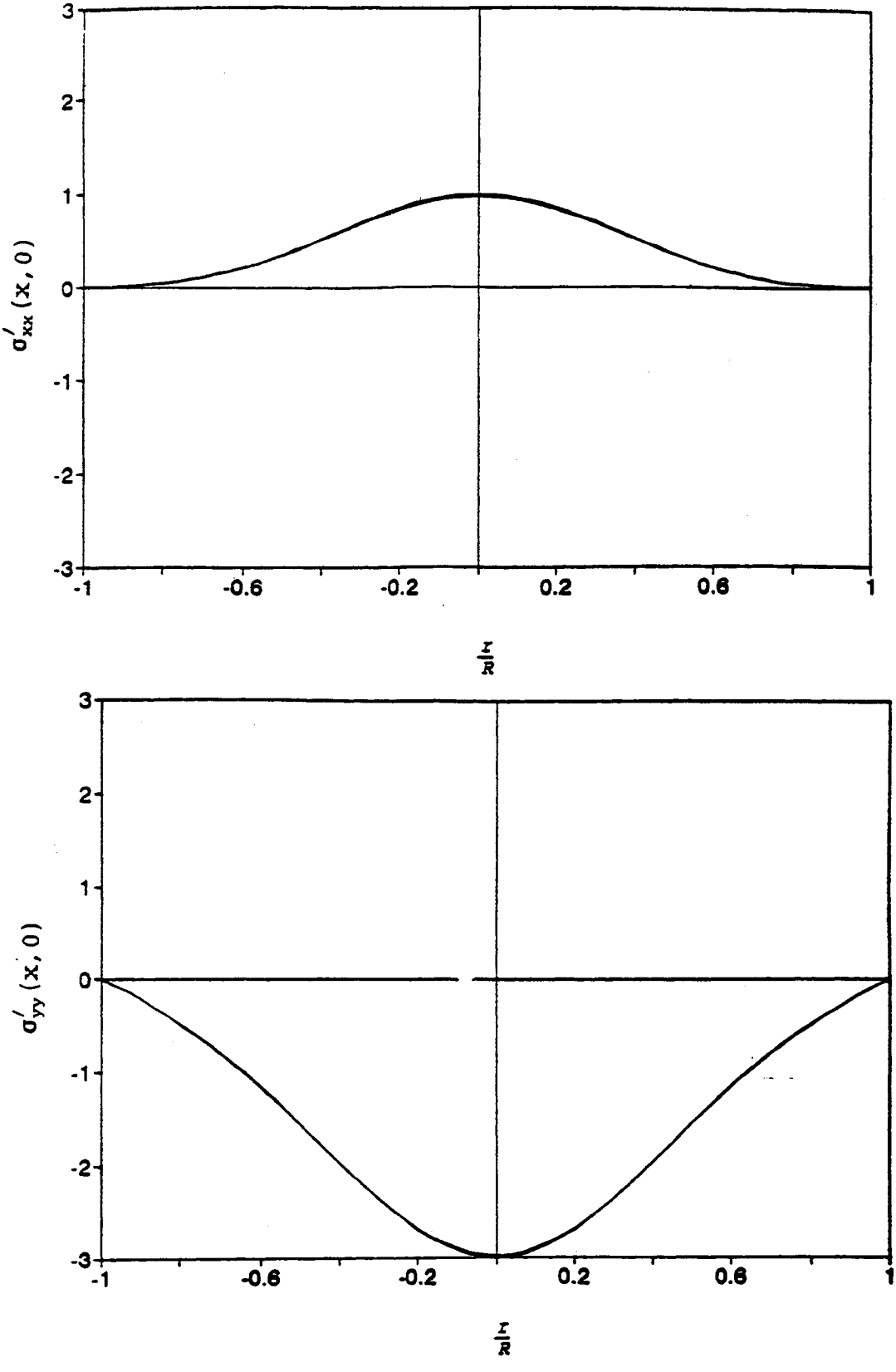

Figure A-2. Stress Distribution Along The Horizontal Axis

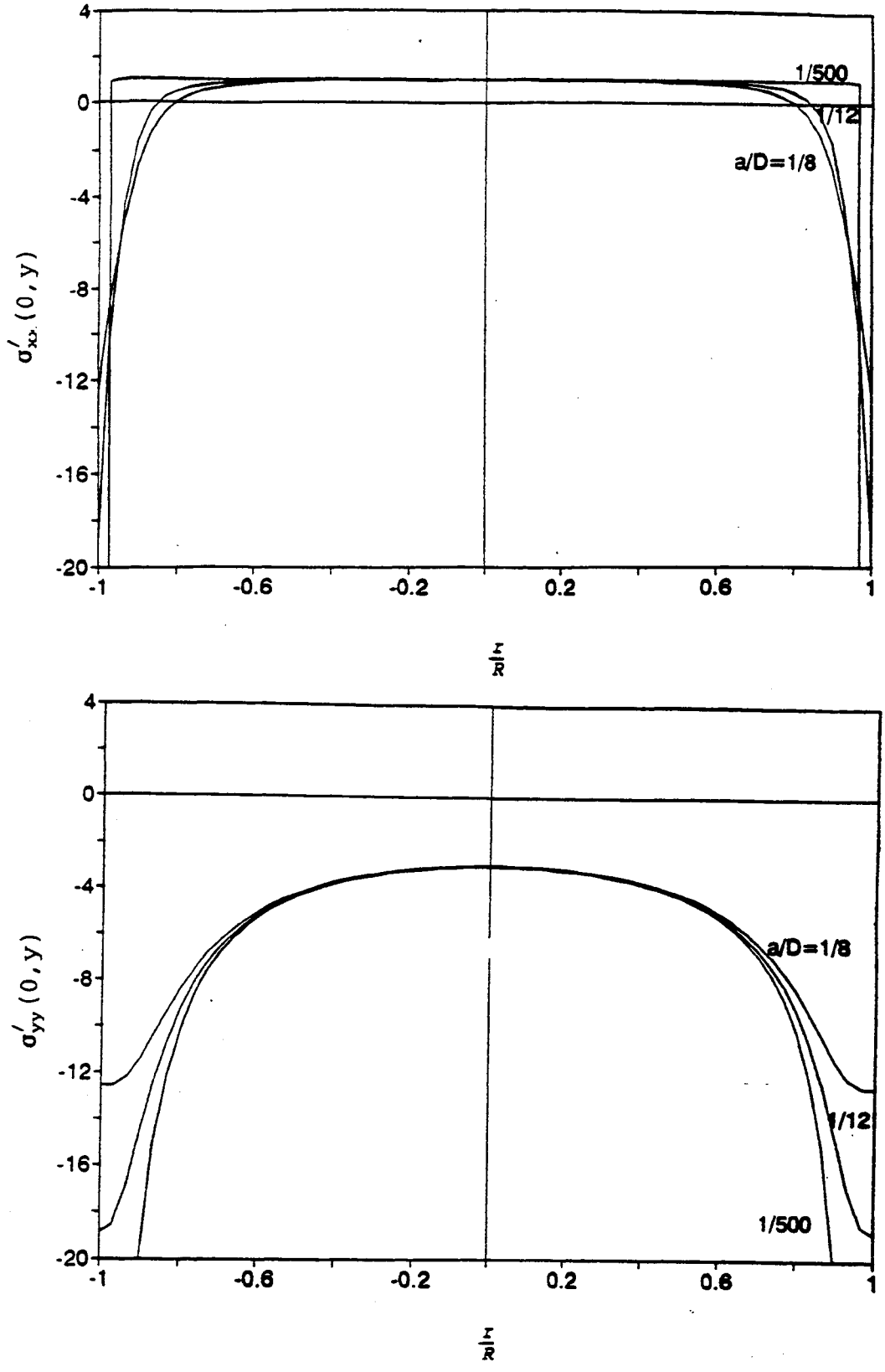

Figure A-3. Stress Distribution Along The Vertical Axis

Plane Stress Conditions

Assuming plane stress condition, let E be the Young's modulus and υ be the Poisson's ratio. According to Hooke's law:

$$\epsilon_{xx} = \frac{1}{E}[\sigma_{xx} - \upsilon\sigma_{yy}]$$
$$\epsilon_{yy} = \frac{1}{E}[\sigma_{yy} - \upsilon\sigma_{xx}] \qquad \text{(A-5)}$$

There are two ways to determine E and υ from a laboratory experiment. We can measure the strain components at any point inside the domain where the corresponding stress components can be calculated using equation (A-2a) and then solve for E and υ from equation (A-5). Or we can measure the total change in length across the X and Y axes which are the integration of (A-5) and than solve for E and υ. The latter is experimentally easier to achieve and the E and υ thus determined are average properties of a block of material. For asphalt concrete, the material properties are not uniform on a point to point basis due to the differences between the aggregate and mortar, but are uniform on a block to block basis. So the second approach is used for asphalt concrete. Let the total change in diameter across the horizontal axis is ΔU and the total change in diameter across the vertical axis is ΔV, then

$$\Delta U = \int_{-R}^{R} \epsilon_{xx}(x,0)dx = \frac{1}{E}\int_{-R}^{R}[\sigma_{xx}(x,0) - \upsilon\sigma_{yy}(x,0)]dx$$
$$\Delta V = \int_{-R}^{R} \epsilon_{yy}(0,y)dy = \frac{1}{E}\int_{-R}^{R}[\sigma_{yy}(0,y) - \upsilon\sigma_{xx}(0,y)]dy \qquad \text{(A-6)}$$

Define

$$I_1 = \int_{-R}^{R} \sigma_{xx}(0,y)dy \qquad I_2 = \int_{-R}^{R} \sigma_{yy}(0,y)dy$$
$$I_3 = \int_{-R}^{R} \sigma_{xx}(x,0)dx \qquad I_4 = \int_{-R}^{R} \sigma_{yy}(x,0)dx \tag{A-7}$$

The values of I_1 to I_4 are calculated using numerical integration and are listed in Table A-1.

Table A-1. Results of Numerical Integrations (times $2P/\pi t$).

Ratio of Loading Strip Width to Sample Diameter (a/D)	Integration Parameters			
	I_1	I_2	I_3	I_4
1/8	-0.09866	-5.63559	0.42395	-1.57078
1/12	-0.06566	-6.41790	0.42688	-1.57078
1/20	-0.03939	-7.41550	0.42837	-1.57078
1/100	-0.00797	-10.60415	0.42917	-1.57078
1/500	-0.00201	-13.81679	0.42920	-1.57078

Solving the equations in (A-6) for υ, we have

$$\upsilon = \frac{I_2\Delta U - I_3\Delta V}{I_1\Delta U - I_4\Delta V} = \frac{I_2 - I_3\frac{\Delta V}{\Delta U}}{I_1 - I_4\frac{\Delta V}{\Delta U}} \tag{A-8}$$

from (A-5)

$$E = \frac{1}{\Delta U}(I_3 - \upsilon I_4) \tag{A-9a}$$

or

$$E = \frac{1}{\Delta V}(I_2 - \upsilon I_1) \tag{A-9b}$$

and the tensile strain at the center of the specimen is

$$\epsilon_t(0,0)=\frac{1}{E}[\sigma_{xx}(0,0)-\upsilon\sigma_{yy}(0,0)] \qquad \text{(A-10)}$$

Substituting the values of I_1 to I_4 into equations (A-8), (A-9a), and (A-10), we can arrive at the expressions for E , υ and ϵ_t (0, 0). However, by observing Table A-1 one can notice that I_1 and I_2 vary with the a/D ratio, but I_3 and I_4 are virtually independent of the a/D ratio. So the expressions for E, υ, and ϵ_t (0, 0) will depend on a/D. In the current ASTM standard (ASTM D4123), equation (A-9a) is used for calculating the resilient modulus, and equation (A-10) is used for calculating the tensile strain. The dimensionless values of the stress components at the center of the specimen can be calculated according to equation (A-4) and the results are listed in Table A-2

Table A-2. Dimensionless Stress Values at the Center of the Specimen

a/D	σ'_{xx} (0,0)	σ'_{yy} (0,0)
1/8	0.98169	-2.98694
1/12	0.99188	-2.99420
1/20	0.99708	-2.99792
1/100	0.99988	-2.99992
1/500	0.99999	-3.00000

It can be seen that σ'_{xx} (0,0) and σ'_{yy} (0,0) do not depend on the a/D ratio. Substitute the values of I_3, I_4, σ'_{xx} (0,0), and σ'_{yy} (0,0) into equations (A-9a) and (A-10) result in

$$E = \frac{1}{\Delta U}\frac{P}{t}(0.2727+\upsilon) \qquad \text{(A-11a)}$$

$$\epsilon_t(0,0) = \frac{\Delta U}{D}\frac{0.99708+2.99792\upsilon}{0.42837+1.57078\upsilon} \qquad \text{(A-11b)}$$

The expression for υ as a function of a/D is summarized in Table A-3. The variation of υ as a function of a/D at different values of $\Delta V/\Delta U$ is plotted in Figure A-4. It has been reported that Poisson's ratio determined in this manner are usually unreasonable. The current practice is to assume a value of υ for each specimen, it is claimed that the resilient modulus E and the tensile strain ϵ_t (0, 0) are relatively insensitive to the variation of υ. Figures A-5 and A-6 show the variations of E and ϵ_t (0, 0) with respect to υ.

Assuming a material parameter before the test makes the test result more subjective and thus less reliable. This problem can be resolved by changing the integration range. The non-unique expression for υ is due to the fact that it involves the terms I_1 and I_2 which are very sensitive to the a/D ratio. From Figures A-2 and A-3 it can be seen that stresses along the horizontal axis do not depend on the a/D ratio, but stresses along the vertical axis do. This is why I_1 and I_2 vary with a/D, but I_3 and I_4 do not. However, stress deviations along the vertical axis happen only near the loaded boundary. Sufficiently far away from the loaded area, stress distributions along the vertical axis are independent of a/D. Therefore, instead of measuring the total change in diameter across the vertical diameter, the longitudinal deformation across the center part of the specimen can be measured where the stress distributions are independent of the a/D ratio. This way the stress concentration problem can be avoided and the stress integrations along the vertical axis are independent of a/D, thus arriving at an unique expression

for υ. The numerical integrations along the center part of the specimen are recalculated and listed in Table A-4.

Table A-3. Expression for Poisson's Ratio, $\upsilon = (I_2 - I_3 \beta) / (I_1 - I_4 \beta)$

a/D	υ
1/8	$\frac{-5.63559 - 0.42395\beta}{-0.09866 + 1.57078\beta}$
1/12	$\frac{-6.41819 - 0.42688\beta}{-0.06796 + 1.57078\beta}$
1/20	$\frac{-7.41550 - 0.42837\beta}{-0.03939 + 1.57078\beta}$
1/100	$\frac{-10.60415 - 0.42917\beta}{-0.00797 + 1.57078\beta}$
1/500	$\frac{-13.81679 - 0.42920\beta}{-0.00201 + 1.57078\beta}$

where $\beta = \Delta V / \Delta U$

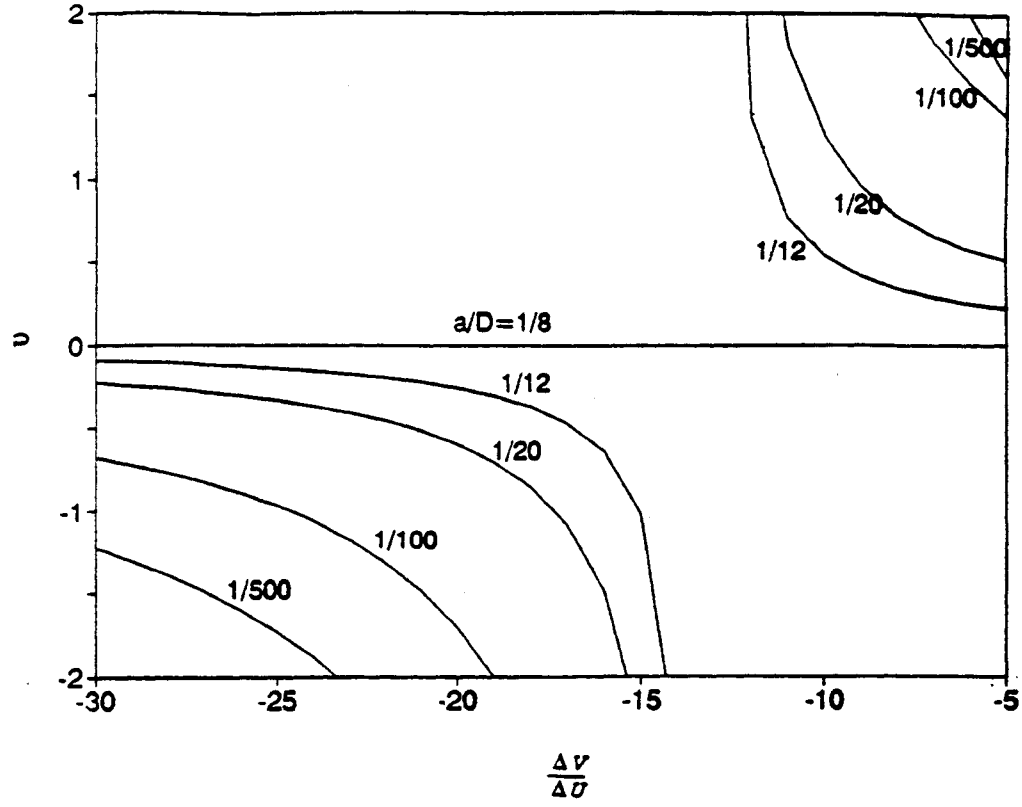

Figure A-4. Poisson's Ratio Versus ΔV/ΔU

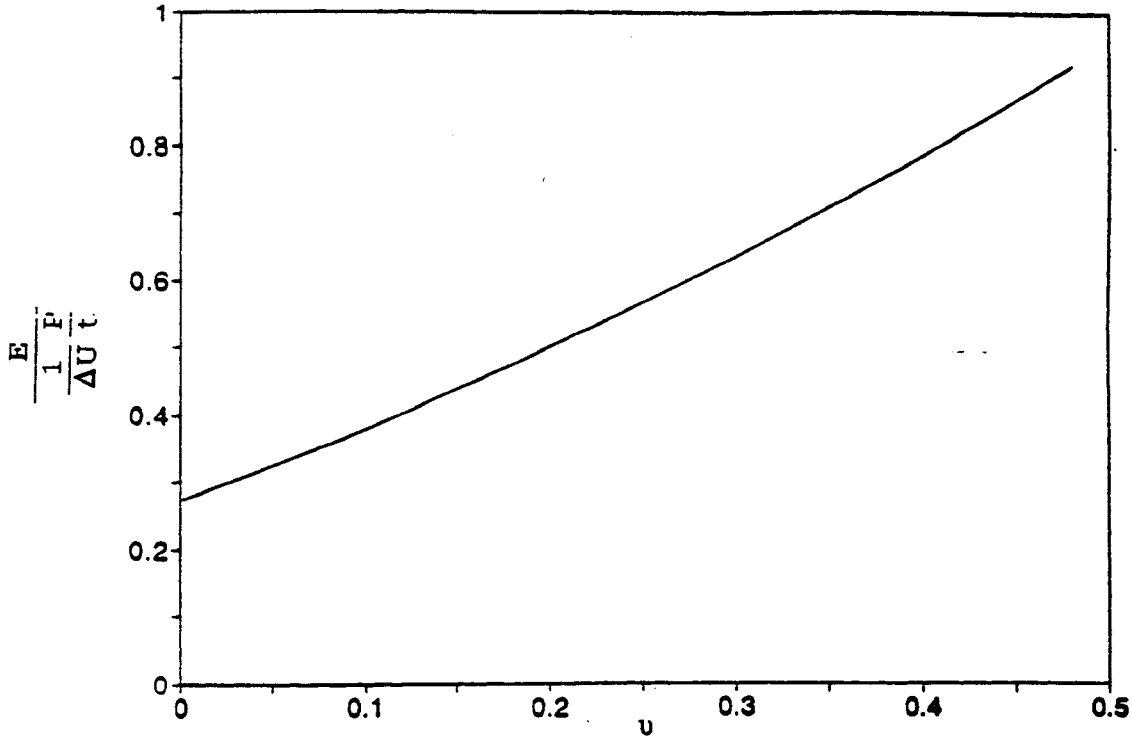

Figure A-5. Young's Modulus Versus Poisson's Ratio

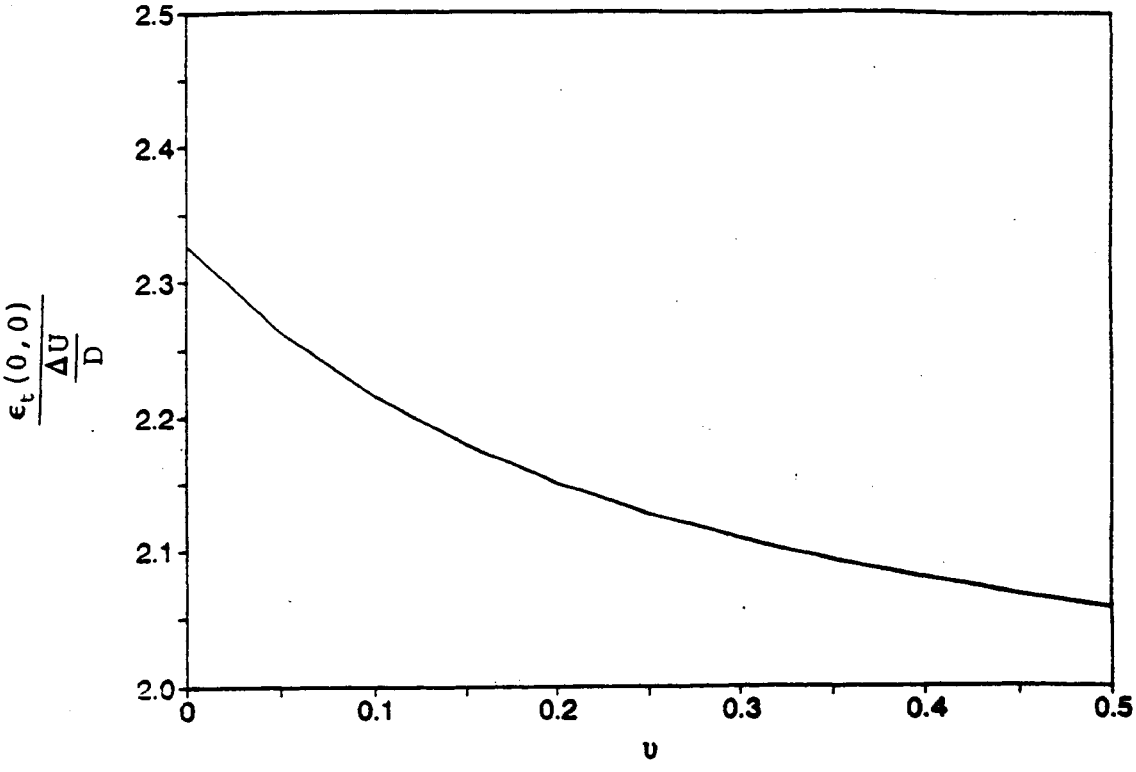

Figure A-6. Tensile Strain Versus Poisson's Ratio

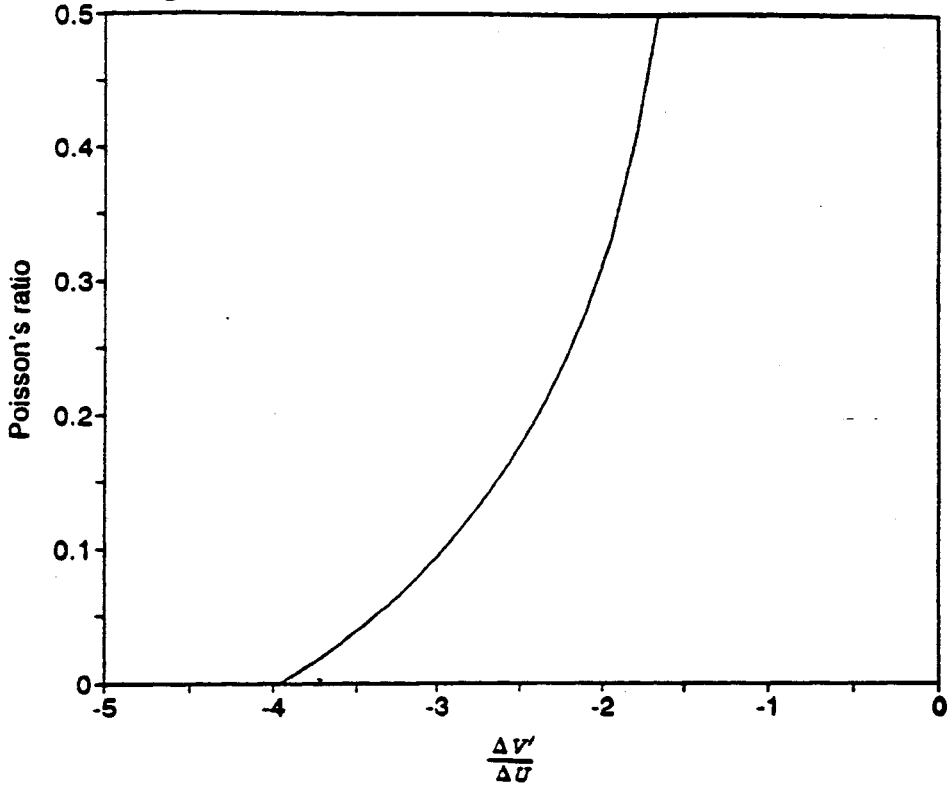

Figure A-7. Poisson's Ratio Versus ΔV'/ΔU

Table A-4. Numerical Integrals Along Part of the Axes

a/D	I_1'	I_2'	I_3'	I_4'
	r = 0.1 R			
1/8	0.098127	-0.29999	0.096896	-0.2961
1/12	0.099169	-0.30074	0.097887	-0.29679
1/20	0.099701	-0.30113	0.098382	-0.29715
1/100	0.099988	-0.30134	0.098665	-0.29734
1/500	0.1	-0.30135	0.098676	-0.29734
	r= 0.3R			
1/8	0.293224	-0.93253	0.26183	-0.83078
1/12	0.296991	-0.93563	0.265605	-0.83221
1/20	0.298917	-0.93721	0.266839	-0.83293
1/100	0.299957	-0.93807	0.267503	-0.83333
1/500	0.299998	-0.93810	0.26753	-0.83334
	r = 0.5R			
1/8	0.48293	-1.67996	0.367453	-1.22528
1/12	0.492377	-1.68954	0.370374	-1.22638
1/20	0.497249	-1.69449	0.371859	-1.22695
1/100	0.49989	-1.69717	0.372659	-1.22725
1/500	0.499996	-1.69728	0.372691	-1.22726
	r =0.7R			
1/8	0.648538	-2.70185	0.412839	-1.46023
1/12	0.676457	-2.73851	0.415794	-1.46067
1/20	0.691393	-2.7581	0.417297	-1.46089
1/100	0.699653	-2.76893	0.418105	-1.46102
1/500	0.699986	-2.76936	0.418137	-1.46102
	r = 0.9 R			
1/8	0.59306	-4.41132	0.423587	-1.56
1/12	0.726165	-4.67495	0.426518	-1.56005
1/20	0.826007	-4.85999	0.428008	-1.56007
1/100	0.896691	-4.98482	0.42881	-1.56008
1/500	0.899867	-4.99031	0.428842	-1.56009

where

$$I_1' = \int_{-r}^{r} \sigma_{xx}(0,y)dy \qquad I_2' = \int_{-r}^{r} \sigma_{yy}(0,y)dy$$
$$I_3' = \int_{-r}^{r} \sigma_{xx}(x,0)dx \qquad I_4' = \int_{-r}^{r} \sigma_{yy}(x,0)dx \tag{A-12}$$

It can be seen that within the range of [-0.5R, 0.5R], all the integrals are virtually independent of the a/D ratio. Let $\Delta V'$ be the total deformation along the vertical axis within the range of $-0.5R \leq y \leq 0.5R$, ΔU be the total deformation across the horizontal axis, then the expression for Poisson's ration becomes:

$$\upsilon = \frac{I_2' - I_3 \frac{\Delta V'}{\Delta U}}{I_1' - I_4 \frac{\Delta V'}{\Delta U}} = \frac{-1.69449 - 0.42837 \frac{\Delta V'}{\Delta U}}{0.49725 + 1.57078 \frac{\Delta V'}{\Delta U}} \tag{A-13}$$

The above expressions do not depend on the a/D ratio, and the relationship between Poisson's ratio and $\Delta V'/\Delta U$ is plotted in Figure A-7. It should be pointed out that we can also measure the longitudinal deformation at any other range within which stress distributions do not depend on the a/D ratio, it can be along either the horizontal or the vertical axis.

Plane Strain Conditions

Again, according to Hooke's law

$$\epsilon_{xx} = \frac{1}{E}[\sigma_{xx} - \upsilon(\sigma_{yy} + \sigma_{zz})]$$

$$\epsilon_{yy} = \frac{1}{E}[\sigma_{yy} - \upsilon(\sigma_{xx} + \sigma_{zz})] \qquad \text{(A-14)}$$

$$\epsilon_{zz} = \frac{1}{E}[\sigma_{zz} - \upsilon(\sigma_{xx} + \sigma_{yy})] = 0$$

eliminate σ_{zz} ,

$$\epsilon_{xx} = \frac{1}{E}[\sigma_{xx} - \upsilon\sigma_{yy} - \upsilon^2(\sigma_{xx} + \sigma_{yy})]$$

$$\epsilon_{yy} = \frac{1}{E}[\sigma_{yy} - \upsilon\sigma_{xx} - \upsilon^2(\sigma_{xx} + \sigma_{yy})] \qquad \text{(A-15)}$$

again by definition,

$$\Delta U = \int_{-R}^{R} \epsilon_{xx}(x,0)dx = \frac{1}{E}[I_3 - \upsilon I_4 - \upsilon^2(I_3 + I_4)]$$

$$\Delta V = \int_{-0.5R}^{0.5R} \epsilon_{yy}(0,y)dy = \frac{1}{E}[I_2' - \upsilon I_1' - \upsilon^2(I_1' + I_2')] \qquad \text{(A-16)}$$

from (A-16)

$$I_2' - \upsilon I_1' - \upsilon^2(I_1' + I_2') = [I_3 - \upsilon I_4 - \upsilon^2(I_3 + I_4)]\frac{\Delta V}{\Delta U} \qquad \text{(A-17)}$$

rearrange

$$[(I_3 + I_4)\frac{\Delta V}{\Delta U} - (I_1' + I_2')]\upsilon^2 + (I_4\frac{\Delta V}{\Delta U} - I_1')\upsilon + (I_2' - I_3\frac{\Delta V}{\Delta U}) = 0 \qquad \text{(A-18)}$$

define

$$a = (I_3+I_4)\frac{\Delta V}{\Delta U}-(I_1'+I_2')$$

$$b = (I_4\frac{\Delta V}{\Delta U}-I_1') \qquad \text{(A-19)}$$

$$c = (I_2'-I_3\frac{\Delta V}{\Delta U})$$

equation (A-18) becomes

$$av^2 + bv + c = 0 \qquad \text{(A-20)}$$

solve for v

$$v = \frac{-b\pm\sqrt{b^2-4ac}}{2a} \qquad \text{(A-21)}$$

If the values of I_1' , I_2' , I_3, and I_4 are substituted into (A-21) (remember $\Delta V / \Delta U < 0$), it can be shown that $a > 0$, $b < 0$, and $c < 0$. So for the Poisson's ratio to be meaningful, we should take the positive root.

$$v = \frac{-b+\sqrt{b^2-4ac}}{2a} \qquad \text{(A-22)}$$

from (A-16),

$$E = \frac{1}{\Delta U}\frac{2P}{\pi t}[I_3-vI_4-v^2(I_3+I_4)] \qquad \text{(A-23)}$$

In summary, for a plane stress condition:

$$\upsilon = \frac{I_2' - I_3\frac{\Delta V}{\Delta U}}{I_1' - I_4\frac{\Delta V}{\Delta U}}$$

$$E = \frac{1}{\Delta U}(I_3 - \upsilon I_4) \qquad \text{(A-24)}$$

$$\epsilon_t(0,0) = \frac{1}{E}[\sigma_{xx}(0,0) - \upsilon\sigma_{yy}(0,0)]$$

and for a plane strain condition:

$$\upsilon = \frac{-b+\sqrt{b^2-4ac}}{2a}$$

$$E = \frac{1}{\Delta U}[I_3 - \upsilon I_4 - \upsilon^2(I_3+I_4)] \qquad \text{(A-25)}$$

$$\epsilon_t(0,0) = \frac{1}{E}[\sigma_{xx}(0,0) - \upsilon\sigma_{yy}(0,0) - \upsilon^2(\sigma_{xx}(0,0)+\sigma_{yy}(0,0))]$$

where

$$\sigma_{xx}(0,0) = \frac{2P}{\pi Dt}$$

$$\sigma_{xx}(0,0) = 3\frac{2P}{\pi Dt} \qquad \text{(A-26)}$$

$$I_1' = 0.49725\frac{2P}{\pi t}$$

$$I_2' = -1.69449\frac{2P}{\pi t}$$

$$I_3 = 0.42837\frac{2P}{\pi t} \qquad \text{(A-27)}$$

$$I_4 = -1.57078\frac{2P}{\pi t}$$

$$a = (I_3+I_4)\frac{\Delta V}{\Delta U}-(I_1'+I_2')$$

$$b = (I_4\frac{\Delta V}{\Delta U}-I_1') \qquad \text{(A-28)}$$

$$c = (I_2'-I_3\frac{\Delta V}{\Delta U})$$

The υ - $\Delta V/\Delta U$ and E - $\Delta V/\Delta U$ relationships for both plane stress and plane strain conditions are plotted in Figures A-8 and A-9. It can be seen that the Poisson's ratios are virtually identical for plane stress and plane strain conditions. The difference in Young's moduli start to show up when $\Delta V /\Delta U > -2.5$.

The following conclusions can be drawn from this analysis:

1. Hondros' solution is suitable for diametral tension test.

2. Unified expressions for E, $\epsilon_t(0,0)$, and υ can be derived if properly selected measurements are obtained within a certain range along the horizontal or vertical axis.

3. The feasibility of designing a device that will allow the installation of either a strain gauge or a extensometer across the center part of the specimen to make the above measurement has been explored by researchers at Penn State University for the Strategic Highway Research Program (SHRP) (21). While there were some problems with matching signal conditioning with the sub-miniature LVDTs used, the last report from the researchers indicate these problems have been solved. Some form of this concept should be pursued in further research programs.

4. This proposed modification to the test method does not require an assumed value of υ. Poisson's ratio, resilient modulus, and tensile strain can all be determined experimentally. The accuracy of experiment can be greatly improved.

Due to time limitations for this program, equipment modifications were not possible. Therefore, the ASTM D4123 standard testing protocol (16) was used to determine the resilient modulus. The Poisson's ratio were assumed to be 0.2 for temperatures -18°C (0°F) and 1°C (34 °F), 0.35 for 25°C (77 °F), and 0.5 for 40°C (104°F).

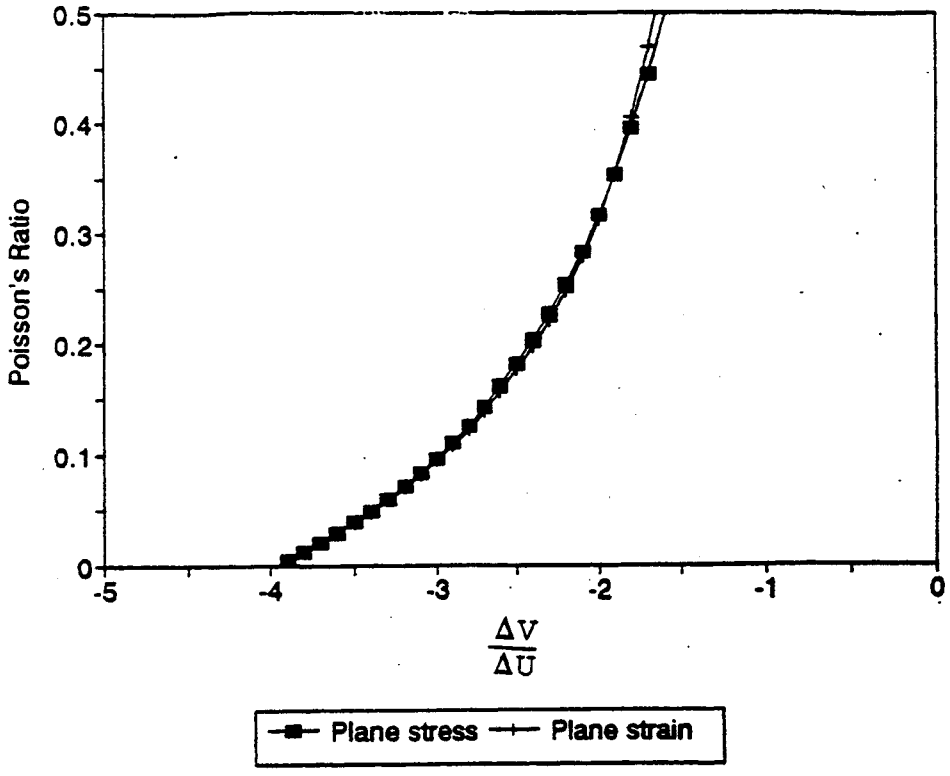

Figure A-8. Poisson's Ratio Versus ΔV/ΔU

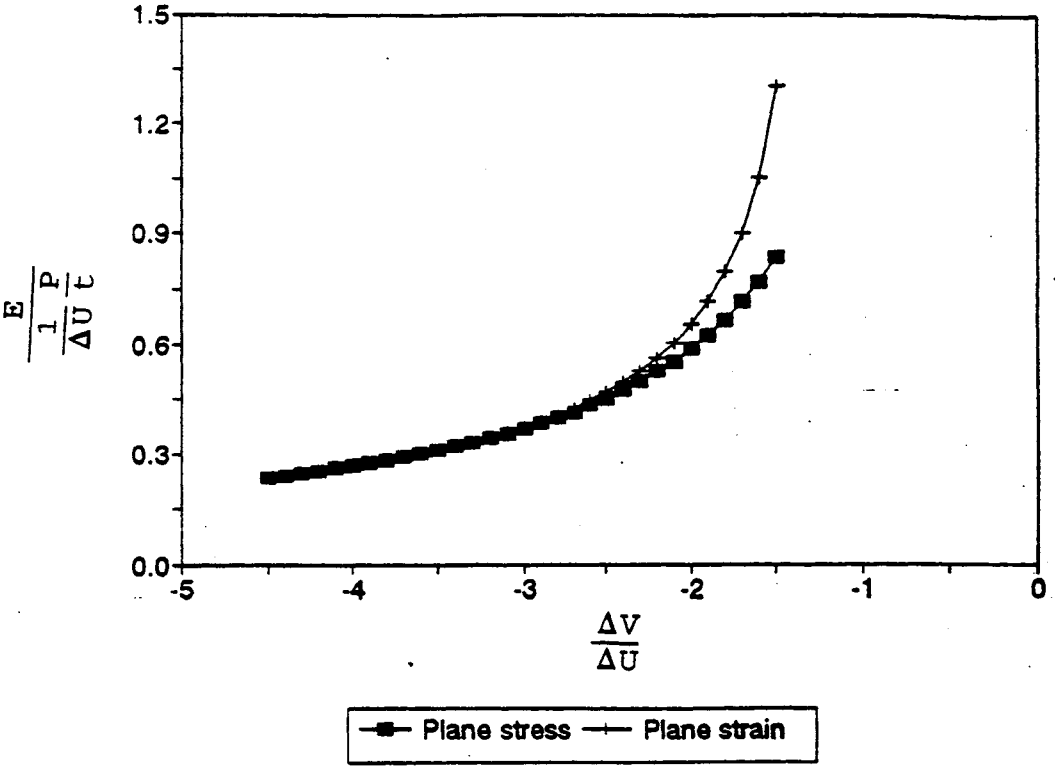

Figure A-9. Young's Modulus Versus ΔV/ΔU

Appendix B

Determination of Maximum Specific Gravity for Cores

INTRODUCTION

Cores were obtained from the Mn/ROAD 5-Year Mainline test sections during the fall of 1993. These cores were used for a range of research programs that included investigations of temperature susceptibility, moisture sensitivity, low temperature behavior, and permanent deformation characteristics. One of the most important mixture property that was expected to influence results from any of these research programs is the air void content of the cores. Therefore, every effort was made to insure an accurate measurement of the in-place voids.

Initial air void determinations for each of the four test sections located in the 5 Year Mainline facility appeared to be lower than anticipated. In order to confirm the results a second set of cores was obtained and tested by the Minnesota Department of Transportation (Mn/DOT) laboratory. The Mn/DOT results showed consistently higher air voids than those reported by the University of Minnesota laboratory. An evaluation of the sampling and testing programs indicated that the differences could be the result of real material differences due to the different sampling locations, variations in the maximum specific gravity test methods used by each laboratory, and/or sample preparation. A limited investigation was conducted by the University of Minnesota to investigate these potential sources for the inter-laboratory differences in reported air voids.

BACKGROUND

Many test methods have been developed for determining maximum specific gravity of paving mixtures. The most commonly cited methods are the American Society for Testing and Materials (ASTM) D2041 and the American Association of State Highway and Transportation Officials (AASHTO) T209 (2,3). Individual state agencies also commonly develop their own version(s) (Mn/DOT 1807 (draft)) that address specific concerns of each agency (4).

In general, all test methods prescribe placing a known mass of oven dried loose mixture in a tared vacuum vessel such as an inverted bell jar or pycnometer. The sample is then covered with a sufficient quantity of water to submerge the sample and a vacuum of less than 30 mm of

mercury absolute pressure is applied for a specified time. During the time the sample is being subjected to a vacuum, it can be agitated either continuously with a mechanical shaker or intermittently by hand. At the end of this procedure, the vacuum is gradually released and the volume determined by either immersing the container and sample in a water bath for 10 $\pm$1 minutes and weighing under water or by filling the container to a known level with water and weighing in air after 10 $\pm$1 minutes. Temperature corrections are made for the volume of water if the test temperature differs from the prescribed temperature. Variations between test methods are summarized in Table 1.

Table 1. Comparison of Variations in Selected Test Methods for Determining Maximum Specific Gravity

Test Method Parameter	ASTM D2041	AASHTO T209	Mn/DOT (Modified AASHTO T209)
Sample Size	Based on Nominal Maximum Agg. Size Min. 1, 000 g for 9.5 mm (3/8-in) Min. 2,000 g for 12.5 mm (1/2-in)	Based on Nominal Maximum Agg. Size Min. 1, 000 g for 9.5 mm (3/8-in) Min. 2,000 g for 12.5 mm (1/2-in)	2,000 to 2050 grams
Length of Time Vacuum Applied	5 to 15 minutes	15 $\pm$2 minutes	15 or less
Method of Agitation	Continuously (mechanical) Intermittently (by hand every 2 minutes)	Continuously (mechanical) Intermittently (by hand every 2 minutes)	Continuously (mechanical)
Use of Release Agent	None allowed	0.01% Concentration Aerosol OT	0.08% Concentration Aerosol OT[1]
Water Temperature Requirement	25°C $\pm$ 0.5 (77°F $\pm$ 0.9)	25°C $\pm$ 0.5 (77°F $\pm$ 0.9)	25°C $\pm$1 (77°F $\pm$1.8)
Procedure for Partially Coated Aggregate	Yes	Yes	Yes

1: Information obtained from MnDOT laboratory in Maplewood but not specified in draft.

When cores are used to determine the theoretical maximum specific gravity, an additional source of potential variation is added. Some laboratories choose to crumble the entire core, which includes the cut aggregate faces, to obtain a loose mixture. Other laboratories remove

the cut faces and then crumble the remaining mixture to obtain the loose mixture sample. Including the cut aggregate faces allows for water absorption by the aggregate during testing which can lead to higher theoretical maximum specific gravities. All of the test methods include a supplemental procedure for testing mixtures with partially coated aggregates which should, theoretically, be followed if cut faces are included. However, in practice this procedure is not commonly used due to length of test time required to obtain results and the increased testing variability associated with the supplemental procedures.

All of the supplemental procedures require the water to be decanted after the under-water mass is determined. The mixture is then spread on a non-absorptive surface and air-dried to a constant weight. Problems with this procedure include the length of time to get a constant mass (usually from 2 to 3.5 hours), and the continual technician attention required to make sure the mixture dries evenly. Both of these factors lead to an increase in the standard deviation for the test method.

Hypothetically, the water absorption problem can also be accentuated by the size of the core used for preparing the loose mixture. The proportion of cut faces in any given sample is a function of the height and diameter of the core used to prepare the sample:

$$A_{cut} = \frac{(1 - (Percent\ Binder + Percent\ Voids))\ (\ Surface\ Area\ of\ Core)}{Mass\ of\ Sample}$$

or

$$A_{cut} = = \frac{[1 - (V_{air} + V_{AC})]\ [(2\pi r)h + 2\pi r^2]}{M}$$

Where:

A_{cut} = Surface area of cut aggregate faces per gram of mixture

V_{air} = Estimated air voids, expressed in decimal form

V_{AC} = Estimated binder content, expressed in decimal form

r = Radius of sample, mm

h = Height of sample, mm

M = Mass of dry sample, grams

For example, if a 4 inch (100 mm) diameter by 2.5 inch (60 mm) high sample has a mass of 1,000 grams, a reported binder content (from construction records) of 5.8 percent, and an assumed air void content of 6 percent, A_{cut} is 31.17 mm^2/g. If the same sample is cut in half, A_{cut} increases to 45.34 mm^2/g of mixture tested. When the core height decreases, the mass decreases proportionally; the radius, however, remains constant. As the surface area of cut faces per gram of mixture tested increases, the influence of water absorption by the aggregate on the theoretical maximum specific gravity should also increase.

RESEARCH PROGRAM

Initially, a total of 12 cores were obtained from the center of each of the four asphalt concrete Mn/ROAD 5-Year Mainline test sections during the sensor placement activities. These cores were tested by the University of Minnesota. The bulk specific gravities were determined according to ASTM D2726. The theoretical maximum specific gravities were determined using ASTM D2041; all aggregates with cut faces were removed.

Additional cores taken from the coring areas of each of the four Mn/ROAD sections were tested at the Mn/DOT laboratory in Maplewood, Minnesota. The bulk specific gravity testing used by Mn/DOT is similar to ASTM D2726 with the only exception being that the sample time in the water bath is 3 to 5 minutes for the Mn/DOT method and it is 1 to 3 minutes for ASTM D2726. The theoretical maximum specific gravity was conducted according to the procedure outlined in the background section; cut faces were included in the sample tested. These results were used to compare results for the different methods of sample preparation and testing.

A second small study was conducted at the University to determine the influence of cut faces on test results. The cores used for this study were taken from the test pad construction at Mn/ROAD for establishing the rolling pattern for the full depth pavement section; this mixture was the same design as that used for section F1 (75 blow mix design) in the 5 Year Mainline section. A total of 30 cores were taken; the top lift was removed and used for another testing program. The remaining base lifts were used to determine both the bulk and theoretical maximum specific gravities per ASTM.

ANALYSIS

Cores from Mn/ROAD 5-Year Main Line

Table 2 shows the bulk and theoretical maximum specific gravity as well as the air voids results from the Mn/ROAD 5-Year Mainline cores for both the University and Mn/DOT laboratories.

Table 2. Comparison of Average Specific Gravity Results Between U of M and Mn/DOT.

Mn/ROAD Cell	Lift	Bulk Specific Gravity		Theoretical Maximum Specific Gravity		Air Voids, %	
		U of M	Mn/DOT	U of M	Mn/DOT	U of M	Mn/DOT
F-1 75 Blow	Wear	2.260	2.293	2.444	2.460	7.5	6.8
	Base 1	2.275	2.278	2.417	2.457	5.9	7.3
	Base 2	2.307	2.282	2.452	2.470	5.9	7.6
F-2 35 Blow	Wear	2.282	2.302	2.370	2.444	3.7	5.9
	Base 1	2.301	2.303	2.380	2.439	3.3	5.6
	Base 2	2.302	2.329	2.390	2.442	3.7	4.6
F-3 50 Blow	Wear	2.265	2.273	2.456	2.444	7.8	7.0
	Base 1	2.293	2.282	NA	2.457	NA	7.1
	Base 2	2.285	2.261	2.437	2.456	6.2	7.9
F-4 Gyratory	Wear	2.273	2.262	2.462	2.458	7.7	8.0
	Bit.	2.297	2.275	2.451	2.465	6.3	7.7
	Base 1	2.285	2.272	2.458	2.467	7.0	7.9
	Base 2	2.310	2.298	2.461	2.470	6.1	7.0

Figure 1 shows that the bulk specific gravity results for both laboratories were randomly distributed around the line of equality. This randomness indicates that there was no bias between the two sets of data. Figure 2 shows the difference in test results between the two laboratories. Using the precision statement included in ASTM D2726 for establishing the

acceptable range of two test results (0.076 for between-laboratories), the between-laboratory test results were well within this limit. In fact, all but one set of test results showed differences of less than 0.030.

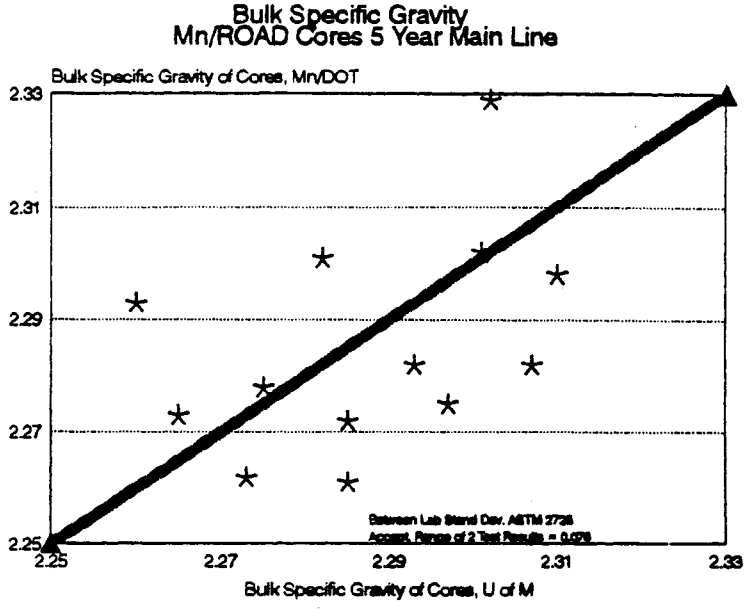

Figure 1. Comparison of Bulk Specific Gravity Between-Laboratories Results.

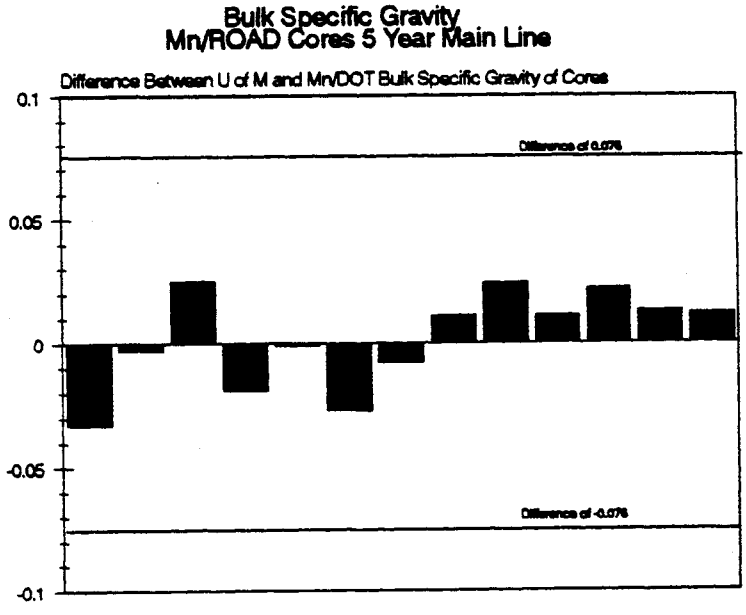

Figure 2. Differences in Between-Laboratory Test Results for Bulk Specific Gravity.

Figure 3 compares the theoretical maximum specific gravities for both laboratories. Unlike the bulk specific gravity comparison, this comparison shows a distinct bias in the data. The Mn/DOT results were consistently slightly higher than the University of Minnesota results in all but two cases . It is probable that this bias was the result of both the differences in the test methods used to determine the maximum specific gravities and whether or not the sample included the cut faces. This hypothesis will be discussed further in the following section. Figure 3 also shows that the results for the lifts in the F2 section tended to be separated from the other results. An examination of the test reports yielded no obvious explanations for the substantial difference in these data such as different operators, or equipment problems. Because the outliers were all from different lifts of the same section, the data could not be reasonably eliminated from the data base as random outliers.

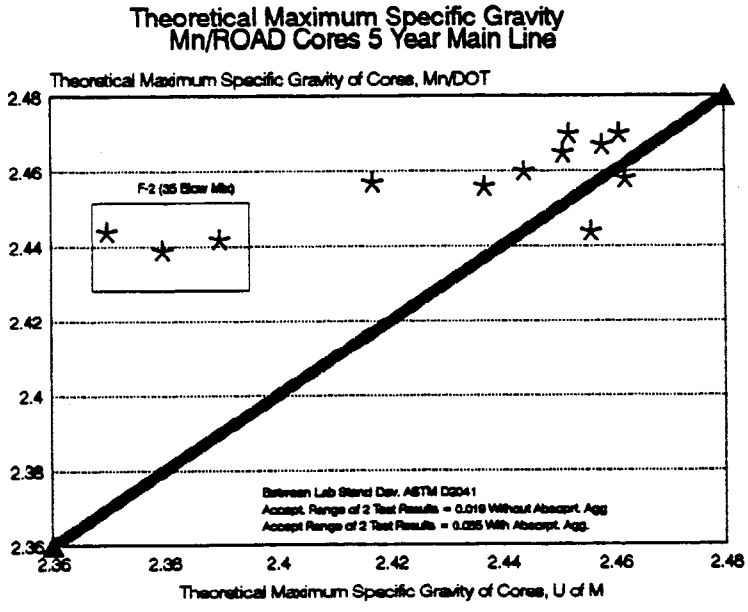

Figure 3. Comparison of Theoretical Maximum Specific Gravity Between-Laboratory Results.

Figure 4 presents the difference in the between-laboratory test results; this figure re-emphasizes the bias in the data. Using the ASTM D2041 criteria for the acceptable range of two between-laboratory test results (0.019), four of the results were greater than this limit. Three of these results belonged to the lifts for the F2 section. This indicates that with the exception of this section, the majority of results met the ASTM precision statement requirements.

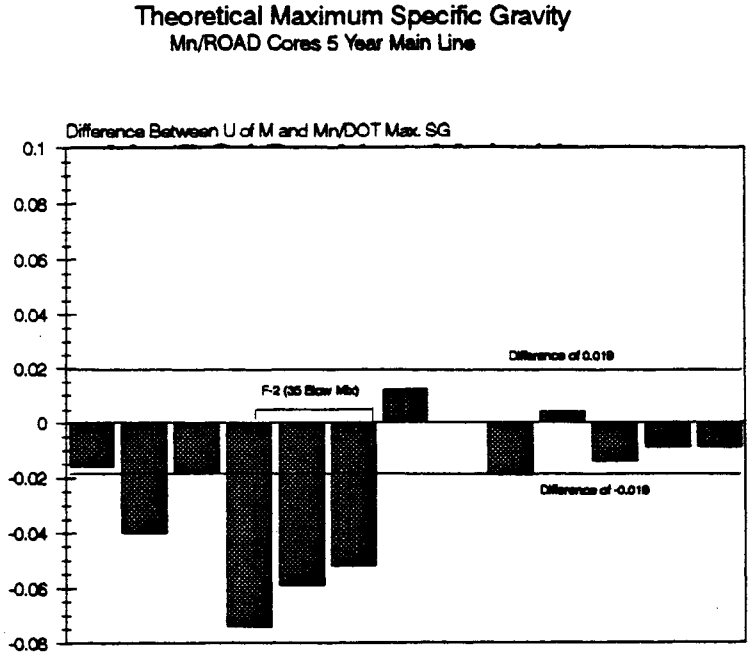

Figure 4. Differences in Between-Laboratory Theoretical Maximum Specific Gravity Results.

Figure 5 shows the determination of air voids follows a trend similar to that seen for the theoretical maximum specific gravity (Figure 3). Using the precision statement from ASTM D3203 that indicates an acceptable between-laboratory range is 3.08 percent voids, none of the results were considered statistically different.

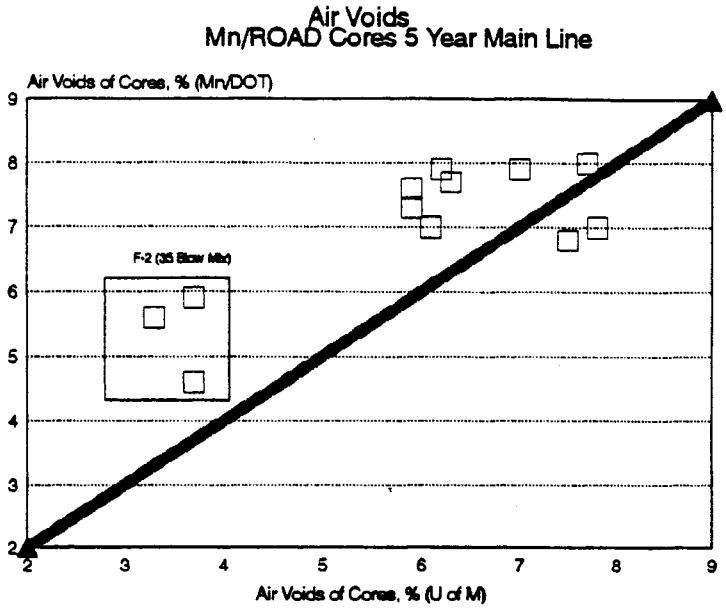

Figure 5. Comparison of Air Voids Between-Laboratory Results.

ASTM D3203 also presents an equation for calculating the standard deviation for air voids rather than using the pre-calculated precision statement values. This equation for calculating the standard deviation of air voids is:

$$\sigma_{air\ voids} = \sqrt{\frac{\overline{y^2}\sigma_x^2 + \overline{x^2}\sigma_y^2}{\overline{y^4}}}$$

Where:

σ_x = Standard deviation for determining bulk specific gravity

σ_y = Standard deviation for determining theoretical maximum specific gravity

y = Mean theoretical maximum specific gravity

x = Mean bulk specific gravity

Using the data in Table 2, an average standard deviation and mean for bulk specific gravity of 0.017 and 2.286, respectively, were obtained. The Mn/DOT data standard deviation and mean for the theoretical maximum specific gravity were 0.010 and 2.456, respectively. Based on these statistics, the standard deviation for air voids should be 0.008 percent voids expressed in decimal form, or 0.8 percent air voids (i.e., 0.008 x 100). The acceptable range of two test results would then be 2.2 percent voids (standard deviation times 2 $\sqrt{2}$ per ASTM C670). While this is a substantially narrower range than reported in ASTM, only two sets of test results would exceeded this range (Figure 6), and both of these were from the F2 section.

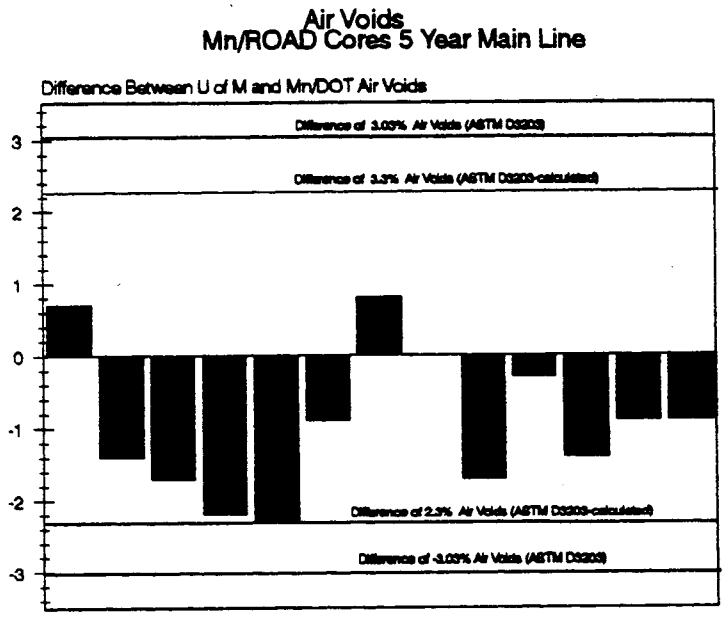

Figure 6. Differences in Between-Laboratory Air Void Results.

Mn/ROAD Test Pad Cores

Table 3 shows the results from the within-laboratory testing of the cores from the Mn/ROAD test pad. Samples were prepared by crumbling the bottom two lifts together without cutting the individual lifts apart. For the samples with the cut faces removed, two cores were used to obtain one sample of loose mixture. Only one core was needed to produce a sufficient amount of loose mixture for testing when the cut faces were left in the mixture.

Table 3. Results for Within-Laboratory Testing.

	Theoretical Maximum Specific Gravity	
	Without Cut Faces	Including Cut Faces
Individual Results for 9 Cores[1]	2.420 2.421 2.427 2.423 2.415 2.435 2.444 2.428 2.417	2.445 2.441 2.446 2.429 2.442 2.430 2.425 2.435 2.466
Average	2.426	2.440
Standard Deviation	0.009	0.012

1: One outlier removed from each data base. Criteria was $\pm$ 2 standard deviations

A t-test was used to answer the question: Does including the cut faces in the sample significantly increase the theoretical maximum specific gravity results? The t-test value was calculated as:

$$t = \frac{\overline{X_1} - \overline{X_2}}{\left[\frac{S_1^2}{n_1} + \frac{S_2^2}{n_2}\right]^{1/2}}$$

Where:

X_1 = mean of first sample set

X_2 = mean of second sample set

s_1^2 = standard deviation of first sample set

s_2^2 = standard deviation of second sample set

n_1 = number of samples in first sample set

n_2 = number of samples in second sample set

To find the critical t-test value, the degree of freedom, ν, also needed to be calculated:

$$\nu = \frac{[\frac{s_1^2}{n_1} + \frac{s_2^2}{n_2}]^2}{\frac{[\frac{s_1^2}{n_1}]^2}{n_1 + 1} + \frac{[\frac{s_2^2}{n_2}]^2}{n_2 + 1}} - 2$$

Using these equations, t equals 2.800 for 17 degrees of freedom. The critical t-test value for a one-tailed test is 1.740 (5). Since the calculated t value is greater than the critical t value, including the cut faces in the sample significantly increased the theoretical maximum specific gravity.

The surface area of cut faces per gram of mixture tested for these samples ranged between 37.19 mm^2/g and 36.37 mm^2/g for assumptions of 4 and 6 percent air voids, respectively for average sample dimensions of 5.5 inches (160 mm) tall and 1,600 grams. The cut surface area per gram would have been increased to between 54.90 and 53.69 mm^2/g (assumed 4 and 6 percent voids, respectively) if the cores had been cut into three equal sized individual lifts prior to testing. While there were not a sufficient number of samples to confirm this hypothesis, the significant increase in test results with the lower cut aggregate surface area is sufficient to recommend removing all cut faces prior to testing.

Adjustment of Theoretical Maximum Specific Gravity for Cut Faces

The inclusion of cut faces in the mixture increased the theoretical maximum specific gravity by an average of 0.017. Figure 7 shows the difference between the University of Minnesota and Mn/DOT data (Table 2) after the University theoretical maximum specific gravity data was increased by 0.017.

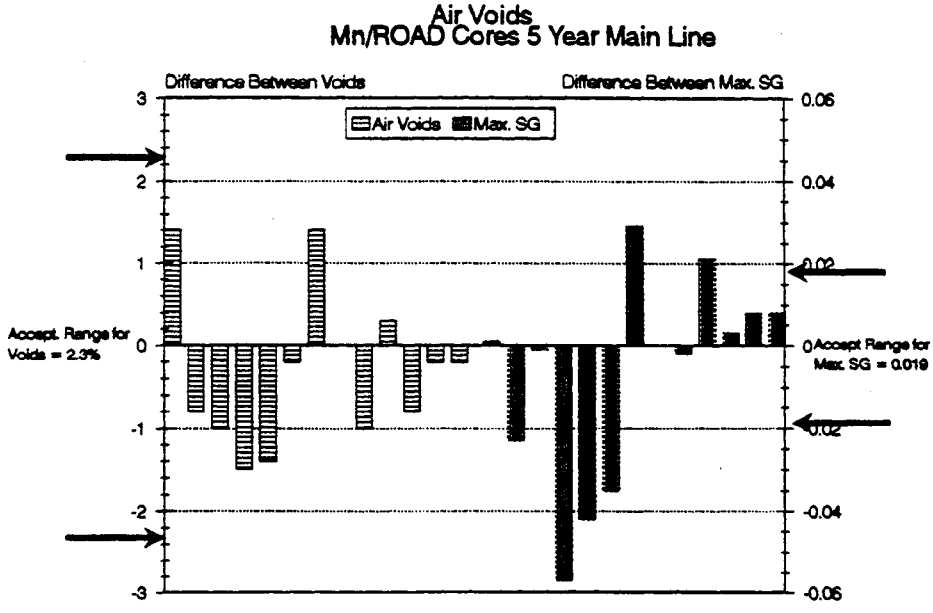

Figure 7. Comparison of Between-Laboratory After Data Adjusted for Cut-Faces.

Figure 7 shows that the difference between the University of Minnesota and Mn/DOT air voids is now less than 1.5 percent voids for all lifts in all sections. This is well within the acceptable range of test results. This figure also shows that the differences in the adjusted theoretical maximum specific gravity are now reasonably well distributed; the previous bias in the test results was removed by adjusting the data for differences caused by including cut aggregate faces in the mixture. A total of six sets of data are now outside of the acceptable range of two between-laboratory test results; three of these belong to the F2 section. Several

reasons for this include differences in test methods (ASTM D2041 versus Mn/DOT 1807 (draft)), real material differences due to the different sampling locations, and a potentially greater testing variability associated with testing cores as opposed to fresh laboratory-prepared loose mix. The last reason is the most probable as the within-laboratory standard deviation for the theoretical maximum specific gravity using cores was an average of 0.011 (Table 3). This standard deviation would increase the acceptable range of two test results to 0.031 for within-laboratory testing; this would be expected to increase further for between-laboratory comparisons. Using this limit all but the F2 maximum specific gravities would be within acceptable limits.

Although it was possible to apply an adjustment to correct the differences in test methods for the Mn/ROAD cores, one does not usually have the luxury of comparative data. It should be kept in mind that these results represent one fairly consistent gradation and the absorption characteristics of one aggregate source. Differing amounts of damage to core faces during extraction or handling and differing aggregate absorption characteristics will have various effects at other construction sites.

CONCLUSIONS AND RECOMMENDATIONS

1. When determining the theoretical maximum specific gravity of a mixture from cores, all cut faces should be removed from the sample prior to testing. Leaving the cut faces in the mixture can significantly increase the maximum specific gravity. This increase will result in increased in air voids.

2. The large difference in the test results for section F2 appears to be unusual when the results for the other sections are considered. This section will be retested by the University if a sufficient number of cores can be salvaged from other testing programs.

BIBLIOGRAPHY

1. Stroup-Gardiner, M., Newcomb, D.E., et. al, "Preliminary Laboratory Test Results for Mn/ROAD 5 Year Mainline Test Sections," draft currently being completed, January, 1994.
2. American Society for Testing and Materials Annual Book of Standards, Vol. 04.03, 1993.
3. American Association of State Highway Transportation Officials, Standard Specifications for Transportation Materials and Materials and Testing, Part II - Test Methods, 1990.
4. State of Minnesota Department of Transportation Bituminous Manual, 1990.
5. Blank, L, Statistical Procedures for Engineering, Management, and Science, McGraw-Hill Book company, 1980.